Potential use of nitrification inhibitors for mitigating N_2O emission from soils

Di Wu

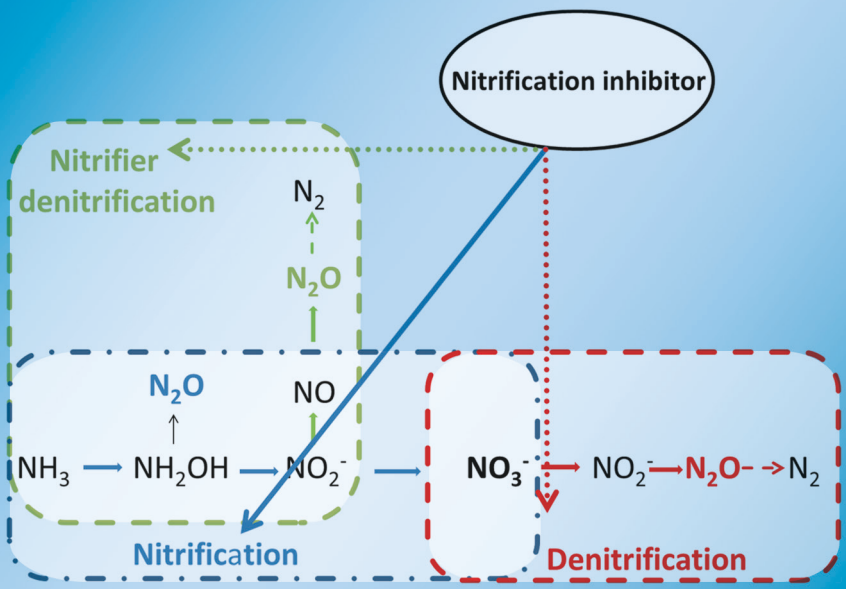

Energie & Umwelt / Energy & Environment
Band / Volume 390
ISBN 978-3-95806-264-1

JÜLICH FORSCHUNGSZENTRUM

Schriften des Forschungszentrums Jülich
Reihe Energie & Umwelt / Energy & Environment Band / Volume 390

Forschungszentrum Jülich GmbH
Institute of Bio- and Geosciences
Agrosphere (IBG-3)

Potential use of nitrification inhibitors for mitigating N_2O emission from soils

Di Wu

Schriften des Forschungszentrums Jülich
Reihe Energie & Umwelt / Energy & Environment Band / Volume 390

ISSN 1866-1793 ISBN 978-3-95806-264-1

Bibliographic information published by the Deutsche Nationalbibliothek.
The Deutsche Nationalbibliothek lists this publication in the Deutsche
Nationalbibliografie; detailed bibliographic data are available in the
Internet at http://dnb.d-nb.de.

Publisher and Distributor: Forschungszentrum Jülich GmbH
Zentralbibliothek
52425 Jülich
Tel: +49 2461 61-5368
Fax: +49 2461 61-6103
Email: zb-publikation@fz-juelich.de
www.fz-juelich.de/zb

Cover Design: Grafische Medien, Forschungszentrum Jülich GmbH

Printer: Grafische Medien, Forschungszentrum Jülich GmbH

Schriften des Forschungszentrums Jülich
Reihe Energie & Umwelt / Energy & Environment, Band / Volume 390

D 5 (Diss., Bonn, Univ., 2017)

ISSN 1866-1793
ISBN 978-3-95806-264-1

The complete volume is freely available on the Internet on the Jülicher Open Access Server (JuSER)
at www.fz-juelich.de/zb/openaccess.

Zusammenfassung

Die Anwendung von Nitrifikationsinhibitoren (NI) zur Reduzierung von Distickstoffoxid-(N_2O)-Emissionen ist eine vielversprechende Strategie zur Verbesserung der Nutzungseffizienz von Stickstoffdüngern und zur Minderung der Emissionen des klimarelevanten Gases N_2O aus landwirtschaftlichen Systemen. Ein besseres Verständnis der Faktoren und Einflussgrößen, die die Effizienz der N_2O-Emissionsminderung bestimmen, ist entscheidend, um optimale NI-Anwendungsstrategien entwickeln und anwenden zu können. Das Wissen über die der N_2O-Produktion und -Komsumption im Boden zugrunde liegenden Prozesse ist allerdings noch immer lückenhaft, wodurch das Verständnis der Mechanismen der N_2O-Emissionsminderung durch NI sowie die Effizienz der N_2O-Emissionsminderung unter verschiedenen Bodenbedingungen erschwert wird. Bisher wurde allgemein angenommen, dass NI keinen direkten Effekt auf den Prozess der Denitrifikation haben und somit auch keinen verringernden Effekt auf N_2O-Emissionen, die durch Denitrifikation entstehen, haben. Die Anwendung von NI könnte allerdings aufgrund der reduzierten Substrat-(NO_3^-)-Nachlieferung in Mikrobereichen des Bodens, in denen Denitrifikation stattfindet, signifikante Auswirkungen auf die Stöchiometrie der Denitrifikationsprodukte haben, wodurch die N_2O-Emissionen aus dem Boden signifikant verringert werden könnten. Darüber hinaus könnten NI-Effekte auf den Prozess der Nitrifizierer-Denitrifikation ebenfalls eine entscheidende Rolle in der N_2O-Emissionsminderung spielen, was bisher allgemein vernachlässigt wurde. Diese Befunde weisen darauf hin, dass NI möglicherweise auch bei hoher Bodenfeuchte zur N_2O-Emissionsminderung verwendet werden könnten.

Das Ziel dieser Arbeit war es, die Steuergrößen und detaillierten Mechanismen, die den Effekt von NI auf N_2O-Emissionen aus landwirtschaftlichen Böden bestimmen, zu untersuchen. Im Rahmen der Arbeit wurde Stabile-Isotopen- und N_2O-Isotopomeranalytik angewendet, um die

Quellen der N_2O-Emissionen aufzuschlüsseln. Die Ergebnisse der Feld- und Laborstudien zeigen, dass NI als effiziente Managementoption zur Verringerung von N_2O-Emissionen verwendet werden können, und zwar nicht nur unter Bodenbedingungen, die die Nitrifikation begünstigen, sondern auch unter Bedingungen, unter denen das Potential für Denitrifikation/Nitrifizierer-Denitrifikation sehr hoch ist, z.B. in N-gedüngten und mit Stroh versetzten feuchten Böden.

In dieser Arbeit wurden maßgeblich Hinweise für deutsche und chinesische Böden darauf gefunden, dass die beobachtete hohe N_2O-Minderungseffizienz von NI unter feuchten Bodenbedingungen höchstwahrscheinlich auf die Inhibitionseffekte von NI auf durch Denitrifikation und Nitrifizierer-Denitrifikation produziertes N_2O zurückzuführen ist. Somit stellt diese Studie einen Fortschritt zum besseren Verständnis der detaillierten Mechanismen von N_2O-Minderungseffekten durch NI in Böden dar. Im Vergleich mit verschiedenen alternativen Strategien, wie die Anwendung von Urease-Inhibitoren und Hippursäure, wurde die Anwendung von NI als verlässlicher und effektiver für die Reduzierung von aus dem Boden ausgestoßenem N_2O aus Feld- auch Laborstudien befunden und könnte somit als vielversprechende Strategie in landwirtschaftlichen Systemen angewendet werden.

Abstract

The use of nitrification inhibitors (NI) to reduce nitrous oxide (N_2O) emissions is a promising strategy to improve N fertilizer use efficiency and to help minimize emissions of the climate-relevant gas N_2O in agricultural systems. Better understanding of factors and drivers controlling the N_2O mitigation effectiveness is crucial for implementing optimal NI application strategies. However, the understanding of the underlying pathways involved in N_2O production and consumption in soils is still fragmentary, which hampers real insight into the N_2O mitigation mechanisms using NIs as well as NI mitigation effectiveness under various soil conditions. It has been generally assumed that nitrification inhibitors have no direct effect on denitrification and therefore should have no mitigation effect on N_2O emissions derived from denitrification. However, the indirect impact of NIs, due to the reduced substrate (NO_3^-) delivery to those microsites where denitrification occurs, may have significant effects on denitrification product stoichiometry that may significantly lower soil-borne N_2O emissions. Moreover, the inhibition effects of NIs on N_2O produced via the nitrifier denitrification pathway could also play an important role, which has generally been neglected. These facts suggest that NI might be used for mitigating N_2O emissions even under conditions of higher soil moisture.

The aim of this study was to in depth explore the driving factors and detailed mechanisms that determine the effect of NIs on N_2O emissions in agricultural soils. Stable isotope and N_2O isotopomer techniques were applied to trace N_2O emissions sources. The obtained results in both field and laboratory studies did indicate that that NIs can be used as an effective management option to mitigate N_2O emissions, not only under soil conditions favouring nitrification, but also in situations when soil denitrification/nitrifier denitrification potential is high, e.g., in N-fertilized and straw-amended moist soils. Significant evidence was found in

this thesis for both German and Chinese soils that the high NI mitigation effectiveness in moist soil conditions is most likely due to the inhibition effects of NIs on N_2O produced by denitrification and nitrifier denitrification. Thus, this study is a step forward in understanding the detailed mechanisms of the N_2O-mitigating effect of NIs in soils. Compared with several alternative strategies such as application of urease inhibitor and hippuric acid, NI addition was found to be more reliable and efficient for reducing soil-emitted N_2O in both field and laboratory studies and thus could be applied as an promising strategy in agricultural systems.

List of publications

I. **Wu, D**., Köster, J.R., Cárdenas, L.M., Brüggemann, N., Lewicka-Szczebak, D., Bol, R., 2016. N_2O source partitioning in soils using ^{15}N site preference values corrected for the N_2O reduction effect. *Rapid Communications in Mass Spectrometry 30, 620–626.*

II. **Wu, D**., Senbayram, M., Well, R., Brüggemann, N., Pfeiffer, B., Loick, N., Stempfhuber, B., Dittert, K., Bol, R., 2017. Nitrification inhibitors mitigate N_2O emissions more effectively under straw-induced conditions favoring denitrification. *Soil Biology and Biochemistry 104, 197–207.*

III. **Wu, D.,** Cárdenas, L. M., Calvet, S., Brüggemann, N., Loick, N., Liu, S., & Bol, R. 2017. The effect of nitrification inhibitor on N_2O, NO and N_2 emissions under different soil moisture levels in a permanent grassland soil. *Soil Biology and Biochemistry 113*, 153-160.

IV. **Wu D**., Zhao, Z., Han, X., Meng, F., Wu, W., Zhou, M., Brüggemann, N., Bol, R., 2017. Potential dual effect of nitrification inhibitor on nitrifier denitrification helps mitigate peak N_2O emissions events in the North China Plain cropping systems. **Under review** in *Soil Biology and Biochemistry*

V. **Wu, D**., Senbayram, M., Blagodatskaya, E., Kuzyakov., Y, Bol, R., 2017. Influence of two different biochars application on CO_2 and N_2O emissions in two different soil types. Draft manuscript

VI. **Wu, D**., Cárdenas, L., Lewicka-Szczebak, D., Brüggemann, N., Well, R., Köster, J.R., Bol, R., 2017. Using the correlation between N_2O $\delta^{18}O$ and α position $\delta^{15}N$ as a tool to spot N_2O reduction process during denitrification in soils. Draft manuscript

VII. Nguyen, Q., **Wu, D**., Kong, X., Bol, R., Petersen, S., Jensen, L., Liu, S., Bruggemann, N., Glud, N., Larsen, M., Bruun, S., 2017. Effects of cattle slurry and nitrification inhibitor

application on spatial soil O_2 dynamics and N_2O production pathways. *Soil Biology and Biochemistry 114: 200-209.*

VIII. Zhao, Z., **Wu, D.,** Bol, R., Shi, Y., Guo, Y., Meng, F., & Wu, W. 2017. Nitrification inhibitor's effect on mitigating N_2O emissions was weakened by urease inhibitor in calcareous soils. *Atmospheric Environment. 166: 142-150.*

IX. Liu, S., Berns, AE., Vereecken, H., **Wu, D**., Brüggemann , N., 2017. Interactive effects of MnO_2, organic matter and pH on abiotic formation of N_2O from hydroxylamine in artificial soil mixtures. *Scientific Reports, 7, 39590.*

X. Nguyen, Q., Jensen L, N., Bol, R., **Wu, D**., Triolo, J., Jensen,. Vazifehkhoran, A., Bruun, S., 2017. Biogas digester hydraulic retention time affects oxygen consumption patterns and greenhouse gas emissions after application of digestate to soil. *Journal of Environmental Quality*

XI. Ciganda, V., Lopez-Aizpun, M.,. Repullo, M. **Wu, D**, Terra, J., Elustondo,D., Clough, T., Cardena, L. Potential inhibitor effect of hippuric acid on nitrous oxide emissions from grassland on a heavy clay soil. **Under review** in *Journal of Plant Nutrition and Soil Science.*

Contents

1. Introduction

1.1 Nitrogen transformations in soil and current problems

Nitrogen (N) inputs to the biosphere increased from 155 to 345 Tg N $year^{-1}$ between 1900 and 2000, in which synthetic N fertilizers are the main contributor (Bouwman et al., 2013). When N fertilizers are applied, usually as urea or anhydrous ammonia (NH_3), the microbial process of nitrification converts a large fraction of the ammonium (NH_4^+) into nitrate (NO_3^-) within 2–3 weeks (Huber et al., 1977). The nitrogen fertilizers not taken up by the target system tend to become mobile, causing serious environmental consequences (Galloway et al., 2004). One of the most serious problems in agriculture is the enhancement of nitrous oxide (N_2O) emissions. Since pre-industrial times, the atmospheric N_2O concentration increased by 44 ppb to 324 ppb in 2011 (IPCC, 2013). Nitrous oxide plays a crucial role in environmental terms since the global warming potential (GWP) of N_2O is 298 times the GWP of CO_2 when calculated over a 100-year period (IPCC, 2013). Besides, N_2O also contributes to the destruction of the ozone layer, which is considered currently to be the single most important ozone-depleting substance and is expected to remain so throughout the 21st century (Ravishankara et al., 2009). Global anthropogenic N_2O emissions are estimated as approx. 6.5 Tg N yr^{-1} in 2010 (IPCC, 2013), of which agricultural soils are the largest source (Ciais et al., 2014). Not surprisingly, many studies have reported that application of N fertilizer in agricultural systems significantly increase N_2O emissions (Meng et al., 2005; Wu et al., 2017). However, as N is commonly the most limiting nutrient for crop production, the application of N fertilizers has significantly increased crop yield in agricultural systems across the globe in the past decades (Sutton et al., 2011). It is a great challenge to cut down N fertilizer input since the demand for food is still increasing, especially in developing countries (Zhu and Chen, 2002). It is therefore urgent to develop effective mitigation strategies that can maintain

food production while at same time reducing N_2O emissions in high N input agricultural systems.

1.2 Different microbial pathways for N_2O production and consumption in soils

It is well recognized that soils are the largest source of atmospheric N_2O (Bouwman et al., 2013). Nevertheless, the underlying N_2O microbial production and consumption processes are still not fully understood. As illustrated in Figure 1, recent studies show that at least three major biochemical processes are involved in soil N_2O production, i.e. nitrification, nitrifier denitrification and denitrification (Butterbach-Bahl et al., 2013; Kool et al., 2011). In terrestrial ecosystems, nitrification plays a key role in the N-cycle. Nitrification is defined as the biological oxidation of NH_4^+ or NH_3 via nitrite (NO_2^-) to NO_3^-. Nitrous oxide is a by-product of the ammonia oxidation process of nitrification. The ammonia monooxygenase (AMO), which is an enzyme bound to the membrane of microorganisms with Cu as a co-factor, catalyses the oxidation of NH_3 to NH_2OH (Arp et al., 2002). Chemolitho-autotrophic ammonia-oxidizing bacteria (AOB), like *Nitrosomonas* spp. were considered to be mainly responsible for the rate-limiting steps of nitrification (Kowalchuk and Stephen, 2001). However, in recent years ammonia-oxidizing archaea (AOA) were also found to play a crucial role in the nitrification process in a range of different soils (Könneke et al., 2005; Treusch et al., 2005). Furthermore, several new studies indicate that heterotrophic nitrification, performed by fungi, could be the predominant NO_3^- production pathway in acid forest soils (Zhang et al., 2013; Zhu et al., 2013).

Denitrification process is the reduction of NO_3^- or NO_2^- to the gases nitric oxide (NO), N_2O and dinitrogen (N_2). Nitrous oxide is an obligate intermediate of denitrification. Denitrification rates depend on oxygen availability, soil moisture, soil type, pH, NO_3^-

concentration, and prominently on the availability of labile organic carbon (C) compounds in the soil (Burford and Bremner, 1975; Loecke and Robertson, 2009). Denitrification has been found to be a function of both eukaryotes and bacteria. Nevertheless, many fungi lack the enzyme N_2O reductase and, thus, in this case the final product is N_2O (Laughlin and Stevens, 2002). **Fungal denitrification** was assumed to play only a small role in the nitrogen cycle. However, since recently it is believed to be a major process in the nitrogen cycle based on more studies at the molecular biological level (Shoun et al., 2012; Sutka et al., 2008).

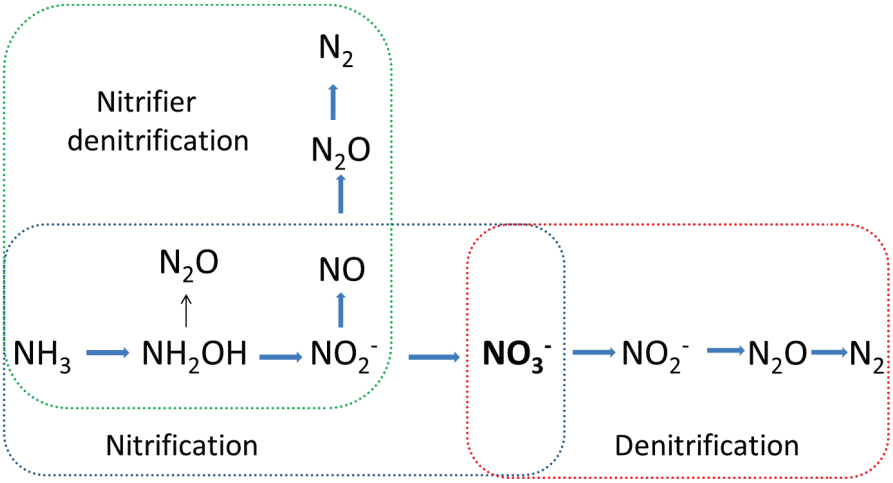

Figure 1. Three major microbial metabolic pathways that are involved in N_2O formation and consumption.

Nitrifier denitrification, which is also conducted by ammonia-oxidising bacteria (AOB), has been well-known in pure cultures for a long time (Hooper, 1968). However, the contribution of nitrifier denitrification has also long been neglected due to methodological constraints. Only recently some unambiguous proofs have been found for nitrifier denitrification as another main process responsible for N_2O emissions in soil (Kool et al., 2011; Zhu et al., 2013). Based on a dual-isotope (^{15}N and ^{18}O) tracing approach, Kool et al. (2011) reported that nitrifier denitrification is a significant source of N_2O in soil and should therefore be

routinely considered as a major contributor to N_2O emissions from soil. Zhu et al. (2013) found that nitrifier denitrification was a significant source of N_2O under low oxygen availability based on a similar approach.

Except for these three main pathways, several other microbial metabolic and abiotic processes can also contribute to N_2O formation and consumption, e.g. chemical decomposition of hydroxylamine during nitrification (**Paper IX**), dissimilatory nitrate reduction to ammonium (DNRA), anaerobic NH_3 oxidation and coupled nitrification-denitrification (Heil et al., 2015; Zhou et al., 2017; Zhu et al., 2011). However, the contributions of these pathways to soil N_2O emissions are still poorly identified and quantified at the field scale (Butterbach-Bahl et al., 2013; Liu et al., 2016).

I.3 Nitrification inhibitors and their effect on N_2O emission

Nitrification inhibitors (NIs) are a group of chemical compounds that can delay the bacterial oxidation of NH_4^+ to NO_2^- in the soil by suppressing the activities of *Nitrosomonas* bacteria in the soil (Zerulla et al., 2001). Different inhibition mechanisms were believed to be involved for various NIs. Nevertheless, a large number of NIs were found to inhibit the first enzymatic step of nitrification through the removal of co-factors by chelating compounds like Cu (Subbarao et al., 2006; McCarty, 1999). This mechanism is also believed to be the case for many commercially used NIs such as nitrapyrin, DCD (dicyandiamide) and DMPP (3,4-dimethylpyrazole phosphate) (Ruser and Schulz, 2015). Nitrification inhibitors first came on the market with the invention of N-serve (trade name for nitrapyrin of Dow Chemical Company) in the 1960s (Prasad and Power, 1995). Since then, many compounds/products have been released that were assumed to inhibit nitrification in soil. However, only a few of them have been widely tested and used commercially, e.g. DCD (Dicyandiamide), DMPP

(3,4-dimethylpyrazole phosphate). Dicyandiamide, which is the dimeric form of cyanamide with relatively high water solubility, has been studied as a NI for more than 50 years (Amberger, 1989). A large number of studies have shown that the addition of DCD could significantly reduce N_2O emission. For example, Cui et al. (2011) reported from an eight-month field experiment in an intensive vegetable production system that N_2O emissions were reduced by 72.7–83.8% with DCD. In a grassland system, Di et al. (2007) found that DCD was very effective in reducing N_2O emissions in four different soils with an average reduction of 70%. In a one-year field experiment in a wheat–maize cropping system, Liu et al. (2013) reported that the DCD treatment significantly decreased annual N_2O emission by 35%. Since about the year 2000, DMPP as a new NI has been introduced into agricultural practice in many countries (Barth et al., 2008; Weiske et al., 2001). In comparison to DCD, DMPP has been shown to be less phytotoxic, and lower application rates are required (Zerulla et al., 2001). Results from a field experiment in a wheat-maize cropping system showed that DMPP decreased annual N_2O emission by 38% (Liu et al., 2013). In another field experiment in a grassland system, DMPP reduced N_2O release by 32% when mixed with slurry (Dittert et al., 2001). In a vegetable production system, DMPP significantly reduced N_2O emissions during the cropping season and winter period, resulting in reduction of annual N_2O emissions by 45% and 40%, respectively, in a two-year experiment (Pfab et al., 2012). Besides the two most popular NIs, some other NI products have also been commercially used. For example, the active ingredients (1,2,4 Triazol and 3-Methylpyrazol) of PIADIN® (SKW, Piesteritc, Germany) have been found act as effective NI; only few published studies have investigated it though (Barneze et al., 2015; Federolf et al., 2016).

In general, the use of NIs has been repeatedly shown to reduce N_2O emissions from agricultural soils, with mitigation effectiveness of about 50% as suggested by recent meta-analysis studies (Qiao et al., 2015; Ruser and Schulz, 2015). However, some studies also

reported that application of NIs failed to reduce N_2O emissions from soils (Dell et al., 2014; Parkin and Hatfield, 2010). Moreover, the knowledge about the underlying mechanisms for the mitigation effect is still limited, especially at high C availability and high soil moisture conditions, suggesting that different processes are involved and that the controlling factors need to be investigated.

1.4 Objectives and hypotheses

The overall objective of this PhD thesis was to explore the mechanisms of NI effects on N_2O emissions in agricultural soils. The specific objectives were:

1. To evaluate and improve the potential use and applicability of N_2O isotopomer techniques for N_2O source partitioning.

2. To explore the detailed mechanisms of NI on nitrogenous gases emissions under different soil moisture conditions with fully automated, high time resolution incubation systems.

3. To evaluate NI mitigation effects on N_2O emissions in field studies with combination of source tracing of N_2O emissions by using N_2O isotopomer techniques.

4. To compare the effectiveness of NI for reducing N_2O emissions from soils with alternative mitigation approaches

2. Methodology

This PhD thesis included several theoretical modelling studies, laboratory incubation experiments and field experiments. In the following section, the main applied methodologies are discussed.

2.1 Measurement of trace gases

Chamber methods are one of the most commonly used approaches for measuring N_2O fluxes from soil. A variety of chamber deployment methods have been used to measure N_2O fluxes from soils (Chadwick et al., 2014). In this thesis, two types of chamber methods were used and thus will be discussed below, i.e. the static chamber method, which was used in **Paper IV**, **V**, **VII**, **VIII**, **X** and **XI**, and dynamic flow-through chamber methods, which was used in **Paper I**, **II**, **III** and **V**.

2.1.1 The static chamber-gas chromatography technique

The static chamber method has been used to measure N_2O for more than 40 years (Delwiche and Rolston, 1976). The advantages of this method are that it is cost-effective as compared to other techniques (e.g. the eddy covariance approach), and it particularly facilitates investigation of field-scale experiments, especially where the fetch area of eddy covariance is a problem (Hensen et al., 2013). However, the static chamber method is also subject to several drawbacks. For example, the considerable variation in chamber methodology often leads to the low quality and reliability flux measurements (Rochette and Eriksen-Hamel, 2008). Besides, constrained by the chamber size and manpower, the measurements are often conducted on a limited soil area with low frequency, which cannot provide the high temporal and spatial resolution required to improve greenhouse gas budgets and policy making (Hensen et al., 2013). To minimize the biases, for example, in the field studies in **Paper IV and VIII** large opaque stainless static chambers (0.5m W×0.5m L×0.15m H) were used for measuring

N_2O emissions (Fig. 2). Air temperature inside the chamber was monitored during gas collection. To get a relatively high time resolution, nitrous oxide emissions were monitored once a day for a continuous duration of 1 week after each fertilization and irrigation event, and then twice a week.

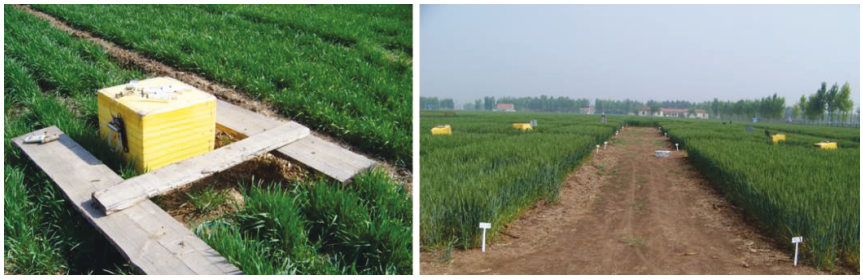

Figure 2. Static chamber used in field experiments described in Paper IV and VIII.

2.1.2 Automated incubation systems for two laboratory experiments

In order to gain a better insight of the underlying N_2O production and consumption pathways in soil, high frequency and well controlled laboratory experiments are needed. In this thesis, two robotized soil incubation systems were used. Both of them applied the dynamic chamber method. The dynamic chamber method introduces an air flow through the headspace of chamber, and the target gas concentrations are measured in the in-coming as well as out-going air. The first incubation experiment **(Paper II)** was conducted in a fully automated continuous flow incubation system with 15 PVC vessels (200 mm height, 200 mm diameter). The details of the experiment are described in the paper chapter. After amendment addition, the incubation pots were sealed and the headspace of each vessel was continuously flushed with ambient air (about 20 ml air min^{-1}). The second incubation experiment **(Paper III)** was carried out in a denitrification incubation system using a He/O_2 atmosphere (Cardenas et al., 2003; Loick et al., 2016). Soils were packed into 12 stainless steel vessels of 140 mm diameter. The atmospheric N_2 was removed by flushing the soil core with a mixture of $He:O_2$

(80:20) in order to measure N_2 fluxes. The dynamic flow-through chamber method together with the auto-sampling system enabled a high gas measuring frequency (maximum 8 seconds measurement time per vessel. The two incubation systems were generally very reliable. However, one issue frequently encountered with these two incubation systems was the unstable flow rate of the outlet. The outlet flow rates were normally relatively stable, but sometimes they fluctuated dramatically. The gas emission rates were only calculated for the times when air flow rates were stable. In some cases, one of the chamber's outlet flow rate would become very low because the pipe was blocked by water vapour or small particles. Therefore, the dynamic flow-through chamber required frequent and precise checks of the flow rate of each chamber. Thus, in the two incubation studies the flow rate was measured manually with a flow meter at least once a day.

Figure 3. The two automatic incubation systems (a) used in Paper II and V and (b) used in Paper I and III .

2.2 Analysis of N_2O isotope signature and ^{15}N site preference

Stable isotope techniques have offered us the potential to interpret the contribution of different microbial processes to N_2O emissions. The N_2O $\delta^{15}N$ and $\delta^{18}O$ values derived from

nitrification are reported to be larger compared with denitrification and nitrifier denitrification, which could be used as an indicator for gaining a first insight of N_2O production pathways (Sutka et al., 2006; Bol et al., 2003). Nevertheless, N_2O $\delta^{15}N$ value can be affected by many factors, e.g. NH_4^+ and NO_3^- origins, isotopic fractionation and soil heterogeneity, while N_2O $\delta^{18}O$ value can be not only affected by the isotope effect of N_2O reduction to N_2, but also be affected by exchanging oxygen with soil water (Baggs, 2011; Ostrom et al., 2007; Well and Flessa, 2009). During the last decade, the developments in mass spectrometric and laser spectroscopic techniques enabled the analysis of the intramolecular ^{15}N distribution in the linear asymmetric N_2O molecule (Brenninkmeijer and Röckmann, 1999; Toyoda and Yoshida, 1999; Köster et al., 2013). The ^{15}N site preference (SP), which is defined as the difference between $\delta^{15}N$ at the central (α position) and the peripheral N atom (β position) in the N_2O molecule, has been shown to differ amongst different N_2O source pathways (Toyoda et al., 2005; Sutka et al., 2006, 2008). In pure culture studies, the SP of N_2O from bacterial denitrification (SP values -11‰ to 0‰) was found to be significantly lower when compared to the SP of nitrification (NH_3 oxidation and hydroxylamine oxidation) derived N_2O (SP values 31‰ to 37‰). Based on these findings, the relative contribution of denitrification and nitrification to the total N_2O emission from soils can be estimated. In our study, a correction for ^{17}O was performed according to Kaiser et al. (2003), assuming a mass-dependent fractionation of ^{17}O and ^{18}O and using the calculations provided by that study. The $\delta^{15}N_{bulk}$, $\delta^{18}O$, and SP were calibrated against two reference gases provided by EMPA (Dübendorf, Switzerland) (Ref 1: $\delta^{15}N_\alpha$: 15.70 ±0.31‰, $\delta^{15}N_\beta$: –3.21 ± 0.37‰, $\delta^{15}N_{bulk}$: 6.24 ± 0.11‰, SP: 18.92 ± 0.66‰, $\delta^{18}O$: 35.16 ± 0.35‰; Ref 2: $\delta^{15}N_\alpha$: 5.55 ± 0.21‰, $\delta^{15}N_\beta$: –12.87 ± 0.32‰, $\delta^{15}N_{bulk}$: –3.66 ± 0.13‰, SP: 18.42 ± 0.50‰, $\delta^{18}O$: 32.73 ± 0.21‰) (Heil et al., 2015). The isotope effects during N_2O reduction on N_2O SP values have been calculated using a Rayleigh-type model, assuming that isotope dynamics followed closed-system behaviour. The model can be described as follows:

$$SP_{N2O-r} = SP_{N2O-0} + \eta_r \ln\left(\frac{C}{C_0}\right)$$

In this equation, $SP_{N2O\text{-}r}$ is the SP value of the remaining substrate (i.e. N_2O), $SP_{N2O\text{-}0}$ is the SP value of the initial substrate, η_r is the net isotope effect associated with N_2O reduction, and C and C_0 are the residual and the initial substrate concentration (i.e. C/C_0 expresses the $N_2O/(N_2O+N_2)$ product ratio).

3. General discussion

3.1 Potential use of N_2O isotopomer analysis for N_2O source tracing in lab and field studies

The N_2O source apportioning to its different production pathways is challenging due to the involvement of the various different microbial pathways and abiotic processes. The newly developed N_2O isotopomer approach has been found to be the one of the most promising techniques to tackle this problem (Köster et al., 2013). However, the shortcomings discussed below are hampering the wider use of the isotopomer approach for quantification of N_2O emission sources in soils.

First of all, overlapping SP values were found from other N_2O production processes, i.e. the SP of N_2O from nitrification and fungal denitrification was reported to be 22 to 37‰, while the SP of N_2O from bacterial denitrification and nitrifier denitrification was reported to be -1 to -11‰ (Rohe et al., 2014; Sutka et al., 2008; Toyoda et al., 2015). Furthermore, there are other microbial N_2O production pathways, such as anammox (anaerobic ammonium oxidation) and DNRA (dissimilatory nitrate reduction to ammonium), for which hardly any characteristic isotopic N_2O signatures have been identified yet.

Moreover, to estimate the N_2O sources correctly, the isotopic fractionation effect of N_2O reduction to N_2 on SP values should not be overlooked (Decock and Six, 2013). The increase in SP in response to reduction would result in a shift away from values associated with denitrification (0%) toward those associated with nitrification (33%) (Sutka et al., 2006). Therefore, the nitrification process as source of N_2O will be overestimated if the fractionation effect of N_2O reduction is not considered. In most of the previous studies, isotope effects during N_2O reduction on N_2O SP values have been calculated using a Rayleigh-type model, assuming that isotope dynamics followed closed-system behavior. However, using a closed-system model with a fixed SP isotope effect may significantly overestimate the N_2O reduction effect on SP values, especially when N_2O reduction rates are high (Wu et al., 2016). Based on our study, we propose the dynamic apparent net isotope effects (NIE) function as an alternative way of examining and calculating SP_0 values, especially when the $N_2O/(N_2O+N_2)$ product ratio is less than 0.1 **(Paper I)**.

Another proposed beneficial use of isotopomer analysis is an indicator for the N_2O reduction to N_2 in field studies. As N_2O reduction to N_2 mainly involves breaking the bond between the central N (α position) and O, the remaining N_2O will therefore be enriched simultaneously in $\delta^{18}O$ and $\delta^{15}N\alpha$. That is, if N_2O reduction is significant, the isotope effect will result in a positive correlation between $\delta^{18}O$ and $\delta^{15}N^{\alpha}$ (Park et al., 2011). Ostrom et al. (2007) reported a slope of 1.7 for the correlation of $\delta^{18}O$ versus $\delta^{15}N^{\alpha}$ when N_2O reduction occurs in the absence of production, and a slope of 0.3 with no N_2O reduction in soil mesocosm and pure culture studies. In **Paper VI**, a possible approach is proposed to identify a significant contribution of the N_2O reduction process by using the correlation and slope between N_2O $\delta^{18}O$ and $\delta^{15}N_{\alpha}$. However, further work is needed to validate this approach *in situ* in field studies with alternative methods.

3.2 Factors affecting the mitigation effectiveness of NIs on N_2O emission

It has been generally assumed that the mitigation effectiveness of NIs on N_2O emission depend on soil properties such as soil water content, soil available C, soil temperature, and different types of NIs (Slangen and Kerkhoff, 1984). The details will be discussed below.

3.2.1 Soil water content and available C

Soil water content is one of, or maybe even the most important factor(s) that control N_2O emissions since it controls the O_2 availability into and also the N_2O diffusion out of the soil (Davidson et al., 2000). In dry soil (water filled pore space (WFPS) <60%), it is generally believed that nitrification is the main source of N_2O production, while in wet soils (WFPS 60-90%), denitrification produces most of N_2O. However, when the soil is even wetter (WFPS>90%) or water-saturated, much of the N_2O is further reduced to N_2 by denitrifiers before it escapes the soil (Davidson et al., 2000). Since most NIs only have an inhibitory effect on nitrification-related bacteria, it should be assumed that NIs show higher N_2O mitigation effectiveness at lower soil water content. Interestingly, Menendez et al. (2012) reported that the use of DMPP reduced N_2O emission more effectively under conditions favouring denitrification, i.e. at 80% water-filled pore space (WFPS), than at 60% WFPS, which provides more suitable conditions for nitrification. Similarly, Di et al. (2014) reported that, while the DCD did not have a significant impact on N_2O emission at 60% field capacity, large reductions were found after DCD application at 100% field capacity and above. In **Paper III**, the highest NI mitigation effect was found at 65% WFPS, the second highest at 80%WFPS, while the lowest was found at 50% WFPS, indicating a more complex relationship between soil water content and the NI mitigation effect on N_2O.

The addition of labile C to soils could stimulate denitrification rates and thus increase N_2O emissions, such as the straw addition in **Paper II**. Therefore, we would assume that NI shows

less effectiveness on N_2O mitigation with labile C addition. However, in the study described in **Paper II**, the N_2O mitigation effect of NI was significantly higher in treatments with straw addition compared to treatments without straw. It can be assumed that this is likely because the indirect effect of NIs on denitrification and the effect of available C interacted with soil water content (**Paper II and III**), which is a novel finding that helps understanding the mechanisms of the N_2O-mitigating effect of NIs in soils in more detail.

3.2.2 Temperature

Soil temperature can affect the stability of NIs in soil. Most reports suggest that NIs are more effective at low temperatures, as higher temperature could increase the degradation of NIs (Prasad and Power, 1995). McCarty and Bremner (1989) showed in a 28-day incubation experiment that with 10 mg kg^{-1} DCD, the inhibition of nitrification decreased from 90% to 23% when temperature increased from 15 to 30 Cº. In a literature review, Kelliher et al. (2008) reported that DCD showed a decreasing trend of N_2O inhibition time with increasing soil temperature. Similarly, Irigoyen et al. (2003) reported that the effectiveness of both DCD and DMPP for stabilising NH_4^+ in soil was drastically decreased at increased soil temperatures. However, Menendez et al. (2012) found that the persistence of DMPP in soil is not influenced by temperature in the range between 10 and 20 °C and the effectiveness of DMPP on mitigating N_2O at the three different temperatures (10, 15, 20 °C) was the same. In all of the incubation studies of this thesis the room temperature was kept constant to avoid the temperature influence. However, in the field studies (**Paper II and VII**) the average soil temperature was significantly higher in the maize season as compared to the wheat season (26.4 °C vs. 10.3 °C), which could be one of the reasons why the N_2O mitigation effect of DMPP was higher in the wheat season.

3.2.3 Types of NIs

Different types of NIs may show different effects on N_2O emissions. In this thesis, two different common synthetic NIs were tested (DMPP and PIADIN®), and both of them showed high N_2O mitigation effectiveness (**Paper II-IV**). However, as the experimental conditions were not the same, it is not possible to directly compare the two NIs. For the two most popular NIs, DCD and DMPP, nevertheless, results described in the literature are contradictory with respect to the mitigation effect on N_2O emissions. For instance, in a 3-year field experiment in a summer barley, maize and winter wheat cropping system, DMPP led on average to a 49% decrease in N_2O release, while DCD decreased N_2O release on average by 26% (Weiske et al., 2001). In contrast, several authors reported that no significant differences in N_2O emissions were found between DCD and DMPP under field conditions (Di and Cameron, 2012; Liu et al., 2013; Soares et al., 2015). Subbarao et al. (2006) pointed out that the mobility of DCD in soil was higher than that of NH_4^+, whereas the relative mobility of DMPP is about the same as NH_4^+, which may make DMPP more effective than DCD. However, Marsden et al. (2016) found that the mobility of DCD and DMPP were similar in soils. In a meta-analysis, Gilsanz et al. (2016) found that DCD exhibited the greater N_2O inhibitory effect in grassland, while DMPP had a greater effect in cropland.

Besides the synthetic NIs, there is type of nature-based NIs, which is named Natural Nitrification Inhibitors (NNIs). It has been found that the seedcake of neem (*Azadirachta indica L.*), a tree from India, could inhibit nitrification (Reddy and Prasad, 1975). A laboratory study showed that neem seedcake amended with urea inhibited 54% nitrification (Abbasi et al., 2011). Patra et al. (2002) reported that the use of two NNIs (Nimin and Mentha spicata) significantly increased fertilizer N use efficiency, and both of them were as effective as DCD. Natural NIs are relatively cheap, compared with synthetic NIs, as they originate from various types of plants and crops. However, the lack of research and product development, the difficulties in the extraction and purification of these compounds make NNIs hard to put into

practice. They were therefore not investigated in this thesis; nevertheless, other alternative N_2O mitigation strategies based on nitrification inhibition (i.e. biochar, urease inhibitor and hippuric acid addition, see section 3.6) were tested.

3.3 Effect of NIs on soil microbes

The study by O'Callaghan et al. (2010) showed that AOB were significantly affected by DCD with reductions in population size and reduced activity. Similarly, DMPP application was found to significantly inhibit the growth of AOB (Di and Cameron, 2011; Li et al., 2008). In **Paper II** the addition of the NI PIADIN was found to delay the emergence of the AOB *amoA* gene abundance peak. However, in the latter phases of the incubation period AOB *amoA* gene abundance was even higher in the NI addition treatments. No significant trend was found for AOA neither in this study nor in the literature, perhaps because AOA growth could be inhibited by high soil N content (Di et al., 2009).

On the other hand, results described in the literature are contradictory with respect to the effect of NIs on no-target microorganism. For instance, Patra et al. (2006) reported a significant reduction of the total number of bacteria after DCD addition under lab condition. Maienza et al. (2014) reported that DMPP addition significantly affected the microbial community structure and reduced fungal growth. In contrast, O'Callaghan et al. (2010) found that the DCD had little impact on the overall soil bacterial activity. So far, there are very few studies about long-term influence of NI addition on soil microorganisms. Only two relatively long-term (seven years) NI application experiments were found. Guo et al. (2013) reported that seven years of DCD application did not significantly affect microbial population abundance and enzymatic activities. Similarly, Dong et al. (2013) found that seven years of – DMPP application to a cambisol in northeast China had little impact on the total abundance of soil bacteria.

3.4 Effect of NIs on denitrification and nitrifier denitrification

The last step of denitrification, i.e. the reduction of N_2O to N_2, has been studied to understand the denitrification process and to establish N_2O mitigation strategies (Senbayram et al., 2012). However, direct measurements of N_2 production via denitrification in soils are challenging due to the high atmospheric N_2 background, especially *in situ* in the field (see **Paper I**). Meanwhile, most indirect methods targeting N_2 production are afflicted with artifacts. For instance, the acetylene inhibition technique, which is still commonly used in many studies, could create a systematic and irreproducible underestimation of N_2 production (Butterbach-Bahl et al., 2013).

The ratio of N_2O to N_2, often used as $N_2O/(N_2O+N_2)$ ratio, can be highly influenced by NO_3^- concentration, available C and O_2 availability in soil (Senbayram et al., 2012; Wu et al., 2017). The $N_2O/(N_2O+N_2)$ ratio increases with increasing NO_3^- concentration and decreasing available C content (Blackmer and Bremner, 1978; Senbayram et al., 2012). It has been suggested that application of NI would decrease $N_2O/(N_2O+N_2)$ ratio by limiting the NO_3^- supply to the soil microsites **(Paper II)**. The lower NO_3^- concentration and available C would therefore decrease the $N_2O/(N_2+N_2O)$ ratio due to the competitive effect of NO_3^- and N_2O as terminal electron acceptors during denitrification **(Paper II and III)**. In an incubation experiment conducted under anoxic conditions, Hatch et al. (2005) found that in two slurry treatments with NIs (DCD and DMPP) N_2 emissions were significantly increased, and $N_2O/(N_2+N_2O)$ ratios were reduced, when compared with the slurry-only treatment. In **paper III**, it was observed that the application of NI increased N_2 production and decreased the $N_2O/(N_2+N_2O)$ ratio. To the best of our knowledge, this is the first time that an alteration of the ratio was observed at oxic incubation conditions.

The potential inhibition effect of NI on nitrifier denitrification has been long time neglected in the field studies. In **paper IV** NI significantly reduced N_2O emissions at high soil moisture conditions in the North China Plain. According to N_2O isotopomer data, nitrifier denitrification is believed to be a main source for N_2O emissions. The NI's efficient mitigation effect on N_2O was assumed attributed to the NI's dual inhibition effect on nitrifier denitrification, i.e., 1) decreasing the substrate of nitrifier denitrification and 2) inhibiting the bacterial that performs nitrifier denitrification. However, studies are needed to further clarify the contribution of nitrifier denitrification on N_2O emissions in the field.

3.5 Effect of NIs on soil oxygen availability

The nitrification process requires oxic conditions for NH_4^+ oxidation, while denitrification as an anaerobic process only occurs at low O_2 partial pressure (Bollmann and Conrad, 1998). The low availability of O_2 evolves either because of high moisture content, or because of high biological O_2 consumption. By using a novel O_2 optode approach, Zhu et al. (2015) found that anoxia rapidly developed due to nitrification after manure addition to soil, and N_2O emission rates increased exponentially after anoxia had developed. In theory, by inhibiting nitrification, NI could therefore decrease O_2 consumption in soil microsites, consequently decrease denitrification rate and N_2O emission. This was further examined by **Paper VII**, with the combination of the O_2 planar optode technique to visualize soil O_2 dynamics and isotopomer technique to trace the sources of emitted N_2O. The application of DMPP was indeed found to reduce the extent of the O_2 depletion zone and altered the sources of N_2O emissions, presumably by interrupting O_2 consumption via inhibiting nitrification. The higher mitigation effect of NI on N_2O emissions with straw addition than without straw could also be partly attributed to the increase of O_2 availability with NI addition **(Paper II)**.

3.6 Alternative approach for N_2O mitigation

In this thesis, three further alternative strategies for reducing soil-emitted N_2O emissions were evaluated in order to compare the effectiveness and reliability with NI addition, including i) biochar amendment with $(NH_4)_2SO_4$, ii) urease inhibitor addition with urea, and iii) hippuric acid addition with artificial urine. According to our studies, the N_2O mitigation effect of biochar largely varied with soil and biochar type (**Paper V**), while the urease inhibitor showed less N_2O mitigation effectiveness as compared with the NI, and even a negative effect when used together with the NI (**Paper VIII**). Furthermore, hippuric acid addition showed no mitigation effect on N_2O emission in the field study when combined with artificial urine **(Paper XI)**. In general, it can be concluded that these alternative approaches showed less N_2O mitigation potential when compared with NI application. A detailed discussion follows below.

3.6.1 Biochar addition

Biochar, which is obtained from the thermochemical conversion of biomass, has been frequently reported to be an effective solution to mitigate greenhouse gas (GHG) emissions, (Cayuela et al., 2014; Lehmann and Joseph, 2009; Yanai et al., 2007). Besides the carbon sequestration potential, in recent years biochar amendment has been frequently reported to reduce N_2O emissions from soils (Chang et al., 2016; Subedi et al., 2016; Yanai et al., 2007). In a meta-analysis based on 30 studies, Cayuela et al. (2014) reported that biochar reduced soil N_2O emissions by 54% in both laboratory and field studies. However, the suppressing effect varies among different kinds of biochar and different soil types (Clough et al., 2010; Taghizadeh-Toosi et al., 2011). Steinbeiss et al. (2009) found that the type of biochar, instead of soil type, is the main driver for all the differences in gas emissions and microbial community. However, in the incubation experiment comparing the influence of different types of biochar on CO_2 and N_2O emissions in different soil types, it was found that the N_2O mitigation effect highly depended on not only biochar type, but also on soil type **(Paper**

V). The underlying mechanisms of the influence of biochar on N_2O production and consumption are still unclear. Several different hypotheses have been proposed, such as the increase in soil aeration status and soil pH, absorption of soil N, and modification of soil microorganism that are involved in N cycle processes (Cayuela et al., 2013; Lehmann et al., 2011; Ouyang et al., 2014).

3.6.2 Urease inhibitor addition

Urease inhibitors (UIs), such as N-(n-butyl) thiophosphoric triamide (NBPT), can regulate the transformation of amide N ($R\text{-}NH_2$) in urea-based fertilizers and urine to ammonium (NH_4^+) ions and slow down urea hydrolysis (Singh et al., 2013). NBPT, when applied with NH_3-based fertilizers, has been found to be able to significantly reduce N_2O emissions and decrease NH_3 emission (Dawar et al., 2011; Singh et al., 2013). Therefore, the combination of NI and UI application might be an effective strategy in reducing N_2O emission. In the study of Ding et al. (2010), NBPT + DCD treatment showed the maximum N_2O mitigation effect when applied with urea as compared with the treatments with NBPT or DCD alone. However, in a meta-analysis study UIs were found not to be effective in reducing N_2O (Akiyama et al., 2010). In **Paper VII** the NBPT application even decreased the mitigation effect of DMPP when mixed together with urea, probably due to some unknown reactions between NBPT and DMPP during mixing. Therefore, the effectiveness of UIs on mitigating N_2O emissions should be further investigated, especially when mixed with NIs.

3.6.3 Hippuric acid addition

Hippuric acid (HA) is a constituent of ruminant urine. In vitro, HA has been shown to reduce N_2O emissions from soil presumably due to the presence of benzoic acid, a break-down product, which has been proven to have antimicrobial activity in acidic media (Bertram et al. 2009). As a result of this antimicrobial activity, the nitrification process is thought to be

inhibited resulting in reduced N_2O emissions. In addition, the concentration of HA in urine has been reported to have a controlling effect on both the hydrolysis of urine-N and on NH_3 volatilization, and thus it may further influence N_2O emission factors by altering substrate supply for microbial mechanisms of N_2O production (van Groenigen et al., 2005). However, in **Paper X**, the N_2O emissions in grasslands were not affected by the addition of different concentrations of HA when applied with artificial urine, indicating that more studies are needed before the practical use of HA for mitigating N_2O emissions in the field can be recommended.

4. Conclusions

This PhD study has investigated the effect of NIs on N_2O emissions when amended with mineral N fertilizers under different soil conditions. In addition, several different pathways for N_2O production in soil were identified to illustrate the mechanisms of the inhibition effect (Fig. 4). Based on our study, the following conclusions can be drawn:

1. The N_2O isotopomer approach proved to be a useful tool to trace sources and pathways of N_2O production and consumption in soils. However, using a fixed fractionation factor may overestimate the N_2O reduction effect on SP values and result in erroneous source partitioning.

2. NI application with mineral N fertilizer was shown to effectively reduce N_2O emissions in both wet and dry soil conditions. Furthermore, NI increased N_2 production and affected the product stoichiometry of denitrification at oxic conditions. The high NI effectiveness under conditions favouring denitrification was likely attributed to the indirect impact of NI on denitrification.

3. In field studies, NI significantly mitigated N_2O emission when compared to urea added alone in a whole winter wheat/summer maize rotation in the North China Plain. The high

effectiveness of NI on mitigating N_2O emission at high soil moisture may be attributed to the NI's dual inhibition effect on nitrifier denitrification, which suggests that NIs can be used as an effective management option to mitigate N_2O emissions in the North China Plain.

4. Alternative N_2O mitigation approaches, such as addition of urease inhibitors and biochar, showed the potential for reducing N_2O emissions, but large variations and uncertainties were observed; therefore more investigations are needed before these strategies can be widely used as reliable and effective mitigation strategy.

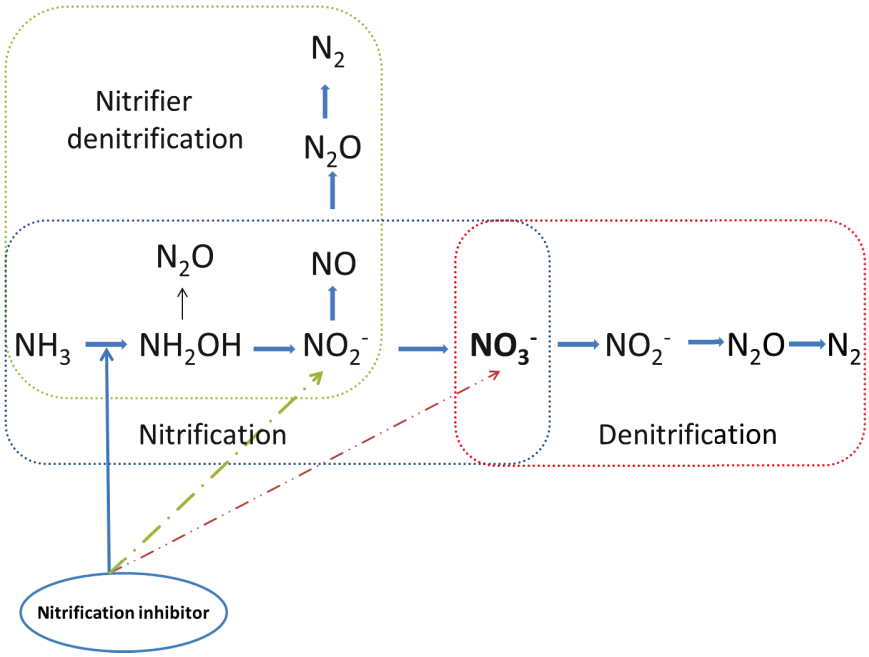

Figure 4. The direct (solid arrow) and indirect effects (dash-dot arrows) of nitrification inhibitors on N_2O production and consumption pathways in soils.

Overall, this thesis provided evidence from both laboratory and field experiments that application of NIs can be used as an effective and reliable management strategy to mitigate N_2O emissions in soils not only under soil conditions favouring nitrification, but also ín situations when soil denitrification/nitrifier denitrification potential is high, e.g. N-fertilized

and straw-amended moist soils. This high mitigation effectiveness in latter situations is likely due to the indirect inhibition effect of NIs on N_2O produced by denitrification and nitrifier denitrification (Fig. 4). Better understanding of these controlling factors is important for making decisions about where and when NIs should be used to minimalize the environmental impact caused by N fertilizer application in agricultural systems.

5. Perspectives

Due to the complexity of N_2O production/consumption pathways and high variability of N_2O emission patterns, source-partitioning of N_2O emitted from soils is methodologically challenging. The N_2O stable isotope and isotopomer approaches can be very useful tools to trace sources and pathways of N_2O production and consumption in soils. However, several obstacles have to be overcome before it can be used as a truly reliable method to help quantifying N_2O emissions and constraining the global N_2O budget in large scales (see General discussion). The most commonly used technique in this thesis for N_2O isotopic measurements is laboratory-based isotope-ratio mass-spectrometry (IRMS) in combination with flask-sampling. Compared to IRMS method used in this thesis, recently developed spectroscopic techniques, like quantum cascade laser absorption spectroscopy (QCLAS), have shown several advantages in terms of precision and throughput (Köster et al., 2013). Most importantly, QCLAS has enabled real-time analysis of N_2O isotope signatures at least in laboratory studies (e.g. Heil et al., 2014), indicating that the isotopomer approach can be a more powerful and effective method for future studies (Mohn et al., 2012).

Nitrification inhibitors have been studied for more than 50 years, and their effectiveness on mitigating N_2O emissions has been well recognized (Ruser and Schulz, 2015). However, the underlying mechanisms that affect the NI mitigation effectiveness are still poorly understood,

even under well-controlled laboratory conditions. In this PhD thesis several important pathways that help understanding N_2O mitigation effectiveness of NI have been identified. Nevertheless, further research is still needed in both laboratory and field studies, especially for identifying the contribution of nitrifier denitrification, which has long been neglected due to methodological constraints.

As NIs could keep nitrogen in the form of NH_4^+ instead of NO_3^- for a longer time in soil, their application might also cause an increase in NH_3 volatilization. Several literature reviews and meta-analysis studies indicated that NI application could increase NH_3 volatilization (Kim et al., 2012; Lam et al., 2017). However, it should be noted that most of the NIs investigated in those studies were DCD. On the contrary, several studies using DMPP found that NI had no effect, or even a mitigation effect on NH_3 volatilization (Li et al., 2008; Menéndez et al., 2006; Wissemeier et al., 2001). In this PhD study, the effect of NIs on NH_3 volatilization was not evaluated due to limited labor resources and methodological constraints. Nevertheless, it is suggested that the effect of NIs on NH_3 volatilization should be investigated in further studies; otherwise the beneficial effect of NIs in decreasing direct N_2O emissions might be overestimated by neglecting an increase in NH_3 volatilization.

The commercially used NIs (e.g. Nitrapyrin, DCD, DMPP) have proved to be non-toxic and both environmentally and ecologically safe (Tindaon et al., 2012; Zerulla et al., 2001). Nevertheless, some worries have been raised in respect of the food safety issue. For example, in year 2013 DCD residues were detected in commercial milk products in New Zealand, and thus led to a debate about safety issues related to the use of NI, with the result of suspending the use of DCD in New Zealand's grazed grasslands. This fact indicates that the over-application of NIs should be treated with more caution, especially when applied in grazed grassland.

It has been known that certain plants can suppress soil nitrification through the release of nitrification inhibitors from their roots, which is a phenomenon termed "biological nitrification inhibition (BNI) (Subbarao et al., 2007). BNI capacity appears to be relatively widespread among a tropical pasture plants with *Brachiaria* spp. (Subbarao et al., 2009). The new understanding of BNI might be used in both genetic and crop system management approaches in agriculture systems, which could also expand the research area of NIs in the future.

6. References

Abbasi, M.K., Hina, M., Tahir, M.M., 2011. Effect of Azadirachta indica (neem), sodium thiosulphate and calcium chloride on changes in nitrogen transformations and inhibition of nitrification in soil incubated under laboratory conditions. Chemosphere 82, 1629–1635.

Akiyama, H., Yan, X., Yagi, K., 2010. Evaluation of effectiveness of enhanced‐efficiency fertilizers as mitigation options for N_2O and NO emissions from agricultural soils: meta‐analysis. Global Change Biology 16, 1837–1846.

Amberger, A., 1989. Research on dicyandiamide as a nitrification inhibitor and future outlook. Communications in Soil Science and Plant Analysis 20, 1933–1955.

Arp, D.J., Sayavedra-Soto, L.A., Hommes, N.G., 2002. Molecular biology and biochemistry of ammonia oxidation by Nitrosomonas europaea. Archives of Microbiology 178, 250–255.

Baggs, E.M., 2011. Soil microbial sources of nitrous oxide: recent advances in knowledge, emerging challenges and future direction. Current Opinion in Environmental Sustainability 3, 321–327.

Barneze, A.S., Minet, E.P., Cerri, C.C., Misselbrook, T., 2015. The effect of nitrification inhibitors on nitrous oxide emissions from cattle urine depositions to grassland under summer conditions in the UK. Chemosphere 119, 122–129.

Barth, G., Von Tucher, S., Schmidhalter, U., 2008. Effectiveness of 3,4-Dimethylpyrazole Phosphate as Nitriflcation Inhibitor in Soil as Influenced by Inhibitor Concentration, Application Form, and Soil Matric Potential. Pedosphere 18, 378–385.

Bertram, J.E., Clough, T.J., Sherlock, R.R., Condron, L.M., O'callaghan, M., Wells, N.S., Ray, J.L., 2009. Hippuric acid and benzoic acid inhibition of urine derived N_2O emissions from soil. Global Change Biology 15, 2067–2077.

Blackmer, A.M., Bremner, J.M., 1978. Inhibitory effect of nitrate on reduction of N_2O to N_2 by soil microorganisms. Soil Biology and Biochemistry 10, 187–191.

Bol, R., Toyoda, S., Yamulki, S., Hawkins, J.M.B., Cardenas, L.M., Yoshida, N., 2003. Dual isotope and isotopomer ratios of N_2O emitted from a temperate grassland soil after fertiliser application. Rapid Communications in Mass Spectrometry 17, 2550–2556.

Bollmann A, Conrad R. Influence of O_2 availability on NO and N_2O release by nitrification and denitrification in soils. 1998. Global Change Biology. 4(4): 387-396.

Bouwman, A.F., Beusen, A.H.W., Griffioen, J., Groenigen, J.W.V., Hefting, M.M., Oenema, O., Puijenbroek, P.J.T.M.V., Seitzinger, S., Slomp, C.P., Stehfest, E., 2013. Global trends and uncertainties in terrestrial denitrification and N_2O emissions. Philosophical Transactions of the Royal Society of London B: Biological Sciences 368, 20130112.

Burford, J.R., Bremner, J.M., 1975. Relationships between the denitrification capacities of soils and total, water-soluble and readily decomposable soil organic matter. Soil Biology and Biochemistry 7, 389–394.

Butterbach-Bahl, K., Baggs, E.M., Dannenmann, M., Kiese, R., Zechmeister-Boltenstern, S., 2013. Nitrous oxide emissions from soils: how well do we understand the processes and their controls? Philos Trans R Soc Lond B Biol Sci 368, 20130122.

Cardenas, L.M., Hawkins, J.M.B., Chadwick, D., Scholefield, D., 2003. Biogenic gas emissions from soils measured using a new automated laboratory incubation system. Soil Biology and Biochemistry 35, 867–870.

Cayuela, M.L., Sánchez-Monedero, M.A., Roig, A., Hanley, K., Enders, A., Lehmann, J., 2013. Biochar and denitrification in soils: when, how much and why does biochar reduce N_2O emissions? Scientific Reports 3.

Cayuela, M.L., van Zwieten, L., Singh, B.P., Jeffery, S., Roig, A., Sánchez-Monedero, M.A., 2014. Biochar's role in mitigating soil nitrous oxide emissions: A review and meta-analysis. Agriculture, Ecosystems & Environment, Environmental Benefits and Risks of Biochar Application to Soil 191, 5–16.

Chadwick, D.R., Cardenas, L., Misselbrook, T.H., Smith, K.A., Rees, R.M., Watson, C.J., McGeough, K.L., Williams, J.R., Cloy, J.M., Thorman, R.E., Dhanoa, M.S., 2014. Optimizing chamber methods for measuring nitrous oxide emissions from plot-based agricultural experiments. European Journal of Soil Science 65, 295–307.

Chang, J., Clay, D.E., Clay, S.A., Chintala, R., Miller, J.M., Schumacher, T., 2016. Biochar Reduced Nitrous Oxide and Carbon Dioxide Emissions from Soil with Different Water and Temperature Cycles. Agronomy Journal 108, 2214–2221.

Ciais, P., Sabine, C., Bala, G., Bopp, L., Brovkin, V., Canadell, J., Chhabra, A., DeFries, R., Galloway, J., Heimann, M., others, 2014. Carbon and other biogeochemical cycles, in: Climate Change 2013: The Physical Science Basis. Contribution of Working Group I to the Fifth Assessment Report of the Intergovernmental Panel on Climate Change. Cambridge University Press, pp. 465–570.

Clough, T.J., Bertram, J.E., Ray, J.L., Condron, L.M., O'Callaghan, M., Sherlock, R.R., Wells, N.S., 2010. Unweathered Wood Biochar Impact on Nitrous Oxide Emissions from a Bovine-Urine-Amended Pasture Soil. Soil Science Society of America Journal 74, 852.

Cui, M., Sun, X.C., Hu, C.X., Di, H.J., Tan, Q.L., Zhao, C.S., 2011. Effective mitigation of nitrate leaching and nitrous oxide emissions in intensive vegetable production systems using a nitrification inhibitor, dicyandiamide. Journal of Soils and Sediments 11, 722–730.

Davidson, E.A., Keller, M., Erickson, H.E., Verchot, L.V., Veldkamp, E., 2000. Testing a Conceptual Model of Soil Emissions of Nitrous and Nitric Oxides Using two functions based on soil nitrogen availability and soil water content, the hole-in-the-pipe model characterizes a large fraction of the observed variation of nitric oxide and nitrous oxide emissions from soils. BioScience 50, 667–680.

Dawar, K., Zaman, M., Rowarth, J.S., Blennerhassett, J., Turnbull, M.H., 2011. Urea hydrolysis and lateral and vertical movement in the soil: effects of urease inhibitor and irrigation. Biology and Fertility of Soils 47, 139–146.

Decock, C., Six, J., 2013. How reliable is the intramolecular distribution of ^{15}N in N_2O to source partition N_2O emitted from soil? Soil Biology and Biochemistry 65, 114–127.

Dell, C.J., Han, K., Bryant, R.B., Schmidt, J.P., 2014. Nitrous Oxide Emissions with Enhanced Nitrogen Fertilizers in a Rainfed System. Agronomy Journal 106, 723–731.

Delwiche, C.C., Rolston, D.E., 1976. Measurement of small nitrous oxide concentrations by gas chromatography. Soil Sci. Soc. Am. J 40.

Di, H.J., Cameron, K.C., Podolyan, A., Robinson, A., 2014. Effect of soil moisture status and a nitrification inhibitor, dicyandiamide, on ammonia oxidizer and denitrifier growth and nitrous oxide emissions in a grassland soil. Soil Biology and Biochemistry 73, 59–68.

Di, H.J., Cameron, K.C., 2012. How does the application of different nitrification inhibitors affect nitrous oxide emissions and nitrate leaching from cow urine in grazed pastures? Soil Use and Management 28, 54–61.

Di, H.J., Cameron, K.C., 2011. Inhibition of ammonium oxidation by a liquid formulation of 3,4-Dimethylpyrazole phosphate (DMPP) compared with a dicyandiamide (DCD) solution in six new Zealand grazed grassland soils. Journal of Soils and Sediments 11, 1032–1039.

Di, H.J., Cameron, K.C., Sherlock, R.R., 2007. Comparison of the effectiveness of a nitrification inhibitor, dicyandiamide, in reducing nitrous oxide emissions in four different soils under different climatic and management conditions. Soil Use and Management 23, 1–9.

Ding, W.X., Yu, H.Y., Cai, Z.C., 2010. Impact of urease and nitrification inhibitors on nitrous oxide emissions from fluvo-aquic soil in the North China Plain. Biology and Fertility of Soils 47, 91–99.

Dittert, K., Bol, R., King, R., Chadwick, D., Hatch, D., 2001. Use of a novel nitrification inhibitor to reduce nitrous oxide emission from ^{15}N-labelled dairy slurry injected into soil. Rapid Commun Mass Spectrom 15, 1291–1296.

Dong, X.X., Zhang, L.L., Wu, Z.J., Li, D.P., Shang, Z.C., Gong, P., 2013. Effects of the nitrification inhibitor DMPP on soil bacterial community in a Cambisol in northeast China. Journal of Soil Science and Plant Nutrition 13, 580–591.

Federolf, C.-P., Westerschulte, M., Olfs, H.-W., Broll, G., Trautz, D., 2016. Enhanced nutrient use efficiencies from liquid manure by positioned injection in maize cropping in northwest Germany. European Journal of Agronomy 75, 130–138.

Galloway, J.N., Dentener, F.J., Capone, D.G., Boyer, E.W., Howarth, R.W., Seitzinger, S.P., Asner, G.P., Cleveland, C.C., Green, P.A., Holland, E.A., Karl, D.M., Michaels, A.F., Porter, J.H., Townsend, A.R., Vöosmarty, C.J., 2004. Nitrogen Cycles: Past, Present, and Future. Biogeochemistry 70, 153–226.

Gilsanz, C., Báez, D., Misselbrook, T.H., Dhanoa, M.S., Cárdenas, L.M., 2016. Development of emission factors and efficiency of two nitrification inhibitors, DCD and DMPP. Agriculture, Ecosystems & Environment 216, 1–8.

Guo, Y.J., Di, H.J., Cameron, K.C., Li, B., Podolyan, A., Moir, J.L., Monaghan, R.M., Smith, L.C., O'Callaghan, M., Bowatte, S., 2013. Effect of 7-year application of a nitrification inhibitor, dicyandiamide (DCD), on soil microbial biomass, protease and deaminase activities, and the abundance of bacteria and archaea in pasture soils. Journal of Soils and Sediments 13, 1–7.

Hatch, D., Trindade, H., Cardenas, L., Carneiro, J., Hawkins, J., Scholefield, D., Chadwick, D., 2005. Laboratory study of the effects of two nitrification inhibitors on greenhouse gas emissions from a slurry-treated arable soil: impact of diurnal temperature cycle. Biology and Fertility of Soils 41, 225–232.

Heil J, Wolf B, Brüggemann N, Emmenegger L, Tuzson B, Vereecken H, Mohn J, 2014. Site-specific ^{15}N isotopic signatures of abiotically produced N_2O. *Geochimica et Cosmochimica Acta* 139, 72–82.

Heil, J., Liu, S., Vereecken, H., Brüggemann, N., 2015. Abiotic nitrous oxide production from hydroxylamine in soils and their dependence on soil properties. Soil Biology and Biochemistry 84, 107–115.

Hensen, A., Skiba, U., Famulari, D., 2013. Low cost and state of the art methods to measure nitrous oxide emissions. Environmental Research Letters 8, 025022.

Hooper, A.B., 1968. A nitrite-reducing enzyme from Nitrosomonas europaea Preliminary characterization with hydroxylamine as electron donor. Biochimica et Biophysica Acta (BBA) - Bioenergetics 162, 49–65.

Huber, D.M., Warren, H.L., Nelson, D.W., Tsai, C.Y., 1977. Nitrification Inhibitors—New Tools for Food Production. BioScience 27, 523–529.

IPCC, 2013. Annex II: Climate System Scenario Tables, in: Climate Change 2013: The Physical Science Basis. Contribution of Working Group I to the Fifth Assessment Report of the Intergovernmental Panel on Climate Change. Cambridge University Press, Cambridge, United Kingdom and New York, NY, USA.

Irigoyen, I., Muro, J., Azpilikueta, M., Aparicio-Tejo, P., Lamsfus, and C., Irigoyen, I., Muro, J., Azpilikueta, M., Aparicio-Tejo, P., Lamsfus, and C., 2003. Ammonium oxidation kinetics in the presence of nitrification inhibitors DCD and DMPP at various temperatures, Ammonium oxidation kinetics in the presence of nitrification inhibitors DCD and DMPP at various temperatures. Soil Research, Soil Research 41, 1177–1183.

Kaiser, J., Röckmann, T., Brenninkmeijer, C.A.M., 2003. Complete and accurate mass spectrometric isotope analysis of tropospheric nitrous oxide. Journal of Geophysical Research: Atmospheres 108, 4476.

Kelliher, F.M., Clough, T.J., Clark, H., Rys, G., Sedcole, J.R., 2008. The temperature dependence of dicyandiamide (DCD) degradation in soils: A data synthesis. Soil Biology and Biochemistry 40, 1878–1882.

Kim, D.G., Saggar, S., Roudier, P., 2012. The effect of nitrification inhibitors on soil ammonia emissions in nitrogen managed soils: a meta-analysis. Nutrient Cycling in Agroecosystems 93, 51–64.

Könneke, M., Bernhard, A.E., de la Torre, J.R., Walker, C.B., Waterbury, J.B., Stahl, D.A., 2005. Isolation of an autotrophic ammonia-oxidizing marine archaeon. Nature 437, 543–546.

Kool, D.M., Dolfing, J., Wrage, N., Van Groenigen, J.W., 2011. Nitrifier denitrification as a distinct and significant source of nitrous oxide from soil. Soil Biology and Biochemistry 43, 174–178.

Köster, J.R., Well, R., Tuzson, B., Bol, R., Dittert, K., Giesemann, A., Emmenegger, L., Manninen, A., Cárdenas, L., Mohn, J., 2013. Novel laser spectroscopic technique for continuous analysis of N_2O isotopomers – application and intercomparison with isotope ratio mass spectrometry. Rapid Communications in Mass Spectrometry 27, 216–222.

Kowalchuk, G.A., Stephen, J.R., 2001. Ammonia-Oxidizing Bacteria: A Model for Molecular Microbial Ecology. Annual Review of Microbiology 55, 485–529.

Lam, S.K., Suter, H., Mosier, A.R., Chen, D., 2017. Using nitrification inhibitors to mitigate agricultural N_2O emission: a double-edged sword? Global Change Biology 23, 485–489.

Laughlin, R.J., Stevens, R.J., 2002. Evidence for fungal dominance of denitrification and codenitrification in a grassland soil. Soil Science Society of America Journal 66, 1540–1548.

Lehmann, J., Joseph, S., 2009. Biochar for environmental management: An introduction. Biochar for Environmental Management: Science and Technology 1–12.

Lehmann, J., Rillig, M.C., Thies, J., Masiello, C.A., Hockaday, W.C., Crowley, D., 2011. Biochar effects on soil biota – A review. Soil Biology and Biochemistry, 19th International Symposium on Environmental Biogeochemistry 43, 1812–1836.

Li, H., Liang, X., Chen, Y., Lian, Y., Tian, G., Ni, W., 2008. Effect of nitrification inhibitor DMPP on nitrogen leaching, nitrifying organisms, and enzyme activities in a rice-oilseed rape cropping system. Journal of Environmental Sciences 20, 149–55.

Liu, C., Wang, K., Zheng, X., 2013. Effects of nitrification inhibitors (DCD and DMPP) on nitrous oxide emission, crop yield and nitrogen uptake in a wheat-maize cropping system. Biogeosciences 10, 2427–2437.

Liu, S., Herbst, M., Bol, R., Gottselig, N., Pütz, T., Weymann, D., Wiekenkamp, I., Vereecken, H., Brüggemann, N., 2016. The contribution of hydroxylamine content to spatial variability of N_2O formation in soil of a Norway spruce forest. Geochimica et Cosmochimica Acta 178, 76–86.

Loecke, T.D., Robertson, G.P., 2009. Soil resource heterogeneity in terms of litter aggregation promotes nitrous oxide fluxes and slows decomposition. Soil Biology and Biochemistry 41, 228–235.

Loick, N., Dixon, E.R., Abalos, D., Vallejo, A., Matthews, G.P., McGeough, K.L., Well, R., Watson, C.J., Laughlin, R.J., Cardenas, L.M., 2016. Denitrification as a source of nitric oxide emissions from incubated soil cores from a UK grassland soil. Soil Biology and Biochemistry 95, 1–7.

Maienza, A., Bååth, E., Stazi, S.R., Benedetti, A., Grego, S., Dell'Abate, M.T., 2014. Microbial dynamics after adding bovine manure effluent together with a nitrification inhibitor (3,4 DMPP) in a microcosm experiment. Biology and Fertility of Soils 50, 869–877.

Marsden, K.A., Marín-Martínez, A.J., Vallejo, A., Hill, P.W., Jones, D.L., Chadwick, D.R., 2016. The mobility of nitrification inhibitors under simulated ruminant urine deposition and rainfall: a comparison between DCD and DMPP. Biology and Fertility of Soils 52, 491–503.

McCarty, G. W., Bremner, J. M., 1989. Laboratory Evaluation of Dicyandiamide as a Soil Nitrification Inhibitor. Communications in Soil Science and Plant Analysis 20, 2049-2065.

McCarty, G.W., 1999. Modes of action of nitrification inhibitors. Biology and Fertility of Soils 29, 1–9.

Menendez, S., Barrena, I., Setien, I., Gonzalez-Murua, C., Estavillo, J.M., 2012. Efficiency of nitrification inhibitor DMPP to reduce nitrous oxide emissions under different temperature and moisture conditions. Soil Biology & Biochemistry 53, 82–89.

Menéndez, S., Merino, P., Pinto, M., González-Murua, C., Estavillo, J.M., 2006. 3,4-Dimethylpyrazol Phosphate Effect on Nitrous Oxide, Nitric Oxide, Ammonia, and Carbon Dioxide Emissions from Grasslands. Journal of Environment Quality 35, 973.

Meng, L., Ding, W., Cai, Z., 2005. Long-term application of organic manure and nitrogen fertilizer on N_2O emissions, soil quality and crop production in a sandy loam soil. Soil Biology and Biochemistry 37, 2037–2045.

Mohn, J., Tuzson, B., Manninen, A., Yoshida, N., Toyoda, S., Brand, W.A., Emmenegger, L., 2012. Site selective real-time measurements of atmospheric N_2O isotopomers by laser spectroscopy. Atmospheric Measurement Techniques 5, 1601–1609.

O'Callaghan, M., Gerard, E.M., Carter, P.E., Lardner, R., Sarathchandra, U., Burch, G., Ghani, A., Bell, N., 2010. Effect of the nitrification inhibitor dicyandiamide (DCD) on microbial communities in a pasture soil amended with bovine urine. Soil Biology & Biochemistry 42, 1425–1436.

Ostrom, N.E., Pitt, A., Sutka, R., Ostrom, P.H., Grandy, A.S., Huizinga, K.M., Robertson, G.P., 2007. Isotopologue effects during N_2O reduction in soils and in pure cultures of denitrifiers. Journal of Geophysical Research: Biogeosciences (2005–2012) 112.

Ouyang, L., Tang, Q., Yu, L., Zhang, R., 2014. Effects of amendment of different biochars on soil enzyme activities related to carbon mineralisation. Soil Research 52, 706–716.

Park, S., Pérez, T., Boering, K.A., Trumbore, S.E., Gil, J., Marquina, S., Tyler, S.C., 2011. Can N_2O stable isotopes and isotopomers be useful tools to characterize sources and microbial pathways of N_2O production and consumption in tropical soils? Global Biogeochemical Cycles 25.

Parkin, T.B., Hatfield, J.L., 2010. Influence of nitrapyrin on N_2O losses from soil receiving fall-applied anhydrous ammonia. Agriculture Ecosystems & Environment 136, 81–86.

Patra, D. D., Anwar, M., Chand, S., Kiran, U., Rajput, D. K., and Kumar, S. (2002). Nimin and Mentha spicata oil as nitrification inhibitors for optimum yield of Japanese mint. *Communications in Soil Science and Plant Analysis* 33, 451-460.

Pfab, H., Palmer, I., Buegger, F., Fiedler, S., Muller, T., Ruser, R., 2012. Influence of a nitrification inhibitor and of placed N-fertilization on N_2O fluxes from a vegetable cropped loamy soil. Agriculture Ecosystems & Environment 150, 91–101.

Prasad, R., Power, J., 1995. Nitrification inhibitors for agriculture, health, and the environment. Advances in Agronomy (USA).

Qiao, C., Liu, L., Hu, S., Compton, J.E., Greaver, T.L., Li, Q., 2015. How inhibiting nitrification affects nitrogen cycle and reduces environmental impacts of anthropogenic nitrogen input. Global Change Biology 21, 1249–1257.

Ravishankara, A.R., Daniel, J.S., Portmann, R.W., 2009. Nitrous oxide (N_2O): the dominant ozone-depleting substance emitted in the 21st century. Science 326, 123–125.

Reddy, R.N.S., Prasad, R., 1975. Studies on the Mineralization of Urea, Coated Urea, and Nitrification Inhibitor Treated Urea in Soil. Journal of Soil Science 26, 304–312.

Rochette, P., Eriksen-Hamel, N.S., 2008. Chamber Measurements of Soil Nitrous Oxide Flux: Are Absolute Values Reliable? Soil Science Society of America Journal 72, 331–342.

Rohe, L., Anderson, T.-H., Braker, G., Flessa, H., Giesemann, A., Lewicka‐Szczebak, D., Wrage‐Mönnig, N., Well, R., 2014. Dual isotope and isotopomer signatures of nitrous oxide from fungal denitrification–a pure culture study. Rapid Communications in Mass Spectrometry 28, 1893–1903.

Ruser, R., Schulz, R., 2015. The effect of nitrification inhibitors on the nitrous oxide (N_2O) release from agricultural soils-a review. Journal of Plant Nutrition and Soil Science 178, 171-188.

Senbayram, M., Chen, R., Budai, A., Bakken, L., Dittert, K., 2012. N_2O emission and the $N_2O/(N_2O+N_2)$ product ratio of denitrification as controlled by available carbon substrates and nitrate concentrations. Agriculture, Ecosystems & Environment 147, 4–12.

Shoun, H., Fushinobu, S., Jiang, L., Kim, S.-W., Wakagi, T., 2012. Fungal denitrification and nitric oxide reductase cytochrome P450nor. Philosophical Transactions of the Royal Society B: Biological Sciences 367, 1186–1194

Singh, J., Kunhikrishnan, A., Bolan, N.S., Saggar, S., 2013. Impact of urease inhibitor on ammonia and nitrous oxide emissions from temperate pasture soil cores receiving urea fertilizer and cattle urine. Science of The Total Environment, Soil as a Source & Sink for Greenhouse Gases 465, 56–63.

Slangen, J., and Kerkhoff, P., 1984. Nitrification inhibitors in agriculture and horticulture: A literature review. Fertilizer Research 5, 1-76.

Soares, J.R., Cantarella, H., Vargas, V.P., Carmo, J.B., Martins, A.A., Sousa, R.M., Andrade, C.A., 2015. Enhanced-Efficiency Fertilizers in Nitrous Oxide Emissions from Urea Applied to Sugarcane. Journal of Environmental Quality 44, 423–430.

Steinbeiss, S., Gleixner, G., Antonietti, M., 2009. Effect of biochar amendment on soil carbon balance and soil microbial activity. Soil Biology and Biochemistry 41, 1301–1310.

Subbarao, G.V., Ito, O., Sahrawat, K.L., Berry, W.L., Nakahara, K., Ishikawa, T., Watanabe, T., Suenaga, K., Rondon, M., Rao, I.M., 2006. Scope and strategies for regulation of nitrification in agricultural systems—challenges and opportunities. Critical Reviews in Plant Sciences 25, 303–335.

Subbarao, G.V., Nakahara, K., Hurtado, M.P., Ono, H., Moreta, D.E., Salcedo, A.F., Yoshihashi, A.T., Ishikawa, T., Ishitani, M., Ohnishi-Kameyama, M., Yoshida, M., Rondon, M., Rao, I.M.,

Lascano, C.E., Berry, W.L., Ito, O., 2009. Evidence for biological nitrification inhibition in Brachiaria pastures. Proceedings of the National Academy of Sciences of the United States of America 106, 17302–17307.

Subbarao, G.V., Tomohiro, B., Masahiro, K., Osamu, I., Samejima, H., Wang, H.Y., Pearse, S.J., Gopalakrishnan, S., Nakahara, K., Hossain, A., Tsujimoto, H., Berry, W.L., 2007. Can biological nitrification inhibition (BNI) genes from perennial Leymus racemosus (Triticeae) combat nitrification in wheat farming? Plant and Soil 299, 55–64.

Subedi, R., Taupe, N., Pelissetti, S., Petruzzelli, L., Bertora, C., Leahy, J.J., Grignani, C., 2016. Greenhouse gas emissions and soil properties following amendment with manure-derived biochars: Influence of pyrolysis temperature and feedstock type. Journal of Environmental Management 166, 73–83.

Sutka, R.L., Adams, G.C., Ostrom, N.E., Ostrom, P.H., 2008. Isotopologue fractionation during N_2O production by fungal denitrification. Rapid Communications in Mass Spectrometry 22, 3989–3996.

Sutka, R.L., Ostrom, N.E., Ostrom, P.H., Breznak, J.A., Gandhi, H., Pitt, A.J., Li, F., 2006. Distinguishing nitrous oxide production from nitrification and denitrification on the basis of isotopomer abundances. Applied and Environmental Microbiology 72, 638–644.

Sutton, M.A., Howard, C.M., Erisman, J.W., Billen, G., Bleeker, A., Grennfelt, P., van Grinsven, H., Grizzetti, B., 2011. The European nitrogen assessment: sources, effects and policy perspectives. Cambridge University Press.

Taghizadeh-Toosi, A., Clough, T.J., Condron, L.M., Sherlock, R.R., Anderson, C.R., Craigie, R.A., 2011. Biochar Incorporation into Pasture Soil Suppresses in situ Nitrous Oxide Emissions from Ruminant Urine Patches. Journal of Environment Quality 40, 468.

Tindaon, F., Benckiser, G., Ottow, J.C.G., 2012. Evaluation of ecological doses of the nitrification inhibitors 3,4-dimethylpyrazole phosphate (DMPP) and 4-chloromethylpyrazole (ClMP) in comparison to dicyandiamide (DCD) in their effects on dehydrogenase and dimethyl sulfoxide reductase activity in soils. Biology and Fertility of Soils 48, 643–650.

Toyoda, S., Yoshida, N., Koba, K., 2015. Isotopocule analysis of biologically produced nitrous oxide in various environments. Mass Spectrometry Reviews http://dx.doi.org/10.1002/mas.21459

Treusch, A.H., Leininger, S., Kletzin, A., Schuster, S.C., Klenk, H.-P., Schleper, C., 2005. Novel genes for nitrite reductase and Amo-related proteins indicate a role of uncultivated mesophilic crenarchaeota in nitrogen cycling. Environmental Microbiology 7, 1985–1995.

van Groenigen, J.W., Kuikman, P.J., de Groot, W.J.M., Velthof, G.L., 2005. Nitrous oxide emission from urine-treated soil as influenced by urine composition and soil physical conditions. Soil Biology and Biochemistry 37, 463–473.

Weiske A, G, B., T, H., J, O., 2001. Influence of the nitrification inhibitor 3,4-dimethylpyrazole phosphate (DMPP) in comparison to dicyandiamide (DCD) on nitrous oxide emissions, carbon dioxide fluxes and methane oxidation during 3 years of repeated application in field experiments. Biology and Fertility of Soils 34, 109–117.

Well, R., Flessa, H., 2009. Isotopologue enrichment factors of N_2O reduction in soils. Rapid Communications in Mass Spectrometry 23, 2996–3002.

Wissemeier, A.H., Linzmeier, W., Gutser, R., Weigelt, W., Schmidhalter, U., 2001. The new nitrification inhibitor DMPP (ENTEC®) — Comparisons with DCD in model studies and field applications. Plant Nutrition. 702–703.

Wu, D., Köster, J.R., Cárdenas, L.M., Brüggemann, N., Lewicka-Szczebak, D., Bol, R., 2016. N_2O source partitioning in soils using ^{15}N site preference values corrected for the N_2O reduction effect. Rapid Communications in Mass Spectrometry 30, 620–626.

Wu, D., Senbayram, M., Well, R., Brüggemann, N., Pfeiffer, B., Loick, N., Stempfhuber, B., Dittert, K., Bol, R., 2017. Nitrification inhibitors mitigate N_2O emissions more effectively under straw-induced conditions favoring denitrification. Soil Biology and Biochemistry 104, 197–207.

Yanai, Y., Toyota, K., Okazaki, M., 2007. Effects of charcoal addition on N_2O emissions from soil resulting from rewetting air-dried soil in short-term laboratory experiments. Soil Science and Plant Nutrition 53, 181–188.

Zerulla, W., Barth, T., Dressel, J., Erhardt, K., Von Locquenghien, K.H., Pasda, G., Radle, M., Wissemeier, A.H., 2001.3,4-Dimethylpyrazole phosphate (DMPP) - a new nitrification inhibitor for agriculture and horticulture. Biology and Fertility of Soils 34, 79–84.

Zhang, Y., Zhang, J., Meng, T., Zhu, T., Müller, C., Cai, Z., 2013. Heterotrophic nitrification is the predominant NO_3^- production pathway in acid coniferous forest soil in subtropical China. Biology and Fertility of Soils 49, 955–957.

Zhou, M., Butterbach-Bahl, K., Vereecken, H., Brüggemann, N., 2017. A meta-analysis of soil salinization effects on nitrogen pools, cycles and fluxes in coastal ecosystems. Global Change Biology 23, 1338–1352.

Zhu, G., Wang, S., Wang, Y., Wang, C., Risgaard-Petersen, N., Jetten, M.S., Yin, C., 2011. Anaerobic ammonia oxidation in a fertilized paddy soil. The ISME Journal 5, 1905–1912.

Zhu, K., Bruun, S., Larsen, M., Glud, R.N., Jensen, L.S., 2015. Heterogeneity of O_2 dynamics in soil amended with animal manure and implications for greenhouse gas emissions. Soil Biology and Biochemistry 84, 96–106.

Zhu, T., Meng, T., Zhang, J., Yin, Y., Cai, Z., Yang, W., Zhong, W., 2013. Nitrogen mineralization, immobilization turnover, heterotrophic nitrification, and microbial groups in acid forest soils of subtropical China. Biology and Fertility of Soils 49, 323–331.

Zhu, X., Burger, M., Doane, T.A., Horwath, W.R., 2013. Ammonia oxidation pathways and nitrifier denitrification are significant sources of N_2O and NO under low oxygen availability. Proceedings of the National Academy of Sciences 110, 6328–6333.

Zhu, Z.L., Chen, D.L., 2002. Nitrogen fertilizer use in China – Contributions to food production, impacts on the environment and best management strategies. Nutrient Cycling in Agroecosystems 63, 117–127.

Acknowledgements

Firstly, I would like to acknowledge the contribution of my main supervisor Prof. Dr. Roland Bol. I am truly grateful for your support and encouragement. Secondly, I would also like to thank my co-supervisor, Prof. Dr. Nicolas Brüggemann for offering me many useful instructions and scientific knowledge. I am also thankful to Prof. Dr. Harry Vereecken, the director of the Agrosphere Institute at the Forschungszentrum Jülich, for the half-yearly

discussions and constructive suggestions. I would also like to thank Holger Wissel and Franz Leistner for the technical support, and colleagues of my workgroup, Liu Shurong and Dr. Zhou Minghua, and many other people who have helped me. Special thanks go to my office mates Katrine Wagner and Dr. Michael Stockinger, for lots of help and wonderful chat during four years.

Particularly, I would like to thank Dr. Mehmet Senbayram, for great support you have offered me in both academic and personal life during my stay in Göttingen. I would also like to thank Klaus Dittert for hosting me in Göttingen University.

I would like to thank Dr. Laura Cárdenas and Dr. Lianhai Wu in Rothamsted Research North Wyke, UK for hosting and taking care of me when I was in there, and the helps from Dr. Nadine Loick and Dr. Salvador Calvet Sanz, the research work would not have been accomplished without their efforts.

Finally, I want to thank for the support of my family and all my friends in Germany and China.

Paper I

N_2O source partitioning in soils using ^{15}N site preference values corrected for the N_2O reduction effect.

Wu, D., Köster, J.R., Cárdenas, L.M., Brüggemann, N., Lewicka-Szczebak, D., Bol, R., 2016.

Rapid Communications in Mass Spectrometry 30, 620–626.

Research Article

Rapid Communications in Mass Spectrometry

Received: 14 October 2015 Revised: 17 December 2015 Accepted: 18 December 2015 Published online in Wiley Online Library

Rapid Commun. Mass Spectrom. **2016**, *30*, 620–626
(wileyonlinelibrary.com) DOI: 10.1002/rcm.7493

N_2O source partitioning in soils using ^{15}N site preference values corrected for the N_2O reduction effect

Di Wu[1]*, Jan Reent Köster[2], Laura M. Cárdenas[3], Nicolas Brüggemann[1], Dominika Lewicka-Szczebak[4] and Roland Bol[1]

[1]Institute of Bio- and Geosciences, Agrosphere (IBG-3), Forschungszentrum Jülich GmbH, 52425 Jülich, Germany
[2]Department of Environmental Sciences, Norwegian University of Life Sciences, 1432 Ås, Norway
[3]Rothamsted Research, North Wyke, Okehampton EX20 2SB, UK
[4]Federal Research Institute for Rural Areas, Forestry and Fisheries, Thünen Institute of Climate-Smart Agriculture, Bundesallee 50, 38116Braunschweig, Germany

RATIONALE: The aim of this study was to determine the impact of isotope fractionation associated with N_2O reduction during soil denitrification on N_2O site preference (SP) values and hence quantify the potential bias on SP-based N_2O source partitioning.
METHODS: The N_2O SP values ($n = 431$) were derived from six soil incubation studies in N_2-free atmosphere, and determined by isotope ratio mass spectrometry (IRMS). The N_2 and N_2O concentrations were measured directly by gas chromatography. Net isotope effects (NIE) during N_2O reduction to N_2 were compensated for using three different approaches: a closed-system model, an open-system model and a dynamic apparent NIE function. The resulting SP values were used for N_2O source partitioning based on a two end-member isotopic mass balance.
RESULTS: The average SP_0 value, i.e. the average SP values of N_2O prior to N_2O reduction, was recalculated with the closed-system model, resulting in −2.6 ‰ (±9.5), while the open-system model and the dynamic apparent NIE model gave average SP_0 values of 2.9 ‰ (±6.3) and 1.7 ‰ (±6.3), respectively. The average source contribution of N_2O from nitrification/fungal denitrification was 18.7% (±21.0) according to the closed-system model, while the open-system model and the dynamic apparent NIE function resulted in values of 31.0% (±14.0) and 28.3% (±14.0), respectively.
CONCLUSIONS: Using a closed-system model with a fixed SP isotope effect may significantly overestimate the N_2O reduction effect on SP values, especially when N_2O reduction rates are high. This is probably due to soil inhomogeneity and can be compensated for by the application of a dynamic apparent NIE function, which takes the variable reduction rates in soil micropores into account.

Nitrous oxide (N_2O) is one of the major climate-relevant trace gases emitted as a result of anthropogenic activities. Although the atmospheric concentrations of N_2O are comparatively low, N_2O has a significant impact on the global climate, as its global warming potential (GWP) is 265 times higher than that of CO_2 when calculated over a 100-year time horizon.[1] Moreover, N_2O makes a major contribution to the destruction of the tropospheric ozone layer.[2] Soils are considered to be the largest source of N_2O emissions.[1] Microbial nitrogen (N) transformation processes, such as nitrification and denitrification, are the major sources of N_2O; however, their relative contribution to N_2O production is often unclear.

Recent developments in mass spectrometric techniques and laser spectroscopic approaches allow the intramolecular ^{15}N distribution to be determined in the linear asymmetric N_2O molecule.[3–6] The so-called ^{15}N site preference (SP), the difference in isotopic ^{15}N content between the central (α position) and the terminal N atom (β position) in the asymmetric N_2O molecule, has been shown to differ clearly amongst different N_2O source pathways,[7–9] and it is assumed to be independent of the $\delta^{15}N$ value of the precursor species.[10] Thus, the SP can provide information about the underlying source processes of N_2O, such as nitrification and denitrification.[11] In several pure culture studies the SP of N_2O originating from bacterial denitrification (SP values −11 ‰ to 0 ‰) was found to be clearly lower that that from nitrification (ammonia oxidation and hydroxylamine oxidation) derived N_2O (SP values 31 ‰ to 37 ‰).[8,9] Based on these findings, the relative contribution of denitrification and nitrification to the total N_2O emission from soils can be estimated. However, definite allocation of the N_2O to these two processes is complicated by similar SP values for other processes such as fungal denitrification and abiotic sources ranging between 32 ‰ and 37 ‰,[7,12] thus overlapping with the SP signatures typical for nitrification. Furthermore, there are other microbial N_2O production pathways, such as archaeal nitrification, anammox (anaerobic ammonium oxidation), or DNRA (dissimilatory nitrate reduction to ammonium), for which hardly any characteristic isotopic N_2O signatures have yet been identified.[13,14]

Another process that could also markedly affect SP values is isotopic fractionation during N_2O reduction to N_2, which tends

* Correspondence to: D. Wu, Institute of Bio- and Geosciences, Agrosphere (IBG-3), Forschungszentrum Jülich GmbH, 52425 Jülich, Germany.
E-mail: w.di@fz-juelich.de

to enrich ^{15}N at the α position of the N_2O molecule,[15,16] thereby increasing SP values according to the degree of reduction.[14,15] To correct this isotopic effect, information on the actual N_2 production via N_2O reduction is needed. However, most indirect methods targeting N_2 production, e.g. the commonly used acetylene inhibition technique, can be influenced by experimental artifacts.[17–20] Direct measurements of N_2 production via denitrification in soils are challenging due to the high atmospheric N_2 background;[20] thus, in most studies using the N_2O isotopomer approach, the N_2 production was not measured.[11,21–25] Therefore, in these studies the use of SP values may have underestimated the proportion of N_2O derived from denitrification, as N_2O reduction cannot be taken into account.

In the present study we focused on SP values obtained from six soil incubation studies conducted in soil incubation systems designed for measuring N_2O as well as N_2 emissions from soil directly by gas chromatography after replacing the air by a He-O_2 atmosphere. These systems facilitate regular gas sampling for N_2O isotopomer analysis by isotope ratio mass spectrometry (IRMS).[6,26] As an advantage, the direct determination of N_2 permits quantification of the N_2O reduction effect on observed SP values and thus allows more accurate N_2O source partitioning estimates.[27] In order to precisely estimate the SP_0 values, i.e. the SP values of N_2O prior to N_2O reduction, the net isotope effect η_{SP} (NIE; according to Jinuntuya-Nortman *et al.*[16]) needs to be known. However, in soil experiments only the apparent η_{SP} can be determined. The apparent η_{SP} value not only depends on the isotopic fractionation associated with N_2O reduction, but it can be also affected by soil heterogeneity and diffusion processes.[27] Since there is no isotopic fractionation for SP during N_2O diffusion, the η_{SP} value during N_2O reduction is believed to be mainly controlled by the rates of enzymatic reduction.[27] Therefore, in most studies a fixed η_{SP} value has generally been used as the fractionation factor because the value was believed to be relatively stable.[27] However, soil heterogeneity may still play an important role, especially for very high N_2O reduction rates when a complete reduction of N_2O to N_2 in isolated soil microsites is possible. For soil conditions in which complete N_2O reduction occurs in isolated soil micropores, no effect on the isotopic composition of the total residual N_2O can be observed, and thus in such cases a higher reduction rate is not associated with a further increase of SP values.[28,29] Hence, even for the (stable) η_{SP} factor the apparent (and measured) isotope effects may be variable depending on the spatially localized distribution of the N_2O reduction in soil.

In the current study, in order to find a better approach for estimating isotope effects during N_2O reduction, we compared three different methods, i.e. a closed-system model,[28] an open-system model,[28] and a dynamic apparent NIE function (our proposed approach) to compensate for the effect of isotope fractionation associated with N_2O reduction on SP values and the subsequent N_2O source partitioning based on SP values.

EXPERIMENTAL

N_2O isotopomer data were obtained from six soil incubation studies [Bol *et al.*,[30] Meijide *et al.*,[31] Bergstermann *et al.*,[32] Köster *et al.*,[33] and Lewicka-Szczebak *et al.*[29], which were conducted at Rothamsted Research in North Wyke, UK, and by Köster *et al.*,[6] which was conducted at the Hanninghof Research Station in Dülmen, Germany].[6,26] A total of 431 data points from soil incubation experiments conducted under conditions explicitly favoring denitrification were obtained (Table 1). In all these studies spot gas samples were collected from the headspace as described in Meijide *et al.*,[31] and the N_2O isotopomer ratios were determined by IRMS, with the isotopomers being those differing in the peripheral (β) and central (α) N-position of the linear molecule. This method does measure the relative abundance of isotopes, particularly in our study the dual isotope and isotopomer signatures of N_2O, i.e. the $\delta^{18}O$ value of N_2O ($\delta^{18}O\text{-}N_2O$), the average $\delta^{15}N$ value ($\delta^{15}N^{bulk}$) and the $\delta^{15}N$ value of the central N-position ($\delta^{15}N^{\alpha}$), as described previously.[3,5] The ^{15}N site preference (SP) was obtained as $SP = 2 \times (\delta^{15}N^{\alpha} - \delta^{15}N^{bulk})$.[3]

Three of these incubation experiments had both anoxic and oxic phases (Table 1). During the anoxic phase the soil samples were incubated under a completely anoxic He atmosphere; thus, no autotrophic nitrification could occur. During the oxic phase of the incubation the O_2 partial pressure (p_{O2}) in the He-O_2 incubation atmosphere was ca 10 to 20 kPa and thus denitrification and nitrification could have occurred simultaneously.

As the N_2O reduction was directly measured in the form of N_2 production, the SP_0 values can be calculated by applying a net isotope effect η_{SP} for the N_2O to N_2 reduction step of denitrification.

In a first step, the isotope effects during N_2O reduction on N_2O SP values have been calculated using a Rayleigh-type model, assuming that isotope dynamics followed closed-system behavior in the six incubation studies. The model can be described as follows:[28,34]

$$SP_{N2O-r} = SP_{N2O-0} + \eta_r \ln\left(\frac{C}{C_0}\right) \quad (1)$$

In this equation, $SP_{N2O\text{-}r}$ is the SP value of the remaining substrate (i.e. N_2O), $SP_{N2O\text{-}0}$ is the SP value of the initial substrate, η_r is the NIE associated with N_2O reduction, and C and C_0 are the residual and the initial substrate concentration (i.e. C/C_0 expresses the $N_2O/(N_2O+N_2)$ product ratio). The error due to the simplified use of η_rSP for the Rayleigh model (Eqn. (1)) instead of separate calculations with $\eta_r^{15}N^{\alpha}$ and $\eta_r^{15}N^{\beta}$ causes a maximal bias of the calculated SP values of 2.1 ‰ for extremely low $N_2O/(N_2O+N_2)$ product ratios (0.00012). However, due to very scarce data on $\eta_r^{15}N^{\alpha}$ and $\eta_r^{15}N^{\beta}$ values,[16] we applied calculations with η_rSP which were much better determined in numerous previous studies. For intermediate product ratios (>0.1), this error is <0.3 ‰, which is below the typical SP measurement precision, hence negligible.

However, as discussed recently by Decock and Six,[35] in reality the behavior of isotope fractionation during N_2O reduction in soils is probably rather characterized as a mixture of processes following closed- as well as open-system isotope dynamics.[35] According to Fry,[28] an open-system model shows a linear response to

Table 1. Soil incubation conditions and average N_2O SP and SP_0 values of the six included studies

Reference	Soil type	Water content	Incubation conditions	SP[‰]	SP_0 (estimated)[‰]
Bol *et al.*[30]	Dystric Gleysol	100% WHC	He (80%), O_2 (20%) (5 days)	5.1 ± 4.6 ‰ (n = 6)	$SP_{0\text{-}c}$ = −2.8 ± 4.2 ‰ $SP_{0\text{-}d}$ = 0.0 ± 3.5 ‰ $SP_{0\text{-}o}$ = 1.9 ± 3.7 ‰
Meijide *et al.*[31]	Chromic Luvisol	85% WFPS	Oxic phase: He (90%), O_2 (10%)(days 1-11); Anoxic phase: He (100%) (days 12–21)	5.0 ± 3.3 ‰ (n = 69)	$SP_{0\text{-}c}$ = −1.6 ± 4.8 ‰ $SP_{0\text{-}d}$ = 0.2 ± 3.3 ‰ $SP_{0\text{-}o}$ = +2.0 ± 3.0 ‰
Bergstermann *et al.*[32]	Chromic Luvisol	90% WFPS	Oxic phase: He (90%), O_2 (10%);Anoxic phase: 100% He (days 6–10)	4.3 ± 3.7 ‰ (n = 109)	$SP_{0\text{-}c}$ = −3.7 ± 9.1 ‰ $SP_{0\text{-}d}$ = +1.1 ± 6.7 ‰ $SP_{0\text{-}o}$ = +1.6 ± 6.7 ‰
Köster *et al.*[6]	Stagnic LuvisolGleyic Podzol;Fluvimollic	65% WHC	He (100%); He (80%), O_2 (20%)	14.8 ± 8.5 ‰ (n = 47)	$SP_{0\text{-}c}$ = 4.7 ± ‰ $SP_{0\text{-}d}$ = 8.1 ± 7.8 ‰ $SP_{0\text{-}o}$ = 10.7 ± 8.0 ‰
Köster *et al.*[33]	Clayey noncalcareous Pelostagnogley	90% WFPS	He (90%), O_2 (10%)	4.9 ± 7.5 ‰ (n = 105)	$SP_{0\text{-}c}$ = −5.2 ± 11.1 ‰ $SP_{0\text{-}d}$ = 0.6 ± 7.1 ‰ $SP_{0\text{-}o}$ = 1.6 ± 7.3 ‰
Lewicka-Szczebak *et al.*[29]	Silty clay loam soil	100% WFPS 94% WFPS 85% WFPS	He (79%), O_2 (21%)	6.0 ± 5.5 ‰ (n = 95)	$SP_{0\text{-}c}$ = −2.9 ± 10.3 ‰ $SP_{0\text{-}d}$ = 1.8 ± 6.0 ‰ $SP_{0\text{-}o}$ = 2.9 ± 5.8 ‰

WHC = Water holding capacity; WFPS = Water filled pore space

increasing substrate consumption and can be modeled as follows:

$$SP_{N2O-r} = SP_{N2O-0} - \eta_r \left(1 - \left(\frac{C}{C_0}\right)\right) \quad (2)$$

It has been suggested that in some cases when extremely low $N_2O/(N_2+N_2O)$ product ratios occur, an open-system model may be more applicable.[29] Published NIE values range from −8.2 ‰ to −2.9 ‰, which indicates that the NIE during N_2O reduction may vary amongst different soils and/or incubation conditions.[6,15,27,35,36] In the majority of previous studies,[6,27] a fixed NIE was used to calculate the N_2O SP_0 values. However, using a temporally variable NIE may significantly affect the SP_0 values, and thus the source partitioning results in the next step. The modelled NIE values determined in Lewicka-Szczebak *et al.*[29] were therefore specifically correlated in this study with the respective measured $N_2O/(N_2O+N_2)$ product ratios to help us to develop a new dynamic apparent NIE function approach:

$$\eta r = -5.9 - 1.1 \ln\left(\frac{C}{C0}\right) \quad (3)$$

An NIE value of 0 was assumed as the maximum value. The SP_0 value can then be calculated using a combination of Eqns. (1) and (3). The differences in SP_0 values and for source partitioning between the open-system model, the closed-system model, as well as the dynamic apparent NIE function, are highlighted in the current study. For the open-system model and the closed-system model an NIE of −5 ‰ was assumed, based on reported average values.[6,25] To differentiate between them, the SP_0 values, based on the closed-system model, the open-system model and the dynamic apparent NIE function are referred to as $SP_{0\text{-}c}$, $SP_{0\text{-}o}$ and $SP_{0\text{-}d}$, respectively.

The N_2O source partitioning was based on an end-member isotopic mass balance equation:

$$SP_{N2O-0} = SP_D \cdot f_{D\text{-}SP} + SP_N \cdot f_{N-SP} \quad (4)$$

In this equation it is assumed that we deal with only two end-members; hence $f_{N\text{-}SP} + f_{D\text{-}SP} = 1$. Here $f_{D\text{-}SP}$ represents the contribution of denitrification, while $f_{N\text{-}SP}$ represents the contribution of both nitrification and fungal denitrification calculated on the basis of the respective SP_0 values. The end-member N_2O SP value for nitrification and fungal denitrification (SP_N) was assumed as 34 ‰, and the N_2O SP value for denitrification (SP_D) was set to −11 ‰, representing the lower end of literature data, thereby largely avoiding negative nitrification/fungal denitrification proportions.[7–9]

RESULTS AND DISCUSSION

Details of the conditions of the six incubation experiments are shown in Table 1. The average SP value was 6.1 ‰ (±6.6) based on 431 single SP values from the six experiments (Fig. 1). After accounting for the N_2O reduction effect, the average $SP_{0\text{-}c}$ and $SP_{0\text{-}o}$ values decreased to −2.6 ‰ (±9.5) and 2.9 ‰ (±6.3), respectively. Sixteen percent of the $SP_{0\text{-}c}$ values were below −11 ‰, which is generally reported to be the lower end of SP values for denitrification in pure-culture incubation experiments,[8,9] while almost no $SP_{0\text{-}o}$ values were below −11 ‰ (Fig. 2).

In many previous studies denitrification and nitrification were assumed to be the two major sources of N_2O.[33] However, with more recent studies at the molecular level, it is believed that fungal denitrification also functions as a major process in the nitrogen cycle and acts as a common N_2O source in different ecosystems.[7,37–39] Fungal denitrification

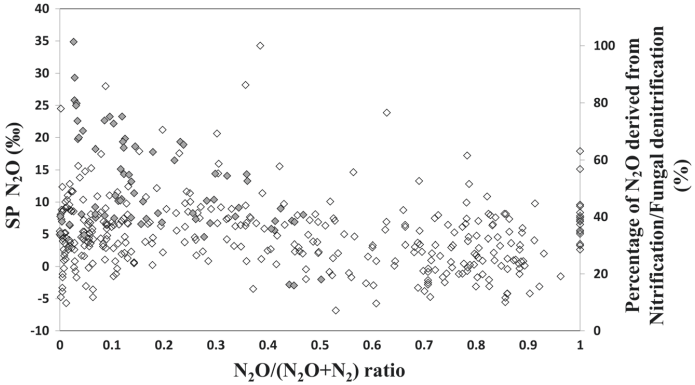

Figure 1. ^{15}N Site preference (SP) values and source partitioning of N_2O as a function of $N_2O/(N_2O+N_2)$ ratio. Left y-axis: N_2O SP values obtained from the six soil incubation experiments using a denitrification incubation system. Right y-axis: Nitrification/fungal denitrification proportion calculated on the basis of N_2O SP values. Grey diamond squares were measured under anaerobic conditions, while white diamond squares were measured under aerobic incubation conditions. The figure includes data from Bol *et al.*,[30] Meijide *et al.*,[31] Bergstermann *et al.*,[32] Köster *et al.*,[6] Köster *et al.*[33] and Lewicka-Szczebak *et al.*[29]

is known to have similar SP values to nitrification; therefore, distinguishing N_2O originating from fungal denitrification and bacterial nitrification is mathematically impossible based on SP values only. Assuming that in these six experiments all the N_2O was produced either by nitrification/fungal denitrification or by bacterial denitrification, SP, $SP_{0\text{-}c}$ and $SP_{0\text{-}o}$ values were used in the two end-member mixing model to partition the emitted N_2O. The proportions of nitrification/fungal denitrification based on the SP, $SP_{0\text{-}c}$ and $SP_{0\text{-}o}$ values were estimated as 38.0% (±14.6), 18.7% (±21.0) and 31.0% (±14.0), respectively. It should be noted that the grey diamond squares in Figs. 1 and 2 should only represent fungal denitrification, as at anoxic conditions bacterial nitrification cannot be active.

However, when $SP_{0\text{-}c}$ values were used, a number of the values of the nitrification/fungal denitrification proportions became negative, while almost none of the nitrification/fungal denitrification proportions estimated by $SP_{0\text{-}o}$ and $SP_{0\text{-}d}$ were below zero (Fig. 2).

In a closed system, substrate is added once and used up progressively over time, whereas, in an open system, substrate is added continually, and product and unused substrate exit permanently.[28] Therefore, when N_2O is continuously produced and partially reduced, N_2O reduction may actually be considered as an open system; however, as the system is not at steady state, i.e. substrate concentration as well as reaction rate are not constant, the open-system model equation (Eqn. (2)) is not the correct one to apply.[27,33] Furthermore, the six incubation experiments were all carried out at high soil moisture, and such conditions favor N_2O accumulation in soil microsites prior to N_2O reduction, justifying the assumption of closed-system isotope dynamics. Moreover, in the study of Köster *et al.*,[6] a logarithmic relation between the N_2O SP value and the $N_2O/(N_2O+N_2)$ product ratio was found, which is typical for a closed system, whereas for an open system a linear relation would be expected.[28] In the other five included studies, neither a logarithmic nor a linear correlation was found between the SP values and the $N_2O/(N_2O+N_2)$ product ratio.

When a very low $N_2O/(N_2O+N_2)$ product ratio occurred, i.e. nearly all the produced N_2O was reduced to N_2, the actual apparent NIE may have been less negative than the assumed fixed value. The reason for this is that although N_2 is produced, no change in SP (N_2O) will be observed, because no N_2O escaped from the soil (see Supplementary Table S1, Supporting Information). This possibly leads to the overestimation of N_2O reduction effects on SP_0 values when a fixed NIE is used. In the study of Lewicka-Szczebak *et al.*,[29] the NIE was found to be positively correlated with the $N_2O/(N_2O+N_2)$ product ratio ($r^2=0.68$, $n=18$, $P=0.002$). Based on dynamic apparent NIE function, the $SP_{0\text{-}d}$ values led to similar results to the $SP_{0\text{-}o}$ values (Fig. 2). The average value of $SP_{0\text{-}d}$ was 1.7 ‰ (±6.3), which was higher than the average value of $SP_{0\text{-}c}$ (−2.6 ‰), but lower than the average value of $SP_{0\text{-}o}$ (2.9 ‰). The proportion of nitrification/fungal denitrification based on $SP_{0\text{-}d}$ was 28.3% (±14.0), which was also between the proportions estimated by the $SP_{0\text{-}c}$and $SP_{0\text{-}o}$ values.

The out-of-range values of $SP_{0\text{-}c}$ and the resulting negative nitrification/fungal denitrification proportions based on the $SP_{0\text{-}c}$ values both clearly indicated an overestimation of the N_2O reduction fractionation effect by applying the closed-system model. However, this overestimation was observed only for samples with very low $N_2O/(N_2O+N_2)$ product ratios (<0.1) (Table 2). The open-system and dynamic apparent NIE function resulted in relatively similar SP_0 results when used to model the N_2O reduction effect, whereas the open-system model gave higher average SP_0 values for the entire range of $N_2O/(N_2O+N_2)$ product ratios. The difference between these three approaches became smaller when the $N_2O/(N_2O+N_2)$ ratio was higher (Table 2). There was almost no difference between the three approaches when the $N_2O/(N_2O+N_2)$ product ratio was above 0.6. In our study the dynamic apparent NIE function compensated well for the

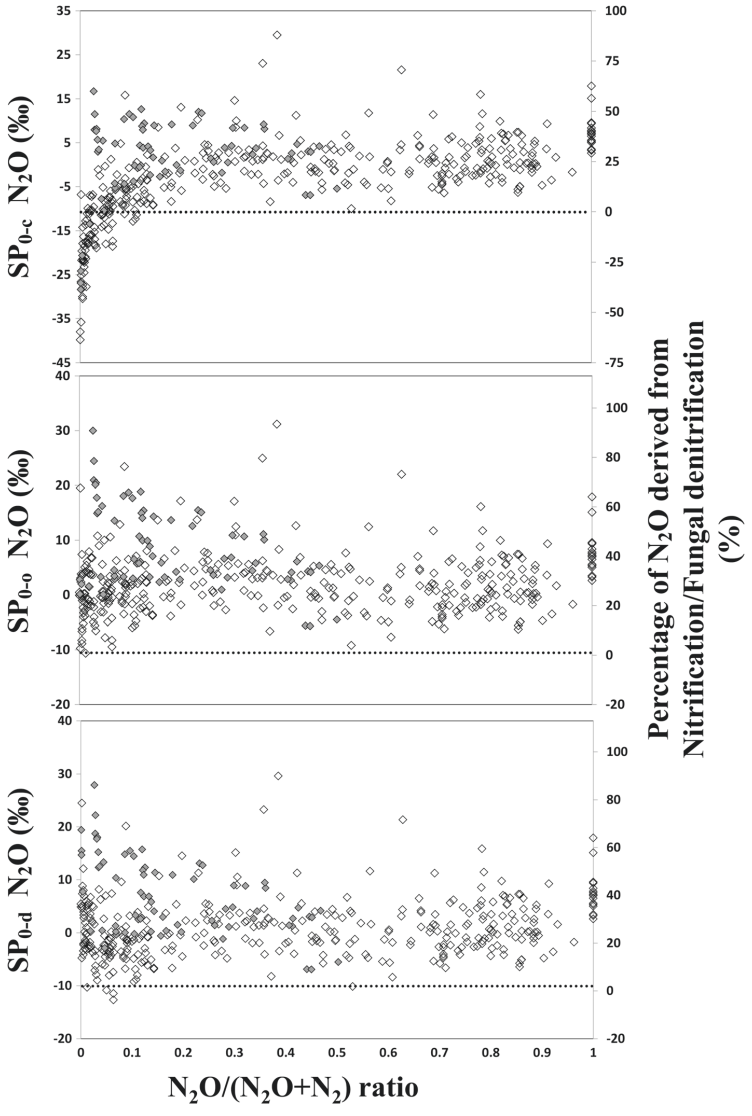

Figure 2. N_2O SP_0 values calculated with the three different approaches and source partitioning based on N_2O SP_0 as a function of $N_2O/(N_2O+N_2)$ ratio. Left y-axis: N_2O SP_0 values obtained from the six soil incubation experiments using a denitrification incubation system. Right y-axis: Nitrification/fungal denitrification proportion calculated on the basis of N_2O SP_0 values. Grey diamond squares were obtained under anaerobic conditions, while white diamond squares were measured under aerobic incubation conditions. N_2O SP_0 values based on the closed-system model are referred to as $SP_{0\text{-}c}$, SP_0 values based on the open-system model are referred to as $SP_{0\text{-}o}$, while SP_0 values based on the dynamic apparent NIE function are referred to as $SP_{0\text{-}d}$. The figures include data from Bol *et al.*,[30] Meijide *et al.*,[31] Bergstermann *et al.*,[32] Köster *et al.*,[6] Köster *et al.*[33] and Lewicka-Szczebak *et al.*[29] Please note the different scaling of the y-axes.

overestimation of the N_2O reduction effect by the closed-system model at extremely low $N_2O/(N_2O+N_2)$ product ratios. Moreover, it also gave the lowest variations for SP_0 within the whole range of $N_2O/(N_2O+N_2)$ ratios (Table 2). Therefore, we propose the dynamic apparent NIE function as an alternative way of examining and calculating SP_0 values,

Rapid Communications in Mass Spectrometry

Table 2. N_2O SP values before and after correction for fractionation during N_2O reduction using three different approaches

$N_2O/(N_2O+N_2)$ratio range	SP [‰]	SP_{0-c} [‰]	SP_{0-o} [‰]	SP_{0-d} [‰]
0–0.1	7.4 ± 7.4	−11.4 ± 10.4	2.6 ± 7.4	1.6 ± 7.5
0.1–0.2	8.5 ± 6.2	−1.5 ± 6.4	4.2 ± 6.3	1.1 ± 6.3
0.2–0.4	8.9 ± 6.5	2.8 ± 6.5	5.4 ± 6.5	3.4 ± 6.5
0.4–0.6	3.8 ± 4.6	0.2 ± 4.5	1.3 ± 4.5	0.1 ± 4.5
0.6–0.8	2.8 ± 5.2	1.1 ± 5.3	1.3 ± 5.2	0.9 ± 5.3
0.8–1.0	3.5 ± 4.7	2.9 ± 4.8	3.0 ± 4.8	2.9 ± 4.8

SP_{0-c} – closed-system model, SP_{0-o} – open-system model, and SP_{0-d} – dynamic apparent NIE function

especially when the $N_2O/(N_2O+N_2)$ product ratio is less than 0.1. It should be noted that in this study the equation for the dynamic calculation of the NIE was still based on limited literature data ($n=18$); however, it already provided an opportunity to rethink the nature of NIE. In order to progress these findings, further soil incubation studies need to be undertaken to determine and subsequently constrain the potential range of NIE associated with the N_2O reduction effect.

No matter which of the SP_0 (SP_{0-c}, SP_{0-o}, or SP_{0-d}) values were used to compensate for the N_2O reduction effect, a marked impact on the SP value was shown, which significantly increased the estimate of the proportion of N_2O derived from denitrification. Several other ways of estimating N_2O reduction have been reported. For example, a strong relationship between N_2O $\delta^{18}O$ and SP values between 2.2 and 2.6 is suggested to be indicative of N_2O significantly affected by reduction.[15,24] It was therefore proposed that the relative N_2O reduction rate can be estimated based on the correlations of the $\delta^{15}N^{\alpha}$, $\delta^{15}N^{\beta}$, and $\delta^{18}O$ values of N_2O.[11] However, it has been argued that the positive relationship may also be caused by a shift from nitrification to denitrification or by other unknown mechanisms.[35]

CONCLUSIONS

The closed-system model tended to overestimate the reduction effect on SP values, when most of produced N_2O was reduced to N_2, which led to an erroneous source-partitioning of N_2O by the two end-member mixing model. This was probably due to the effect of inhomogeneous distribution of reduction rates and the partially complete N_2O reduction in soil isolated micropores. The dynamic apparent NIE function, in which NIE decreases with increasing reduction rate, provided more realistic values, especially at the low end $N_2O/(N_2O+N_2)$ product ratios (<0.1).

Acknowledgements

This study was supported by the Chinese Scholarship Council (Scholarship No. 201306350130). The authors thank Professor Dr Reinhard Well, Dr Ana Meijide and Dr Anja Bergstermann for providing the N_2O isotopomer raw data. Rothamsted Research North Wyke receives strategic funding from the Biotechnology and Biological Sciences Research Council (BBSRC), UK.

REFERENCES

[1] G. Myhre, D. Shindell, F.-M. Bréon, W. Collins, J. Fuglestvedt, J. Huang, D. Koch, J.-F. Lamarque, D. Lee, B. Mendoza, T. Nakajima, A. Robock, G. Stephens, T. Takemura, H. Zhang, Anthropogenic and natural radiative forcing, in *Climate Change 2013: The Physical Science Basis. Contribution of Working Group I to the Fifth Assessment Report of the Intergovernmental Panel on Climate Change*, (Eds: T. F. Stocker, D. Qin, G.-K. Plattner, M. Tignor, S.K. Allen, J. Boschung, A. Nauels, Y. Xia, V. Bex, P. M. Midgley). Cambridge University Press, Cambridge, UK and New York, NY, USA.

[2] A. R. Ravishankara, J. S. Daniel, R. W. Portmann. Nitrous oxide (N_2O): the dominant ozone-depleting substance emitted in the 21st century. *Science* **2009**, *326*, 123.

[3] S. Toyoda, N. Yoshida. Determination of nitrogen isotopomers of nitrous oxide on a modified isotope ratio mass spectrometer. *Anal. Chem.* **1999**, *71*, 4711.

[4] H. Waechter, J. Mohn, B. Tuzson, L. Emmenegger, M. W. Sigrist. Determination of N_2O isotopomers with quantum cascade laser based absorption spectroscopy. *Optics Express* **2008**, *16*, 9239.

[5] J. R. Köster, R. Well, B. Tuzson, R. Bol, K. Dittert, A. Giesemann, L. Emmenegger, A. Manninen, L. Cárdenas, J. Mohn. Novel laser spectroscopic technique for continuous analysis of N_2O isotopomers – application and intercomparison with isotope ratio mass spectrometry. *Rapid Commun. Mass Spectrom.* **2013**, *27*, 216.

[6] J. R. Köster, R. Well, K. Dittert, A. Giesemann, D. Lewicka-Szczebak, K.-H. Mühling, A. Herrmann, J. Lammel, M. Senbayram. Soil denitrification potential and its influence on N_2O reduction and N_2O isotopomer ratios. *Rapid Commun. Mass Spectrom.* **2013**, *27*, 2363.

[7] R. L. Sutka, G. C. Adams, N. E. Ostrom, P. H. Ostrom. Isotopologue fractionation during N_2O production by fungal denitrification. *Rapid Commun. Mass Spectrom.* **2008**, *22*, 3989.

[8] R. L. Sutka, N. E. Ostrom, P. H. Ostrom, J. A. Breznak, H. Gandhi, A. J. Pitt, F. Li. Distinguishing nitrous oxide production from nitrification and denitrification on the basis of isotopomer abundances. *Appl. Environ. Microbiol.* **2006**, *72*, 638.

[9] S. Toyoda, H. Mutobe, H. Yamagishi, N. Yoshida, Y. Tanji. Fractionation of N_2O isotopomers during production by denitrifier. *Soil Biol. Biochem.* **2005**, *37*, 1535.

[10] S. Toyoda, N. Yoshida, T. Miwa, Y. Matsui, H. Yamagishi, U. Tsunogai, Y. Nojiri, N. Tsurushima. Production mechanism and global budget of N_2O inferred from its isotopomers in the western North Pacific. *Geophys. Res. Lett.* **2002**, *29*, 7.

[11] S. Park, T. Perez, K. A. Boering, S. E. Trumbore, J. Gil, S. Marquina, S. C. Tyler. Can N_2O stable isotopes and isotopomers be useful tools to characterize sources and microbial pathways of N2O production and consumption in tropical soils? *Global Biogeochem. Cycles* **2011**, *25*, GB1001.
[12] J. Heil, S. Liu, H. Vereecken, N. Brüggemann. Abiotic nitrous oxide production from hydroxylamine in soils and their dependence on soil properties. *Soil Biol. Biochem.* **2015**, *84*, 107.
[13] N. E. Ostrom, P. H. Ostrom. The isotopomers of nitrous oxide: analytical considerations and application to resolution of microbial production pathways. in *Handbook of Environmental Isotope Geochemistry*, (Ed: M. Baskaran). Springer, **2012**, pp. 453–76.
[14] M.-Y. Jung, R. Well, D. Min, A. Giesemann, S.-J. Park, J.-G. Kim, S.-J. Kim, S.-K. Rhee. Isotopic signatures of N_2O produced by ammonia-oxidizing archaea from soils. *ISME J.* **2014**, *8*, 1115.
[15] N. E. Ostrom, A. Pitt, R. Sutka, P. H. Ostrom, A. S. Grandy, K. M. Huizinga, G. P. Robertson. Isotopologue effects during N_2O reduction in soils and in pure cultures of denitrifiers. *J. Geophys. Res. Biogeosciences* **2007**, *112*, G02005.
[16] M. Jinuntuya-Nortman, R. L. Sutka, P. H. Ostrom, H. Gandhi, N. E. Ostrom. Isotopologue fractionation during microbial reduction of N_2O within soil mesocosms as a function of water-filled pore space. *Soil Biol. Biochem.* **2008**, *40*, 2273.
[17] S. P. Seitzinger, L. P. Nielsen, J. Caffrey, P. B. Christensen. Denitrification measurements in aquatic sediments: a comparison of three methods. *Biogeochemistry* **1993**, *23*, 147.
[18] J. C. Yeomans, E. G. Beauchamp. Limited inhibition of nitrous oxide reduction in soil in the presence of acetylene. *Soil Biol. Biochem.* **1978**, *10*, 517.
[19] R. E. Terry, J. M. Duxbury. Acetylene decomposition in soils. *Soil Sci. Soc. Am. J.* **1985**, *49*, 90.
[20] P. M. Groffman, M. A. Altabet, J. K. Böhlke, K. Butterbach-Bahl, M. B. David, M. K. Firestone, A. E. Giblin, T. M. Kana, L. P. Nielsen, M. A. Voytek. Methods for measuring denitrification: diverse approaches to a difficult problem. *Ecol. Appl.* **2006**, *16*, 2091.
[21] T. Pérez, D. Garcia-Montiel, S. Trumbore, S. Tyler, P. de Camargo, M. Moreira, M. Piccolo, C. Cerri. Nitrous oxide nitrification and denitrification ^{15}N enrichment factors from amazon forest soils. *Ecol. Appl.* **2006**, *16*, 2153.
[22] N. E. Ostrom, R. Sutka, P. H. Ostrom, A. S. Grandy, K. M. Huizinga, H. Gandhi, J. C. von Fischer, G. P. Robertson. Isotopologue data reveal bacterial denitrification as the primary source of N_2O during a high flux event following cultivation of a native temperate grassland. *Soil Biol. Biochem.* **2010**, *42*, 499.
[23] S. Toyoda, M. Yano, S. Nishimura, H. Akiyama, A. Hayakawa, K. Koba, S. Sudo, K. Yagi, A. Makabe, Y. Tobari, N. O. Ogawa, N. Ohkouchi, K. Yamada, N. Yoshida. Characterization and production and consumption processes of N_2O emitted from temperate agricultural soils determined via isotopomer ratio analysis. *Global Biogeochem. Cycles* **2011**, *25*, GB2008.
[24] R. Well, I. Kurganova, V. Lopes de Gerenyu, H. Flessa. Isotopomer signatures of soil-emitted N_2O under different moisture conditions – A microcosm study with arable loess soil. *Soil Biol. Biochem.* **2006**, *38*, 2923.
[25] J. R. Köster, L. Cárdenas, M. Senbayram, R. Bol, R. Well, M. Butler, K. H. Mühling, K. Dittert. Rapid shift from denitrification to nitrification in soil after biogas residue application as indicated by nitrous oxide isotopomers. *Soil Biol. Biochem.* **2011**, *43*, 1671.
[26] L. M. Cárdenas, J. M. B. Hawkins, D. Chadwick, D. Scholefield. Biogenic gas emissions from soils measured using a new automated laboratory incubation system. *Soil Biol. Biochem.* **2003**, *35*, 867.
[27] D. Lewicka-Szczebak, R. Well, J. R. Köster, R. Fuß, M. Senbayram, K. Dittert, H. Flessa. Experimental determinations of isotopic fractionation factors associated with N_2O production and reduction during denitrification in soils. *Geochim. Cosmochim. Acta* **2014**, *134*, 55.
[28] B. Fry. *Stable Isotope Ecology*. Springer, New York, **2006**.
[29] D. Lewicka-Szczebak, R. Well, R. Bol, A. S. Gregory, G. P. Matthews, T. Misselbrook, W. R. Whalley, L. M. Cardenas. Isotope fractionation factors controlling isotopocule signatures of soil-emitted N_2O produced by denitrification processes of various rates. *Rapid Commun. Mass Spectrom.* **2015**, *29*, 269.
[30] R. Bol, S. Toyoda, S. Yamulki, J. M. B. Hawkins, L. M. Cardenas, N. Yoshida. Dual isotope and isotopomer ratios of N_2O emitted from a temperate grassland soil after fertiliser application. *Rapid Commun. Mass Spectrom.* **2003**, *17*, 2550.
[31] A. Meijide, L. M. Cárdenas, R. Bol, A. Bergstermann, K. Goulding, R. Well, A. Vallejo, D. Scholefield. Dual isotope and isotopomer measurements for the understanding of N_2O production and consumption during denitrification in an arable soil. *Eur. J. Soil Sci.* **2010**, *61*, 364.
[32] A. Bergstermann, L. Cárdenas, R. Bol, L. Gilliam, K. Goulding, A. Meijide, D. Scholefield, A. Vallejo, R. Well. Effect of antecedent soil moisture conditions on emissions and isotopologue distribution of N_2O during denitrification. *Soil Biol. Biochem.* **2011**, *43*, 240.
[33] J. R. Köster, L. Cárdenas, R. Bol, D. Lewicka-Szczebak, M. Senbayram, R. Well, A. Giesemann, K. Dittert. Anaerobic digestates lower N_2O emissions compared to cattle slurry by affecting rate and product stoichiometry of denitrification – An N_2O isotopomer case study. *Soil Biol. Biochem.* **2015**, *84*, 65.
[34] A. Mariotti, J. C. Germon, P. Hubert, P. Kaiser, R. Letolle, A. Tardieux, P. Tardieux. Experimental determination of nitrogen kinetic isotope fractionation: some principles; illustration for the denitrification and nitrification processes. *Plant Soil* **1981**, *62*, 413.
[35] C. Decock, J. Six. How reliable is the intramolecular distribution of ^{15}N in N_2O to source partition N_2O emitted from soil? *Soil Biol. Biochem.* **2013**, *65*, 114.
[36] R. Well, H. Flessa. Isotopologue enrichment factors of N_2O reduction in soils. *Rapid Commun. Mass Spectrom.* **2009**, *23*, 2996.
[37] R. J. Laughlin, R. J. Stevens. Evidence for fungal dominance of denitrification and codenitrification in a grassland soil. *Soil Sci. Soc. Am. J.* **2002**, *66*, 1540.
[38] H. Shoun, S. Fushinobu, L. Jiang, S.-W. Kim, T. Wakagi. Fungal denitrification and nitric oxide reductase cytochrome P450nor. *Philos. Trans. R. Soc. B Biol. Sci.* **2012**, *367*, 1186.
[39] W. Wei, K. Isobe, Y. Shiratori, T. Nishizawa, N. Ohte, S. Otsuka, K. Senoo. N_2O emission from cropland field soil through fungal denitrification after surface applications of organic fertilizer. *Soil Biol. Biochem.* **2014**, *69*, 157.

SUPPORTING INFORMATION

Additional supporting information may be found in the online version of this article at the publisher's website.

Paper II

Nitrification inhibitors mitigate N_2O emissions more effectively under straw-induced conditions favoring denitrification.

Wu, D., Senbayram, M., Well, R., Brüggemann, N., Pfeiffer, B., Loick, N., Stempfhuber, B., Dittert, K., Bol, R., 2017

Soil Biology and Biochemistry 104, 197–207.

Soil Biology & Biochemistry 104 (2017) 197–207

Contents lists available at ScienceDirect

Soil Biology & Biochemistry

journal homepage: www.elsevier.com/locate/soilbio

Nitrification inhibitors mitigate N_2O emissions more effectively under straw-induced conditions favoring denitrification

Di Wu [a, *], Mehmet Senbayram [b], Reinhard Well [c], Nicolas Brüggemann [a], Birgit Pfeiffer [d], Nadine Loick [e], Barbara Stempfhuber [f], Klaus Dittert [d], Roland Bol [a]

[a] Institute of Bio- and Geosciences, Agrosphere (IBG-3), Forschungszentrum Jülich GmbH, 52425 Jülich, Germany
[b] Institute of Plant Nutrition and Soil Science, University of Harran, Osmanbey, 63000, Sanliurfa, Turkey
[c] Thünen Institute of Climate-Smart Agriculture, Federal Research Institute for Rural Areas, Forestry and Fisheries, Bundesallee 50, 38116 Braunschweig, Germany
[d] Department of Crop Science, Section of Plant Nutrition and Crop Physiology, University of Göttingen, Carl-Sprengel-Weg 1, 37075 Göttingen, Germany
[e] Rothamsted Research, North Wyke, Okehampton, Devon EX20 2SB, UK
[f] Helmholtz-Zentrum München, German Research Center for Environmental Health, Environmental Genomics, Ingolstädter Landstraße 1, 85764 Neuherberg, Germany

ARTICLE INFO

Article history:
Received 7 June 2016
Received in revised form
17 October 2016
Accepted 30 October 2016

Keywords:
Nitrification inhibitor
Nitrification
Denitrification
Nitrous oxide
Isotope
Gene abundance

ABSTRACT

The application of reactive nitrogen (N) in the form of synthetic/organic fertilizers plays a central role in supporting a larger human population, but also contributes to global warming through the emission of nitrous oxide (N_2O). The use of nitrification inhibitors (NIs) has repeatedly been shown to minimize N_2O emissions; however, their effectiveness in reducing N_2O emissions varies greatly under different environmental conditions. A better understanding of how and to what extent NIs can mitigate fertilizer-related soil-borne N_2O emissions under a range of different conditions is required. In the present study, we carried out a soil incubation experiment in a fully automated continuous-flow incubation system under conditions favoring either nitrification- or denitrification-derived N_2O emissions. Additionally, the abundance of AOB *amoA*, and AOA *amoA* genes was quantified and N_2O isotopic signatures were analyzed. We mixed a common NI (PIADIN®) with mineral fertilizer (ammonium sulfate) and examined the N_2O mitigation potential of the NI in a fertilized sandy soil (low denitrification potential) and a sandy soil mixed with wheat straw (high denitrification potential) at 70% water holding capacity (WHC). In non-NI treatments, the addition of straw led to a drastic increase of CO_2 and N_2O emissions compared to the non-straw-amended soils, suggesting stimulated microbial activity and higher denitrification rate. The NI reduced N_2O emissions in the straw-amended treatment by 41%, whereas in the treatment without straw this was only 17%. With the combination of N_2O isotopic signatures and functional gene abundances, fungal denitrification was considered to be the major process contributing to the higher N_2O fluxes specifically in straw-amended soils. Overall, our study indicated that NI can be used as an effective method for mitigating N_2O emissions in cropland specifically when the denitrification potential is high, e.g. in moist N-fertilized and straw-amended soils.

1. Introduction

Synthetic N fertilizers have been estimated to currently sustain almost 50% of the world's population (Sutton et al., 2011). However, only 47% of the reactive nitrogen added globally to cropland is converted into harvested products, meaning that more than half of the nitrogen used for crop fertilization is currently lost into the environment (Lassaletta et al., 2014). The N fertilizers not taken up by the target system tend to be transformed into gaseous (NO, N_2O, or N_2) or leachable forms (e.g. NO_3^-), potentially causing environmental consequences, as the N escapes into the atmosphere or cascades via the terrestrial systems into the aquatic systems (Fowler et al., 2013). When N fertilizers are applied such as urea or anhydrous ammonia, the microbial process of nitrification converts a large fraction of the ammonium into nitrate (NO_3^-) within 2–3 weeks (Huber et al., 1977). This NO_3^- is highly mobile in soil and may

* Corresponding author.
E-mail address: w.di@fz-juelich.de (D. Wu).

http://dx.doi.org/10.1016/j.soilbio.2016.10.022
0038-0717/

cause a number of environmental problems, such as ground water pollution and greenhouse gas emissions.

Nitrous oxide (N_2O) is an important greenhouse gas and has become the most important stratospheric ozone-depleting gas of the 21st century (Bouwman et al., 2002; Ravishankara et al., 2009). Globally, soils are the largest anthropogenic source of N_2O, and agricultural activities are responsible for about 59% of the anthropogenic N_2O emissions (Ciais et al., 2014). The increasing use of N fertilizers in agriculture is the major reason for the high anthropogenic N_2O emissions by enhancing the microbial processes which lead to nitrification and denitrification (Firestone and Davidson, 1989). Until recently, denitrification was considered to be the dominant process responsible for the increase in atmospheric N_2O (Baggs, 2008; Senbayram et al., 2009). Denitrification has been found to be a function of both eukaryotes and bacteria, however, many fungi lack N_2O reductase and thus the final product is N_2O (Laughlin and Stevens, 2002). Denitrification is a key process of the global N cycle because it leads to significant N losses from agricultural systems by converting NO_3^- and NO_2^- into NO_x, N_2O and elemental N_2 (Bouwman et al., 2013). N_2O emissions from soil denitrification have been projected to reach 14.2 Tg N yr^{-1} by 2050 on the global scale (Bouwman et al., 2013). The rate of denitrification and N_2/N_2O partitioning is regulated by a number of complex interrelated factors, e.g. oxygen availability, soil moisture, pH, NO_3^- concentration, and the availability of labile carbon (C) compounds in the soil (Burford and Bremner, 1975; Dittert et al., 2005; Loecke and Robertson, 2009).

In the recent past, crop straw incorporation has become more popular worldwide. China, for example, accounts for around 30% of global crop straw production. In the past, most of the straw produced was burnt in China, whereas nowadays approx. 46% of this straw is returned to the soil due to the prohibition on burning straw enacted by the government (Jiang et al., 2012). The labile soil C pool, which turns over relatively rapidly, originates from the addition of fresh residues such as plant straw, plant roots and living organisms, and predominantly regulates the denitrification potential. With respect to the impact of crop straw incorporation on N_2O emissions, contradictory observations have been reported (Baggs et al., 2000; Zou et al., 2005). Thus, understanding the impact of straw incorporation on the production of N_2O and therefore developing specific management practices to reduce N_2O fluxes in straw-amended soils may contribute significantly to global efforts to mitigate greenhouse gas emissions.

Nitrification inhibitors (NIs) are compounds that can reduce the bacterial oxidation of NH_4^+ to NO_2^- by inhibiting the activity of ammonia-oxidizing bacteria, e.g. of the genus *Nitrosomas*, in the soil (Zerulla et al., 2001). Most of the NIs inhibit the enzyme ammonia monooxygenase (AMO), which catalyzes the first step of nitrification (Subbarao et al., 2006). The use of NIs has repeatedly been shown to lower N_2O emissions from agricultural soils; however, their effectiveness in reducing N_2O emission varies greatly (Prasad and Power, 1995; Qiao et al., 2015; Ruser and Schulz, 2015). The application of NI was reported to reduce N_2O emission mainly due to inhibited nitrification rate (Zerulla et al., 2001). However, recent studies indicated that denitrification-derived N_2O emissions may also be affected indirectly by NI (Hatch et al., 2005; Ruser and Schulz, 2015). Menendez et al. (2012) reported that the use of NI 3,4-dimethylpyrazole phosphate (DMPP) reduced N_2O emission more effectively under conditions favoring denitrification, i.e. at 80% water-filled pore space (WFPS), than at 60% WFPS, which provides more suitable conditions for nitrification. Similarly, Di et al. (2014) reported that, while the NI dicyandiamide (DCD) did not have a significant impact on N_2O emission at 60% field capacity, large reductions were found after DCD application at 100% field capacity and above.

In the past, sources of soil-borne N_2O emissions were identified using various inhibitors, sterilization or addition of substrates (Baggs, 2008; Khalil et al., 2004; Stevens et al., 1993). Recent developments in mass spectrometric and laser spectroscopic techniques have enabled the analysis of the intramolecular ^{15}N distribution in the linear asymmetric N_2O molecule (Brenninkmeijer and Röckmann, 1999; Toyoda and Yoshida, 1999; Köster et al., 2013a). The ^{15}N site preference (SP), the difference between $\delta^{15}N$ at the central (α position) and the peripheral N atom (β position) in the N_2O molecule, has been shown to differ amongst different N_2O source pathways (Sutka et al., 2008, 2006; Toyoda et al., 2005). The combination of $\delta^{15}N^{bulk}$, $\delta^{18}O$ and SP signatures of N_2O has recently been used to determine the sources of N_2O emitted from soil, e.g. bacterial denitrification (including nitrifier denitrification), nitrification (i.e. ammonium oxidation via hydroxylamine), or fungal denitrification (Sutka et al., 2008, 2006; Toyoda et al., 2005). The advantages of this isotopic approach are that it is a non-invasive, source or process tracer method, enabling convenient low-cost gas sampling, which facilitates the investigation of both laboratory incubation and field-scale experiments (Baggs, 2008; Decock and Six, 2013).

The first objective of this study was to evaluate the effects of mineral N fertilizer and straw incorporation on N_2O production. Secondly, we compared the effectiveness of NI application for mitigating N_2O emissions in N-fertilized soils under two contrasting conditions: incubation of sandy soil with low organic matter (OM) content (favoring nitrification-derived N_2O), and incubation of sandy soil amended with wheat straw (favoring denitrification-derived N_2O). We set up a laboratory incubation trial under fully controlled conditions and determined CO_2 and N_2O gas fluxes with high temporal resolution using a continuous-flow robotized incubation system. Key functional genes (i.e., genes encoding ammonia monooxygenase (*amoA*) of ammonia-oxidizing bacteria (AOB), and *amoA* of ammonia-oxidizing archaea (AOA)) involved in ammonia oxidation were quantified in order to investigate the effect of the application of NI and straw on nitrification activities. To determine the major processes contributing to N_2O emissions, SP values and a two-end-member mixing model were used to source-partition N_2O emissions.

2. Materials and methods

2.1. Soil

The soil was collected from farmland close to Gifhorn, Lower Saxony, Germany (52° 34′ 9.5″ N, 10° 45′ 26.6″ E). Arable crops (oilseed rape, wheat, barley, potato) had been grown prior to soil sampling. The soil was classified as sandy soil (sand 81.8%, silt 14.8%, clay 3.5%). The initial soil contained 1.5% total C, 0.09% total N, 0.1 mg NH_4^+–N kg^{-1} dry soil,11.4 mg NO_3^--N kg^{-1} dry soil, and had a pH of 6.3. The upper 2 cm of the soil and roots were removed, and soil was collected from the first 10 cm below the removed layer.

2.2. Automated soil incubation experiment

The incubation experiment was carried out at the Institute of Applied Plant Nutrition, University of Göttingen, Germany, in a fully automated continuous flow incubation system with 15 PVC vessels (200 mm height, 200 mm diameter). The experiment consisted of four treatments in three replicates each, i.e. soil amended with i) mineral N fertilizer only (ammonium sulfate, AS), ii) NI (PIADIN®, SKW Piesteritz, Germany) mixed with mineral N fertilizer (AS-NI), iii) straw and mineral N fertilizer (SW), iv) straw and NI mixed with mineral N fertilizer (SW-NI), and a non-amended control (CO). Prior to incubation, the soil was pre-incubated for 7 days at 45% water

holding capacity (WHC) to allow the microbial activity to stabilize. Then, soil moisture was adjusted to 70% WHC, equivalent to 67% WFPS, in order to create semi-anoxic conditions (Dobbie and Smith, 2001). In the straw treatments, wheat straw (0.7% total N, 43.7% total C) was mixed with soil at a rate of 4.1 t ha^{-1} (equivalent to 2.6 g wheat straw kg^{-1}dry soil), and 5.7 kg fresh sandy soil. All soils in each incubation vessel were packed at a bulk density of approx. 0.9 g cm^{-3}. Ammonium sulfate was applied at a rate of 150 kg N ha^{-1} (equivalent to 0.47 g in solution in each vessel) in all fertilizer treatments. The NI was pre-mixed with 10 ml ammonium sulfate solution at a rate of 6 L product/ha (equivalent to 19 μl per vessel). The solution was then applied to the top layer. After adding fertilizer without or with NI, the incubation pots were sealed and the headspace (50 mm height) of each vessel was continuously flushed with ambient air (approx. 20 ml air min^{-1}). The temperature of the incubation room was set at 22 °C.

2.3. Measurement of trace gases

For online trace gas concentration analysis of N_2O and CO_2, samples from each incubation vessel's outlet were directed sequentially to a gas chromatograph via two multi-positional valves (12 and 16 ports) by a software-controlled electric actuator (Trilution, Gilson, Inc., Middleton, WI, USA) and an interface module (508 Interface Module, Gilson, Inc.). The gas sample was then analyzed by gas chromatography (450-GC, Bruker, Germany), employing a thermal conductivity detector (TCD) for the quantification of CO_2, and an electron capture detector (ECD) for N_2O. N_2O and CO_2 emissions in the inlet and outlet of each vessel were measured approximately every 8 h. The outlet flux rate for each incubation pot was measured manually every day with a portable gas flow meter (GFM Pro Gas Flowmeter, Thermo Fisher Scientific, Waltham, MA, USA). Flow rate and the concentration difference in CO_2 and N_2O from each incubation vessel's inlet and outlet were used to determine the flux rates.

2.4. Analysis of NH_4^+ and NO_3^-

Soil samples of about 15 g taken from the upper 5 cm were collected from each vessel on four occasions (day 13, 26, 40 and 51) during the experiment using a small soil core sampler, and the small holes were closed after sampling. The soil samples were immediately frozen in liquid nitrogen and stored at −80 °C for further analysis. The samples were extracted with 0.01 M $CaCl_2$ (1:5 w/v) by shaking for 1 h. The extracts were then filtered through Whatman 602 filter paper and stored at −20 °C until analysis. The concentrations of NH_4^+ and NO_3^- in soil extracts were measured colorimetrically using an auto-analyzer (SKALAR, The Netherlands).

2.5. Quantification of bacterial and archaeal amoA gene copies

To quantify the bacterial (AOB) and archaeal (AOA) ammonia monooxygenase genes (*amoA*), genomic DNA was isolated from the soil samples by employing the PowerSoil™ DNA isolation kit (MO BIO Laboratories Inc., Carlsbad, CA, USA). The concentration of DNA extracts was determined using a NanoDrop ND-1000 spectrophotometer (NanoDrop Technologies, Wilmington, DE, USA). For gene copy number quantification, an iCycler (Bio-Rad, Hercules, CA, USA) and the Power SYBR Green PCR Master Mix (Invitrogen, ThermoFisher Scientific, Waltham, MA, USA) were used for real-time PCR. Gene-specific absolute DNA standards with a defined number of gene copies were prepared by cloning the respective gene fragments (generated by the primer pairs given in the supplementary material, using the following standard sources: fosmid clone 54d9 for *amoA* (AOA), and *Nitrosomonas* sp. for *amoA* (AOB) into the pCR2.1 vector of the TA cloning kit (Invitrogen) as described in the manual. The plasmids were isolated from the clones using the Nucleo Spin Kit (Macherey-Nagel, Düren, Germany) according to the manufacturer's instructions, sequenced to ensure the correct insert was present and quantified using the Quant-iT dsDNA BR assay kit and a Qubit fluorometer (Invitrogen). The copy number per microliter was calculated based on the DNA concentration, the molecular weight and length of the plasmid, containing the respective gene fragment. Dilution series of each standard were prepared and applied in triplicate to each qPCR. Each reaction was performed in a 20 μl volume containing 1 ng of 1:10 diluted DNA and of each primer and 12.5 μl of Power SYBR Green PCR Master Mix. Cycling conditions were as follows: 15 min at 95 °C, 46 cycles of 20 s at 95 °C, 30 s at 55 °C for *amoA* (AOA), and 57 °C for *amoA* (AOB) 62 °C, followed by a plate read for 15 s at 80 °C to avoid detection of unspecific products. Product specificity was confirmed by melting curve analysis and visualization in agarose gels showing specific products at the expected size. Quantification of bacterial and archaeal *amoA* genes was done in triplicate. For *amoA* (AOB) and (AOA), PCR efficiencies were 70–73% and 75–83%, and standard curves had R^2 values of >0.99 and >0.97, respectively.

To estimate the possible inhibition of PCR reactions by co-extracted polyphenolic compounds or other inhibiting substances in soil DNA extracts, different dilutions of the respective standard were mixed with the same volume of 1:10 diluted DNA extract used for quantification of the respective genes. For *amoA* (AOB) and *amoA* (AOA), inhibition was not detected or was negligible.

2.6. Isotope analysis and source partitioning

For isotope analysis, gas samples were taken from each incubation vessel by attaching 120 ml serum bottles to the outlets in flow-through mode (with an inlet and an outlet needle) for around 2 h. N_2O $\delta^{15}N^{bulk}$ (i.e., the average $\delta^{15}N$ over the N_2O molecule), $\delta^{15}N_\alpha$ (i.e., $\delta^{15}N$ at the central position of the N_2O molecule), and $\delta^{18}O$ isotope signatures were then determined by analyzing *m/z* 44, 45, and 46 of intact N_2O^+ molecular ions, and *m/z* 30 and 31 of NO^+ fragment ions (Toyoda and Yoshida, 1999) on an isotope ratio mass spectrometer (IsoPrime 100, Elementar Analysensysteme, Hanau, Germany) at Forschungszentrum Jülich, Germany. The $\delta^{15}N$ at the terminal position of the N_2O molecule, $\delta^{15}N_\beta$, was calculated according to $\delta^{15}N_\beta = 2 \cdot \delta^{15}N^{bulk} - \delta^{15}N_\alpha$. The details of correction and calibration are described in Heil et al. (2015). We measured the N_2O concentration in the ambient air (C_0) and the corresponding $\delta^{15}N$, $\delta^{18}O$ or SP value (S_0), as well as the N_2O concentration (C_1) and $\delta^{15}N$, $\delta^{18}O$ or SP value (S_1) at the vessel outlet. We then estimated the soil-released N_2O concentration as the difference between the N_2O concentration at the vessel outlet and that of the air. Based on this, the $\delta^{15}N$, $\delta^{18}O$ or SP value of soil-derived (S_{der}) N_2O was calculated using the following equation:

$$S_{der} = (S_1 \cdot C_1 - S_0 \cdot C_0)/(C_1 - C_0) \quad (1)$$

S_{der} = being soil derived from either the $\delta^{15}N$, $\delta^{18}O$ or SP values.

The source partitioning of N_2O production was based on a two-end-member isotopic mass balance equation:

$$SP_{N2O-0} = SP_D \cdot f_{D-SP} + SP_N \cdot f_{N-SP} \quad (2)$$

In this equation, it is assumed that we are only dealing with two end-members, hence $f_{N\text{-}SP} + f_{D\text{-}SP} = 1$. Distinguishing N_2O originating from fungal denitrification and bacterial nitrification based on SP values is mathematically impossible, as fungal denitrification is known to have SP values similar to those of nitrification (Sutka et al., 2008, 2006). Therefore, the isotopic signatures of the end-

members were defined as 37‰ for both bacterial nitrification and fungal denitrification, and −2‰ for bacterial denitrification (Sutka et al., 2006; Toyoda et al., 2005). In this equation, $f_{D\text{-}SP}$ and $f_{N\text{-}SP}$ represent the contribution of denitrification and nitrification/fungal denitrification to total N_2O release calculated on the basis of SP values, respectively.

2.7. Calculations and statistical analysis

The cumulative gas emissions were calculated by linear interpolation between measured fluxes. Emission rates were expressed as arithmetic means and standard error of the mean (SEM) of the three replicates, and log-transformed for statistical analysis. Tukey's HSD post-hoc tests were used to reveal significant pairwise differences among treatments. Statistical analyses were performed using SPSS version 13.0 (SPSS Inc., Chicago, IL, USA), with $p < 0.05$ used as the criterion for statistical significance.

3. Results

3.1. Gas emissions

Maximum daily CO_2 emissions occurred almost immediately after onset of treatments (within 20 h) in the CO, AS and AS-NI, and decreased gradually to background levels within 30 days (Fig. 1). Here, maximum rates were 48.9 ± 1.5, 51.4 ± 5.4, 50.0 ± 0.2 kg CO_2–C ha^{-1} day^{-1} in CO, AS and AS-NI, respectively. Overall, both maximum daily CO_2 fluxes and cumulative CO_2 fluxes during the whole incubation period were similar in CO, AS and AS-NI, indicating no significant effect of mineral N or NI on soil organic matter mineralization. The addition of straw induced a significant increase in respiration in SW and SW-NI, and maximum CO_2 emissions were reached within three days after the start of treatments. Afterwards, fluxes of CO_2 decreased gradually almost to background levels within 56 days (Fig. 1). In SW and SW-NI, maximum CO_2 emissions (74.5 ± 7.1 and 77.2 ± 5.4 kg CO_2–C ha^{-1} day^{-1} in SW and SW-NI, respectively) were measured 45 h after the start of treatments. The cumulative CO_2 emissions for CO, AS, AS-NI, SW and SW-NI were 412.5 ± 18.1, 408.0 ± 37.2, 405.8 ± 1.2, 1161.0 ± 59.8 and 1168.5 ± 53.4 kg CO_2–C ha^{-1}, respectively (Fig. 1). We divided the incubation period into three phases according to the changes in N_2O emissions (Fig. 1): phase I (0–10 days), phase II (11–28 days), and phase III (29–55 days). There were two major N_2O peak events, one immediately after the start of treatments in phase I, and the other appearing after about 30–40 days in phase III (Fig. 1). After about 13 days, N_2O fluxes sharply increased in SW and SW-NI,

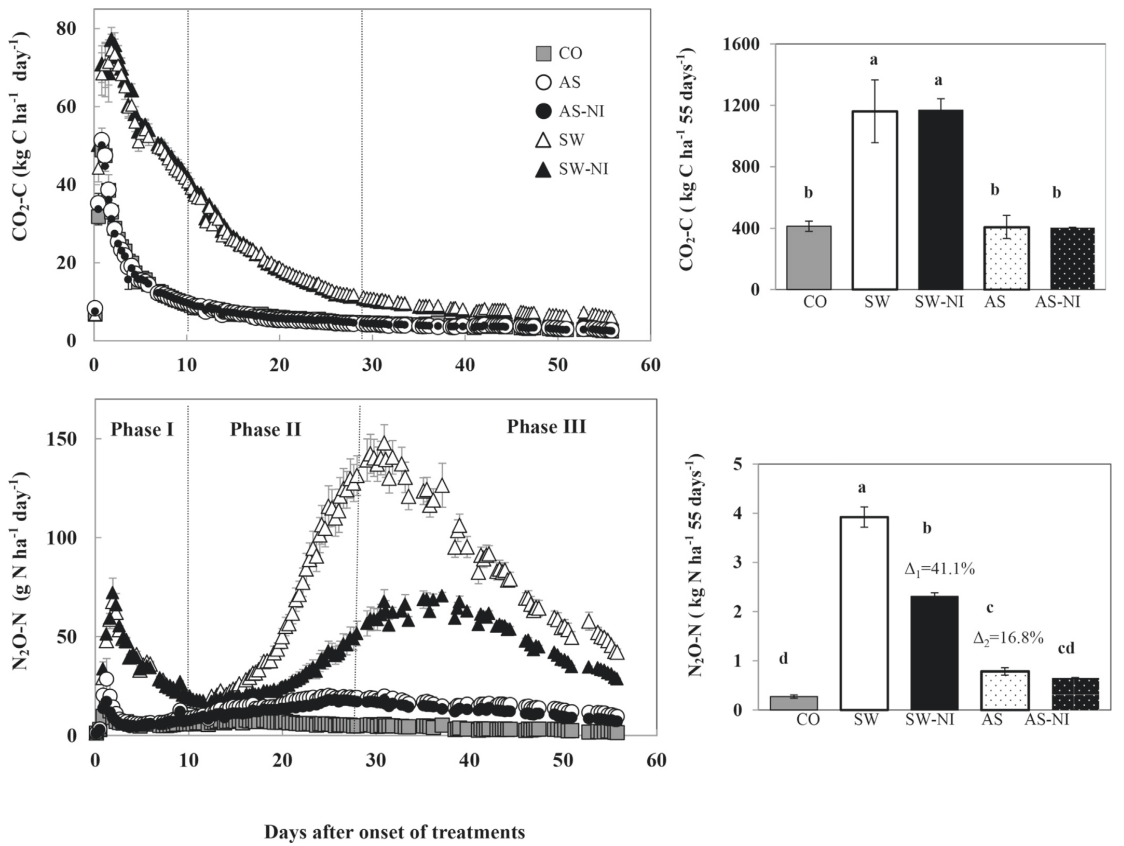

Fig. 1. Time course of fluxes and cumulative emissions of CO_2 and N_2O of soil left unamended (CO), after application of mineral-N only (AS), mineral-N + nitrification inhibitor (AS-NI), mineral-N + straw (SW) or mineral-N + straw + NI (SW-NI), during the 56 days of the incubation experiment at 70% WHC. Error bars show the standard error of the mean of each treatment (n = 3). In some cases error bars are smaller than the symbols. Different lowercase letters indicate significant differences at the $p < 0.05$ level between treatments.

whereas there was only a slight gradual increase in AS and AS-NI. N_2O fluxes reached their maximum after 26 days in AS and AS-NI, after 32 days in SW and after 38 days in SW-NI, respectively. Maximum N_2O fluxes in SW and SW-NI during the second peak event were 5- and 4-fold higher compared to AS and AS-NI, respectively (Fig. 1). Cumulative N_2O emissions during the 56 days of incubation were 275.0 ± 57.8, 784.9 ± 130.0, 652.9 ± 15.6, 3921.1 ± 353.9, and 2310.4 ± 128.9 g N_2O–N ha^{-1} in CO, AS, AS-NI, SW and SW-NI, respectively (Fig. 1).

3.2. NH_4^+ and NO_3^- concentrations in soil

The NH_4^+ concentration decreased gradually with no significant ($p > 0.05$) difference between treatments up to day 26 (Fig. 2). However, after day 26, the concentration of NH_4^+ in the soil was significantly higher in both NI treatments (AS-NI and SW-NI) compared to AS and SW, indicating lower nitrification rates. At the last sampling date, the NH_4^+ concentrations were 48.1% and 40.5% higher ($p < 0.05$) in AS-NI and SW-NI compared to AS and SW, respectively. No difference in NH_4^+ concentrations was found between AS-NI and SW-NI or between AS and SW. The NO_3^- concentration remained low (close to the level of CO) up to day 13 in all treatments. However, the NO_3^- concentration increased almost linearly in all mineral-N treatments, being more pronounced in non-NI treatments (AS and SW). At the end of incubation (after 51 days), the NO_3^- concentration was 22.7% higher in AS compared to AS-NI, and 24.3% higher in SW compared to SW-NI.

3.3. The archaeal and bacterial amoA gene abundances

The bacterial *amoA* gene copy numbers ranged from 5.9×10^5 to 3.3×10^6 in all treatments. As shown in Fig. 3, at 14 days the AOB *amoA* gene abundance was significantly higher in all mineral N treatments. However, the effect was significantly less pronounced in both NI treatments. At 26 days, the AOB *amoA* gene abundance was similar in all treatments. In the further course of the experiment, it only increased significantly in the two NI treatments at 52 days.

The archaeal *amoA* gene copy numbers ranged from 3.5×10^4 to 6.7×10^5. The AOA *amoA* abundance was almost identical in all treatments at 14 days; however, it only increased significantly in CO at 26 days. Both AS-NI and SW-NI treatments showed an increasing trend. In contrast, in AS and SW treatments AOA populations were constantly low during the whole incubation time.

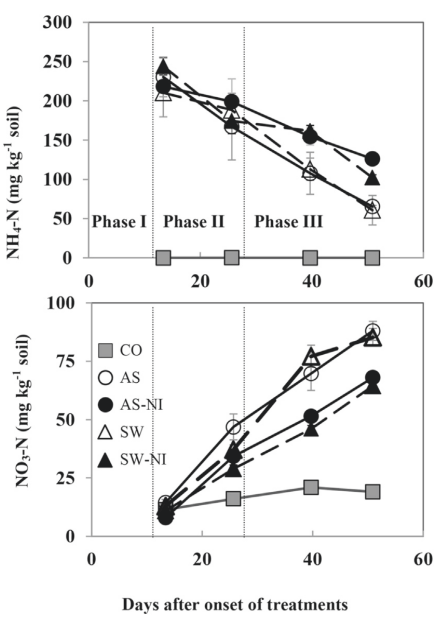

Fig. 2. Time course of NH_4^+ (mg NH_4^+–N kg^{-1} dry soil) and NO_3^- (mg NO_3^-N kg^{-1} dry soil), concentration of soil left unamended (CO), after application of mineral-N only (AS), mineral-N + nitrification inhibitor (AS-NI), mineral-N + straw (SW) or mineral-N + straw + NI (SW-NI), during the 56 days of the incubation experiment at 70% WHC. Error bars show the standard error of the mean of each treatment (n = 3). In some cases error bars are smaller than the symbols.

3.4. $\delta^{15}N^{bulk}$, $\delta^{18}O$ and isotopomers of N_2O

The N_2O isotope trends during the course of the experiment are shown in Fig. 4. During the incubation period, the N_2O $\delta^{15}N^{bulk}$ values in the control (CO) treatment remained almost constant (between 4‰ and 10‰), whereas the N_2O $\delta^{15}N^{bulk}$ values in all the other treatments showed a declining trend. The $\delta^{18}O$ values of N_2O showed a very similar trend to $\delta^{15}N^{bulk}$ values (Fig. 4). The average $\delta^{18}O$ value in CO was 37.4 ± 1.2‰ and remained almost constant during the incubation time. Similar to the $\delta^{15}N^{bulk}$ values, the $\delta^{18}O$ values showed a decreasing trend over time in all N treatments. Overall, there was a significant positive correlation between the $\delta^{15}N^{bulk}$ and $\delta^{18}O$ values ($p < 0.01$; $R^2 = 0.86$).

The SP values ranged from 6.6 to 32.1‰ in all treatments. The average SP value was 13.4 ± 0.7‰, 16.8 ± 0.6‰, 16.0 ± 0.5‰, 24.5 ± 1.9‰ and 19.5 ± 1.5‰ in CO, AS, AS-NI, SW and SW-NI, respectively. Overall, SP values in CO, AS and AS-NI were relatively stable during the incubation period, whereas SP values in SW and SW-NI showed a clear upward trend.

An end-member map with SP as a function of $\delta^{18}O$ is shown in Fig. 5a. The ranges of end-member isotopic signatures were defined according to literature data: SP values for bacterial denitrification from −11 to 0‰ (Toyoda et al., 2005; Sutka et al., 2006), SP values for nitrification from +33 to +37‰ (Sutka et al., 2006), and SP values for fungal denitrification from +34 to +37‰ (Sutka et al., 2008; Rohe et al., 2014), while $\delta^{18}O$ for bacterial denitrification ranged from +10 to +20‰ (Toyoda et al., 2005; Snider et al., 2013; Lewicka-Szczebak et al., 2014), $\delta^{18}O$ for nitrification from +40 to +50‰ (Sutka et al., 2006) and $\delta^{18}O$ for fungal denitrification from +30 to +40‰ (Sutka et al., 2008; Rohe et al., 2014). During the incubation time, SP values in CO were consistently in the transition zone between bacterial denitrification and bacterial nitrification, while there was a shift of SP values in SW and SW-NI from higher $\delta^{18}O$ and lower SP values to lower $\delta^{18}O$ and higher SP values (Fig. 5a). The amounts of N_2O emitted from different sources during the three phases were calculated according to equation (2). As shown in Fig. 5b, bacterial denitrification seems to be the dominant source (more than 50%) of emitted N_2O during phase I (0–10 days) in all treatments. However, in phase II (11–28 days) and phase III (29–55 days), the share of bacterial denitrification of emitted N_2O decreased drastically, suggesting another dominant process (see Discussion).

4. Discussion

4.1. Mineral N content and CO_2 fluxes

When mineral N (in the form of NH_4^+) or organic N fertilizers are applied, nitrification converts most of the NH_4^+ into highly mobile NO_3^- within some days or weeks, depending on the soil properties and other environmental conditions. In the present study, NH_4^+

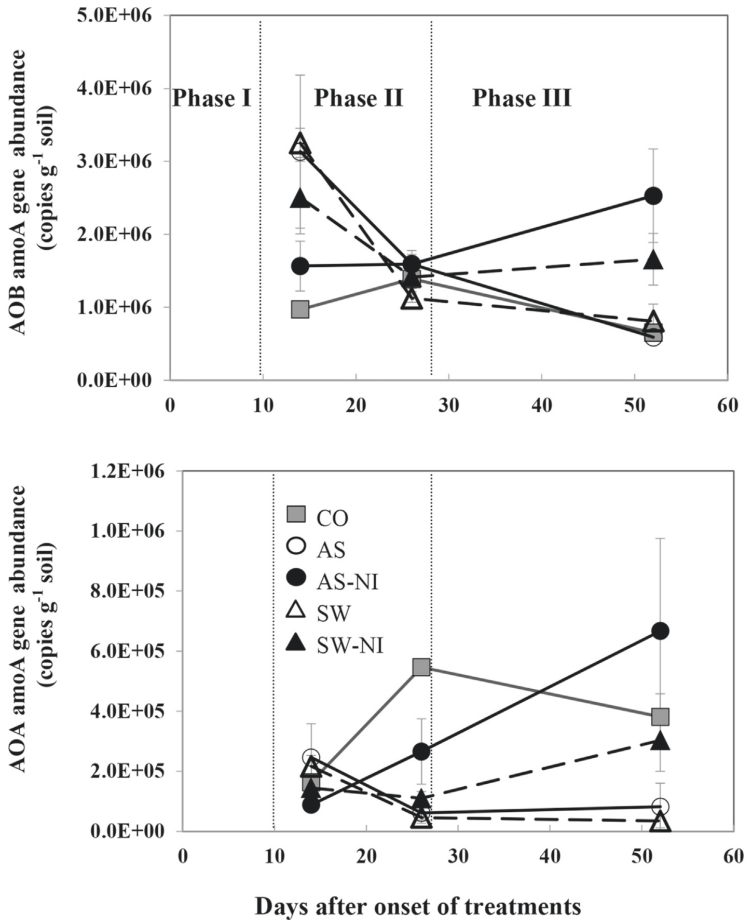

Fig. 3. AOB and AOA *amoA* gene abundance of soil left unamended (CO), after application of mineral-N only (AS), mineral-N + nitrification inhibitor (AS-NI), mineral-N + straw (SW) or mineral-N + straw + NI (SW-NI), during the 56 days of the incubation experiment at 70% WHC. Error bars show the standard error of the mean of each treatment (n = 3).

concentrations in both AS-NI and SW-NI were still significantly higher than in AS and SW after 51 days, respectively. Additionally, NO_3^- concentrations were about 20% lower in both NI treatments (AS-NI, SW-NI) than in AS and SW at the end of the incubation period (after 51 days), indicating that NI significantly inhibited the nitrification process in our experiment.

The addition of straw induced a significant increase in respiration, and maximum CO_2 emissions were reached within 4–6 days. Assuming that the mineralization of soil organic carbon is unaffected by the amendments (i.e. no priming effect), cumulative CO_2 losses for the entire incubation period can be used to calculate the approximate fraction of the added carbon substrates which is mineralized during the incubation. The mineralization of the substrate C can then be estimated as the difference between cumulative CO_2–C evolved in straw-amended soil minus that of the control soil. At the end of the incubation period, the calculated share of mineralized straw-derived C was 59% in all straw-amended soils. This clearly suggests that soil amended with straw has a strongly enhanced soil microbial activity, induced by the supply of labile C. Numerous studies reported that the amendment of soil with organic matter containing readily decomposable organic carbon may trigger denitrification by enhancing respiration (through the creation of anoxic microsites) and by providing energy for denitrifiers (Burford and Bremner, 1975; Firestone, 1982; Köster et al., 2015; Weier et al., 1993). In line with a number of previous reports, our experiment clearly showed that NIs do not have a direct impact on CO_2 emissions (organic matter mineralization) and microbial respiration in the soil (Menendez et al., 2012; Pereira et al., 2010; Tian et al., 2015), which could also indicate that NI do not have a direct effect on either heterotrophic microbial activity or on denitrification.

4.2. Effect of N fertilizer and straw addition on N_2O emissions

Soil supplied with N fertilizers emits more N_2O from the various biological processes in soil, i.e. nitrification, denitrification and fungal or nitrifier denitrification (Kumar et al., 2000; Wrage et al., 2004). In the present experiment, cumulative N_2O emissions were about 3-fold higher in soils treated with mineral N alone compared to the non-fertilized control. Cumulative emission in the

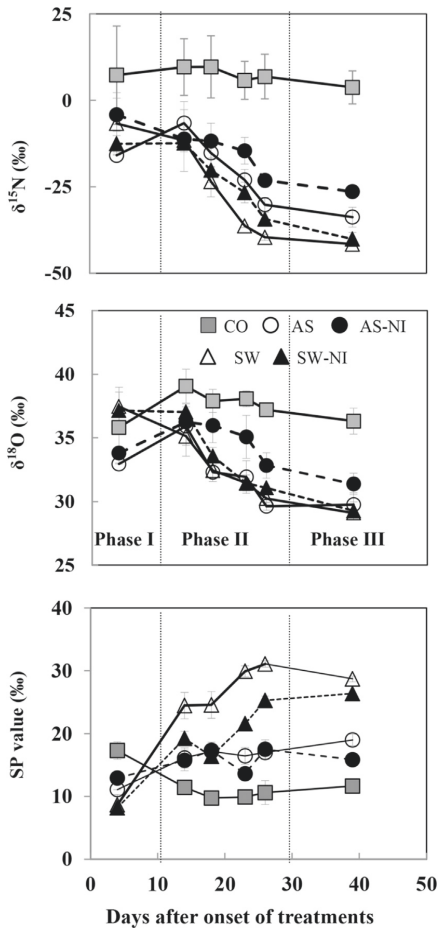

Fig. 4. The N_2O $\delta^{15}N^{bulk}$, δ ^{18}O and SP values of soil left unamended (CO), after application of mineral-N only (AS), mineral-N + nitrification inhibitor (AS-NI), mineral-N + straw (SW) or mineral-N + straw + NI (SW-NI), during the 56 days of the incubation experiment at 70% WHC. Error bars show the standard error of the mean of each treatment (n = 3). In some cases error bars are smaller than the symbols.

AS treatment was of the same order as those obtained in similar incubation trials (Hatch et al., 2005; Köster et al., 2011).

Overall, there were two significant peak events (Fig. 1). The first occurred immediately after the start of treatments (2–3 days) and gradually decreased almost to background levels within 2 days in AS and AS-NI, and within 12 days in SW and SW-NI treatments. As NH_4^+ and SP values (see also discussion in 4.5) did not suggest that any significant nitrification/fungal denitrification occurred during the initial period of the experiment, observed N_2O fluxes seem to have originated mainly from bacterial denitrification as shown in a similar experiment by Senbayram et al. (2009). A significant decline in N_2O emission up to day 15 in all treatments may be attributed to the change in the product ratio of denitrification ($N_2O/(N_2O + N_2)$) due to depletion of NO_3^- at the microsites where denitrification occurs (Köster et al., 2015). When NO_3^- concentrations fall below a threshold value at the denitrifying microsites, studies have shown that under such conditions the N_2O reduction rate will increase and N_2 fluxes can become larger than the N_2O fluxes (Cleemput, 1998; Weier et al., 1993).

In our study, the addition of straw did increase the 56-day cumulative N_2O emissions (SW; 3921 g N_2O–N ha^{-1}) about 5-fold compared to N fertilizer only (AS; 785 g N_2O–N ha^{-1}). It is commonly accepted that the addition of organic matter to soil increases, in particular, the rate of denitrification, as it introduces substrate to the soil which could stimulate microbial growth and activity, and hence promote oxygen consumption that creates temporary anoxic microsites favoring denitrification (Myrold and Tiedje, 1985; Goek and Ottow, 1988; Nishio et al., 2001). However, recent studies show great variations in the effects on N_2O emissions of organic matter amendment to soil, ranging from an increase (Hu et al., 2014; Li et al., 2013; Tang et al., 2014) to a decrease in N_2O emission (Ma et al., 2007; Yamulki, 2006), indicating that other factors (e.g. soil NO_3^- concentration) may also play a role in the overall impact. In soils with a higher denitrification potential, the product stoichiometry of denitrification is known to switch quickly from non–N_2O–emitting ($N_2O/(N_2O + N_2)$ ratio close to zero) to almost exclusively N_2O-emitting conditions ($N_2O/(N_2O + N_2)$ ratio close to one) when soil NO_3^- concentration rises (Senbayram et al., 2012). In our study, when NO_3^- concentration started to increase beyond day 15, the N_2O fluxes also rose drastically at the same time, especially in the straw-amended treatments (SW and SW-NI). However, in those treatments where only mineral-N was added (as ammonium sulfate) there was only found to be a minor effect of N addition on N_2O emissions. Thus, the results confirmed our hypothesis that soils with high native or added organic matter and NO_3^- content have the potential to emit large amounts of N_2O.

4.3. Effect of NI on N_2O emissions

Recent meta-analyses suggested that NI application reduced N_2O emission by 38–44% (Akiyama et al., 2010; Qiao et al., 2015). It is generally accepted that NIs have no direct effect on denitrification, and their effect on N_2O emission has been attributed to their effect on NH_4^+ oxidation (Müller et al., 2002; Zerulla et al., 2001). In our experiment, we compared the effectiveness of NI application for mitigating N_2O emissions under two contrasting soil conditions, i) sandy soil with low OM content (conditions where nitrification may be the dominant source of emitted N_2O), and ii) sandy soil amended with straw application (conditions where denitrification may be the dominant source of emitted N_2O). Both daily and cumulative N_2O fluxes clearly showed that the effectiveness of NI for mitigating N_2O emissions was more significant in soils treated with straw than non-straw-amended treatments. This is reflected in the larger decrease in N_2O emissions due to NI addition in the SW treatment (1611 g N ha^{-1} or 41.1% lower N_2O) compared to the AS treatment (132 g N ha^{-1} or 16.8% lower N_2O). Therefore, the present study clearly suggests that the effectiveness of NI use for mitigating N_2O emissions seems to be more pronounced under conditions favoring denitrification, i.e. high soil moisture and high labile C content in soil. Firstly, we presume that NI application may decrease O_2 consumption in soil microsites by inhibiting nitrification, thereby suppressing N_2O emission from denitrification. Whereas the nitrification process requires oxic conditions for NH_4^+ oxidation, denitrification, which is an anaerobic process, will only occur at low O_2 availability (Bollmann and Conrad, 1998). Low availability of O_2 could either be caused by high moisture content or high biological O_2 consumption. By using oxygen optodes, Zhu et al. (2015) found anoxia rapidly developing due to nitrification after the addition of manure to soil, and N_2O emission rates increased exponentially after anoxia had developed. Therefore, by inhibiting nitrification, NI could decrease O_2 consumption in soil microsites,

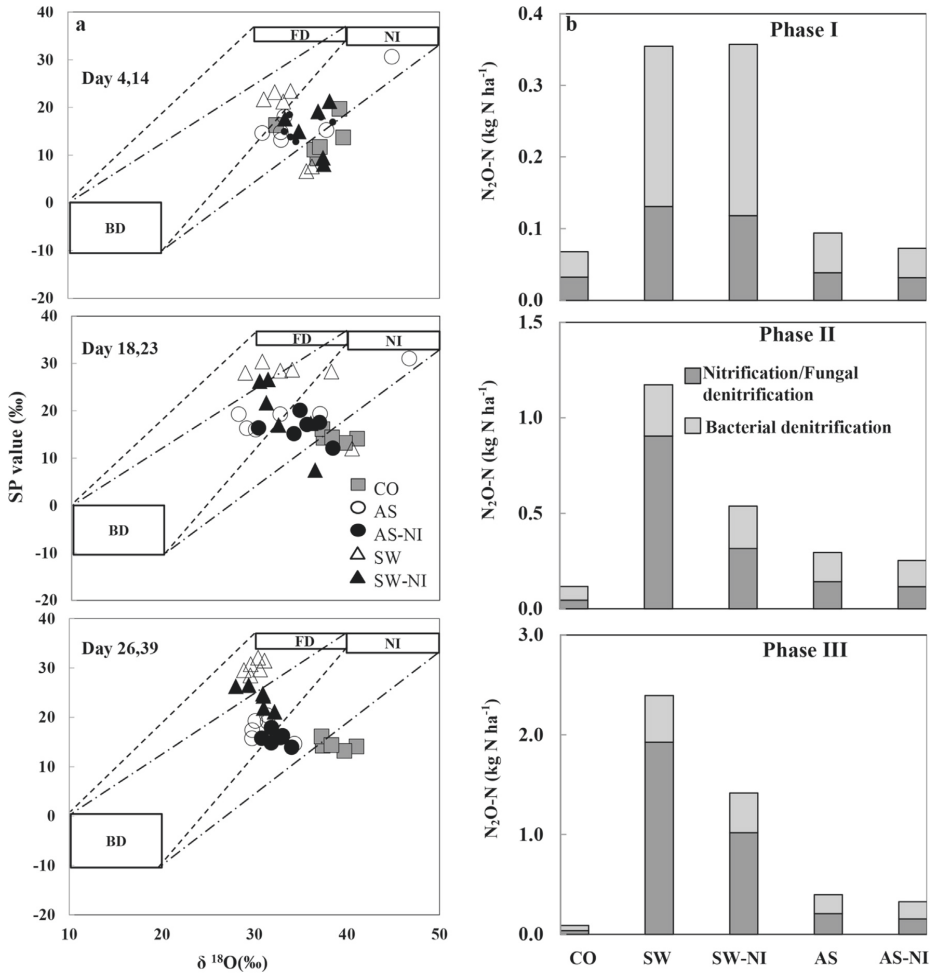

Fig. 5. (a) End-member map of nitrification (NI), bacterial denitrification (BD) and fungal denitrification (FD) with the relationship between SP and $\delta^{18}O$; (b) source partitioning (bacterial nitrification/fungal denitrification vs bacterial denitrification) of soil left unamended (CO), after application of mineral-N only (AS), mineral-N + nitrification inhibitor (AS-NI), mineral-N + straw (SW) or mineral-N + straw + NI (SW-NI), during the 56 days of the incubation experiment at 70% WHC.

consequently decreasing denitrification rates and N_2O emissions (Fig. 1). Secondly, NI could suppress NO_3^- production (Fig. 2) and limit denitrification. Since nitrification supplies NO_3^- as a substrate for denitrification, this inhibits nitrification by the use of NI in N fertilizers in oxic or semi-oxic situations. This may effectively lower the amount of NO_3^- in soils and thus of N_2O emissions (Dobbie and Smith, 2003; Ruser and Schulz, 2015). The low NO_3^- concentration in conjunction with high labile C content could lead to a lower $N_2O/(N_2O + N_2)$ product ratio of denitrification, as was shown in earlier studies (Köster et al., 2015; Miller et al., 2008; Senbayram et al., 2012), and therefore decrease N_2O emissions. Although N_2 emission data was not available in this experiment, Hatch et al. (2005) reported that NI sharply reduced N_2O emissions in a similar incubation study, specifically during anoxic phases with a smaller $N_2O/(N_2O + N_2)$ ratio in NI treatments compared to non-NI treatments.

4.4. The AOB and AOA amoA gene abundance

The AOB *amoA* gene abundances were significantly higher in SW and AS compared to SW-NI and AS-NI at 14 days. However, AOB *amoA* gene abundances in SW and AS were significantly lower than SW-NI and AS-NI at 52 days (Fig. 3). The latter clearly suggests that the addition of NI delayed the emergence of the AOB *amoA* gene abundance peak, which agrees with an earlier study by Di et al. (2014).

There was no significant difference between CO and the other treatments in AOA population abundance at an early stage of the incubation (Fig. 3). However, AOA amoA gene abundance in CO was significantly higher than in the other treatments when N_2O emissions peaked at 26 days. Furthermore, at the end of the incubation experiment the treatments which had the highest NO_3^- content (AS and SW) showed the lowest AOA abundance (Fig. 3), indicating that

AOA growth was inhibited by high soil N content, which agrees with previous reports (Di et al., 2009).

No quantitative relationship was found between N_2O flux and AOB or AOA *amoA* gene abundances; besides when the highest N_2O emission occurred both AOA and AOB populations were relatively low. The application of straw did not have a significant impact on either AOB or AOA *amoA* gene abundances. These results therefore indicate that nitrification should not be responsible for the much higher N_2O emissions in the straw-amended treatments.

4.5. N_2O isotopomer trends and isotopomer-based N_2O source partitioning

N_2O $\delta^{15}N$ values derived for nitrification were reported to be larger than denitrification (Sutka et al., 2006). However, due to the wide range and large variations of reported $\delta^{15}N$ values, e.g. due to different origin, fractionation, soil heterogeneity, natural abundance, $\delta^{15}N^{bulk}$ values are unreliable for use in the source partitioning of N_2O emissions (Baggs, 2008). In our study, the $\delta^{15}N^{bulk}$ values of N_2O showed a declining trend during the incubation trial in all treatments, except for CO (Fig. 4). The decreasing trend in $\delta^{15}N^{bulk}$ values occurred almost precisely when NO_3^- started to increase due to nitrification, which indicates that the decrease was not likely due to a shift from nitrification to denitrification. We presume that the decrease in $\delta^{15}N^{bulk}$ values in the fertilized treatments was likely due to the higher $\delta^{15}N^{bulk}$ values of the original soil NO_3^- as compared to the applied mineral N and the shift of the N_2O source from soil N to mineral fertilizer N, especially in view of the constantly high $\delta^{15}N^{bulk}$ values (4–10‰) of CO.

As oxygen (O) of N_2O precursors, especially nitrite, is exchanged with the O of soil water during nitrification and denitrification, the $\delta^{18}O$ value of N_2O has been shown to reflect the isotope signature of the water and the associated isotope effect (Casciotti et al., 2007; Kool et al., 2009; Rohe et al., 2014), as well as the isotope effect of N_2O reduction to N_2 (Ostrom et al., 2007; Well and Flessa, 2009). As yet, little pure culture data is available, indicating that the $\delta^{18}O$ ranges of nitrification and fungal denitrification might be distinct (Rohe et al., 2014; Sutka et al., 2006). In our study, we combined the $\delta^{18}O$ values of N_2O with SP values in an end-member map in order to distinguish nitrification and fungal denitrification. As can be seen in Fig. 5a, most of the isotopic data spots of SW and SW-NI treatments were in the fungal denitrification zone instead of being in the nitrification zone in the later phases, when the highest N_2O emissions occurred, indicating that fungal denitrification was most likely responsible for the higher N_2O emissions in the straw-amended treatments. The source partitioning (Fig. 5b) provided only a rough estimation for N_2O sources, as the calculations were based on average end-member values without including the N_2O reduction effect, which may lead to some uncertainty in the final source apportionment (Wu et al., 2016).

During the initial phase of the experiment, the lower SP values in the SW and SW-NI treatments clearly indicated that bacterial denitrification was the major source of N_2O emissions, in line with previous reports in comparable soils and treatments which showed that 95% of the emitted N_2O originated from denitrification (Senbayram et al., 2009; Köster et al., 2015). Interestingly, SP values increased over time in all N-fertilized treatments, indicating the dominance of other processes in N_2O emission, e.g. nitrification, or fungal denitrification, or increasing N_2O reduction. It is unlikely that the upshift in SP values was dominated by N_2O reduction to N_2, since $\delta^{18}O$ did not increase simultaneously (Ostrom et al., 2007; Park et al., 2011). Furthermore, higher SP values were found in the later phases of incubation when the soils have higher nitrate and lower labile C, which would be the opposite case if the upshift were due to the N_2O reduction effect. Taking into account the fact that $\delta^{18}O$/SP values were closer to the fungal denitrification/nitrification end-member region (Fig. 5a) in both SW and SW-NI as compared to AS and AS-NI, we therefore speculate that fungal denitrification was the major source of N_2O fluxes in straw-amended treatments at later phases of the experiment.

Additionally, straw decomposition can enhance fungal biomass (Allison and Killham, 1988), and the higher CO_2 fluxes in SW and SW-NI indicated not only a higher substrate availability (especially for denitrifiers), but also higher oxygen consumption, which could therefore encourage denitrification to take place. A similar phenomenon was observed by Köster et al. (2011), where SP values increased while $\delta^{18}O$ values were more constant over time after biogas residue application at 80% WFPS. However, the authors hypothesized that this observation may indicate a rapid shift from denitrification to nitrification due to depletion of organic carbon over the course of the incubation. In our experiment, 58.7% of C amended in the straw treatments was still in the soil at the end of the incubation, based on cumulative CO_2 fluxes. In addition, the CO_2 emission rate in straw-amended treatments stayed clearly higher during the whole incubation period compared to the treatments without straw addition (Fig. 1). Therefore, the increase in SP values cannot be linked directly to the depletion of available C. Adding labile C, as was present in SW and SW-NI, led to 5-fold higher N_2O emissions compared to non-straw-amended treatments. Additionally, the observed N_2O yields in straw-amended treatments were far beyond the expected N_2O yield (0.1–1% of added NH_4^+) from autotrophic nitrification (Well et al., 2008). Hence, the high N_2O fluxes and SP values cannot be attributed to nitrification.

On the basis of the combined information provided by both N_2O isotopomer analysis and AOA and AOB abundance analysis, we conclude that fungal denitrification should be the major process contributing to the higher N_2O emissions in straw-amended treatments. Fungal denitrification was assumed to play only a small role in the N cycle. However, based on the outcomes of recent studies using both molecular biological techniques and isotopomers, it is now thought that fungal denitrification may function as a major process in the N cycle (Shoun et al., 2012; Sutka et al., 2008). Laughlin and Stevens (2002) reported on the basis of the substrate-induced-respiration-inhibition (SIRIN) approach that fungi are responsible for most of the N_2O production in a grassland soil. In cropland soil, fungi have also been identified using SIRIN as the main contributor to the observed N_2O emission after organic fertilizer application (Wei et al., 2014). In an incubation experiment that was comparable to ours, but performed under completely anoxic conditions (excluding nitrification) by Köster et al. (2013b), the authors observed higher SP values at later stages of the experiment, thereby also suggesting an increasing dominance of fungal denitrification during the course of the experiment. It should be noted that in the current study the N_2O reduction effect on SP values was neglected, as it is impossible to quantify without N_2 data, which were not available. We may thus underestimate the emission of N_2O from bacterial denitrification to a certain degree (Wu et al., 2016). However, it is well accepted that the isotopomer-based N_2O source partitioning calculations provide only rough estimates of the pathways contributing to N_2O production due to the complexity and interrelation between the processes involved (Decock and Six, 2013; Lewicka-Szczebak et al., 2014). Furthermore, the precise ranges of SP values of other processes, e.g. heterotrophic nitrification, aerobic denitrification, co-denitrification, are still unknown. That is to say, a final proof of our hypothesis of fungal denitrification as the dominant process in N_2O production is currently not possible based solely on SP values or the apportionment of the ^{18}O vs SP values in the plotted data.

5. Conclusions

Straw incorporation in conjunction with mineral N fertilizer in cropland triggered higher soil-borne N_2O emissions. We found indications based on isotopomer values that the N_2O emissions were initially predominantly derived from bacterial denitrification (day 0–10), but later on (day 11–55) in the experimental period likely mainly resulted from fungal denitrification. The results of our study showed that use of NI has great potential (41% mitigation of N_2O emission) for mitigating N_2O fluxes especially under our experimental conditions (high soil moisture, straw amended) favoring denitrification.

Acknowledgements

The authors thank the Institute of Applied Plant Nutrition (IAPN), University of Göttingen, for financial support. This study was supported by the Chinese Scholarship Council (scholarship no. 201306350130).

Appendix A. Supplementary data

Supplementary data related to this article can be found at http://dx.doi.org/10.1016/j.soilbio.2016.10.022.

References

Akiyama, H., Yan, X.Y., Yagi, K., 2010. Evaluation of effectiveness of enhanced-efficiency fertilizers as mitigation options for N_2O and NO emissions from agricultural soils: meta-analysis. Glob. Change Biol. 16, 1837–1846.
Allison, M.F., Killham, K., 1988. Response of soil microbial biomass to straw incorporation. J. Soil Sci. 39, 237–242.
Baggs, E.M., 2008. A review of stable isotope techniques for N_2O source partitioning in soils: recent progress, remaining challenges and future considerations. Rapid Commun. Mass Spectrom. 22, 1664–1672.
Baggs, E.M., Rees, R.M., Smith, K.A., Vinten, A.J.A., 2000. Nitrous oxide emission from soils after incorporating crop residues. Soil Use Manag. 16, 82–87.
Bollmann, A., Conrad, R., 1998. Influence of O_2 availability on NO and N_2O release by nitrification and denitrification in soils. Glob. Change Biol. 4, 387–396.
Bouwman, A.F., Beusen, A.H.W., Griffioen, J., Groenigen, J.W.V., Hefting, M.M., Oenema, O., Puijenbroek, P.J.T.M.V., Seitzinger, S., Slomp, C.P., Stehfest, E., 2013. Global trends and uncertainties in terrestrial denitrification and N_2O emissions. Phil. Trans. R. Soc. Lond. B: Biol. Sci. 368, 20130112.
Bouwman, A.F., Boumans, L.J.M., Batjes, N.H., 2002. Emissions of N_2O and NO from fertilized fields: summary of available measurement data. Glob. Biogeochem. Cycles 16, 1058.
Brenninkmeijer, C.A.M., Röckmann, T., 1999. Mass spectrometry of the intramolecular nitrogen isotope distribution of environmental nitrous oxide using fragment-ion analysis. Rapid Commun. Mass Spectrom. 13, 2028–2033.
Burford, J.R., Bremner, J.M., 1975. Relationships between the denitrification capacities of soils and total, water-soluble and readily decomposable soil organic matter. Soil Biol. Biochem. 7, 389–394.
Casciotti, K.L., Boehlke, J.K., McIlvin, M.R., Mroczkowski, S.J., Hannon, J.E., 2007. Oxygen isotopes in nitrite: analysis, calibration, and equilibration. Anal. Chem. 79, 2427–2436.
Ciais, P., Sabine, C., Bala, G., Bopp, L., Brovkin, V., Canadell, J., Chhabra, A., DeFries, R., Galloway, J., Heimann, M., others, 2014. Carbon and other biogeochemical cycles. In: Climate Change 2013: The Physical Science Basis. Contribution of Working Group I to the Fifth Assessment Report of the Intergovernmental Panel on Climate Change. Cambridge University Press, pp. 465–570.
Cleemput, O. van, 1998. Subsoils: chemo-and biological denitrification, N_2O and N_2 emissions. Nutr. Cycling Agroecosyst. 52, 187–194.
Decock, C., Six, J., 2013. How reliable is the intramolecular distribution of ^{15}N in N_2O to source partition N_2O emitted from soil? Soil Biol. Biochem. 65, 114–127.
Di, H.J., Cameron, K.C., Shen, J.P., Winefield, C.S., O'Callaghan, M., Bowatte, S., He, J.Z., 2009. Nitrification driven by bacteria and not archaea in nitrogen-rich grassland soils. Nat. Geosci. 2, 621–624.
Di, H.J., Cameron, K.C., Podolyan, A., Robinson, A., 2014. Effect of soil moisture status and a nitrification inhibitor, dicyandiamide, on ammonia oxidizer and denitrifier growth and nitrous oxide emissions in a grassland soil. Soil Biol. Biochem. 73, 59–68.
Dittert, K., Lampe, C., Gasche, R., Butterbach-Bahl, K., Wachendorf, M., Papen, H., Sattelmacher, B., Taube, F., 2005. Short-term effects of single or combined application of mineral N fertilizer and cattle slurry on the fluxes of radiatively active trace gases from grassland soil. Soil Biol. Biochem. 37, 1665–1674.
Dobbie, K.E., Smith, K.A., 2001. The effects of temperature, water-filled pore space and land use on N2O emissions from an imperfectly drained gleysol. European Journal of Soil Science 52, 667–673.
Dobbie, K.E., Smith, K.A., 2003. Impact of different forms of N fertilizer on N_2O emissions from intensive grassland. Nutr. Cycling Agroecosyst. 67, 37–46.
Firestone, M., 1982. Biological Denitrification. Nitrogen in Agricultural Soils, 8. ASA-CSSA-SSSA, Madison, pp. 289–326.
Firestone, M., Davidson, E., 1989. Microbiological Basis of NO and N_2O Production and Consumption in Soil. John Wiley and Sons Ltd, Chichester.
Fowler, D., Coyle, M., Skiba, U., Sutton, M.A., Cape, J.N., Reis, S., Sheppard, L.J., Jenkins, A., Grizzetti, B., Galloway, J.N., Vitousek, P., Leach, A., Bouwman, A.F., Butterbach-Bahl, K., Dentener, F., Stevenson, D., Amann, M., Voss, M., 2013. The global nitrogen cycle in the twenty-first century. Phil. Trans. R. Soc. B 368, 20130164.
Goek, M., Ottow, J.C.G., 1988. Effect of cellulose and straw incorporation in soil on total denitrification and nitrogen immobilization at initially aerobic and permanent anaerobic conditions. Biol. Fertil. Soils 5, 317–322.
Hatch, D., Trindade, H., Cardenas, L., Carneiro, J., Hawkins, J., Scholefield, D., Chadwick, D., 2005. Laboratory study of the effects of two nitrification inhibitors on greenhouse gas emissions from a slurry-treated arable soil: impact of diurnal temperature cycle. Biol. Fertil. Soils 41, 225–232.
Heil, J., Liu, S., Vereecken, H., Brüggemann, N., 2015. Abiotic nitrous oxide production from hydroxylamine in soils and their dependence on soil properties. Soil Biol. Biochem. 84, 107–115.
Huber, D.M., Warren, H.L., Nelson, D.W., Tsai, C.Y., 1977. Nitrification inhibitors—new tools for food production. BioScience 27, 523–529.
Hu, Y.L., Wu, F.P., Zeng, D.H., Chang, S.X., 2014. Wheat straw and its biochar had contrasting effects on soil C and N cycling two growing seasons after addition to a Black Chernozemic soil planted to barley. Biol. Fertil. Soils 50, 1291–1299.
Jiang, D., Zhuang, D., Fu, J., Huang, Y., Wen, K., 2012. Bioenergy potential from crop residues in China: availability and distribution. Renew. Sustain. Energ. Rev. 16, 1377–1382.
Khalil, K., Mary, B., Renault, P., 2004. Nitrous oxide production by nitrification and denitrification in soil aggregates as affected by O_2 concentration. Soil Biol. Biochem. 36, 687–699.
Kool, D.M., Müller, C., Wrage, N., Oenema, O., Van Groenigen, J.W., 2009. Oxygen exchange between nitrogen oxides and H_2O can occur during nitrifier pathways. Soil Biol. Biochem. 41, 1632–1641.
Köster, J.R., Cárdenas, L., Bol, R., Lewicka-Szczebak, D., Senbayram, M., Well, R., Giesemann, A., Dittert, K., 2015. Anaerobic digestates lower N_2O emissions compared to cattle slurry by affecting rate and product stoichiometry of denitrification – an N_2O isotopomer case study. Soil Biol. Biochem. 84, 65–74.
Köster, J.R., Cárdenas, L., Senbayram, M., Bol, R., Well, R., Butler, M., Mühling, K.H., Dittert, K., 2011. Rapid shift from denitrification to nitrification in soil after biogas residue application as indicated by nitrous oxide isotopomers. Soil Biol. Biochem. 43, 1671–1677.
Köster, J.R., Well, R., Tuzson, B., Bol, R., Dittert, K., Giesemann, A., Emmenegger, L., Manninen, A., Cárdenas, L., Mohn, J., 2013a. Novel laser spectroscopic technique for continuous analysis of N_2O isotopomers – application and intercomparison with isotope ratio mass spectrometry. Rapid Commun. Mass Spectrom. 27, 216–222.
Köster, J.R., Well, R., Dittert, K., Giesemann, A., Lewicka-Szczebak, D., Mühling, K.-H., Herrmann, A., Lammel, J., Senbayram, M., 2013b. Soil denitrification potential and its influence on N_2O reduction and N_2O isotopomer ratios. Rapid Commun. Mass Spectrom. 27, 2363–2373.
Kumar, U., Jain, M.C., Pathak, H., Kumar, S., Majumdar, D., 2000. Nitrous oxide emission from different fertilizers and its mitigation by nitrification inhibitors in irrigated rice. Biol. Fertil. Soils 32, 474–478.
Lassaletta, L., Billen, G., Grizzetti, B., Garnier, J., Leach, A.M., Galloway, J.N., 2014. Food and feed trade as a driver in the global nitrogen cycle: 50-year trends. Biogeochemistry 118, 225–241.
Laughlin, R.J., Stevens, R.J., 2002. Evidence for fungal dominance of denitrification and codenitrification in a grassland soil. Soil Sci. Soc. Am. J. 66, 1540–1548.
Lewicka-Szczebak, D., Well, R., Köster, J.R., Fuß, R., Senbayram, M., Dittert, K., Flessa, H., 2014. Experimental determinations of isotopic fractionation factors associated with N_2O production and reduction during denitrification in soils. Geochim. et Cosmochimi. Acta 134, 55–73.
Li, L.J., Han, X.Z., You, M.Y., Horwath, W.R., 2013. Nitrous oxide emissions from Mollisols as affected by long-term applications of organic amendments and chemical fertilizers. Sci. Total Environ. 452, 302–308.
Loecke, T.D., Robertson, G.P., 2009. Soil resource heterogeneity in terms of litter aggregation promotes nitrous oxide fluxes and slows decomposition. Soil Biol. Biochem. 41, 228–235.
Ma, J., Li, X.L., Xu, H., Han, Y., Cai, Z.C., Yagi, K., 2007. Effects of nitrogen fertiliser and wheat straw application on CH_4 and N_2O emissions from a paddy rice field. Soil Res. 45, 359–367.
Menendez, S., Barrena, I., Setien, I., Gonzalez-Murua, C., Estavillo, J.M., 2012. Efficiency of nitrification inhibitor DMPP to reduce nitrous oxide emissions under different temperature and moisture conditions. Soil Biol. Biochem 53, 82–89.
Miller, M.N., Zebarth, B.J., Dandie, C.E., Burton, D.L., Goyer, C., Trevors, J.T., 2008. Crop residue influence on denitrification, N_2O emissions and denitrifier community abundance in soil. Soil Biol. Biochem 40, 2553–2562.
Müller, C., Stevens, R.J., Laughlin, R.J., Azam, F., Ottow, J.C.G., 2002. The nitrification inhibitor DMPP had no effect on denitrifying enzyme activity. Soil Biol. Biochem. 34, 1825–1827.
Myrold, D.D., Tiedje, J.M., 1985. Establishment of denitrification capacity in soil:

effects of carbon, nitrate and moisture. Soil Biol. Biochem. 17, 819–822.
Nishio, T., Komada, M., Arao, T., Kanamori, T., 2001. Simultaneous determination of transformation rates of nitrate in soil. Jpn. Agric. Res. Q. 35, 11–17.
Ostrom, N.E., Pitt, A., Sutka, R., Ostrom, P.H., Grandy, A.S., Huizinga, K.M., Robertson, G.P., 2007. Isotopologue effects during N2O reduction in soils and in pure cultures of denitrifiers. J. Geophys. Res.: Biogeosciences 2005–2012, 112.
Park, S., Pérez, T., Boering, K.A., Trumbore, S.E., Gil, J., Marquina, S., Tyler, S.C., 2011. Can N_2O stable isotopes and isotopomers be useful tools to characterize sources and microbial pathways of N_2O production and consumption in tropical soils? Glob. Biogeochem. Cycles 25 (1).
Pereira, J., Fangueiro, D., Chadwick, D.R., Misselbrook, T.H., Coutinho, J., Trindade, H., 2010. Effect of cattle slurry pre-treatment by separation and addition of nitrification inhibitors on gaseous emissions and N dynamics: a laboratory study. Chemosphere 79, 620–627.
Prasad, R., Power, J., 1995. Nitrification inhibitors for agriculture, health, and the environment. Adv. Agron. (USA) 263–268.
Qiao, C., Liu, L., Hu, S., Compton, J.E., Greaver, T.L., Li, Q., 2015. How inhibiting nitrification affects nitrogen cycle and reduces environmental impacts of anthropogenic nitrogen input. Glob. Change Biol. 21, 1249–1257.
Ravishankara, A.R., Daniel, J.S., Portmann, R.W., 2009. Nitrous oxide (N_2O): the dominant ozone-depleting substance emitted in the 21st century. Science 326, 123–125.
Rohe, L., Anderson, T.-H., Braker, G., Flessa, H., Giesemann, A., Lewicka-Szczebak, D., Wrage-Mönnig, N., Well, R., 2014. Dual isotope and isotopomer signatures of nitrous oxide from fungal denitrification–a pure culture study. Rapid Commun. Mass Spectrom. 28, 1893–1903.
Ruser, R., Schulz, R., 2015. The effect of nitrification inhibitors on the nitrous oxide (N_2O) release from agricultural soils-a review. J. Plant Nutr. Soil Sci. 178, 171–188.
Senbayram, M., Chen, R., Budai, A., Bakken, L., Dittert, K., 2012. N_2O emission and the $N_2O/(N_2O + N_2)$ product ratio of denitrification as controlled by available carbon substrates and nitrate concentrations. Agric. Ecosyst. Environ. 147, 4–12.
Senbayram, M., Chen, R., Mühling, K.H., Dittert, K., 2009. Contribution of nitrification and denitrification to nitrous oxide emissions from soils after application of biogas waste and other fertilizers. Rapid Commun. Mass Spectrom. 23, 2489–2498.
Shoun, H., Fushinobu, S., Jiang, L., Kim, S.-W., Wakagi, T., 2012. Fungal denitrification and nitric oxide reductase cytochrome P450nor. Philos. Trans. R. Soc. B: Biol. Sci. 367, 1186–1194.
Snider, D.M., Venkiteswaran, J.J., Schiff, S.L., Spoelstra, J., 2013. A new mechanistic model of δ18O-N2O formation by denitrification. Geochimica et Cosmochimica Acta 112, 102–115.
Stevens, R.J., Laughlin, R.J., Atkins, G.J., Prosser, S.J., 1993. Automated determination of nitrogen-15-labeled dinitrogen and nitrous oxide by mass spectrometry. Soil Sci. Soc. Am. J. 57, 981.
Subbarao, G.V., Ito, O., Sahrawat, K.L., Berry, W.L., Nakahara, K., Ishikawa, T., Watanabe, T., Suenaga, K., Rondon, M., Rao, I.M., 2006. Scope and strategies for regulation of nitrification in agricultural systems—challenges and opportunities. Crit. Rev. Plant Sci. 25, 303–335.
Sutka, R.L., Adams, G.C., Ostrom, N.E., Ostrom, P.H., 2008. Isotopologue fractionation during N_2O production by fungal denitrification. Rapid Commun. Mass Spectrom. 22, 3989–3996.
Sutka, R.L., Ostrom, N.E., Ostrom, P.H., Breznak, J.A., Gandhi, H., Pitt, A.J., Li, F., 2006. Distinguishing nitrous oxide production from nitrification and denitrification on the basis of isotopomer abundances. Appl. Environ. Microbiol. 72, 638–644.
Sutton, M.A., Howard, C.M., Erisman, J.W., Billen, G., Bleeker, A., Grennfelt, P., van Grinsven, H., Grizzetti, B., 2011. The European Nitrogen Assessment: Sources, Effects and Policy Perspectives. Cambridge University Press.
Tang, H.M., Xiao, X.P., Tang, W.G., Wang, K., Sun, J.M., Li, W.Y., Yang, G.L., 2014. Effects of winter cover crops straws incorporation on CH_4 and N_2O emission from double-cropping paddy fields in southern China. PLoS One 9, e108322.
Tian, Z., Wang, J.J., Liu, S., Zhang, Z., Dodla, S.K., Myers, G., 2015. Application effects of coated urea and urease and nitrification inhibitors on ammonia and greenhouse gas emissions from a subtropical cotton field of the Mississippi delta region. Sci. Total Environ. 533, 329–338.
Toyoda, S., Mutobe, H., Yamagishi, H., Yoshida, N., Tanji, Y., 2005. Fractionation of N_2O isotopomers during production by denitrifier. Soil Biol. Biochem. 37, 1535–1545.
Toyoda, S., Yoshida, N., 1999. Determination of nitrogen isotopomers of nitrous oxide on a modified isotope ratio mass spectrometer. Anal. Chem. 71, 4711–4718.
Weier, K.L., Doran, J.W., Power, J.F., Walters, D.T., 1993. Denitrification and the dinitrogen/nitrous oxide ratio as affected by soil water, available carbon, and nitrate. Soil Sci. Soc. Am. J. 57, 66–72.
Wei, W., Isobe, K., Shiratori, Y., Nishizawa, T., Ohte, N., Otsuka, S., Senoo, K., 2014. N_2O emission from cropland field soil through fungal denitrification after surface applications of organic fertilizer. Soil Biol. Biochem. 69, 157–167.
Well, R., Flessa, H., 2009. Isotopologue enrichment factors of N_2O reduction in soils. Rapid Commun. Mass Spectrom. 23, 2996–3002.
Well, R., Flessa, H., Xing, L., Xiaotang, J., Römheld, V., 2008. Isotopologue ratios of N_2O emitted from microcosms with NH_4^+ fertilized arable soils under conditions favoring nitrification. Soil Biol. Biochem. Spec. Sect.: Enzym. Environ. III 40, 2416–2426.
Wrage, N., Velthof, G.L., Laanbroek, H.J., Oenema, O., 2004. Nitrous oxide production in grassland soils: assessing the contribution of nitrifier denitrification. Soil Biol. Biochem. 36, 229–236.
Wu, D., Köster, J.R., Cárdenas, L.M., Brüggemann, N., Lewicka-Szczebak, D., Bol, R., 2016. N_2O source partitioning in soils using ^{15}N site preference values corrected for the N_2O reduction effect. Rapid Commun. Mass Spectrom. 30, 620–626.
Yamulki, S., 2006. Effect of straw addition on nitrous oxide and methane emissions from stored farmyard manures. Agric. Ecosyst. Environ. 112, 140–145.
Zerulla, W., Barth, T., Dressel, J., Erhardt, K., Von Locquenghien, K.H., Pasda, G., Radle, M., Wissemeier, A.H., 2001. 3,4-Dimethylpyrazole phosphate (DMPP) - a new nitrification inhibitor for agriculture and horticulture. Biol. Fertil. Soils 34, 79–84.
Zhu, K., Bruun, S., Larsen, M., Glud, R.N., Jensen, L.S., 2015. Heterogeneity of O_2 dynamics in soil amended with animal manure and implications for greenhouse gas emissions. Soil Biol. Biochem. 84, 96–106.
Zou, J., Huang, Y., Jiang, J., Zheng, X., Sass, R.L., 2005. A 3-year field measurement of methane and nitrous oxide emissions from rice paddies in China: effects of water regime, crop residue, and fertilizer application. Glob. Biogeochem. Cycles 19, GB2021.

Paper III

The effect of nitrification inhibitor on N_2O, NO and N_2 emissions under different soil moisture levels in a permanent grassland soil

Wu, D., Cárdenas, L. M., Calvet, S., Brüggemann, N., Loick, N., Liu, S., & Bol, R. 2017

Soil Biology and Biochemistry 113, 153-160.

Soil Biology & Biochemistry 113 (2017) 153–160

Contents lists available at ScienceDirect

Soil Biology & Biochemistry

journal homepage: www.elsevier.com/locate/soilbio

The effect of nitrification inhibitor on N_2O, NO and N_2 emissions under different soil moisture levels in a permanent grassland soil

Di Wu [a, *], Laura M. Cárdenas [b], Salvador Calvet [c], Nicolas Brüggemann [a], Nadine Loick [b], Shurong Liu [a], Roland Bol [a]

[a] Institute of Bio- and Geosciences, Agrosphere (IBG-3), Forschungszentrum Jülich GmbH, Jülich, Germany
[b] Rothamsted Research, North Wyke, Okehampton, Devon EX20 2SB, UK
[c] Institute of Animal Science and Technology, Universitat Politècnica de Valencia, Spain

ARTICLE INFO

Article history:
Received 7 December 2016
Received in revised form
30 May 2017
Accepted 5 June 2017

Keywords:
Nitrification inhibitor
Denitrification
Nitrous oxide
Nitric oxide
Dinitrogen
Isotopomer

ABSTRACT

Emissions of gaseous forms of nitrogen from soil, such as nitrous oxide (N_2O) and nitric oxide (NO), have shown great impact on global warming and atmospheric chemistry. Although in soil both nitrification and denitrification could cause N_2O and NO emissions, most studies demonstrated that denitrification is the dominant process responsible for the increase of atmospheric N_2O, while nitrification produces mostly NO. The use of nitrification inhibitors (NIs) has repeatedly been shown to reduce both N_2O and NO emissions from agricultural soils; nevertheless, the efficiency of the mitigation effect varies greatly. It is generally assumed that nitrification inhibitors have no direct effect on denitrification. However, the indirect impact, due to the reduced substrate (nitrate) delivery to microsites where denitrification occurs, may have significant effects on denitrification product stoichiometry that may significantly lower soil-borne N_2O emissions. Soil-water status is considered to have a remarkable effect on the relative fluxes of nitrogen gases. The effect and mechanism of NI on N_2O, NO and N_2 emission under different soil water-filled pore space (WFPS) is still not well explored. In the present study, we conducted a soil incubation experiment in an automated continuous-flow incubation system under a He/O_2 atmosphere. Ammonium sulfate was applied with and without NI (DMPP) to a permanent UK grassland soil under three different soil moisture conditions (50, 65, and 80% WFPS). With every treatment, glucose was applied to supply enough available carbon for denitrification. Emissions of CO_2, N_2O, NO and N_2 were investigated. Additionally, isotopic signatures of soil-emitted N_2O were analyzed. Generally, higher WFPS led to higher N_2O and NO emissions, while N_2 emissions were only detected at high soil moisture condition (80% WFPS). Different processes were responsible for N_2O and NO emission in different phases of the incubation period. The application of DMPP did significantly reduce both N_2O and NO emissions at all three soil moisture conditions. Furthermore, DMPP application increased N_2 emissions and decreased the $N_2O/(N_2O + N_2)$ product ratio at 80% WFPS.

1. Introduction

Emissions of nitrogenous gases from agricultural soil, such as nitrous oxide (N_2O), nitric oxide (NO) and dinitrogen (N_2), represent a loss of N fertilizer and a reduction of plants N use efficiency (Bouwman et al., 2013). Grasslands, which are the dominant global ecosystem and cover 17% world surface, are also one of the main sources of N_2O and NO emissions (Cárdenas et al., 2007; Stehfest and Bouwman, 2006). Both N_2O and NO have great impact on global environmental change and atmospheric chemistry. Nitrous oxide has a global warming potential of about 300 times that of CO_2 and is considered as the major cause of ozone layer depletion in the 21st century (Bouwman et al., 2002; Myhre et al., 2013). Global anthropogenic N_2O emissions are estimated as approx. 6.5 Tg N yr^{-1} in 2010 (IPCC, 2013), of which soils are the largest source (Ciais et al., 2014). Although both nitrification and denitrification could produce N_2O in soil, recent studies suggested that denitrification is the dominant process responsible for the increase in atmospheric N_2O (Baggs, 2008). Denitrifying activity could be exhibited by both

* Corresponding author. Institute of Bio- and Geosciences, Agrosphere (IBG-3), Forschungszentrum Jülich GmbH, 52425 Jülich, Germany.
E-mail address: w.di@fz-juelich.de (D. Wu).

http://dx.doi.org/10.1016/j.soilbio.2017.06.007
0038-0717/

bacteria and fungi. However, fungal denitrification pathway, which recently has been found to be a major process in the nitrogen cycle, is not capable of reducing N_2O to N_2 (Laughlin and Stevens, 2002; Shoun et al., 2012). Anthropogenic nitrogen oxide (NO_x = NO + NO_2) emissions were estimated as approx. 43 TgN yr^{-1} in 2010 globally (IPCC, 2013). The atmospheric lifetime of NO_x is relatively short (1–2 days), but as they are readily deposited on land and water surfaces (soil, plants, open waters), they lead to eutrophication and acidification of ecosystems (Crutzen, 1979). A recent study indicates that NO also plays an important role in haze formation of urban air pollution (Guo et al., 2014). In soil, NO can be produced by both nitrification and denitrification, as NO is not only a facultative by-product of the nitrification pathway, but also an obligatory intermediate of the denitrification pathway (Skiba et al., 1997). Nevertheless, nitrification is believed to be the main source of NO, as the diffusion of NO is restricted at high soil moisture contents and NO produced from denitrification is reduced to N_2O before it escapes to the soil surface (Davidson, 1992; Firestone and Davidson, 1989; Skiba et al., 1997). Yet some studies showed that denitrification could also be a major source of NO emission from soils (Cárdenas et al., 1993; Loick et al., 2016; Pereira et al., 2010; Sanhueza et al., 1990).

Nitrification inhibitors (NIs) have been widely tested and studied for the purpose of decreasing nitrate leaching and mitigating greenhouse gas (GHG) emissions. Nitrification inhibitors are a group of chemical compounds that can reduce the bacterial oxidation of ammonium (NH_4^+) to nitrite (NO_2^-) in the soil by inhibiting the activity of ammonia-oxidizing bacteria, e.g., of the genus *Nitrosomas*, in the soil (Zerulla et al., 2001). Most of NIs inhibit the first enzymatic step of nitrification, which is catalyzed by the enzyme ammonia monooxygenase (AMO) (Subbarao et al., 2006). A large number of NIs are known, but only a few of them, such as dicyandiamide (DCD) and 3, 4-Dimethylpyrazole phosphate (DMPP), have been widely and commercially used (Ruser and Schulz, 2015). The addition of NIs has been frequently reported to reduce both N_2O and NO emissions from agricultural soils, although their efficiency varies greatly in different environments (Pereira et al., 2010; Ruser and Schulz, 2015). Interestingly, some authors reported that the use of the NI reduced N_2O emission more effectively under higher soil moisture level, which is more favoured by denitrification (Di et al., 2014; Menendez et al., 2012). Although previous studies showed that most NIs did not have a direct effect on denitrification (Bremner and Yeomans, 1986; Müller et al., 2002), other studies suggested that denitrification-derived N_2O emission may also be affected by NIs indirectly via altering the product stoichiometry of denitrification (Hatch et al., 2005; Wu et al., 2017). As a key process of the global N cycle, denitrification leads to significant N losses from agricultural systems by converting NO_3^- and NO_2^- into NO, N_2O and N_2 (Bouwman et al., 2013). However, the product stoichiometry of denitrification, which is usually studied as $N_2O/(N_2O + N_2)$ product ratio, is affected by factors such as soil NO_3^- concentration, water-filled pore space (WFPS), and soil available carbon (C) (Weier et al., 1993). The effects of these factors on the product ratio are still not well understood, as the direct and precise measurements of N_2 production via denitrification in soils are challenging due to the high N_2 abundance in the atmosphere.

The difference between ^{15}N at the central (α position) and the terminal N atom (β position) in the asymmetric N_2O molecule (^{15}N site preference, SP) has been shown as useful indicators of N_2O production and consumption processes in soils (bacterial nitrification: 34–37‰, bacterial denitrification: -10-0‰) (Sutka et al., 2008, 2006; Toyoda et al., 2005). The advantages of this isotopic technique are that it is a non-invasive, source-process tracking method, enabling convenient low-cost gaseous sampling, which facilitates investigation of both laboratory incubation and field-scale experiments (Decock and Six, 2013). The limitations of this technique have also been demonstrated, e.g., the uncertainties of N_2O source partitioning due to the overlapping or unknown SP signature of various pathways (Baggs, 2008; Decock and Six, 2013).

The first objective of this study was to examine the effectiveness of NI on mitigating N_2O and NO emissions at different soil moisture conditions in a UK grassland soil, as NIs have been widely used in grazed grassland. Furthermore, as the same soil was used in previous studies to investigate the sources and fate of N pools involving nitrogenous gas emissions (Loick et al., 2016), we further explored the effect of different soil moisture conditions on the fluxes, with and without the presence of NI, and sources of N_2O, NO and N_2, in order to gain a better understanding of the different processes involved, thereby helping to develop better management strategies to mitigate N_2O and NO emissions.

2. Material and methods

2.1. Soil

The soil was collected from a permanent grassland in North Wyke, Devon, UK (50° 46′ 10″ N, 3° 54′ 05″ E) to a depth of 15 cm in November 2013. The soil was classified as clayey pelostagnogley soil (Clayden and Hollis, 1985) (44% clay, 40% silt, 15% sand) and contained 0.5% total N and 11.7% organic matter, with a pH of 5.6. Root and plant residues were removed and the soil was sieved to <2 mm and stored at 4° C since 7 days before rewetting.

2.2. Automated soil incubation experiment

The incubation experiment was carried out at Rothamsted Research, North Wyke, UK, in a denitrification incubation system using a He/O_2 atmosphere (Cárdenas et al., 2003; Loick et al., 2016). Soils were packed into 12 stainless steel vessels of 140 mm diameter at a bulk density of 0.8 g cm^{-3}, which is similar to previous studies (Loick et al., 2016; Meijide et al., 2010). The atmospheric N_2 was removed by flushing the soil core with a mixture of $He:O_2$ (80:20) in order to measure N_2 fluxes. The experiment consisted of 6 treatments in total, i.e. soil amended with mineral N fertilizer (ammonium sulfate) and glucose (AS), or NI (DMPP) mixed with ammonium sulfate and glucose, at 50, 65, and 80% WFPS, respectively (AS50, DMPP50, AS65, DMPP65, AS80, DMPP80). The incubation experiment was conducted in two consecutive runs due to limited numbers of vessels. Prior to incubation, the soil was pre-incubated for 7 days at a soil moisture level that after taking the later amendment into account would achieve the final required WFPS. Ammonium sulfate was applied at a rate of 150 kg N ha^{-1} and glucose was applied at a rate providing 400 kg C ha^{-1}. DMPP was added at rate of 1.5 kg ha^{-1}. The amendment was dissolved in 50 ml water and added to each vessel. The temperature of the incubation cabinet was set at 22 °C.

2.3. Measurement of trace gases

For online trace gas concentration analysis of N_2O and CO_2, gas samples from each incubation vessel were measured every two hours and quantified using a gas chromatograph (Clarus 500, Perkin Elmer Instruments, Beaconsfield, UK), fitted with a flame ionization detector (FID) and methanizer for the quantification of CO_2, and an electron capture detector (ECD) for N_2O. Nitric oxide (NO) emissions were quantified using a chemiluminescence analyzer (Sievers NOA280I. GE Instruments, Colorado, USA). Dinitrogen (N_2) emissions were measured by using a gas chromatograph fitted with a helium ionization detector (VICI AG International, Schenkon, Switzerland) and are presented as average fluxes per day. The flow

rate from each incubation vessel's outlet was measured daily (Loick et al., 2016). Gas concentrations were determined from a 1 ml sample via GC. The gas-flow through the system was determined and fluxes calculated by dividing the gas concentration by the flow rate of the He/O_2 atmosphere through the vessel and the core surface area. Units were then extrapolated to give fluxes in kg N or C per ha per day.

2.4. Isotopomer analysis

Gas samples for isotopic analysis were taken from each incubation vessel by attaching 120-mL serum bottles to the outlets in flow-through mode (with an inlet and an outlet needle) for approx. 1 h during the incubation time. The N_2O $\delta^{15}N^{bulk}$ (i.e., the average $\delta^{15}N$ over the N_2O molecule), $\delta^{15}N_\alpha$ (i.e., $\delta^{15}N$ at the central position of the N_2O molecule), and $\delta^{18}O$ isotope signatures were then determined by analysing *m/z* 44, 45, and 46 of intact N_2O^+ molecular ions, and *m/z* 30 and 31 of NO^+ fragment ions (Toyoda and Yoshida, 1999) on an isotope ratio mass spectrometer (IsoPrime 100, Elementar Analysensysteme, Hanau, Germany). The $\delta^{15}N$ at the terminal position of the N_2O molecule, $\delta^{15}N_\beta$, was calculated according to $\delta^{15}N_\beta = 2 \cdot \delta^{15}N^{bulk} - \delta^{15}N_\alpha$. The details for correction and calibration are described in Heil et al. (2015). The isotope effects during N_2O reduction on N_2O SP values have been calculated using a Rayleigh-type model, assuming that isotope dynamics followed closed-system behaviour. The model can be described as follows:

$$SP_{N_2O\text{-}r} = SP_{N_2O\text{-}0} + \eta_r \ln\left(\frac{C}{C_0}\right)$$

In this equation, $SP_{N2O\text{-}r}$ is the SP value of the remaining substrate (i.e. N_2O), $SP_{N2O\text{-}0}$ is the SP value of the initial substrate, η_r is the net isotope effect (NIE) associated with N_2O reduction, and C and C_0 are the residual and the initial substrate concentration (i.e. C/C_0 expresses the $N_2O/(N_2O + N_2)$ product ratio). In this study an NIE of −4‰ was used based on previously reported average values (Lewicka-Szczebak et al., 2014).

2.5. Analyses of soil

Soil samples were taken at the beginning and end of each incubation to determine the NH_4^+ and total oxidised N ($TON = NO_3^- + NO_2^-$) contents. It is assumed that total oxidised N is nearly exclusively made of NO_3^-, as NO_2^- contents in the soil samples are negligibly small (Burns et al., 1996). The soil samples were extracted with 2 M KCl by shaking for 1 h. The extracts were then filtered through Whatman 602 filter paper (Searle, 1984). The concentrations of NH_4^+ and NO_3^- in soil extracts were measured colorimetrically using a Skalar SANL^{PLUS} Analyzer (Skalar Analytical B.V., Breda, Netherlands).

2.6. Calculations and statistical analysis

The total gas emissions were calculated by linear interpolation between measured fluxes. Emission rates are expressed as arithmetic means of the four replicates. Tukey's HSD post-hoc tests were used to reveal significant pairwise differences among treatments. Statistical analyses were done using R, with $P < 0.05$ used as the criterion for statistical significance.

3. Results

3.1. Gas fluxes

The incubation period was characterized by three phases with different nitrogen gas emission patterns (Figs. 1–3): phase I (0–5 days) with a sharp and high N_2O emission peak, but low or no NO and N_2 emissions; phase II (5–20 days) with low or no N_2O and NO, but relatively high N_2 emissions; and phase III (20–43 days) with slowly decreasing N_2 emission and slowly increasing N_2O and NO emissions.

Nitrous oxide emissions were consistently low at 50% WPFS during all three phases in both AS and DMPP treatments (Fig. 1). Maximum average fluxes of 12.0 ± 1.3 and 7.2 ± 0.1 g N ha^{-1} day^{-1} were observed at the end of phase III in AS and DMPP treatments at 50% WFPS, respectively. At 65% and 80% WFPS, the first N_2O emissions peaks both occurred in phase I about 1.5 days after amendment application. At 80% WFPS the peak was approx. 10-fold larger than at 65% WFPS. The fluxes decreased drastically after the peak and showed constant low emissions rates of approx. 10–15 g N ha^{-1} day^{-1} till the end of phase II. The fluxes then started to increase gradually and peaked at the end of phase III. The second N_2O peak at 65% WFPS was significantly larger than the first peak, while at 80% WFPS it was much lower than the first one but lasted much longer. During the observation period the total N_2O emissions increased with increasing WFPS, while DMPP significantly reduced total N_2O emissions compared with the AS treatments at all three different soil moisture levels.

Fluxes of NO were much lower than those of N_2O (Fig. 2), and total NO emissions were about 8% of total N_2O emissions. NO fluxes showed a gradually increasing trend in all treatments during the 43 days incubation period. They were very low during phase I in all treatments, then started to rise after phase I, with higher NO fluxes in the AS treatments compared to the DMPP treatments (Fig. 2). In all treatments, NO emissions peaked closed to the end of phase III. Larger average NO emissions were observed in treatments with higher soil moisture. The application of DMPP significantly reduced NO emissions compared with the AS treatments at all three soil moisture conditions.

Gaseous nitrogen (N_2) production occurred only at 80% WFPS, where higher N_2 fluxes were observed in the DMPP treatment than in the mineral-N only treatment (Fig. 3). In phase I, the first N_2 fluxes peaked at similar time to N_2O and then decreased until about day 4. In phase II the N_2 fluxes rose again and showed another peak with a maximum at day 12 and then started to decrease and stayed low till the end of the incubation. The cumulative N_2 emissions were 16.4% higher (albeit not statistically significant) in the DMPP treatment compared with the AS treatment.

Carbon dioxide emissions peaked at about 1–1.5 days after amendment application and decreased immediately to about 10 kg C ha^{-1} day^{-1} after 5 days and stayed low for the rest of the incubation for all treatments (Fig. S1).

3.2. NH_4^+ and NO_3^- concentrations in soil

Table 1 shows the concentrations of ammonium (NH_4^+) and nitrate (NO_3^-) in the soil before and after the incubation. The initial soil NH_4^+ and NO_3^- content was 4.2 ± 0.03 and 182.8 ± 2.3 mg N kg^{-1} dry soil, respectively. At the end of the incubation, NO_3^- concentrations at 65% WFPS and 80% WFPS in AS and DMPP treatments were significantly higher than the initial NO_3^- concentration, while no significant difference was found between those at 50% WFPS and the initial NO_3^- concentration. The NO_3^- concentrations at all three soil moisture levels were significantly lower in DMPP treatments compared to those without inhibitor. Ammonium contents at the

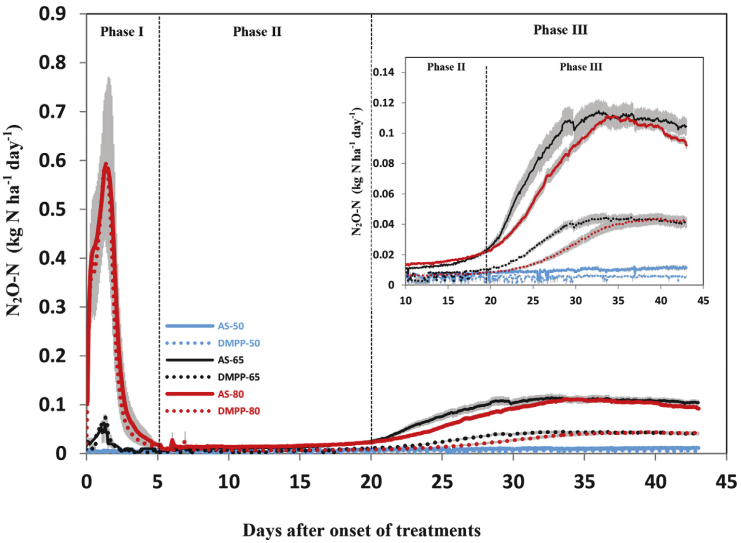

Fig. 1. Fluxes of N_2O of soil with only mineral-N at 50% WFPS (AS-50), or mineral-N+ nitrification inhibitor at 50% WFPS (DMPP-50), or only mineral-N at 65% WFPS (AS-65), or mineral-N + nitrification inhibitor at 65% WFPS (DMPP-65), or only mineral-N at 80% WFPS (AS-80), or mineral-N + nitrification inhibitor at 80% WFPS (DMPP-80), during the 43 days of the incubation experiment. Error bars show the standard error of the mean of each treatment (n = 3).

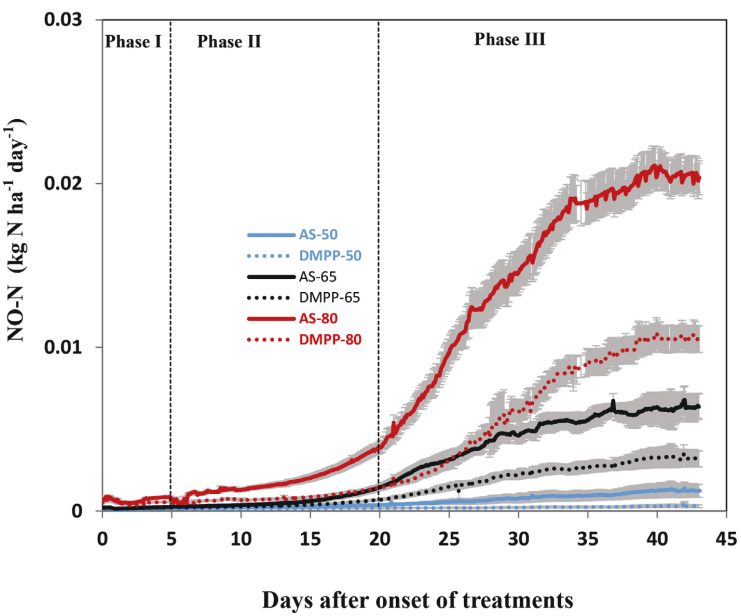

Fig. 2. Fluxes of NO of soil with only mineral-N at 50% WFPS (AS-50), or mineral-N+ nitrification inhibitor at 50% WFPS (DMPP-50), or only mineral-N at 65% WFPS (AS-65), or mineral-N + nitrification inhibitor at 65% WFPS (DMPP-65), or only mineral-N at 80% WFPS (AS-80), or mineral-N + nitrification inhibitor at 80% WFPS (DMPP-80), during the 43 days of the incubation experiment. Error bars show the standard error of the mean of each treatment (n = 3).

end of the incubation were larger than at the beginning in all treatments, and they were larger by 22, 89 and 108% in DMPP treatments compared to the AS treatments at 50, 65, 80% WFPS, respectively (although not statistically significant at 50 and 65% WFPS).

3.3. *Isotopic signatures of soil-emitted N_2O*

The SP values ranged from −6.4–41.0‰ in all treatments during the incubation period (Table 2). At day 0, the N_2O SP values were lower in the higher WFPS treatments, indicating a higher bacterial

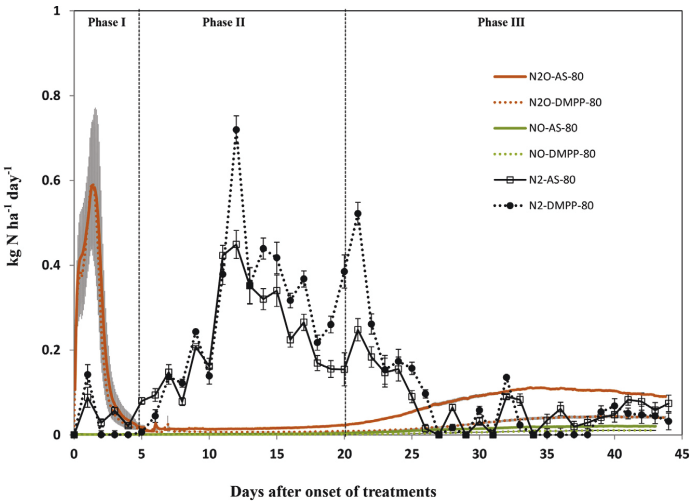

Fig. 3. Fluxes of N_2O, NO and N_2 of soil with only mineral-N at 80% WFPS (AS-80), or mineral-N+ nitrification inhibitor at 80% WFPS (DMPP-80) during the 43 days of the incubation experiment. Error bars show the standard error of the mean of each treatment (n = 3).

Table 1
Nitrate (NO_3^-) and ammonium (NH_4^+) at the end of the experiment of soil with only mineral-N at 50% WFPS (AS-50), or mineral-N + nitrification inhibitor at 50% WFPS (DMPP-50), or only mineral-N at 65% WFPS (AS-65), or mineral-N + nitrification inhibitor at 65% WFPS (DMPP-65), or only mineral-N at 80% WFPS (AS-80), or mineral-N + nitrification inhibitor at 80% WFPS (DMPP-80), during the 43 days of the incubation experiment. Means denoted by a different letter in the same column differ significantly according to the Tukey's HSD post-hoc tests at alfa = 0.05. The capital letters indicate comparison among different soil moisture levels, while the small letters indicate comparison between treatments with or without NI at the same soil moisture level.

Parameter	NO_3^- (mg N kg-1 dry soil)	NH_4^+ (mg N kg-1 dry soil)
Initial	182.8 ± 2.3	4.18 ± 0.03
AS-50	222.0 ± 10.1 $^{A\ a}$	249.7 ± 63.3 $^{A\ a}$
DMPP-50	167.7 ± 2.5 $^{A\ b}$	305.0 ± 35.4 $^{A\ a}$
AS-65	420.5 ± 21.2 $^{B\ a}$	87.5 ± 56.1 $^{B\ a}$
DMPP-65	332.4 ± 16.7 $^{B\ b}$	165.4 ± 65.9 $^{B\ a}$
AS-80	383.3 ± 3.0 $^{B\ a}$	64.0 ± 11.2 $^{B\ a}$
DMPP-80	277.9 ± 10.4 $^{B\ b}$	139.2. ±14.2 $^{B\ b}$

denitrification proportion of N_2O at these soil moisture levels. However, at 80% WPFS, where the highest N_2O peak occurred on day 1, the SP values were 24.4‰ and 35.4‰ in AS and DMPP treatments, respectively, indicating that other major sources (nitrification or fungal denitrification) were involved in the N_2O production. During phase II and phase III, the SP values at all treatments were relatively stable, ranging from 27.9 to 41.0‰ at 50% WFPS, from 26.7 to 32.9‰ at 65% WFPS, and from 19.3 to 27.7‰ at 80% WFPS.

4. Discussion

4.1. Tracing N_2O, N_2 and NO emissions pathways under different WFPS conditions

Soil moisture is a key factor that determines N cycle in soils (Galloway et al., 2004). Several studies found that soil N mineralization rate increased with increasing soil moisture (Bengtson et al., 2005; Zaman and Chang, 2004), while N immobilization was less sensitive to soil moisture (Booth et al., 2005). Nevertheless, compared to N mineralization and immobilization, nitrification rate is more sensitive to moisture, and is believed to increase with increasing soil moisture to a certain content and decline when moisture is above it (Manzoni et al., 2012). It is generally accepted that under oxic conditions nitrification is the main process for N_2O production, while denitrification dominates N_2O production under anoxic conditions. In our study higher soil moisture levels led to higher N_2O emissions, which is in agreement with an earlier study by Davidson et al. (2000), who demonstrated that the highest N_2O fluxes should be expected when denitrification dominates at

Table 2
Site preference (SP) values (‰) of N_2O of soil with only mineral-N at 50% WFPS (AS-50), or mineral-N+ nitrification inhibitor at 50% WFPS (DMPP-50), or only mineral-N at 65% WFPS (AS-65), or mineral-N + nitrification inhibitor at 65% WFPS (DMPP-65), or only mineral-N at 80% WFPS (AS-80)), or mineral-N + nitrification inhibitor at 80% WFPS (DMPP-80), during the 43 days of the incubation experiment. Symbol "-" represents SP values that were not measured at that day, while "*" indicates missing or out of range values due to analytical reasons; the standard error was not given if the replicates were less than three.

Date	Phase I			Phase II		Phase III			
	Day 0	Day 1	Day 3	Day 13	Day 20	Day25	Day 30	Day 34	Day 43
AS-50	20.7 ± 8.4	–	–	–	38.2 ± 3.8	31.6 ± 0.7	30.3 ± 0.7	–	27.9 ± 0.2
DMPP-50	*	–	–	–	*	41.0	38.0	–	*
AS-65	11.3 ± 6.0	–	–	–	*	32.5 ± 1.0	28.7 ± 1.0	–	30.9 ± 0.8
DMPP-65	*	–	–	–	*	32.9	26.7	–	28.4
AS-80	2.3 ± 0.7	24.4 ± 3.7	26.5 ± 4.2	23.8 ± 2.6	–	–	–	27.7 ± 0.9	26.2 ± 2.0
DMPP-80	−6.4	35.4 ± 2.7	31.7 ± 6.8	19.3 ± 0.5	–	–	–	26.9 ± 1.2	24.7 ± 1.5

60–90% WFPS. We assume that the much higher N_2O emissions at 80% WFPS compared with lower soil moisture treatments in phase I were due to enhanced denitrification, which was triggered by the addition of glucose, oxygen depletion, and the soil residual NO_3^- (Fig. 1). This is supported by the initial peaks of N_2 emissions at 80% WFPS in both AS and DMPP treatments, and the absence of N_2 emission in the lower soil moisture treatments (Fig. 3). Furthermore, the smaller SP values observed on day 0 (Table 2) at higher soil moisture also indicated that a larger proportion of N_2O was initially derived from bacterial denitrification (Sutka et al., 2006). Although the smaller SP values might also be interpreted as nitrifier denitrification, it is unlikely the case for our study due to the high available C and high soil moisture condition in phase I (Kool et al., 2011). It should be noted that in our experiment the nitrate concentration in the initial soil was quite high, probably due to the mineralization during long-time storage and pre-incubation. The high nitrate content may have affected the N_2/N_2O ratio towards higher N_2O portions in phase I (Senbayram et al., 2012). Therefore, the results of the same experiment using a soil with lower nitrate content might be different.

According to the SP values (Table 2), the major source of the N_2O peak in phase I at WFPS 80% could have been either nitrification or fungal denitrification, as the overlapping SP signature between the processes makes it impossible to distinguish these two N_2O production pathways (Sutka et al., 2008). However, the fact that the NI showed no effect on the first N_2O emissions peak suggested that the source was unlikely nitrification (Fig. 1). Much larger N_2 emissions occurred at 80% WFPS in phase II, which is in line with Davidson et al. (2000), who suggested N_2 will become the main end product of denitrification when soil moisture is above 80% WFPS. The high N_2O reduction was likely promoted by the developed anaerobic condition caused by the high respiration in phase I. It has been found that nitrate can inhibit N_2O reduction to N_2 and the reduction process only occurs when nitrate content in soil is low (Cleemput, 1998; Senbayram et al., 2012). Therefore, in phase II the observed much larger N_2 emissions at WPFS 80% indicated that the soil NO_3^- content may have fallen below a threshold value at the denitrifying microsites (Fig. 3). At this high soil moisture level, and in combination with the abundant available C and low NO_3^- concentration, this would lead to a low $N_2O/(N_2O + N_2)$ product stoichiometry of denitrification (Senbayram et al., 2012). The N_2O reduction process was likely conducted by bacterial denitrification, as most of the fungal denitrification systems seem to lack N_2O reductase, leaving N_2O as the final product (Shoun et al., 2012). The large decrease of N_2 fluxes after phase II can be explained by the depleted available C as shown by the smaller CO_2 emissions compared to phase I.

An increasing trend of N_2O fluxes was observed in every treatment in phase III (Fig. 1). This increase is probably due to the slowly growing nitrifying bacteria, as the grassland soil used in the current study has not been fertilized for over 20 years. A similar delay in N_2O emission after fertilization was observed by Brümmer et al. (2008) for a previously unfertilized agricultural soil in Burkina Faso after adding ammonium nitrate to the soil. In fact, at the end of phase III, emissions had still not gone down to background levels. Nevertheless, the emissions were smaller, slower and of longer duration compared to the first peak. The incubation was therefore stopped as the system seemed to have reached steady state. This may affect the estimation of the NI's reduction potential, but should have no significant effect on our final conclusion.

In our study the high average N_2O SP values observed at all three soil moisture conditions during phase III indicated that N_2O emissions mainly originated from nitrification or fungal denitrification (Table 2). It could be assumed that the larger N_2O emissions observed at high soil moisture condition were possibly produced through denitrification (Bollmann and Conrad, 1998). However, in our study the lower NH_4^+ at the end of the experiment with rising soil moisture content indicated nitrification was likely also enhanced by higher soil moisture (Table 1). Although the high soil moisture is generally believed to favor denitrification, it could also accelerate nitrification if the conditions are still oxic, which might occur through diffusion of atmospheric oxygen from the headspace in our study (Cheng et al., 2014; Chen et al., 2015; Loick et al., 2016). Furthermore, the fact that the NI significantly decreased N_2O emission in this phase at all three soil moisture conditions would indicate that nitrification is an important process in regulating N_2O emissions. The marginal N_2 fluxes and the smaller SP values observed at WFPS 80% during phase III indicate that very likely bacterial denitrification was also involved. Thus, we conclude that both nitrification and denitrification were responsible for the observed larger N_2O emissions at 80% WFPS soil moisture condition.

It was suggested that the highest NO fluxes should be expected at 30–60% WFPS, when nitrification dominates, as the NO can diffuse out of the soil before it is consumed, whereas at high soil moisture, when gas diffusion is lower, NO emission should be low, as it is reduced to N_2O before escaping the soil (Bollmann and Conrad, 1998; Davidson et al., 2000; Skiba et al., 1997). In the present study, however, the NO emissions significantly increased with increasing WFPS from 50% to 80%, which therefore suggests that the larger amounts of NO at 80% WFPS are probably produced through denitrification (Fig. 2). Although many studies did suggest that emitted NO is mainly produced by nitrification (Scheer et al., 2008; Skiba et al., 1997, 1993), several studies have challenged this assumption and found denitrification could also be a major source of NO emission from soils (Cárdenas et al., 1993; Loick et al., 2016; Pereira et al., 2010; Sanhueza et al., 1990). To distinguish the relative contributions of nitrification and denitrification to NO and N_2O production, the N_2O/NO emission ratio has been proposed as a useful indicator. When the N_2O/NO emission ratio is < 1, soil conditions are favourable for nitrification, whereas emission ratios >10 are associated with denitrification and restricted aeration (Lipschultz et al., 1981; Skiba et al., 1993). During the first phase of our incubation experiment, the average N_2O/NO ratios in AS treatments were 70, 151, and 383 at 50, 65, 80% WFPS, respectively. This clearly reinforced our assumption that N-fluxes were mainly associated with denitrification in phase I, when increasing soil moisture increased the contribution of denitrification. In phase II and III, when NO emissions increased sharply, the average N_2O/NO ratios were 18, 22, and 7 at 50, 65, 80% WFPS, respectively. The significantly lower ratios at 80% WFPS confirm our hypothesis that the higher NO emissions at 80% WFPS might be caused by a higher nitrification rate, as mentioned previously, although both nitrification and denitrification were likely involved. Similarly, Cheng et al. (2014) reported NO and N_2O emissions of a forest soil that were favoured at 90% WHC, whereas both NO and N_2O emissions showed a positive relationship with gross nitrification rates, indicating that nitrification was likely the dominant process. Furthermore, the significant mitigation effect of NI on NO emissions at all three soil moisture conditions also suggests the importance of nitrification as an important pathway in our study.

4.2. Effect of NI on N_2O, NO and N_2 emissions

Nitrification inhibitor application significantly reduced total N_2O emissions during observation period at all three soil moisture conditions. This agrees with recent review and meta-analysis studies which suggested that NIs are highly effective for reducing N_2O emissions at various soil conditions (Gilsanz et al., 2016; Qiao et al., 2015; Ruser and Schulz, 2015). In our study, the NI showed no significant effect on N_2O and N_2 emission in phase I, in line with

previous reports which showed that NIs did not have a direct effect on denitrification (Bremner and Yeomans, 1986; Müller et al., 2002). However, in phase II the $N_2O/(N_2+N_2O)$ product ratios in the NI treatments were much smaller than the ratios in the AS treatments (Fig. 3). We assume this is because the use of NI limited the NO_3^- supply to the soil microsites, the lower NO_3^- concentration and available C would therefore decrease the $N_2O/(N_2+N_2O)$ ratio due to the competitive effect of NO_3^- and N_2O as terminal electron acceptors during denitrification (Senbayram et al., 2012; Wu et al., 2017).

The assumption that NIs could reduce N_2O emission under denitrification conditions by decreasing the $N_2O/(N_2+N_2O)$ ratio has been brought forward by several authors, but has still not been directly proven (Ruser and Schulz, 2015; Wu et al., 2017). Hatch et al. (2005) found that two slurry treatments with NIs (DCD and DMPP) could significantly increase N_2 emissions and reduce $N_2O/(N_2+N_2O)$ ratios compared with slurry-only treatment. However, the results were observed in an incubation experiment conducted under anoxic conditions (100% helium atmosphere). In the present study, although the soil moisture was high, the atmosphere of the soil surface was kept oxic (20% oxygen and 80% helium), which is more comparable with the field condition. To the best of our knowledge, our study is the first one showing that NI could promote N_2 emissions under oxic conditions.

Most studies investigating the use of NIs did not consider the mitigation effect on NO emissions, which can be significant after fertilization (Pereira et al., 2015). Several recent studies reported a wide range of NO mitigation effects ranging from 35 to 80% when the NI was applied with mineral fertilizer N or slurry (Akiyama et al., 2010; Pereira et al., 2015, 2010). In our study, application of the NI significantly reduced NO emissions at all three soil moisture conditions, which is likely due to the inhibition effect of NI on nitrification process, indicating that the overlooked mitigation effect of NI on NO emissions should be taken into account when evaluating NI's mitigation effect on GHG emissions.

In this study the effect of NI on NH_3 volatilization was not evaluated, nevertheless, it should be noted that the beneficial effect of NI application in decreasing N_2O and NO emissions might be overestimated by the potentially increased NH_3 volatilization, especially when applied with ammonium-based fertilizer (Kim et al., 2012; Lam et al., 2017).

5. Conclusions

The combination of the measurement of N_2O, NO and N_2 fluxes and N_2O isotopomer analysis provided insight into the different pathways involved in the production of nitrogen gases in soil at different soil moisture conditions. Our study showed that higher soil moisture in a grassland soil was associated with higher N_2O, NO and N_2 emissions, and those different processes were responsible for N_2O and NO emissions in three phases of the incubation period. To the best of our knowledge, our study is the first showing that NI could indirectly affect the product stoichiometry of denitrification under atmospheric oxic conditions. The fact that the NI significantly reduced both N_2O and NO emissions at all three soil moisture conditions suggests that NIs could be used as an effective approach to mitigate GHGs emissions at various soil moisture conditions.

Acknowledgements

Rothamsted Research is sponsored by the BBSRC. This study was in part funded by BBSRC project BB/K001051/1 and supported by the Chinese Scholarship Council (scholarship no. give number 201306350130).

Appendix A. Supplementary data

Supplementary data related to this article can be found at http://dx.doi.org/10.1016/j.soilbio.2017.06.007.

References

Akiyama, H., Yan, X., Yagi, K., 2010. Evaluation of effectiveness of enhanced-efficiency fertilizers as mitigation options for N_2O and NO emissions from agricultural soils: meta-analysis. Global Change Biology 16, 1837–1846.
Baggs, E.M., 2008. A review of stable isotope techniques for N_2O source partitioning in soils: recent progress, remaining challenges and future considerations. Rapid Communications in Mass Spectrometry 22, 1664–1672.
Bengtson, P., Falkengren-Grerup, U., Bengtsson, G., 2005. Relieving substrate limitation-soil moisture and temperature determine gross N transformation rates. Oikos 111, 81–90.
Bollmann, A., Conrad, R., 1998. Influence of O_2 availability on NO and N_2O release by nitrification and denitrification in soils. Global Change Biology 4, 387–396.
Booth, M.S., Stark, J.M., Rastetter, E., 2005. Controls on nitrogen cycling in terrestrial ecosystems: a synthetic analysis of literature data. Ecological Monographs 75, 139–157.
Bouwman, A.F., Boumans, L.J.M., Batjes, N.H., 2002. Emissions of N_2O and NO from fertilized fields: summary of available measurement data. Global Biogeochemical Cycles 16, 1058.
Bouwman, A.F., Beusen, A.H.W., Griffioen, J., Groenigen, J.W.V., Hefting, M.M., Oenema, O., Puijenbroek, P.J.T.M.V., Seitzinger, S., Slomp, C.P., Stehfest, E., 2013. Global trends and uncertainties in terrestrial denitrification and N_2O emissions. Philosophical Transactions of the Royal Society of London B: Biological Sciences 368, 20130112.
Bremner, J.M., Yeomans, J.C., 1986. Effects of nitrification inhibitors on denitrification of nitrate in soil. Biology and Fertility of Soils 2, 173–179.
Brümmer, C., Brüggemann, N., Butterbach-Bahl, K., Falk, U., Szarzynski, J., Vielhauer, K., Wassmann, R., Papen, H., 2008. Soil-atmosphere exchange of N_2O and NO in near-natural savanna and agricultural land in Burkina Faso (W. Africa). Ecosystems 11, 582–600.
Burns, L.C., Stevens, R.J., Laughlin, R.J., 1996. Production of nitrite in soil by simultaneous nitrification and denitrification. Soil Biology and Biochemistry 28, 609–616.
Cárdenas, L.M., Rondón, A., Johansson, C., Sanhueza, E., 1993. Effects of soil moisture, temperature, and inorganic nitrogen on nitric oxide emissions from acidic tropical savannah soils. Journal of Geophysical Research: Atmospheres 98, 14783–14790.
Cárdenas, L.M., Hawkins, J.M.B., Chadwick, D., Scholefield, D., 2003. Biogenic gas emissions from soils measured using a new automated laboratory incubation system. Soil Biology and Biochemistry 35, 867–870.
Cárdenas, L.M., Chadwick, D., Scholefield, D., Fychan, R., Marley, C.L., Jones, R., Bol, R., Well, R., Vallejo, A., 2007. The effect of diet manipulation on nitrous oxide and methane emissions from manure application to incubated grassland soils. Atmospheric Environment 41, 7096–7107.
Chen, Z., Ding, W., Xu, Y., Müller, C., Rütting, T., Yu, H., Fan, J., Zhang, J., Zhu, T., 2015. Importance of heterotrophic nitrification and dissimilatory nitrate reduction to ammonium in a cropland soil: evidences from a ^{15}N tracing study to literature synthesis. Soil Biology and Biochemistry 91, 65–75.
Cheng, Y., Wang, J., Wang, S.-Q., Zhang, J.-B., Cai, Z.-C., 2014. Effects of soil moisture on gross N transformations and N_2O emission in acid subtropical forest soils. Biology and Fertility of Soils 50, 1099–1108.
Ciais, P., Sabine, C., Bala, G., Bopp, L., Brovkin, V., Canadell, J., Chhabra, A., DeFries, R., Galloway, J., Heimann, M., Jones, C., Le Quéré, C., Myneni, R.B., Piao, S., Thornton, P., 2013. Carbon and other biogeochemical cycles. In: Stocker, T.F., Qin, D., Plattner, G.-K., Tignor, M., Allen, S.K., Boschung, J., Nauels, A., Xia, Y., Bex, V., Midgley, P.M. (Eds.), Climate Change 2013: The Physical Science Basis. Contribution of Working Group I to the Fifth Assessment Report of the Intergovernmental Panel on Climate Change. Cambridge University Press, Cambridge, United Kingdom and New York, NY, USA, pp. 465–570.
Clayden, B., Hollis, J.M., 1985. Criteria for Differentiating Soil Series. Soil Survey Technical Monograph, N0O. 17, Harpenden, UK.
Cleemput, O. van, 1998. Subsoils: chemo-and biological denitrification, N_2O and N_2 emissions. Nutrient Cycling in Agroecosystems 52, 187–194.
Crutzen, P.J., 1979. The role of NO and NO_2 in the chemistry of the troposphere and stratosphere. Annual Review of Earth and Planetary Sciences 7, 443–472.
Davidson, E.A., 1992. Sources of nitric oxide and nitrous oxide following wetting of dry soil. Soil Science Society of America Journal 56, 95.
Davidson, E.A., Keller, M., Erickson, H.E., Verchot, L.V., Veldkamp, E., 2000. Testing a Conceptual Model of Soil Emissions of Nitrous and Nitric Oxides Using two functions based on soil nitrogen availability and soil water content, the hole-in-the-pipe model characterizes a large fraction of the observed variation of nitric oxide and nitrous oxide emissions from soils. BioScience 50, 667–680.
Decock, C., Six, J., 2013. How reliable is the intramolecular distribution of ^{15}N in N_2O to source partition N_2O emitted from soil? Soil Biology and Biochemistry 65, 114–127.
Di, H.J., Cameron, K.C., Podolyan, A., Robinson, A., 2014. Effect of soil moisture status and a nitrification inhibitor, dicyandiamide, on ammonia oxidizer and denitrifier growth and nitrous oxide emissions in a grassland soil. Soil Biology and

Biochemistry 73, 59–68.
Firestone, M., Davidson, E., 1989. Microbiological Basis of NO and N_2O Production and Consumption in Soil. John Wiley & Sons Ltd, Chichester.
Galloway, J.N., Dentener, F.J., Capone, D.G., Boyer, E.W., Howarth, R.W., Seitzinger, S.P., Asner, G.P., Cleveland, C.C., Green, P.A., Holland, E.A., Karl, D.M., Michaels, A.F., Porter, J.H., Townsend, A.R., Vöosmarty, C.J., 2004. Nitrogen cycles: past, present, and future. Biogeochemistry 70, 153–226.
Gilsanz, C., Báez, D., Misselbrook, T.H., Dhanoa, M.S., Cárdenas, L.M., 2016. Development of emission factors and efficiency of two nitrification inhibitors, DCD and DMPP. Agriculture, Ecosystems & Environment 216, 1–8.
Guo, S., Hu, M., Zamora, M.L., Peng, J., Shang, D., Zheng, J., Du, Z., Wu, Z., Shao, M., Zeng, L., Molina, M.J., Zhang, R., 2014. Elucidating severe urban haze formation in China. Proceedings of the National Academy of Sciences 111, 17373–17378.
Hatch, D., Trindade, H., Cardenas, L., Carneiro, J., Hawkins, J., Scholefield, D., Chadwick, D., 2005. Laboratory study of the effects of two nitrification inhibitors on greenhouse gas emissions from a slurry-treated arable soil: impact of diurnal temperature cycle. Biology and Fertility of Soils 41, 225–232.
Heil, J., Liu, S., Vereecken, H., Brüggemann, N., 2015. Abiotic nitrous oxide production from hydroxylamine in soils and their dependence on soil properties. Soil Biology and Biochemistry 84, 107–115.
IPCC, 2013. Annex II: climate system scenario tables. In: Climate Change 2013: the Physical Science Basis. Contribution of Working Group I to the Fifth Assessment Report of the Intergovernmental Panel on Climate Change. Cambridge University Press, Cambridge, United Kingdom and New York, NY, USA.
Kim, D.G., Saggar, S., Roudier, P., 2012. The effect of nitrification inhibitors on soil ammonia emissions in nitrogen managed soils: a meta-analysis. Nutrient Cycling in Agroecosystems 93, 51–64.
Kool, D.M., Dolfing, J., Wrage, N., Van Groenigen, J.W., 2011. Nitrifier denitrification as a distinct and significant source of nitrous oxide from soil. Soil Biology and Biochemistry 43, 174–178.
Lam, S.K., Suter, H., Mosier, A.R., Chen, D., 2017. Using nitrification inhibitors to mitigate agricultural N_2O emission: a double-edged sword? Global Change Biology 23, 485–489.
Laughlin, R.J., Stevens, R.J., 2002. Evidence for fungal dominance of denitrification and codenitrification in a grassland soil. Soil Science Society of America Journal 66, 1540–1548.
Lewicka-Szczebak, D., Well, R., Köster, J.R., Fuß, R., Senbayram, M., Dittert, K., Flessa, H., 2014. Experimental determinations of isotopic fractionation factors associated with N_2O production and reduction during denitrification in soils. Geochimica et Cosmochimica Acta 134, 55–73.
Lipschultz, F., Zafiriou, O.C., Wofsy, S.C., McElroy, M.B., Valois, F.W., Watson, S.W., 1981. Production of NO and N_2O by soil nitrifying bacteria. Nature 294, 641–643.
Loick, N., Dixon, E.R., Abalos, D., Vallejo, A., Matthews, G.P., McGeough, K.L., Well, R., Watson, C.J., Laughlin, R.J., Cardenas, L.M., 2016. Denitrification as a source of nitric oxide emissions from incubated soil cores from a UK grassland soil. Soil Biology and Biochemistry 95, 1–7.
Manzoni, S., Schimel, J.P., Porporato, A., 2012. Responses of soil microbial communities to water stress: results from a meta-analysis. Ecology 93, 930–938.
Meijide, A., Cardenas, L.M., Bol, R., Bergstermann, A., Goulding, K., Well, R., Vallejo, A., Scholefield, D., 2010. Dual isotope and isotopomer measurements for the understanding of N_2O production and consumption during denitrification in an arable soil. European Journal of Soil Science 61, 364–374.
Menendez, S., Barrena, I., Setien, I., Gonzalez-Murua, C., Estavillo, J.M., 2012. Efficiency of nitrification inhibitor DMPP to reduce nitrous oxide emissions under different temperature and moisture conditions. Soil Biology & Biochemistry 53, 82–89.
Müller, C., Stevens, R.J., Laughlin, R.J., Azam, F., Ottow, J.C.G., 2002. The nitrification inhibitor DMPP had no effect on denitrifying enzyme activity. Soil Biology and Biochemistry 34, 1825–1827.
Myhre, G., Shindell, D., Bréon, F.-M., Collins, W., Fuglestvedt, J., Huang, J., Koch, D., Lamarque, J.-F., Lee, D., Mendoza, B., Nakajima, T., Robock, A., Stephens, G., Takemura, T., Zhang, H., 2013. Anthropogenic and natural radiative forcing. In: Stocker, T.F., Qin, D., Plattner, G.-K., Tignor, M., Allen, S.K., Boschung, J., Nauels, A., Xia, Y., Bex, V., Midgley, P.M. (Eds.), Climate Change 2013: the Physical Science Basis. Contribution of Working Group I to the Fifth Assessment Report of the Intergovernmental Panel on Climate Change. Cambridge University Press, Cambridge, United Kingdom and New York, NY, USA, pp. 659–740.
Pereira, J., Fangueiro, D., Chadwick, D.R., Misselbrook, T.H., Coutinho, J., Trindade, H., 2010. Effect of cattle slurry pre-treatment by separation and addition of nitrification inhibitors on gaseous emissions and N dynamics: a laboratory study. Chemosphere 79, 620–627.
Pereira, J., Coutinho, J., Fangueiro, D., Trindade, H., 2015. Nitric oxide and nitrous oxide emissions from cattle-slurry and mineral fertiliser treated with nitrification inhibitor to an agricultural soil: a laboratory approach. Spanish Journal of Agricultural Research 13, 0305.
Qiao, C., Liu, L., Hu, S., Compton, J.E., Greaver, T.L., Li, Q., 2015. How inhibiting nitrification affects nitrogen cycle and reduces environmental impacts of anthropogenic nitrogen input. Global Change Biology 21, 1249–1257.
Ruser, R., Schulz, R., 2015. The effect of nitrification inhibitors on the nitrous oxide (N_2O) release from agricultural soils-a review. Journal of Plant Nutrition and Soil Science 178, 171–188.
Sanhueza, E., Hao, W.M., Scharffe, D., Donoso, L., Crutzen, P.J., 1990. N_2O and NO emissions from soils of the northern part of the Guayana Shield, Venezuela. Journal of Geophysical Research: Atmospheres 95, 22481–22488.
Scheer, C., Wassmann, R., Butterbach-Bahl, K., Lamers, J.P.A., Martius, C., 2008. The relationship between N_2O, NO, and N_2 fluxes from fertilized and irrigated dryland soils of the Aral Sea Basin, Uzbekistan. Plant and Soil 314, 273.
Searle, P.L., 1984. The Berthelot or indophenol reaction and its use in the analytical chemistry of nitrogen. A review. Analyst 109, 549–568.
Senbayram, M., Chen, R., Budai, A., Bakken, L., Dittert, K., 2012. N_2O emission and the $N_2O/(N_2O+N_2)$ product ratio of denitrification as controlled by available carbon substrates and nitrate concentrations. Agriculture, Ecosystems & Environment 147, 4–12.
Shoun, H., Fushinobu, S., Jiang, L., Kim, S.-W., Wakagi, T., 2012. Fungal denitrification and nitric oxide reductase cytochrome P450nor. Philosophical Transactions of the Royal Society B: Biological Sciences 367, 1186–1194.
Skiba, U., Smith, K.A., fowler, D., 1993. Nitrification and denitrification as sources of nitric oxide and nitrous oxide in a sandy loam soil. Soil Biology and Biochemistry 25, 1527–1536.
Skiba, U., Fowler, D., Smith, K.A., 1997. Nitric oxide emissions from agricultural soils in temperate and tropical climates: sources, controls and mitigation options. Nutrient Cycling in Agroecosystems 48, 139–153.
Stehfest, E., Bouwman, L., 2006. N_2O and NO emission from agricultural fields and soils under natural vegetation: summarizing available measurement data and modeling of global annual emissions. Nutrient Cycling in Agroecosystems 74, 207–228.
Subbarao, G.V., Ito, O., Sahrawat, K.L., Berry, W.L., Nakahara, K., Ishikawa, T., Watanabe, T., Suenaga, K., Rondon, M., Rao, I.M., 2006. Scope and strategies for regulation of nitrification in agricultural systems—challenges and opportunities. Critical Reviews in Plant Sciences 25, 303–335.
Sutka, R.L., Ostrom, N.E., Ostrom, P.H., Breznak, J.A., Gandhi, H., Pitt, A.J., Li, F., 2006. Distinguishing nitrous oxide production from nitrification and denitrification on the basis of isotopomer abundances. Applied and Environmental Microbiology 72, 638–644.
Sutka, R.L., Adams, G.C., Ostrom, N.E., Ostrom, P.H., 2008. Isotopologue fractionation during N_2O production by fungal denitrification. Rapid Communications in Mass Spectrometry 22, 3989–3996.
Toyoda, S., Yoshida, N., 1999. Determination of nitrogen isotopomers of nitrous oxide on a modified isotope ratio mass spectrometer. Analytical Chemistry 71, 4711–4718.
Toyoda, S., Mutobe, H., Yamagishi, H., Yoshida, N., Tanji, Y., 2005. Fractionation of N_2O isotopomers during production by denitrifier. Soil Biology and Biochemistry 37, 1535–1545.
Weier, K.L., Doran, J.W., Power, J.F., Walters, D.T., 1993. Denitrification and the dinitrogen/nitrous oxide ratio as affected by soil water, available carbon, and nitrate. Soil Science Society of America Journal 57, 66–72.
Wu, D., Senbayram, M., Well, R., Brüggemann, N., Pfeiffer, B., Loick, N., Stempfhuber, B., Dittert, K., Bol, R., 2017. Nitrification inhibitors mitigate N_2O emissions more effectively under straw-induced conditions favoring denitrification. Soil Biology and Biochemistry 104, 197–207.
Zaman, M., Chang, S.X., 2004. Substrate type, temperature, and moisture content affect gross and net N mineralization and nitrification rates in agroforestry systems. Biology and Fertility of Soils 39, 269–279.
Zerulla, W., Barth, T., Dressel, J., Erhardt, K., Von Locquenghien, K.H., Pasda, G., Radle, M., Wissemeier, A.H., 2001. 3,4-Dimethylpyrazole phosphate (DMPP) - a new nitrification inhibitor for agriculture and horticulture. Biology and Fertility of Soils 34, 79–84.

Paper IV

Potential dual effect of nitrification inhibitor on nitrifier denitrification helps mitigate peak N_2O emissions events in the North China Plain cropping systems.

Wu D., Zhao, Z., Han, X., Meng, F., Wu, W., Zhou, M., Brüggemann, N., Bol, R., 2017

Under review in *Soil Biology and Biochemistry*

Elsevier Editorial System(tm) for Soil Biology and Biochemistry

Manuscript Draft

Manuscript Number:

Title: Potential dual effect of nitrification inhibitor on nitrifier denitrification helps mitigate peak N2O emissions events in the North China Plain cropping systems

Article Type: Research Paper

Keywords: Nitrous oxide; isotopomer; nitrification inhibitor; nitrifier denitrification

Corresponding Author: Mr. Fanqiao MENG,

Corresponding Author's Institution: China Agricultural University

First Author: Di Wu

Order of Authors: Di Wu; Zichao Zhao; Xiao Han; Fanqiao MENG; Wenliang Wu; Minghua Zhou; Nicolas Brüggemann; Roland Bol

Manuscript Region of Origin: GERMANY

Suggested Reviewers: Zengming Chen Dr.
Assistent Professor, Chinese Academy of Sciences,Institute of Soil Science
zmchen@issas.ac.cn
Expert in N2O emission and nitrogen cycle of North China area

Laura Cardenas Dr.
Professor, Rothamsted Research, North Wyke
laura.cardenas@rothamsted.ac.uk
Expert in nitrification/denitrification process in soil

Klaus Dittert Dr.
Professor, Georg-August-Universität Göttingen
klaus.dittert@agr.uni-goettingen.de
Expert in nitrification inhibitor area

Potential dual effect of nitrification inhibitor on nitrifier denitrification helps mitigate peak N_2O emissions events in the North China Plain cropping systems

Di Wu[1, 2*], Zichao Zhao[1,*], Xiao Han[1], Fanqiao Meng[1,+], Wenliang Wu[1], Minghua Zhou[2], Nicolas Brüggemann[2], Roland Bol[2]

[1] College of Resources and Environmental Sciences, China Agricultural University, Beijing, 100193, China

[2] Institute of Bio- and Geosciences, Agrosphere (IBG-3), Forschungszentrum Jülich GmbH, 52425 Jülich, Germany

* These authors contributed equally to this work.

[+]Corresponding author

Email address: mengfq@cau.edu.cn

Keywords: Nitrous oxide; isotopomer; nitrification inhibitor; nitrifier denitrification

Abstract

The winter wheat–summer maize rotation system in the North China Plain is a major source of nitrous oxide (N_2O) emissions due to high nitrogen (N) fertilizer and irrigation water inputs. However, the detailed understanding of the contribution of N_2O production sources is still insufficient due to the complexity of N_2O generation in soils and lack of relevant field studies. Moreover, the efficiency and mechanism of N_2O mitigation approaches in this area, such as of the use of nitrification inhibitors, remains still poorly understood. To elucidate the producing pathways of nitrous oxide from this rotation system and to evaluate the effect of a widely used nitrification inhibitor (DMPP) on mitigating N_2O emissions, we monitored N_2O emission fluxes and analyzed isotopomer ratios of soil-emitted N_2O during one rotation year. Results indicate that the application of DMPP significantly mitigated N_2O emissions by 67% in winter wheat and 47% in summer maize season. Isotopomer analysis revealed that in N-fertilized treatment, nitrification accounted for max. 41% N_2O emissions peaks observed after fertilization and irrigation events, while nitrifier denitrification pathway was likely to be the main source that accounts for the rest of N_2O emissions. The high effectiveness of the nitrification inhibitor on mitigating N_2O emission at high soil moisture may be attributed to the dual inhibitory effect on nitrifier denitrification, i.e., decreasing substrate of nitrifier denitrification and inhibiting bacterial activities which carry nitrifier denitrification. Our study also pointed to a wider range of applicable moisture conditions for the use of nitrification inhibitors than previous assumed in the soil of the North China Plain.

1. Introduction

Emissions of nitrous oxide (N_2O) have shown great impact on global warming and stratospheric ozone depletion (Bouwman et al., 2002; Ravishankara et al., 2009). Agricultural soils are the major source of atmospheric N_2O (IPCC, 2014). High N applications generally lead to larger N_2O emissions. However, the sustainability of high agricultural productivity largely depends on use of synthetic nitrogen (N) fertilizers (Sutton et al. 2011). To secure crop production, the winter wheat–summer maize rotation system in the North China Plain (NCP), which accounts for about 40% of wheat and maize yield in China (National Bureau of Statistics of China, 2016), has been amended with large amounts of N fertilizer, leading to a number of environmental problems, such as groundwater pollution and greenhouse gas (GHG) emissions (Ju et al., 2004; Shi et al., 2013). Nitrous oxide emission is one important pathway for gaseous N loss in the NCP (Meng et al., 2005). In soil, N_2O production is mainly related to the type and activity of the microbial processes involved. Nitrification and denitrification have been found to be the key sources of N_2O emissions (Baggs 2011; Butterbach-Bahl et al., 2013). Previous studies suggested that nitrification accounted for 80-90% of N_2O emission in the NCP due to the large supply of ammonium-based N fertilizers and weak denitrification potential in the soil (Ju et al., 2004; Wan et al., 2009; Ding et al., 2010).

Recently, nitrifier denitrification has been identified as another main process responsible for N_2O emissions in soil, which is supported by an increasing number of studies based on a multi-isotope tracing approach (Kool et al., 2011; Zhu et al., 2013; Huang et al., 2014). However, the contribution of nitrifier denitrification to soil N_2O emissions is still unclear due to the lack of actual field measurements. Indeed, several recent studies pointed to the overlooked major role of nitrifier denitrification on N_2O emissions in the NCP, thereby highlighting that the contribution of nitrification (ammonia oxidation) on N_2O emissions has been overestimated (Zhang et al.,

2016), since most previous studies did not distinguish between the contribution of nitrification and nitrifier denitrification (Huang et al., 2014).

Nitrification inhibitors (NI) are a group of compounds that can decrease the bacterial oxidation of NH_4^+ to NO_2^- by inhibiting the activity of *Nitrosomas* sp. in the soil (Zerulla et al., 2001). The use of nitrification inhibitors (NIs) has repeatedly been shown to reduce N_2O emissions from cropland soils, with mitigation efficiency of 38-44% as suggested by recent meta-analysis studies (Qiao et al., 2015). Different factors, e.g. soil moisture, oxygen content, soil available C, have been found to affect the mitigation effect of NI on N_2O emission, which indicated that the extent to which NI inhibits N_2O emissions might dependent on different pathways of N_2O production (Hatch et al., 2005; Menendez et al., 2012; Wu et al., 2017).

The difference between ^{15}N at the central (α position) and the terminal N atom (β position) in the asymmetric N_2O molecule has been found to differ clearly amongst different N_2O source pathways (bacterial nitrification: 34-37‰, nitrifier denitrification and bacterial denitrification: -11-2‰) (Sutka et al., 2006; Frame and Casciotti 2010; Toyoda et al., 2015), and it is assumed to be independent of the $\delta^{15}N$ value of the precursor species (Toyoda et al., 2011; Decock and Six 2013). Thus, it has potential to be used to gain information about the underlying N_2O source processes. The advantages of this isotopic technique approach include: non-invasive, low-cost gaseous sampling, and facilitating investigation of both incubation and field scale experiments (Lewicka-Szczebak et al., 2016). However, deploying N_2O SP values for N_2O source partitioning to nitrification and denitrification processes is complicated by the similar SP values for fungal denitrification/ nitrification and nitrifier denitrification/ bacteria denitrification (Sutka et al., 2006; Rohe et al., 2014). Furthermore, there are other microbial N_2O production pathways, such as archaeal nitrification, anammox (anaerobic ammonium oxidation), or DNRA (dissimilatory nitrate

92 reduction to ammonium), for which hardly any characteristic isotopic N_2O signatures have been
93 identified yet (Decock and Six 2013).
94 The objectives of our study were (a) to evaluate the effect of application of NI with urea on
95 mitigating N_2O emissions during one winter wheat–summer maize rotation in the NCP; (b) to
96 illustrate the main processes contributing to N_2O emissions in the NCP by investigating the iso-
97 topic signature of N_2O during peak emission events.
98
99 **2. Materials and methods**
100 2.1 Study site and field management
101 The experiment was conducted in Huantai County, Shandong province, North China (36°57.75'N;
102 117°59.21'E). Wheat (*Triticum aestivum L.*) was planted on 10th October 2015 and harvested on
103 13th June 2016, while maize (*Zea mays L.*) was planted on 20th June 2016 and harvested on 2nd
104 October 2016. The average air temperature and precipitation for winter wheat season and summer
105 maize season was 10.3°C/234 mm and 26.4 °C/481 mm, respectively. The soil was classified as
106 aquic inceptisol (a calcareous, fluvo-aquic clay loam) and consisted of 38% clay (< 0.002 mm),
107 32 % silt (0.002–0.02 mm) and 30 % sand (0.02–2 mm). The soil had a bulk density of 1.4 g cm^{-3},
108 pH in water of 7.7, soil organic carbon of 10.0 g kg^{-1} and total N content of 1.1 g kg^{-1}.
109 The field experiment included three treatments: CK (no fertilizer N input), U (urea), and NI
110 (urea plus nitrification inhibitor (DMPP). Each treatment had three replicates. Urea was applied
111 at a rate of 300 kg N ha^{-1} (50 % as basal fertilization and 50 % as top-dressing fertilization) for
112 the wheat season and maize season, respectively. The nitrification inhibitor (DMPP) was thor-
113 oughly mixed with urea and then spread on the surface of soil at a rate of 1% of the applied urea
114 N. The straw of wheat and maize were both returned to field after harvest. Irrigation was carried

115 out immediately after fertilization twice in the wheat season and once in the maize season (75
116 mm each).
117
118 2.2 Gas sampling and flux measurement
119 The static chamber-gas chromatography technique was used for measuring N_2O fluxes (Shi et al.
120 2013; Zhou et al. 2014). The N_2O emissions were monitored once every day for one week imme-
121 diately following fertilization and irrigation events, and then twice a week afterwards. Gas sam-
122 pling for flux measurements were performed between 9:00 and 11:00 a.m. local time and ana-
123 lyzed on a gas chromatograph (7820A, Agilent, Shanghai, China) within 24 hours. The flux was
124 calculated as a linear slope of the concentration evolution over the chamber closure time. Gas
125 samples for isotopomer analyses were collected from the static flux chamber after 90 minutes
126 closure time.
127
128 2.3 Isotope analysis
129 The N_2O $\delta^{15}N_{bulk}$ (i.e., the average $\delta^{15}N$ over the N_2O molecule), $\delta^{15}N_\alpha$ (i.e., $\delta^{15}N$ at the central
130 position of the N_2O molecule), and $\delta^{18}O$ isotope signatures were determined by analyzing *m/z* 44,
131 45, and 46 of intact N_2O^+ molecular ions, and *m/z* 30 and 31 of NO^+ fragment ions (Toyoda and
132 Yoshida 1999) on an isotope ratio mass spectrometer (IsoPrime 100, Elementar Analysensysteme,
133 Hanau, Germany) in the laboratory at Forschungszentrum Jülich, Germany. The $\delta^{15}N$ at the ter-
134 minal position of the N_2O molecule, $\delta^{15}N_\beta$, was calculated according to $\delta^{15}N_\beta = 2 \cdot \delta^{15}N_{bulk} - \delta^{15}N_\alpha$.
135 The details for correction and calibration are described in Heil et al. (2015). The collected N_2O is
136 a mixture of atmospheric and soil-emitted N_2O. We measured the N_2O concentration in ambient
137 air (C_0) and the corresponding $\delta^{15}N$ or $\delta^{18}O$ value (δ_0), and the N_2O concentration (C_1) and the
138 corresponding δ value (δ_1) from the closed chambers. We then calculated the soil-released N_2O

concentration as the difference between the N_2O concentration of the chamber headspace and that of ambient air. Based on this, the δ value of soil-released N_2O was calculated using the following equation:

$$\delta = (\delta_1 \cdot C_1 - \delta_0 \cdot C_0) / (C_1 - C_0) \quad (1)$$

The δ values of soil-released N_2O were not calculated when $(C_1 - C_0) < 20$ ppb, i.e. when the soil-emitted N_2O was marginal, since at this condition and within the precision of the analysis the propagated error of the calculation was too large (Yano et al. 2014).

The source partitioning of N_2O production was based on a two-end-member isotopic mass balance equation:

$$SP_{N2O\text{-}0} = SP_D \cdot f_{D\text{-}SP} + SP_N \cdot f_{N\text{-}SP} \quad (2)$$

This equation is based on the assumption of only two end members, hence $f_{N\text{-}SP} + f_{D\text{-}SP} = 1$. As nitrifier denitrification is known to have SP values similar to those of bacterial denitrification (Sutka et al., 2006; Frame and Casciotti 2010; Toyoda et al., 2015), distinguishing N_2O originating from bacterial denitrification and nitrifier denitrification based on SP values is mathematically impossible. Therefore, the isotopic signatures of the end members were defined as 37‰ for bacterial nitrification and –2‰ for both bacterial denitrification and nitrifier denitrification (Toyoda et al., 2005; Sutka et al., 2006; Toyoda et al., 2015; Wu et al., 2017). In this equation $f_{D\text{-}SP}$ and $f_{N\text{-}SP}$ represent the contribution of denitrification (both bacterial denitrification and nitrifier denitrification) and nitrification to total N_2O release calculated on the basis of SP values, respectively.

2.4 Auxiliary measurements

In addition to N_2O flux measurements, air temperature, precipitation, soil temperature (0–5 cm), soil moisture (0–10 cm), soil NO_3^- (0–10 cm) and soil NH_4^+ content (0–10 cm) were also measured. Daily air temperature and precipitation were continuously recorded at a meteorological station (AR5, Xinyuanshijie technology Co. Ltd, Beijing, China). Soil temperature and moisture were measured at the time of gas sample collection. Soil temperature was determined with a digital thermometer (JM 624, Jinming Instrument Co. Ltd, Tianjin, China). Soil moisture was converted into water-filled pore space (WFPS; %) and calculated by the following equation:

WFPS = water content (%, w/w) × BD/total soil porosity (%) × 100% (3)

Where total soil porosity=1-(BD/2.65), with 2.65 g cm^{-3} as the mineral particle density of the soil, and BD is the soil bulk density (g cm^{-3}). The soil NO_3^- and NH_4^+ content was analyzed using a continuous flow analyzer (Auto Analyzer 3, BRAN+LUEBBE Co. Ltd., Hamburg, Germany). Details of the measurements can be found in Shi et al. (2013).

2.5 Statistical analysis

Statistical analyses were conducted using the R version 3.2.2 software. Statistically significant differences were tested using Tukey's HSD post-hoc tests at a 5% significant level. Correlation and linear or nonlinear regression analyses were used to test relationships between N_2O fluxes and other factors.

3. Results

187 3.1 Seasonal variations and controlling factors of N_2O emissions

188 The mean soil temperature at 5 cm depth ranged from -5°C to 22°C and from 18°C to 29°C in the
189 wheat season and maize season, respectively, while the mean soil moisture (WFPS) ranged from
190 12.8 to 81.9% in wheat season and from 42.4 to 82.5% in maize season (Fig. 1). Soil NH_4^+ con-
191 tents ranged from 0 to 62.0 mg N kg^{-1} in the wheat season and from 0 to 10.3 mg N kg^{-1} in the
192 maize season, while NO_3^- contents ranged from 1.0 to 233.0 mg N kg^{-1} in the wheat season and
193 from 0.8 to 173.2 mg N kg^{-1} in maize season (Fig. 2). The NH_4^+ concentrations in the NI treat-
194 ment were significantly higher after N fertilizer application compared with U and CK treatment
195 during the winter wheat season, while no significant difference was found among three treat-
196 ments in summer maize season. Soil NO_3^- contents sharply increased after each fertilization and
197 irrigation event in U and NI treatments. Soil NO_3^- concentrations in U and NI treatments were
198 both significantly higher compared with CK, while no significant difference was found for soil
199 NO_3^- concentrations between the NI and U treatment during most of wheat and maize season
200 (Fig. 2).

201 In general, N_2O emissions were stimulated by N fertilizer application and irrigation, and then
202 sharply declined. Throughout the one-year experimental period, four pronounced N_2O flux peaks
203 were observed (Fig. 3). In the U treatment, peak event I (242.0 μg N m^{-2} h^{-1}) and peak event II
204 (64.6 μg N m^{-2} h^{-1}) that occurred in the winter wheat season (17 October, 2015 and 1 April, 2016)
205 were significantly lower than peak event III (687.3 μg N m^{-2} h^{-1}) and peak event IV(400.4 μg N
206 m^{-2} h^{-1}), which occurred in the summer maize season (21 June, 2016 and 21 July, 2016). Each of
207 the four peak fluxes was detected when soil moisture was relatively high (Peak event I-IV: WFPS
208 61, 82, 82 and 72%, respectively). The N_2O emissions were relatively low between two fertiliz-
209 ing/irrigating events, mostly below 20 μg N m^{-2} h^{-1}. Compared with the U treatment, the applica-
210 tion of DMPP significantly reduced peak N_2O emissions by 95.6%, 78.7%, 82.6% and 54.5%, in

211 peak events I-IV, respectively. The cumulative N_2O emissions during the summer maize season
212 were higher than those in the winter wheat season (Table 1). Application of DMPP significantly
213 reduced N_2O emissions by 67.0% for the winter wheat season and 46.8% for the summer maize
214 season compare with U treatment. The annual N_2O emissions factor (EF) was 0.32% in U treat-
215 ment and 0.11% in NI treatment (Table 1). The N_2O fluxes were significantly correlated with soil
216 temperature and soil moisture (WFPS) in all treatments (Table 2). In contrast, N_2O fluxes were
217 significantly correlated with NH_4^+ concentrations only in the CK treatment, and with NO_3^- con-
218 centrations only in the U treatment (Table 2).
219
220 3.2 Isotopomer ratios of soil-emitted N_2O and source partitioning
221 The isotopic signature of emitted N_2O from the control was not shown in the figure as the N_2O
222 concentration was too closed to the ambient air. In general, in both urea and NI treatments the
223 $\delta^{15}N_{bulk}$ values of soil-emitted N_2O increased with time after peak event occurred (Fig. S1). The
224 $\delta^{15}N_{bulk}$ values of soil-emitted N_2O from the urea treatment were more depleted than those from
225 the NI treatment. A similar trend was observed for the $\delta^{18}O$ values of N_2O, ranging from 23.1‰
226 to 30.2‰ (Fig. S2). The average SP values of soil-emitted N_2O in the U and NI treatments were
227 12.9‰ and 16.7‰, respectively, ranging from 1.6‰ to 23.7‰ in the U treatment and from 4.3‰
228 to 34.9‰ in the NI treatment. During each peak event, SP values in the U treatment were lower
229 than in the NI treatment (Fig. 4). Nitrification proportion based on the two-end-member model
230 was shown on the y axis of Figure 4. For the total amount of N_2O emitted during the four meas-
231 ured periods, nitrification accounted for 36.8% in the U treatment and 45.8% in the NI treatment,
232 respectively. On the other hand, on the four peak events the average amount of N_2O derived from
233 nitrification was 36.3 % in the U treatment and 74.1 % in the NI treatment (Fig. 4).
234

4. Discussion

In our study, the N_2O emissions factor of the urea treatment (EF=0.32%) was lower than for other agricultural fields in the NCP (EF=0.82-2.7%) (Cai et al., 2013; Zhou et al., 2016), but was similar to a study conducted previously in the same field (Shi et al., 2013). The soil N_2O fluxes were significantly and positively correlated with soil moisture and soil temperature, in line with previous studies which showed that higher N_2O emissions were observed in warmer and wetter condition (Table 2) (Li et al., 2010). The relatively higher soil NH_4^+ concentrations in the NI treatment during the winter wheat season was likely attributed to the inhibition effect of NI on NH_4^+ oxidation process. The soil NH_4^+ contents observed in the U and NI treatments were both very low during summer maize season. This was probably due to the higher temperature in summer, which increased the rate of NH_3 volatilization (Cai et al., 2002). In contrast, no significant effect of NI application on soil NO_3^- concentrations was found, which is in line with several previous field studies (Weiske et al., 2001; Ding et al., 2010), most likely due to the combined effects of denitrification, soil leaching and soil heterogeneity. The N_2O fluxes in the U treatments showed a significant positive correlation with soil NO_3^-, and a negative (albeit not significant) correlation with soil NH_4^+ concentrations (Table 2), indicating N_2O emissions were dominated by the NH_4^+ transformation process.

The application of NI significantly mitigated N_2O emissions during the four peak events, and reduced the total N_2O emissions by 56.4% for the whole rotation year. This agrees with previous studies which demonstrated that NI could significantly reduce N_2O emissions in the NCP (Ding et al., 2010; Liu et al., 2013). The high mitigation efficiency of NI may be explained by the large contribution of nitrification-derived N_2O in the NCP, as suggested by previous studies (Ju et al., 2004; Wan et al., 2009; Ding et al., 2010). It has been generally assumed that in soil at WFPS 30-

70% nitrification is the main source of N_2O, while denitrification is the main contributor at WFPS 70-90% (Granli and Boeckman 1994; Davidson et al., 2000). However, in our study the mean soil moisture (WFPS 74.2%) during the four N_2O peaks was above the range favorable for nitrification, indicating that nitrification was less likely to be the primary N_2O source during the four peak events. According to the SP values and the two end-member mixing model, nitrification only accounted for less than half (on average 41%) of the N_2O production in the U treatment during the four peak events (Fig. 4). The 41% of nitrification's contribution would be the maximum value, as the N_2O reduction effect on SP and contribution of fungal denitrification were neglected in this study, which would both lead to the overestimation of the N_2O derived from nitrification to a certain degree (Wu et al., 2016). This result is not in agreement with previous studies, which found that about 80-90% N_2O emissions in the NCP were derived from nitrification (Ju et al., 2004; Wan et al., 2009). However, it should be noted that none of those aforementioned studies which reported nitrification being the main source of N_2O emissions in the NCP could actually distinguish between nitrification and nitrifier denitrification. This means that the contribution of nitrification as N_2O source can be largely overestimated under conditions where nitrifier denitrification is pronounced.

Despite the lack of sufficient evidence from field studies, nitrifier denitrification has been found recently in soil incubation studies as a major source of N_2O emission from soil, which may in fact account for 30-66% of soil N_2O emissions (Kool et al., 2011; Zhu et al., 2013). In our study, the lower SP values in the U treatments can be the evidence for a larger contribution of nitrifier denitrification (0 to -10‰) (Toyoda et al., 2015). Moreover, the high NH_4^+-N fertilizer input and the semi-aerobic conditions, as induced by ammonia fertilizer application and irrigation, together with the high soil pH and low C availability, would create conditions favorable for nitrifier denitrification (Kool et al., 2011). Huang et al. (2014) reported that nitrifier

283 denitrification accounted for 44-58% of total N_2O emissions at 70% WFPS in the NCP. In the
284 study of Zhang et al. (2016) nitrifier denitrification accounted for about 30% of total N_2O emis-
285 sions, and the contribution increased greatly with higher fertilizer content of the soil.

286 During the four peak events, NI significantly reduced about 80% of N_2O emissions. Interest-
287 ingly, significantly larger proportions of nitrification-derived N_2O were found in NI treatment
288 compared with U treatment (average 74 % vs 36%) (Fig. 4). This indicates that in NI treatment
289 beside nitrification other N_2O production sources (e.g. nitrifier denitrification or denitrifier
290 denitrification) must be also inhibited by NI. Otherwise, we would have observed smaller propor-
291 tion of nitrification-derived N_2O in NI treatment compared to U treatment, since NI would inhibit
292 most of N_2O derived from nitrification. We therefore presume that NI also inhibited N_2O pro-
293 duced by nitrifier denitrification. The efficient N_2O mitigation effect of NI on the four N_2O peak
294 events at high soil moisture is thus likely attributed to the "dual inhibitory effect" of NI on
295 nitrifier denitrification. Firstly, by delaying the bacterial oxidation of NH_4^+ in soil, NI decreased
296 the substrate of nitrifier denitrification. Secondly, NI inhibited the nitrifier denitrification process
297 by decreasing the activity of *Nitrosomas* bacteria, which performs nitrifier denitrification (Kool et
298 al., 2011; Zerulla et al., 2001).

299 In our study one other possible, but unlikely main N_2O production pathway could be denitrifier
300 denitrification. The low SP values observed in the U treatment could also be interpreted as a large
301 contribution of denitrifier denitrification. However, it fails to explain the high NI mitigation effi-
302 ciency during the four peak events. Moreover, the correlations between N_2O fluxes and soil NH_4^+
303 / NO_3^- in the urea application treatment suggested that denitrification is unlikely to be the domi-
304 nant process (Table 2). Finally, a large number of studies have proven that the contribution of
305 denitrifier denitrification on N_2O emissions is minor in the NCP, due to the low denitrification

potential caused by high pH and low soil C availability (White et al., 2002; Ding et al., 2007; Wan et al., 2009; Ju et al., 2011).

Therefore, we conclude that nitrifier denitrification is more likely to be the major source that accounts for the rest N_2O emissions than denitrifier denitrification. Nevertheless, a final proof of our hypothesis on nitrifier denitrification is still missing due to the limitations of methods for identifying nitrifier denitrification in the field. Further studies that scrutinize different N_2O production processes are still needed in order to develop the optimum method for mitigating N_2O emissions.

5. Conclusions

The application of NI significantly mitigated N_2O emission by 56% compared to urea alone in a whole winter wheat–summer maize rotation period. We found evidence based on N_2O isotopomer signatures that nitrification contributed to less than 41% of N_2O peak emissions, while nitrifier denitrification was more likely a significant source of the remaining N_2O emissions. The high effectiveness of NI on mitigating N_2O emission at high soil moisture condition may be attributed to the dual inhibitory effect of the NI on nitrifier denitrification, which suggests that NI can be used as an efficient management option to mitigate N_2O emissions even at high soil moisture conditions in the NCP.

Acknowledgements

This study was supported by the State's Key Project of Research and Development Plan (2016YFD0800104) and the Chinese Scholarship Council (scholarship no. 201306350130).

330

331

332

333

334 References

335 Baggs, E.M., 2011. Soil microbial sources of nitrous oxide: recent advances in knowledge, emerging chal-
336 lenges and future direction. Current Opinion in Environmental Sustainability 3, 321–327.

337 Bouwman, A.F., Boumans, L.J.M., Batjes, N.H., 2002. Emissions of N_2O and NO from fertilized fields:
338 Summary of available measurement data. Global Biogeochemical Cycles 16, 1058.

339 National Bureau of Statistics of China., 2016 China statistical yearbook. China Statistics Press, Beijing

340 Butterbach-Bahl, K., Baggs, E.M., Dannenmann, M., Kiese, R., Zechmeister-Boltenstern, S., 2013. Nitrous
341 oxide emissions from soils: how well do we understand the processes and their controls? Philos Trans R
342 Soc Lond B Biol Sci 368, 20130122.

343 Cai, G.X., Chen, D.L., Ding, H., Pacholski, A., Fan, X.H., Zhu, Z.L., 2002. Nitrogen losses from fertilizers ap-
344 plied to maize, wheat and rice in the North China Plain. Nutrient Cycling in Agroecosystems 63, 187–195.

345 Cai, Y., Ding, W., Luo, J., 2013. Nitrous oxide emissions from Chinese maize–wheat rotation systems: A 3-
346 year field measurement. Atmospheric Environment 65, 112–122.

347 Davidson, E.A., Keller, M., Erickson, H.E., Verchot, L.V., Veldkamp, E., 2000. Testing a Conceptual Model
348 of Soil Emissions of Nitrous and Nitric Oxides Using two functions based on soil nitrogen availability and
349 soil water content, the hole-in-the-pipe model characterizes a large fraction of the observed variation of
350 nitric oxide and nitrous oxide emissions from soils. BioScience 50, 667–680.

351 Decock, C., Six, J., 2013. How reliable is the intramolecular distribution of ^{15}N in N_2O to source partition
352 N2O emitted from soil? Soil Biology and Biochemistry 65, 114–127.

353 Ding, W., Cai, Y., Cai, Z., Yagi, K., Zheng, X., 2007. Nitrous oxide emissions from an intensively cultivated
354 maize–wheat rotation soil in the North China Plain. Science of The Total Environment 373, 501–511.

355 Ding, W.X., Yu, H.Y., Cai, Z.C., 2010. Impact of urease and nitrification inhibitors on nitrous oxide emis-
356 sions from fluvo-aquic soil in the North China Plain. Biology and Fertility of Soils 47, 91–99.

357 Frame, C.H., Casciotti, K.L., 2010. Biogeochemical controls and isotopic signatures of nitrous oxide pro-
358 duction by a marine ammonia-oxidizing bacterium. Biogeosciences 7, 2695–2709.

359 Granli, T., Boeckman, O.C. Norsk H. as F., 1994. Nitrous oxide from agriculture. Norwegian Journal of
360 Agricultural Sciences (Norway).

361 Hatch, D., Trindade, H., Cardenas, L., Carneiro, J., Hawkins, J., Scholefield, D., Chadwick, D., 2005. Labora-
362 tory study of the effects of two nitrification inhibitors on greenhouse gas emissions from a slurry-treated
363 arable soil: impact of diurnal temperature cycle. Biology and Fertility of Soils 41, 225–232.

364 Heil, J., Liu, S., Vereecken, H., Brüggemann, N., 2015. Abiotic nitrous oxide production from hydroxyla-
365 mine in soils and their dependence on soil properties. Soil Biology and Biochemistry 84, 107–115.

366 Huang, T., Gao, B., Hu, X.-K., Lu, X., Well, R., Christie, P., Bakken, L.R., Ju, X.-T., 2014. Ammonia-oxidation
367 as an engine to generate nitrous oxide in an intensively managed calcareous Fluvo-aquic soil. Scientific
368 Reports 4.

IPCC ., 2014: Climate Change 2014: Synthesis Report. Available at: https://www.ipcc.ch/pdf/assessment-report/ar5/syr/SYR_AR5_FINAL_full_wcover.pdf

Ju, X., Liu, X., Zhang, F., Roelcke, M., 2004. Nitrogen Fertilization, Soil Nitrate Accumulation, and Policy Recommendations in Several Agricultural Regions of China. AMBIO: A Journal of the Human Environment 33, 300–305.

Ju, X., Lu, X., Gao, Z., Chen, X., Su, F., Kogge, M., Römheld, V., Christie, P., Zhang, F., 2011. Processes and factors controlling N_2O production in an intensively managed low carbon calcareous soil under sub-humid monsoon conditions. Environmental Pollution 159, 1007–1016.

Kool, D.M., Dolfing, J., Wrage, N., Van Groenigen, J.W., 2011. Nitrifier denitrification as a distinct and significant source of nitrous oxide from soil. Soil Biology and Biochemistry 43, 174–178.

Köster, J.R., Cárdenas, L., Senbayram, M., Bol, R., Well, R., Butler, M., Mühling, K.H., Dittert, K., 2011. Rapid shift from denitrification to nitrification in soil after biogas residue application as indicated by nitrous oxide isotopomers. Soil Biology and Biochemistry 43, 1671–1677.

Lewicka-Szczebak, D., Augustin, J., Giesemann, A., Well, R., 2016. Isotopic fractionation of N_2O to quantify N_2O reduction to N_2 - validation with Helium incubation and ^{15}N gas flux methods. Biogeosciences Discuss. 2016, 1–50.

Li, H., Qiu, J., Wang, L., Tang, H., Li, C., Van Ranst, E., 2010. Modelling impacts of alternative farming management practices on greenhouse gas emissions from a winter wheat–maize rotation system in China. Agriculture, Ecosystems & Environment 135, 24–33.

Liu, C., Wang, K., Zheng, X., 2013. Effects of nitrification inhibitors (DCD and DMPP) on nitrous oxide emission, crop yield and nitrogen uptake in a wheat-maize cropping system. Biogeosciences 10, 2427–2437.

Menendez, S., Barrena, I., Setien, I., Gonzalez-Murua, C., Estavillo, J.M., 2012. Efficiency of nitrification inhibitor DMPP to reduce nitrous oxide emissions under different temperature and moisture conditions. Soil Biology & Biochemistry 53, 82–89.

Meng, L., Ding, W., Cai, Z., 2005. Long-term application of organic manure and nitrogen fertilizer on N_2O emissions, soil quality and crop production in a sandy loam soil. Soil Biology and Biochemistry 37, 2037–2045.

Ostrom, N.E., Pitt, A., Sutka, R., Ostrom, P.H., Grandy, A.S., Huizinga, K.M., Robertson, G.P., 2007. Isotopologue effects during N_2O reduction in soils and in pure cultures of denitrifiers. Journal of Geophysical Research: Biogeosciences (2005–2012) 112.

Qiao, C., Liu, L., Hu, S., Compton, J.E., Greaver, T.L., Li, Q., 2015. How inhibiting nitrification affects nitrogen cycle and reduces environmental impacts of anthropogenic nitrogen input. Global Change Biology 21, 1249–1257.

Ravishankara, A.R., Daniel, J.S., Portmann, R.W., 2009. Nitrous oxide (N_2O): the dominant ozone-depleting substance emitted in the 21st century. Science 326, 123–125.

Rohe, L., Anderson, T.-H., Braker, G., Flessa, H., Giesemann, A., Lewicka-Szczebak, D., Wrage-Mönnig, N., Well, R., 2014. Dual isotope and isotopomer signatures of nitrous oxide from fungal denitrification–a pure culture study. Rapid Communications in Mass Spectrometry 28, 1893–1903.

Senbayram, M., Chen, R., Budai, A., Bakken, L., Dittert, K., 2012. N_2O emission and the $N_2O/(N_2O+N_2)$ product ratio of denitrification as controlled by available carbon substrates and nitrate concentrations. Agriculture, Ecosystems & Environment 147, 4–12.

Shi, Y., Wu, W., Meng, F., Zhang, Z., Zheng, L., Wang, D., 2013. Integrated management practices significantly affect N_2O emissions and wheat–maize production at field scale in the North China Plain. Nutrient Cycling in Agroecosystems 95, 203–218.

Sutka, R.L., Ostrom, N.E., Ostrom, P.H., Breznak, J.A., Gandhi, H., Pitt, A.J., Li, F., 2006. Distinguishing nitrous oxide production from nitrification and denitrification on the basis of isotopomer abundances. Applied and Environmental Microbiology 72, 638–644.

Sutton, M.A., Howard, C.M., Erisman, J.W., Billen, G., Bleeker, A., Grennfelt, P., van Grinsven, H., Grizzetti, B., 2011. The European nitrogen assessment: sources, effects and policy perspectives. Cambridge University Press.

Toyoda, S., Mutobe, H., Yamagishi, H., Yoshida, N., Tanji, Y., 2005. Fractionation of N_2O isotopomers during production by denitrifier. Soil Biology and Biochemistry 37, 1535–1545.

Toyoda, S., Yano, M., Nishimura, S., Akiyama, H., Hayakawa, A., Koba, K., Sudo, S., Yagi, K., Makabe, A., Tobari, Y., 2011. Characterization and production and consumption processes of N_2O emitted from temperate agricultural soils determined via isotopomer ratio analysis. Global Biogeochemical Cycles 25.

Toyoda, S., Yoshida, N., 1999. Determination of nitrogen isotopomers of nitrous oxide on a modified isotope ratio mass spectrometer. Analytical Chemistry 71, 4711–4718.

Toyoda, S., Yoshida, N., Koba, K., 2015. Isotopocule analysis of biologically produced nitrous oxide in various environments. Mass Spectrometry Reviews 36: 135–160.

Wan, Y., Ju, X., Ingwersen, J., Schwarz, U., Stange, C.F., Zhang, F., Streck, T., 2009. Gross Nitrogen Transformations and Related Nitrous Oxide Emissions in an Intensively Used Calcareous Soil. Soil Science Society of America Journal 73, 102–112.

Weiske A, G, B., T, H., J, O., 2001. Influence of the nitrification inhibitor 3,4-dimethylpyrazole phosphate (DMPP) in comparison to dicyandiamide (DCD) on nitrous oxide emissions, carbon dioxide fluxes and methane oxidation during 3 years of repeated application in field experiments. Biology and Fertility of Soils 34, 109–117.

Well, R., Flessa, H., 2009. Isotopologue enrichment factors of N_2O reduction in soils. Rapid Communications in Mass Spectrometry 23, 2996–3002.

White, R.E., Cai, G., Chen, D., Fan, X.H., Pacholski, A., Zhu, Z.L., Ding, H., 2002. Gaseous nitrogen losses from urea applied to maize on a calcareous fluvo-aquic soil in the North China Plain. Soil Research 40, 737–748.

Wu, D., Köster, J.R., Cárdenas, L.M., Brüggemann, N., Lewicka-Szczebak, D., Bol, R., 2016. N_2O source partitioning in soils using 15N site preference values corrected for the N_2O reduction effect. Rapid Communications in Mass Spectrometry 30, 620–626.

Wu, D., Senbayram, M., Well, R., Brüggemann, N., Pfeiffer, B., Loick, N., Stempfhuber, B., Dittert, K., Bol, R., 2017. Nitrification inhibitors mitigate N_2O emissions more effectively under straw-induced conditions favoring denitrification. Soil Biology and Biochemistry 104, 197–207.

Yano, M., Toyoda, S., Tokida, T., Hayashi, K., Hasegawa, T., Makabe, A., Koba, K., Yoshida, N., 2014. Isotopomer analysis of production, consumption and soil-to-atmosphere emission processes of N_2O at the beginning of paddy field irrigation. Soil Biology and Biochemistry 70, 66–78.

Zerulla, W., Barth, T., Dressel, J., Erhardt, K., Von Locquenghien, K.H., Pasda, G., Radle, M., Wissemeier, A.H., 2001. 3,4-Dimethylpyrazole phosphate (DMPP) - a new nitrification inhibitor for agriculture and horticulture. Biology and Fertility of Soils 34, 79–84.

Zhang, W., Li, Y., Xu, C., Li, Q., Lin, W., 2016. Isotope signatures of N_2O emitted from vegetable soil: Ammonia oxidation drives N_2O production in NH_4^+-fertilized soil of North China. Scientific Reports 6, 29257.

Zhou, M., Zhu, B., Butterbach-Bahl, K., Wang, X., Zheng, X., 2014. Nitrous oxide emissions during the non-rice growing seasons of two subtropical rice-based rotation systems in southwest China. Plant and Soil 383, 401–414.

Zhou, Y., Zhang, Y., Tian, D., Mu, Y., 2016. Impact of dicyandiamide on emissions of nitrous oxide, nitric oxide and ammonia from agricultural field in the North China Plain. Journal of Environmental Sciences, Changing Complexity of Air Pollution 40, 20–27.

Zhu, X., Burger, M., Doane, T.A., Horwath, W.R., 2013. Ammonia oxidation pathways and nitrifier denitrification are significant sources of N_2O and NO under low oxygen availability. Proceedings of the National Academy of Sciences 110, 6328–6333.

Table captions

Table 1 Total N_2O emissions and emission factors for different treatments for the observation period 2015-2016. Values in the same column followed by different superscript letters are significantly different ($P<0.05$).

Table 2 Correlations between N_2O flux and soil temperature, WFPS, NO_3^--N or NH_4^+-N. Asterisks denote significance ($^*P < 0.05$, n = 77).

Figure captions

Figure 1 Temporal variation of (a) air temperature, mean soil temperature, precipitation and (b) soil WFPS during the experimental period. The dotted line arrows indicate irrigation events.

Figure 2 Temporal variations of NH_4^+ (a) and NO_3^- (b) concentrations of different treatments during the experimental period. The solid line arrows indicate N fertilizer application events.

Figure 3 N_2O fluxes of soil for different treatments during the experimental period. The solid line arrows indicate N fertilizer application events.

Figure 4 ^{15}N Site preference (SP) values and source partitioning of N_2O. Left y axis: N_2O SP values of the U treatment (urea alone) and the NI treatment (urea + DMPP) during the experimental period. Right Y axis: Nitrification proportion calculated on the basis of N_2O SP values and two-end-member model. Vertical bars denote the standard error of the mean (n=3).

Figure S1 $\delta^{15}N_{bulk}$ of N_2O of the U treatment (urea alone) and the NI treatment (urea + DMPP) during the experimental period. Vertical bars denote the standard error of the mean (n=3).

Figure S2 $\delta^{18}O$ of N_2O of the U treatment (urea alone) and the NI treatment (urea + DMPP) during the experimental period. Vertical bars denote the standard error of the mean (n=3).

Table 1

Treatment	Winter Wheat		Summer Maize		Annual	
	N_2O (kg N ha^{-1})	EF (%)	N_2O (kg N ha^{-1})	EF (%)	N_2O (kg N ha^{-1})	EF (%)
CK	0.14±0.02[a]	-	0.25±0.03[a]	-	0.39±0.04[a]	-
U	1.11±0.21[c]	0.32	1.23±0.09[c]	0.33	2.33±0.20[c]	0.32
NI	0.37±0.06[b]	0.08	0.65±0.01[b]	0.13	1.02±0.04[b]	0.11

Table 2

Treatment	Soil T	WFPS	NO_3^--N	NH_4^+-N
CK	0.43*	0.33*	0.21	0.41*
U	0.33*	0.35*	0.31*	-0.14
NI	0.47*	0.27*	0.15	-0.03

Figure. 1

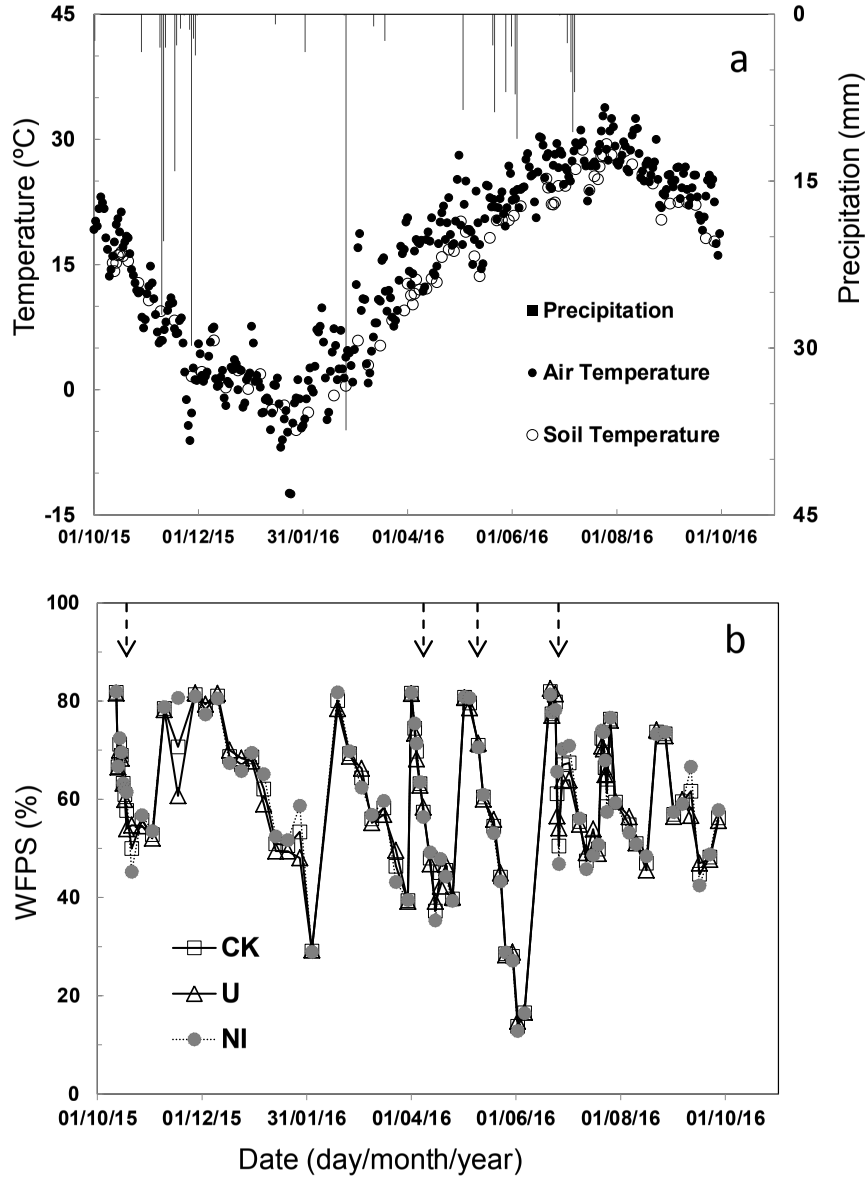
a
Temperature (ºC)
Precipitation (mm)
45
30
15
0
-15
0
15
30
45
Precipitation
Air Temperature
Soil Temperature
01/10/15
01/12/15
31/01/16
01/04/16
01/06/16
01/08/16
01/10/16
b
WFPS (%)
100
80
60
40
20
0
CK
U
NI
Date (day/month/year)

Figure. 2

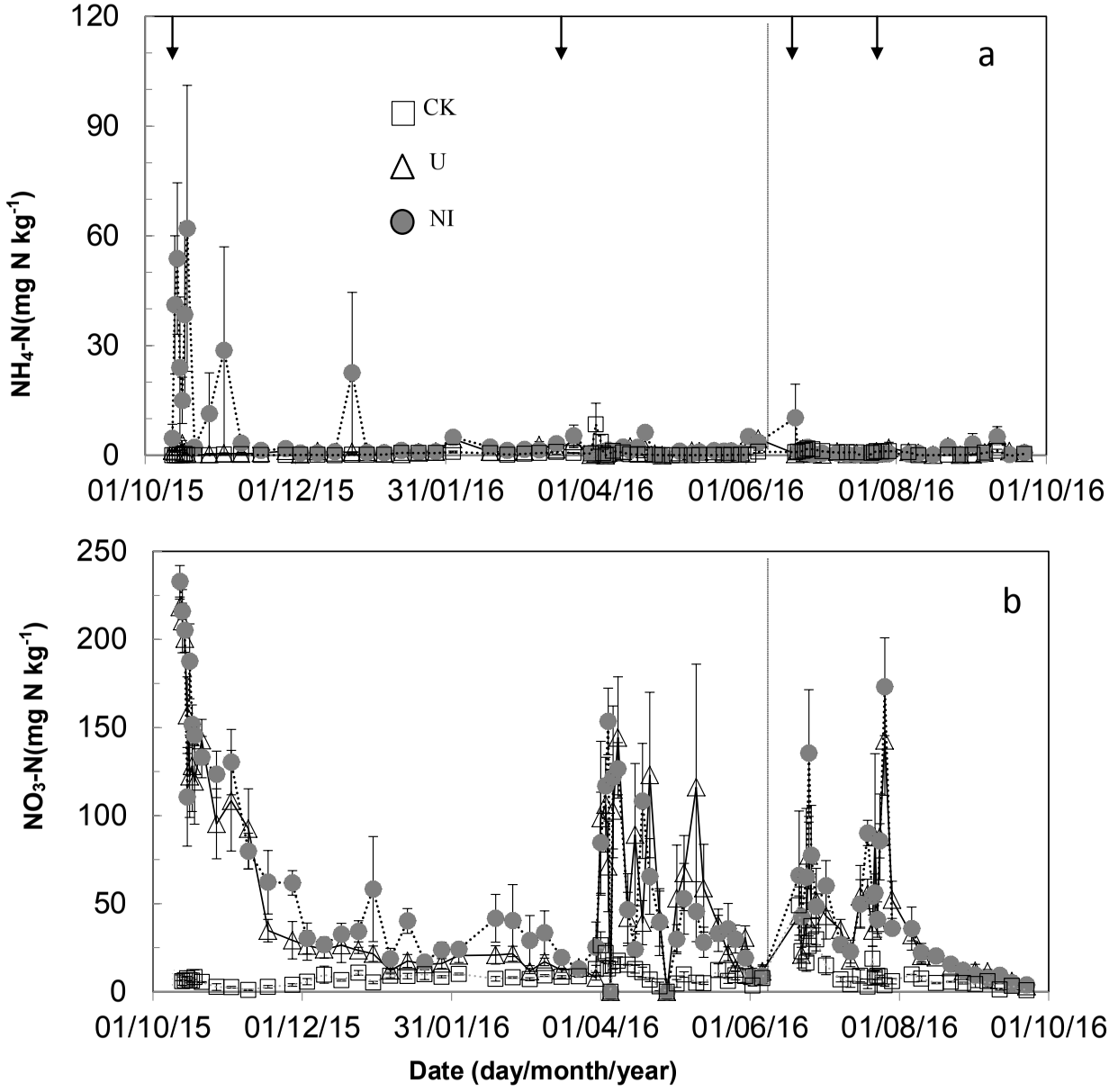
a
b
CK
U
NI
NH_4-N(mg N kg^{-1})
NO_3-N(mg N kg^{-1})
120
90
60
30
0
250
200
150
100
50
01/10/15
01/12/15
31/01/16
01/04/16
01/06/16
01/08/16
01/10/16
Date (day/month/year)

Figure. 3

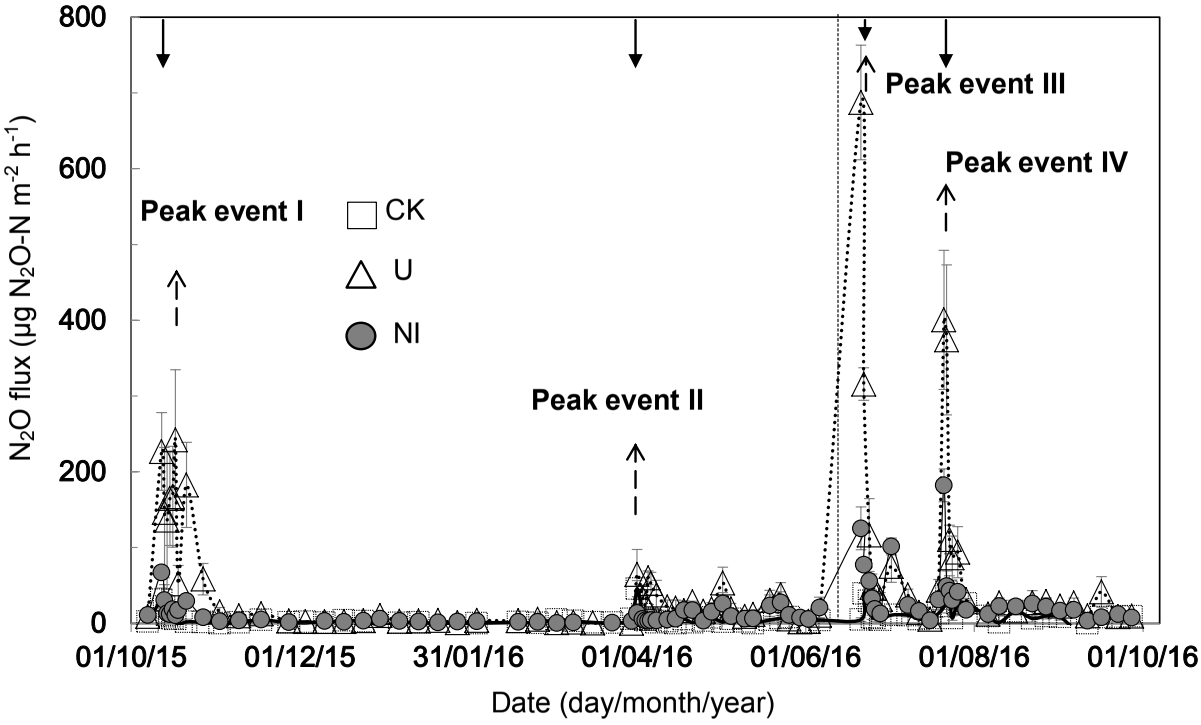
800
600
400
200
0
N2O flux (µg N2O-N m-2 h-1)
Peak event I
CK
U
NI
Peak event II
Peak event III
Peak event IV
01/10/15
01/12/15
31/01/16
01/04/16
01/06/16
01/08/16
01/10/16
Date (day/month/year)

Figure. 4

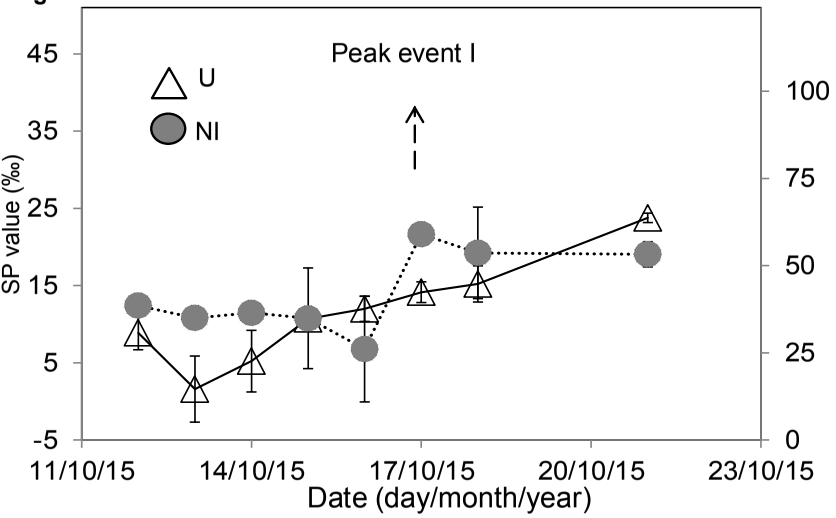
Peak event I
U
NI
SP value (‰)
Percentage of N_2O derived from nitrification (%)
45
35
25
15
5
-5
100
75
50
25
0
11/10/15
14/10/15
17/10/15
20/10/15
23/10/15
Date (day/month/year)

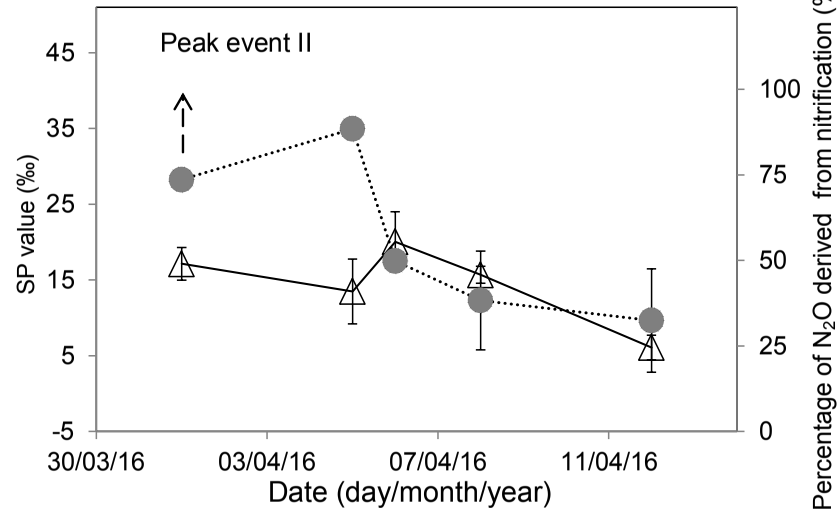
Peak event II
SP value (‰)
Percentage of N_2O derived from nitrification (%)
45
35
25
15
5
-5
100
75
50
25
0
30/03/16
03/04/16
07/04/16
11/04/16
Date (day/month/year)

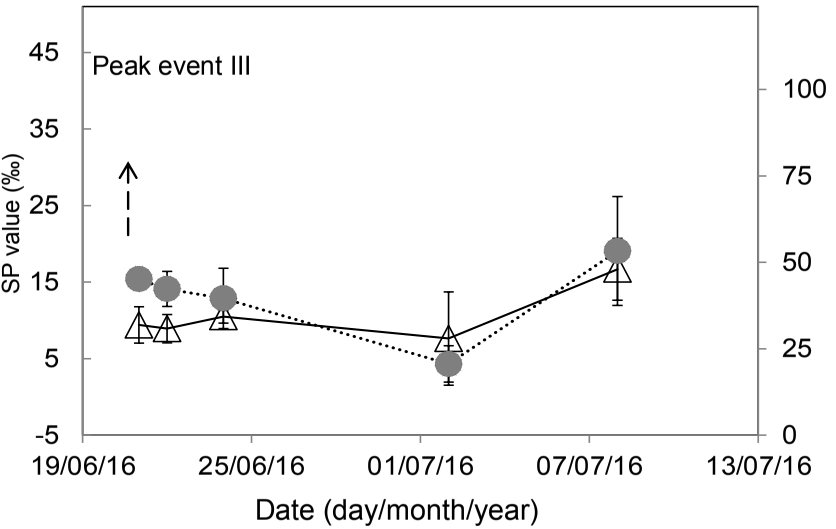
Peak event III
SP value (‰)
Percentage of N_2O derived from nitrification (%)
45
35
25
15
5
-5
100
75
50
25
0
19/06/16
25/06/16
01/07/16
07/07/16
13/07/16
Date (day/month/year)

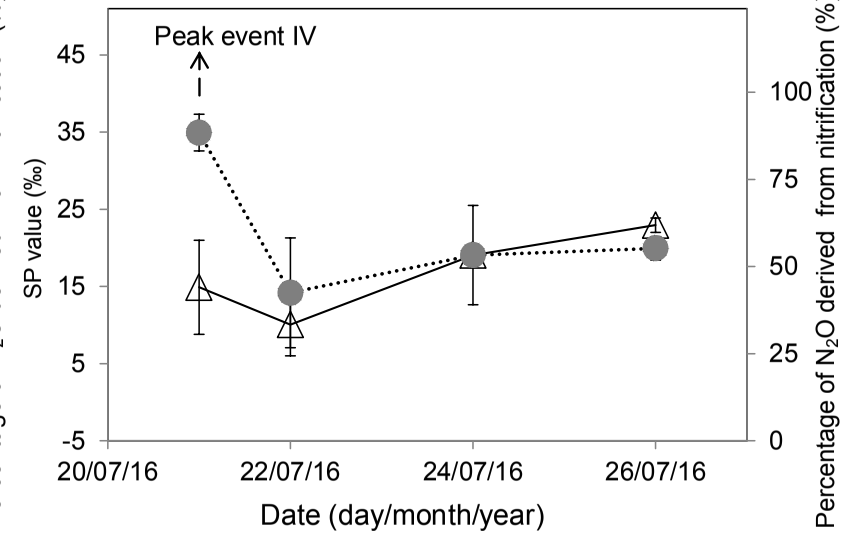
Peak event IV
SP value (‰)
Percentage of N_2O derived from nitrification (%)
45
35
25
15
5
-5
100
75
50
25
0
20/07/16
22/07/16
24/07/16
26/07/16
Date (day/month/year)

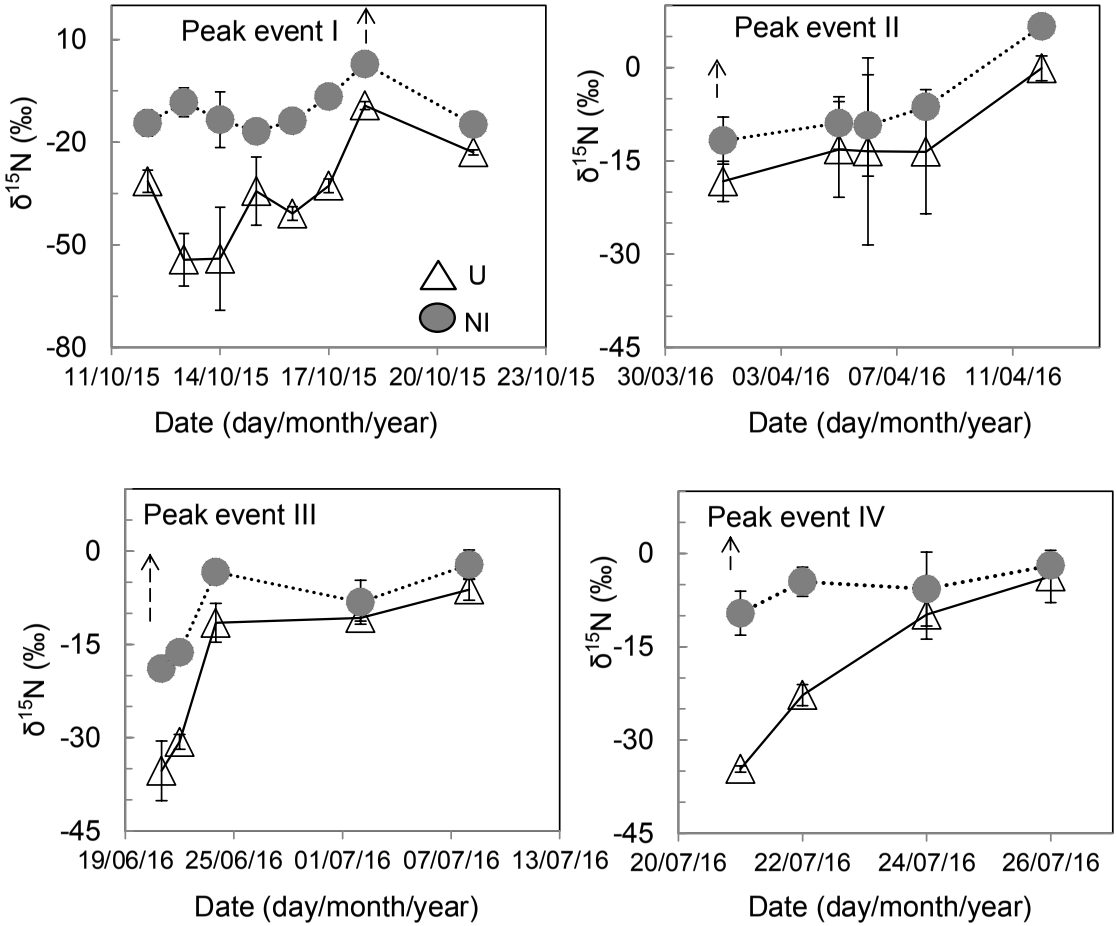

Figure S1 $\delta^{15}N_{bulk}$ of N_2O of the U treatment (urea alone) and the NI treatment (urea + DMPP) during the experimental period. Vertical bars denote the standard error of the mean (n=3).

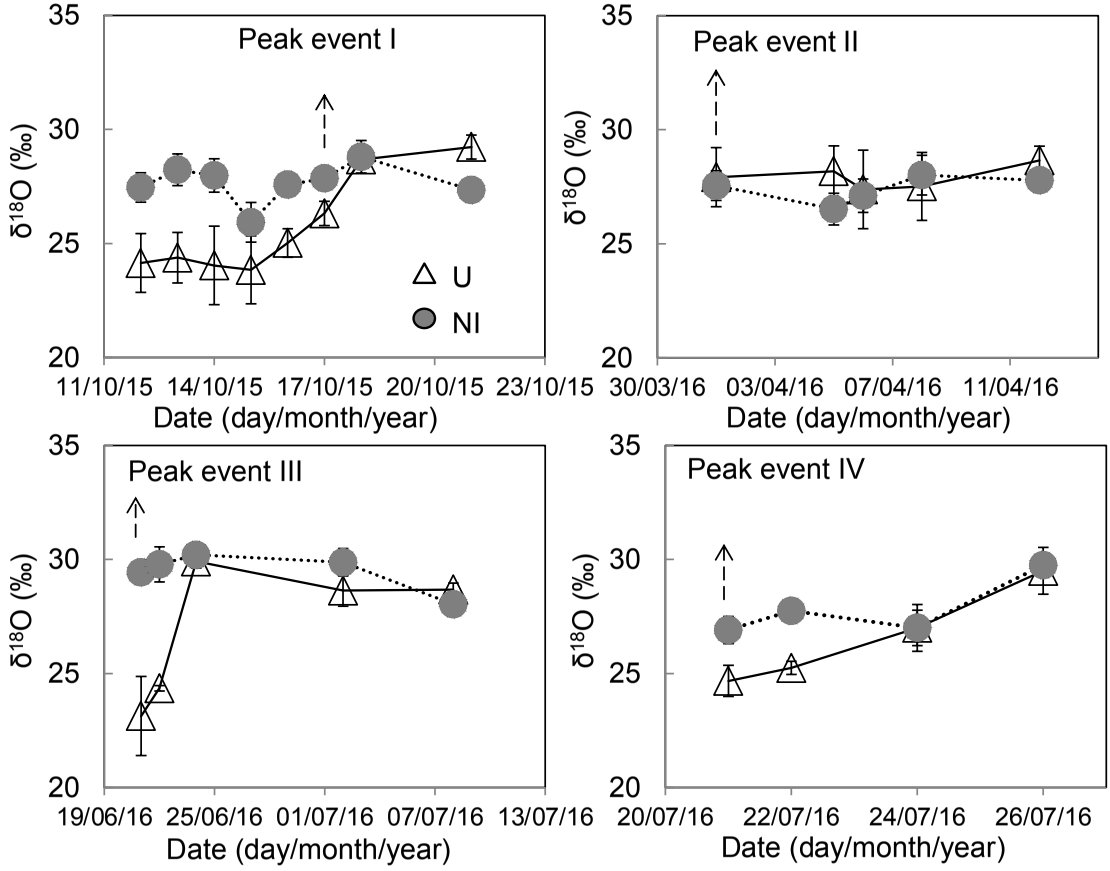

Figure S2 $\delta^{18}O$ of N_2O of the U treatment (urea alone) and the NI treatment (urea + DMPP) during the experimental period. Vertical bars denote the standard error of the mean (n=3).

Paper V

Influence of two different biochars application on CO_2 and N_2O emissions in two different soil types.

Wu, D., Senbayram, M., Blagodatskaya, E., Kuzyakov, Y., Bol, R., 2017

Draft manuscript

Influence of two different biochars application on CO_2 and N_2O emissions in two different soil types

Di Wu[1], Mehmet Senbayram[2], Evgenia Blagodatskaya[3], Nicolas Brüggemann[1], Yakov Kuzyakov[3], Roland Bol[1]

1 Institute of Bio- and Geosciences, Agrosphere (IBG-3), Forschungszentrum Jülich GmbH, 52425 Jülich, Germany

2 Institute of Plant Nutrition and Soil Science, University of Harran, Osmanbey, 63000, Sanliurfa, Turkey

3. Department of Soil Science of Temperate Ecosystems, Büsgen-Institute, University of Göttingen, 37007 Göttingen, Germany.

Abstract

Emissions of greenhouse gases (GHGs), e.g. carbon dioxide (CO_2) and nitrous oxide (N_2O) have shown great impact on global warming and atmospheric chemistry. Biochar addition has been proposed as a potential option for reducing greenhouse gas emissions through carbon sequestration and mitigating N_2O emissions. However, mixed results were observed in both laboratory and field studies about the mitigation effects of biochar application on CO_2 and N_2O emissions. The influences of biochar on carbon (C) mineralization and nitrogen (N) transformation processes in soil are still unclear, resulting in a poor understanding of the mechanisms of biochar's mitigation effect. Here we carried out a 62 day soil incubation experiment to investigate the influence of two biochar (olive biochar and corn biochar) on CO_2 and N_2O emissions from two different soil types. In acidic sandy soil, application of olive biochar induced a pronounced positive priming effect for CO_2 emissions during the early phases of incubation, while corn biochar amendment showed negative prime effect and significantly reduced the cumulative CO_2 emissions during 62 day incubation. In alkaline clay soil no significant influences of two biochar on CO_2 emissions were observed. Both olive biochar and corn biochar significantly reduced N_2O emissions in acidic sandy soil, while none of them had significantly effect on N_2O emissions in alkaline clay soil. We propose that the N_2O mitigation effect of biochar was likely due to the oxygen and C depletion caused by the biochar priming effect, which promoted the last denitrification step -N_2O to N_2 reduction.

1. Introduction

Both carbon dioxide (CO_2) and nitrous oxide (N_2O) are the important long-lived greenhouse gases (GHGs) forcing global warming. Biochar, which is obtained from the thermos-chemical conversion of biomass (Lehmann and Joseph, 2009), has been frequently reported to be an effective solution to mitigate greenhouse gas (GHG) emissions, e.g. CO_2 and N_2O (Cayuela et al., 2014; Yanai et al., 2007).

Besides well-known CO_2, nitrous oxide is another potent greenhouse gas, which has been increased since pre-industrial times through human activities (Bouwman et al., 2002; IPCC, 2013). The global warming potential (GWP) of N_2O is 298 times the GWP of CO_2 when calculated over a 100-year period (IPCC, 2013). Soils are considered to be the largest source of N_2O emissions, while biochemical nitrogen (N) transformations such as nitrification and denitrification are thought to be the major sources of N_2O (Baggs, 2011; Butterbach-Bahl and Dannenmann, 2011). Increased N_2O emissions are generally attributed to aplication of N fertilizer; however, application of N fertilizer also is one of the key contributors for the increasing agricultural productivity (Fowler et al., 2013; Sutton et al., 2011). It is therefore a great challenge to develop mitigation strategies that could maintain food production while reducing N_2O emissions in high N input agricultural systems.

Wide variations in the biochar's greenhouse emissions mitigation effect have been reported among different kinds of biochar and different soil types (Clough et al., 2010; Taghizadeh-Toosi et al., 2011). The effect of biochar amendment on soil CO_2 evolution, which is known as biochar priming effect, has been reported as positive, neutral and negative. For example, Chang et al., (2016) and Chintala et al. (2014) found that biochar showed negative priming effect on mineralization of carbon and reduce CO_2 emission, whereas Zimmerman et al. (2011) reported both positive and negative priming effect under different types of biochar amendment. Similarly, contro-

versial results about the suppression effects of biochar application on N_2O emissions were observed in both laboratory and field studies (Cayuela et al., 2014; Chang et al., 2016; Nelissen et al., 2014). Several hypotheses have been proposed to understand the mechanism, such as biochar's effect of increasing soil aeration and soil pH, absorbing N in soil, and modifying the soil microorganism that involve in N cycle process (Cayuela et al., 2013; Lehmann et al., 2011). The inconsistent findings and explanations from different studies emphasize the need to compare the influence of different biochars on GHGs emissions under different types of soil to reveal the underlying mechanism.

The objective of this incubation study was to investigate the influence of two different biochars application on CO_2 and N_2O emissions in two different soil types and thus gain an insight into the underlying mechanisms of biochar's influence on CO_2 and N_2O emissions.

2. Material and methods

2.1 Properties of biochar and soil

The olive mill and corn cob biochars were both pressed two times and pyrolized one month after. The olive biochar substrate includes the olives only. The pyrolysis temperature was 400℃. Important biochar properties are listed in Table 1. The sandy soil (sand 81.8%, silt 14.8%, clay 3.5%) was collected from farmland close to Gifhorn, Lower Saxony, Germany (52° 34' 9.5" N, 10° 45' 26.6" E). Arable crops (oilseed rape, wheat, barley, potato) had been grown prior to soil sampling. The clay soil (sand 17.8%, silt 26.2%, clay 56.0%) was collected from soil in Turkey. The upper 2 cm of soil and roots were removed and the 10-15 cm soil horizon beneath was collected. Before use, both of the soils are air dried and sieved <4mm. n. Important soil properties are presented in Table 2.

Table 1. The characteristics of the two biochar (olive biochar, corn biochar) used in the experiment.

Biochar	N (%)	C (%)	C/N
Olive pulp biochar	0.65	49.2	76.3
Corn cub biochar	0.67	78.0	116.4

Table 2. The characteristics of the two soil (sandy soil, clay soil) used in the experiment

Soil	Total N (%)	Total C (%)	NH_4^+ (mg N kg^{-1})	NO_3^- (mg N kg^{-1})	pH
Sandy soil	0.11	2.34	0.50	1.41	6.3
Clay soil	0.09	1.52	1.91	9.86	7.8

2.2 Incubation experiment and gas measurement

The incubation experiment was carried out at institute of Applied Plant Nutrition, University of Göttingen, Germany, with in total 24 PVC vessels, among them 15 vessels with a fully automated incubation system, as describe by Wu et al. (2017) and 9 similar vessels with manual sampling system. In biochar treatments 19.9 g olive pulp biochar or 12.6 g corn cob biochar was thoroughly mixed with soil, equilibrant to 9.8g C addition. Soil moisture was adjusted to 70% water holding capacity (WHC). In each vessel 1.5 kg dry soils were packed in with bulk density 0.9 cm^{-3}. Ammonium sulfate ($(NH_4)_2 SO_4$) was used as mineral N fertilizer and applied at a rate of 150 kg N ha^{-1} (equivalent to 2.2 g per pot). Four treatments were applied to the two soils, i.e. i) soil

amended with N fertilizer (ammonium sulfate) only (AS), ii) olive pulp biochar amended with N fertilizer.(Olive+AS) iii) Corn cub amended with N fertilizer (Corn+AS) and iv) non-amended control (Control). The headspace of each vessel was continuously flushed with ambient air (about 20 ml air min^{-1}). For the gas concentration analysis of N_2O and CO_2 with the automated incubation system, samples from each incubation vessel's outlet was directed to a gas chromatograph sequentially via two multi-positional valves with electric actuator controlled by Trilution software (Gilson Inc., Middleton, WI, USA) and an interface module (508 interface module, Gilson Inc.). The concentrations were measured about 3 times per day; the specific applied system has previously been described in detail by Wu et al. (2017). For the manual sampling system, gas samples were taken approximately 1 time per day from the headspace of additional 9 PVC vessels, which were identical to those in the online system. The outlet flux rate for each incubation vessel was measured every day manually with a portable gas flow meter (GFM Pro Gas Flowmeter, Thermo Fisher Scientific, Waltham, MA, USA).

2.3 Soil sampling and analysis of NH_4^+ and NO_3^-

Soil samples from the upper 10 cm were collected at the end of incubation from each vessel and were stored at -80°C until further analyses. For mineral N analysis the soil samples were extracted with 0.01 M $CaCl_2$ (1:5 w/v) by shaking for 1 h. The extracts were then filtered through Whatman 602 filter paper and stored at −20 °C until analysis. The concentrations of NH_4^+ and NO_3^- in soil extracts were measured colorimetrically using an autoanalyzer (SKALAR, The Netherlands).

2.4 Calculations and statistical analysis

The cumulative gas emissions were calculated by linear interpolation between measured daily fluxes. Emission rates were expressed as arithmetic means of the three replicates and ANOVA tests were used to reveal significant pairwise differences among the three treatments at $P < 0.05$. Statistical analyses were conducted using R.

3. Results

3.1 CO_2 and N_2O gas emissions

The incubation period was divided to three phases regarding the CO_2 and N_2O emissions patterns (Fig. 1 and 3): phase I (0-15 days), phase II (15-30 days) and phase III (30-62 days). During phase I, maximum CO_2 emission rates were observed in all treatments. In sandy soil, maximum rates were 8.2 ±0.6, 9.5±0.4, 19.1±3.6 and 8.0±0.9 kg CO_2-C ha^{-1} day^{-1} in the Control, AS, Olive+AS and Corn+AS, respectively. Application of olive biochar induced a pronounced CO_2 emission peak after onset of treatments (19 hours), while the CO_2 emissions peaks were not obvious in other treatments. This suggested the olive biochar stimulated a significant increase in respiration in Olive+AS treatments. After phase I, the fluxes of CO_2 decreased to the background levels in all treatments except for AS treatment until the end of incubation period. During phase II and phase III, the N fertilizer only treatment had larger CO_2 emission rates over time compared with other treatments. The cumulative CO_2 emission for the Control, AS, Olive+AS and Corn+AS were 320.8±7.6, 394.0±12.2, 409.4±45.7 and 347.0±11.6 CO_2-C kg C ha^{-1}, respectively (Fig. 2). Compare to N-fertilizer only treatment, in sandy soil corn biochar addition significantly reduced the cumulative CO_2 emissions, while no significant different was found in olive biochar treatment.

The CO_2 emissions in clay soil were generally greater than those in sandy soil. The emission patterns were similar for all treatments during whole incubation period. During phase I, maximum

CO_2 emission rates were observed in all clay soil treatments at approx. day 2 with no significant difference in between, ranging from 32.4-38.6 kg CO_2-C ha^{-1} day^{-1}. The CO_2 fluxes decreased drastically after the peak till the end of phase I, and then decreased gradually during phase II and phase III. In contrast with sandy soil, the biochar treatments had larger CO_2 emission compared with mineral N only treatment during phase II and phase III. The cumulative CO_2 emission for the Control, AS, Olive+AS and Corn+AS were 744.3±40.4, 814.3.0±19.1, 885.3±71.7 and 920.1±44.9 CO_2-C kg C ha^{-1}, respectively (Fig. 2). No significant difference was found on cumulative CO_2 emissions between N-fertilizer only treatments and biochar amendment treatments.

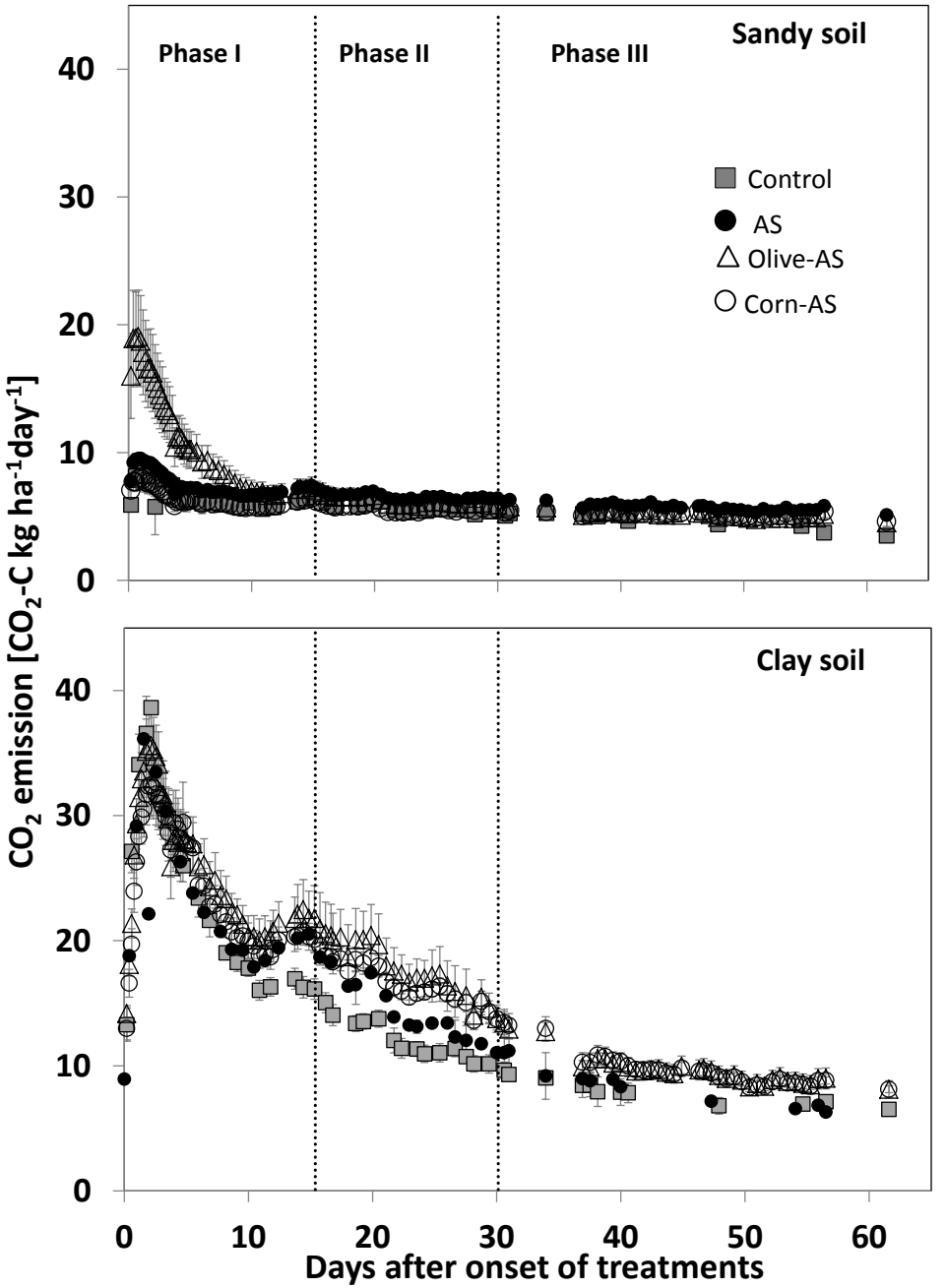
Phase I
Phase II
Phase III
Sandy soil
Control
AS
Olive-AS
Corn-AS
Clay soil
CO2 emission [CO2-C kg ha-1day-1]
0
10
20
30
40
0
10
20
30
40
50
60
Days after onset of treatments

Figure 1. CO_2 fluxes in the four treatments from sandy soil and clay soil. Data presented are the average of soil cores. Error bars show the standard error of the mean of each treatment (n = 3).

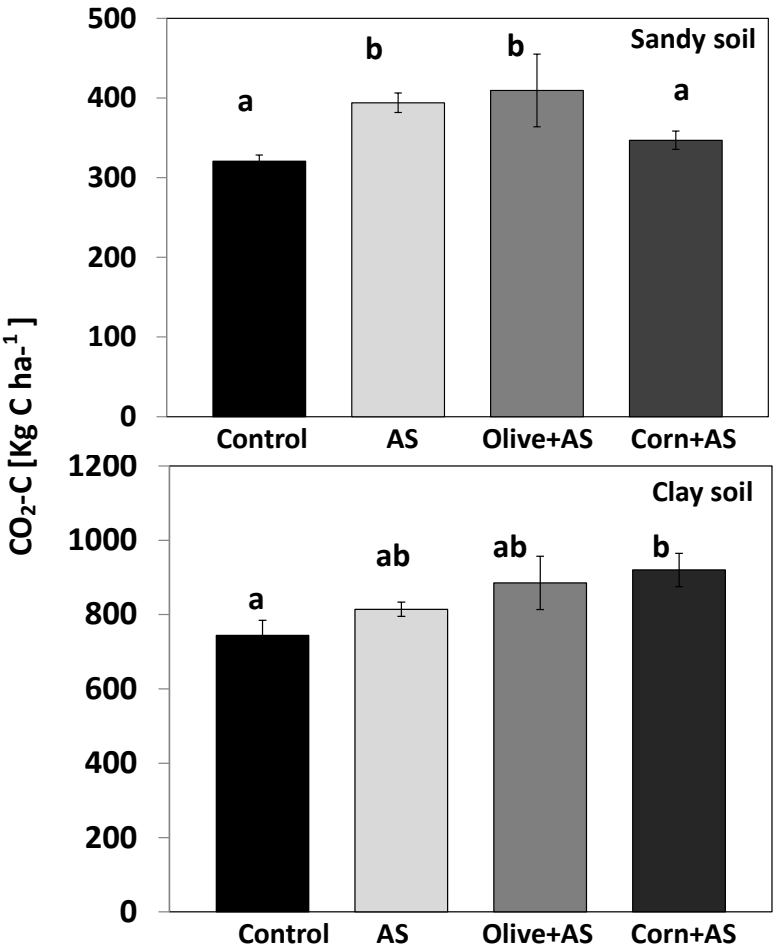

Figure 2. Cumulative CO_2 emissions during 62 days incubation period in the four treatments from sandy soil and clay soil. Error bars show the standard error of the mean of each treatment (n = 3). Different small letters indicate significant differences at the $p < 0.05$ level between treatments.

The N_2O emissions patterns were strongly affected by the different types of biochar amendment and different types of soils. In sandy soil, the N_2O emissions peak emerged at the end of phase I in Olive+AS treatment, while in Corn+AS and AS only treatments the peak emerged both at the end of phase II (Fig. 3), whereas both biochar applications reduced the peak N_2O emissions compare with N-fertilizer only treatment. After peaked, N_2O emission in Olive+AS drastically decreased to close to zero in phase II and stayed constantly low during phase III, while the N_2O emission in AS and Corn+AS treatments gradually decreased after peaked in phase II and remained higher rate in phase III compared with the Control and Olive+AS treatment. The cumulative N_2O emissions over the 62 days incubation period were 38.0 ±6.4, 392.5±30.5, 124.2±11.9 and 286.9±10.3 g N_2O-N ha^{-1} day^{-1} in the Control, AS, Olive+AS, and Corn+AS respectively. Both olive biochar and corn biochar application significantly reduced N_2O emission (68.4% and 26.9% respectively) compared to N-fertilizer only treatment.

In clay soil, N fertilizer application induced larger N_2O emissions, while biochar application showed no significant influence on N_2O emission. The N_2O emission in N fertilized treatment peaked in phase I and gradually decreased to background level during phase II. The cumulative N_2O emissions were 27.5 ±1.8, 121.7±19.8, 99.1±9.9 and 80.2±9.6 g N_2O-N ha^{-1} day^{-1} in the Control, AS, Olive+AS, and Corn+AS respectively. No significant difference was found on cumulative N_2O emissions between biochar amendment treatments and N-fertilizer only treatment.

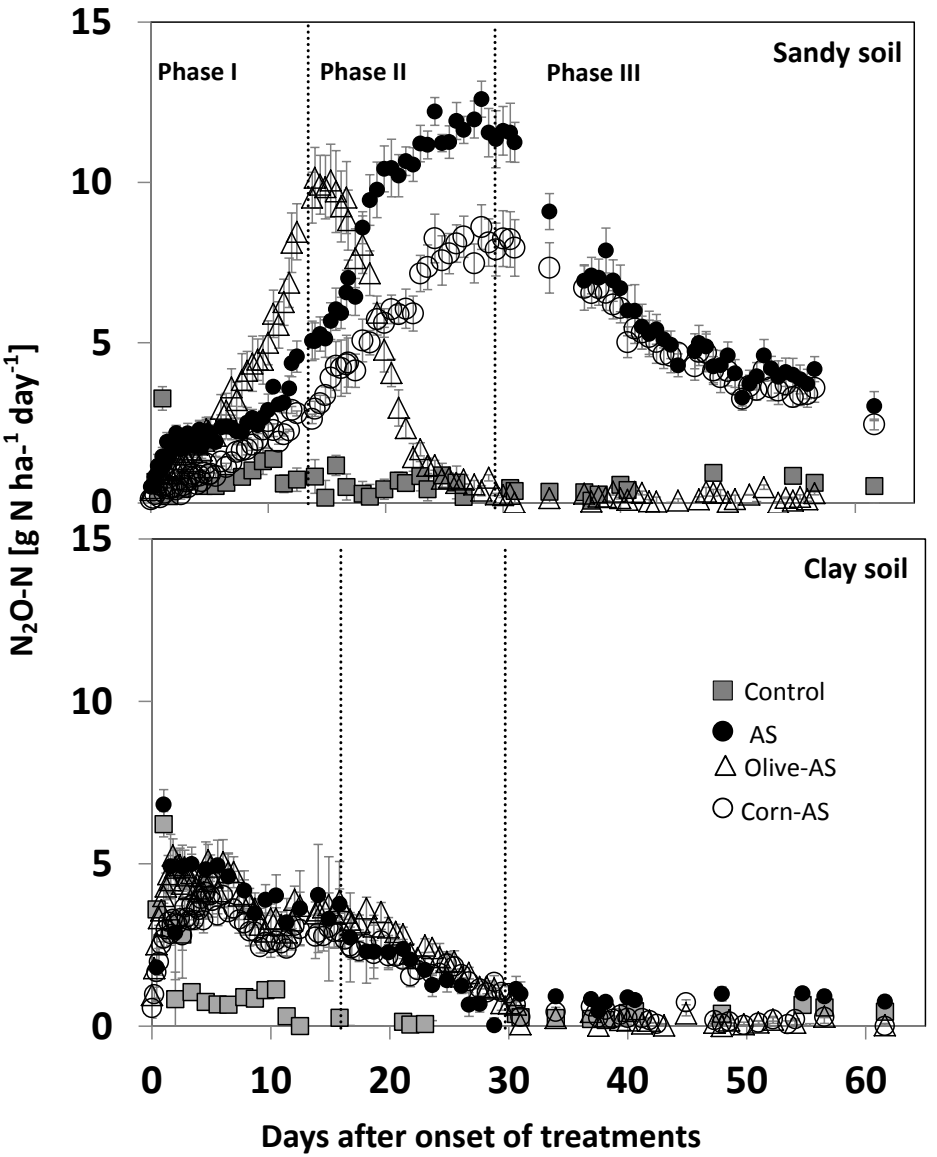

Figure 3. N_2O fluxes in the four treatments from sandy soil and clay soil. Data presented are the average of soil cores. Error bars show the standard error of the mean of each treatment (n = 3).

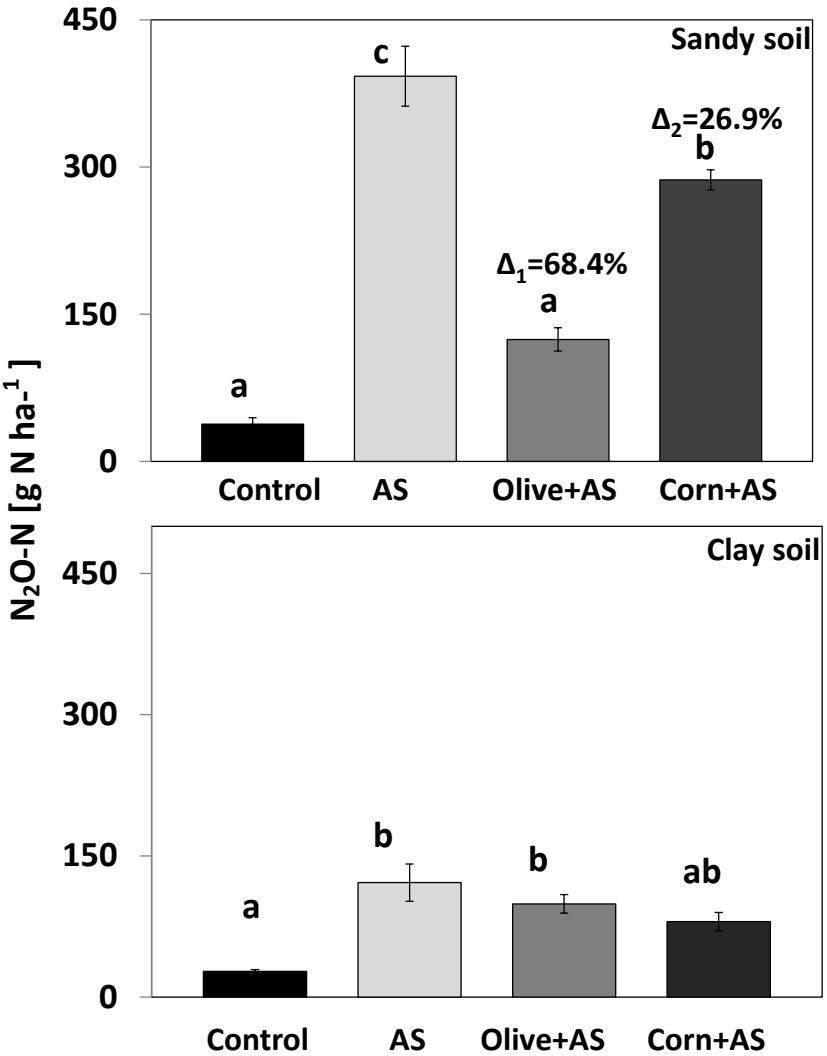

Figure 4. Cumulative N_2O emissions during 62 days incubation period in the four treatments from sandy soil and clay soil. Error bars show the standard error of the mean of each treatment (n = 3). Different small letters indicate significant differences at the $p < 0.05$ level between treatments.

3.2 NH_4^+ and NO_3^- concentrations in soil

In sandy soil, no significant difference was found between biochar amended treatments and N only treatment; whereas two biochar amended treatments had relatively lower NO_3^- concentration and higher NH_4^+ concentration compared to N-only treatment (Table 3).

In clay soil, olive biochar had highest NO_3^- concentration compared to other treatments (albeit not statistically different). Compare to treatments in sandy soil, treatments in clay soils in general had significantly higher NO_3^- content in the end of the incubation.

Table 3. NH_4^+ and NO_3^- concentrations in four treatments from sand soil and clay soil treatments at the end of incubation.

Soil type	Treatment	NH_4^+ (mg N kg^{-1} soil)	NO_3^- (mg N kg^{-1} soil)
Sandy soil	Control	0.15±0.02	5.02±0.23
	AS	0.11±0.01	35.85±2.52
	Olive+AS	0.23±0.07	30.51±0.71
	Corn+AS	0.13±0.01	30.64±3.19
Clay soil	Control	0.13±0.01	7.79±0.40
	AS	0.12±0.01	41.74±1.55
	Olive+AS	0.07±0.01	45.96±1.81
	Corn+AS	0.10±0.00	39.43±1.79

4. Discussion

In our study, depending on soil and biochar types both positive and negative effects of biochar addition on soil CO_2 evolution were observed. This agrees with previous studies which demonstrated that the priming effect induced by biochar addition may be various (Chang et al., 2016; Subedi et al., 2016). The clear different CO_2 emission patterns that observed with olive biochar addition between two soils indicate that it cannot only be attributed to the liable C induced by biochar. We presumed the contrasting influence of olive biochar on CO_2 emissions during different phases in sand soil was likely due to biochar's shift from positive priming effect to negative priming effect during incubation period (Zimmerman et al. 2011). Up to now no consensus has been reached about why and how biochar could reduce N_2O emissions (Cayuela et al., 2014). Several mechanisms have been proposed, for instance, biochar could reduce N_2O emission by improving soil porosity and aeration (Yanai et al., 2007). However, this is unlikely to be the main mechanism in our study, because we would rather observe a more significant N_2O mitigation effect from clay soils, especially considering the high soil moisture condition (70% WHC) in our experiment.

Biochar's liming effect has been suggested one of the key factors that influence N_2O emissions (Cayuela et al., 2013). It has also been suggested that increase of soil pH introduced by biochar application could drive denitrification to N_2O reduction to N_2 (van Zwieten et al., 2010). In our study biochar amendment significantly reduced N_2O emissions for the acidic sandy soil, whereas no significant influence was found for the alkaline clay soil. Cayuela et al. (2014) found that the efficiency of biochar's N_2O mitigation effect did not differ with slightly acidic or alkaline soils. In our study about two times greater N_2O emissions were observed for the acidic sandy soil than for the alkaline clay soil, which is in lined with the findings of other authors that suggested N_2O emissions are negatively correlated with soil pH (Bandibas et al., 1994; Van Den Heuvel et al., 2011).

However, as indicated by our second experiment, in our study biochar's priming pH was unlikely to be the key factors for regulating N_2O emissions, other factors, such as different N_2O production microbial pathway and C content of soil may have dominated the influence of soil pH (Subedi et al., 2016).

There are at least two main processes of N_2O production in soils: nitrification and denitrification (Butterbach-Bahl et al., 2013). Before we could gain insight into the mechanisms of biochar's mitigation effect, a general understanding of the sources of N_2O emissions is essential. Soil water content is one of the most important factors that control N_2O emissions since it controls O_2 availability in soils and also N_2O diffusion out of soil. It is generally believed that in wet soils (WFPS 60-90%), denitrification produced most of N_2O (Ciarlo et al., 2007; Davidson et al., 2000). Based on the our high soil moisture (70%WHC) and the findings of our previous study (Wu et al., 2017), we hypothesized that in the acidic sandy soil denitrification was the major source for N_2O emissions, with the same soil type at same soil moisture. In Olive-AS, the N_2O emission peak was reduced by the olive biochar, and occurred 18 days earlier than that of N fertilizer only treatment. The earlier emerged N_2O peak was likely attributed to the enhanced development of anoxic condition in Olive-AS soils compared with AS, which created a favored condition for denitrification process. The anoxic condition was caused by the positive priming effect of olive biochar addition in phase I, leading to the consumption of the limited supply of oxygen in soils at 70% WHC (Singh et al., 2010), which was evidenced by the significantly increased CO_2 emissions (Fig. 1). The reduced N_2O peak observed in both biochar addition treatments might be explained by the decreased $N_2O/ (N_2+N_2O)$ ratio, as biochar could facilitate the transfer of electrons to soil denitrification microorganisms and promote the reduction of N_2O to N_2 (Cayuela et al., 2013). In Olive-AS the sharper decline of N_2O emissions could be attributed to the depleted available C caused by priming effect, since available carbon is likely to be the limited factor for denitrification, ac-

cording to the high soil NO_3^- contents in end of the incubation (Table 2). On the other hand, as indicated by CO_2 emissions, the corn biochar induced no priming effect, and therefore caused no oxygen and C depletion. The N_2O emissions were reduced by corn biochar in phase I and phase II, but N_2O emissions peak time was not shifted to earlier day, and the emissions rates were not reduced in phase III (Fig. 1 and 3). This provides good support for our previous assumption that biochar priming effect caused oxygen and C depletion in soil, and therefore induced earlier N_2O emission peak and less pronounced N_2O emissions in latter phases in sandy soil. On the other hand, we presumed that nitrification is likely the major source of N_2O emission our ns in alkaline clay soil for the following reasons. The two times smaller cumulative N_2O emissions but two times larger cumulative CO_2 emissions in clay soil compare to sandy soil may be attributed to the different N_2O production pathways. Compare to sandy soil, the higher NO_3^- content in clay soil at the end of incubation suggested that the denitrification rate was more limited, possibly due to the lower initial total C content in soils. This suggests that a smaller contribution of denitrification derived N_2O emissions from clay soil. The N_2O and CO_2 emissions of all treatments in clay soil were positively related during the incubation period, which is in lined with previous studies (Huang et al., 2004; Singh et al., 2010). However, the N_2O and CO_2 emissions of olive addition treatment in sandy soil showed significant negative correlation during phase I, whereas no positive correlation was found for N_2O and CO_2 emissions from sandy soil during the incubation period. This could further support our hypothesis that the microbial N_2O production processes that involved were different in sandy soil and clay soil. Steinbeiss et al. (2009) found that the type of biochar, instead of soil type, is the main driver for all the differences in gas emissions and microbial community. In our study, however, the significant different gas emissions patterns observed in different type treatments indicates that both biochar type and soil type are the key factors accounting for the differences. Olive biochar and corn biochar showed clear different influences on

CO_2 and N_2O emissions in sandy soil. The reasons for this difference might be attributed the different C:N ratio of biochar amendment, which may affect the soil N cycle and N_2O emissions pattern (Atkinson et al., 2010; Ellis et al., 1996). In our study, the olive biochar had a higher C:N ratio than corn biochar (117 vs. 68), and smaller cumulative N_2O emissions in sandy soil. This is consistent with the finding of Huang et al. (2004) who found that cumulative emissions of N_2O were negatively correlated with the C:N ratio in plant residues addition.

5. Conclusion

Our study shows that biochar application can be effective in mitigating N_2O emissions, depending on biochar type and soil type. Both olive and corn biochars significantly reduced N_2O emissions in acidic sandy soil, whereas none of them had significantly effect on N_2O emissions in alkaline clay soil. We propose that the mitigation effect was probably due to the C depletion caused by the biochar priming effect and promoted N_2O to N_2 reduction step of denitrification process, while the different influences of biochar on N_2O emissions in sandy soil and clay soil were likely due to the different microbial processes involved in N_2O production.

Acknowledgements

The authors thank Institute of Applied Plant Nutrition (IAPN), University of Göttingen for the financial support. This study was supported by the Chinese Scholarship Council (scholarship no. 201306350130).

References

Atkinson, C.J., Fitzgerald, J.D., Hipps, N.A., 2010. Potential mechanisms for achieving agricultural benefits from biochar application to temperate soils: a review. Plant and Soil 337, 1–18.

Baggs, E.M., 2011. Soil microbial sources of nitrous oxide: recent advances in knowledge, emerging challenges and future direction. Current Opinion in Environmental Sustainability 3, 321–327.

Bandibas, J., Vermoesen, A., De Groot, C.J., Cleemput, O.V., 1994. The effect of different moisture regimes and soil characteristics on nitrous oxide emission and consumption by different soils Soil Science 158, 106–114.

Bouwman, A.F., Boumans, L.J.M., Batjes, N.H., 2002. Emissions of N_2O and NO from fertilized fields: Summary of available measurement data. Global Biogeochemical Cycles 16, 1058.

Butterbach-Bahl, K., Baggs, E.M., Dannenmann, M., Kiese, R., Zechmeister-Boltenstern, S., 2013. Nitrous oxide emissions from soils: how well do we understand the processes and their controls? Philos Trans R Soc Lond B Biol Sci 368, 20130122.

Butterbach-Bahl, K., Dannenmann, M., 2011. Denitrification and associated soil N_2O emissions due to agricultural activities in a changing climate. Current Opinion in Environmental Sustainability 3, 389–395.

Cayuela, M.L., Sánchez-Monedero, M.A., Roig, A., Hanley, K., Enders, A., Lehmann, J., 2013. Biochar and denitrification in soils: when, how much and why does biochar reduce N_2O emissions? Scientific Reports 3.

Cayuela, M.L., van Zwieten, L., Singh, B.P., Jeffery, S., Roig, A., Sánchez-Monedero, M.A., 2014. Biochar's role in mitigating soil nitrous oxide emissions: A review and meta-analysis. Agriculture, Ecosystems & Environment, Environmental Benefits and Risks of Biochar Application to Soil 191, 5–16.

Chang, J., Clay, D.E., Clay, S.A., Chintala, R., Miller, J.M., Schumacher, T., 2016. Biochar Reduced Nitrous Oxide and Carbon Dioxide Emissions from Soil with Different Water and Temperature Cycles. Agronomy Journal 108, 2214–2221.

Chintala, R., Schumacher, T.E., Kumar, S., Malo, D.D., Rice, J.A., Bleakley, B., Chilom, G., Clay, D.E., Julson, J.L., Papiernik, S.K., Gu, Z.R., 2014. Molecular characterization of biochars and their influence on microbiological properties of soil. Journal of Hazardous Materials 279, 244–256.

Ciarlo, E., Conti, M., Bartoloni, N., Rubio, G., 2007. The effect of moisture on nitrous oxide emissions from soil and the $N_2O/(N_2O+N_2)$ ratio under laboratory conditions. Biology and Fertility of Soils 43, 675–681.

Clough, T.J., Bertram, J.E., Ray, J.L., Condron, L.M., O'Callaghan, M., Sherlock, R.R., Wells, N.S., 2010. Unweathered Wood Biochar Impact on Nitrous Oxide Emissions from a Bovine-Urine-Amended Pasture Soil. Soil Science Society of America Journal 74, 852.

Davidson, E.A., Keller, M., Erickson, H.E., Verchot, L.V., Veldkamp, E., 2000. Testing a Conceptual Model of Soil Emissions of Nitrous and Nitric Oxides Using two functions based on soil nitrogen availability and soil water content, the hole-in-the-pipe model characterizes a large fraction of the observed variation of nitric oxide and nitrous oxide emissions from soils. BioScience 50, 667–680.

Ellis, S., Dendooven, L., Goulding, K.W.T., 1996. Quantitative assessment of Soil nitrate disappearance and N2O evolution during denitrification: Nitrate disappearance during denitrification. Soil Biology and Biochemistry 28, 589–595.

Fowler, D., Coyle, M., Skiba, U., Sutton, M.A., Cape, J.N., Reis, S., Sheppard, L.J., Jenkins, A., Grizzetti, B., Galloway, J.N., Vitousek, P., Leach, A., Bouwman, A.F., Butterbach-Bahl, K., Dentener, F., Stevenson, D., Amann, M., Voss, M., 2013. The global nitrogen cycle in the twenty-first century. Phil. Trans. R. Soc. B 368, 20130164.

Huang, Y., Zou, J., Zheng, X., Wang, Y., Xu, X., 2004. Nitrous oxide emissions as influenced by amendment of plant residues with different C:N ratios. Soil Biology and Biochemistry 36, 973–981.

IPCC, 2013. Annex II: Climate System Scenario Tables, in: Climate Change 2013: The Physical Science Basis. Contribution of Working Group I to the Fifth Assessment Report of the Intergovernmental

Panel on Climate Change. Cambridge University Press, Cambridge, United Kingdom and New York, NY, USA.
Lehmann, J., Joseph, S., 2009. Biochar for environmental management: An introduction. Biochar for Environmental Management: Science and Technology 1–12.
Lehmann, J., Rillig, M.C., Thies, J., Masiello, C.A., Hockaday, W.C., Crowley, D., 2011. Biochar effects on soil biota – A review. Soil Biology and Biochemistry, 19th International Symposium on Environmental Biogeochemistry 43, 1812–1836.
Nelissen, V., Saha, B.K., Ruysschaert, G., Boeckx, P., 2014. Effect of different biochar and fertilizer types on N_2O and NO emissions. Soil Biology and Biochemistry 70, 244–255.
Singh, B.P., Hatton, B.J., Singh, B., Cowie, A.L., Kathuria, A., 2010. Influence of Biochars on Nitrous Oxide Emission and Nitrogen Leaching from Two Contrasting Soils. Journal of Environmental Quality 39, 1224–1235.
Steinbeiss, S., Gleixner, G., Antonietti, M., 2009. Effect of biochar amendment on soil carbon balance and soil microbial activity. Soil Biology and Biochemistry 41, 1301–1310.
Subedi, R., Taupe, N., Pelissetti, S., Petruzzelli, L., Bertora, C., Leahy, J.J., Grignani, C., 2016. Greenhouse gas emissions and soil properties following amendment with manure-derived biochars: Influence of pyrolysis temperature and feedstock type. Journal of Environmental Management 166, 73–83. Sutton, M.A., Howard, C.M., Erisman, J.W., Billen, G., Bleeker, A., Grennfelt, P., van Grinsven, H., Grizzetti, B., 2011. The European nitrogen assessment: sources, effects and policy perspectives. Cambridge University Press.
Taghizadeh-Toosi, A., Clough, T.J., Condron, L.M., Sherlock, R.R., Anderson, C.R., Craigie, R.A., 2011. Biochar Incorporation into Pasture Soil Suppresses in situ Nitrous Oxide Emissions from Ruminant Urine Patches. Journal of Environment Quality 40, 468.
Van Den Heuvel, R.N., Bakker, S.E., Jetten, M.S.M., Hefting, M.M., 2011. Decreased N2O reduction by low soil pH causes high N_2O emissions in a riparian ecosystem. Geobiology 9, 294–300.
van Zwieten, L., Kimber, S., Morris, S., Downie, A., Berger, E., Rust, J., Scheer, C., 2010. Influence of biochars on flux of N_2O and CO_2 from Ferrosol. Soil Research 48, 555–568.
Wu, D., Senbayram, M., Well, R., Brüggemann, N., Pfeiffer, B., Loick, N., Stempfhuber, B., Dittert, K., Bol, R., 2017. Nitrification inhibitors mitigate N_2O emissions more effectively under straw-induced conditions favoring denitrification. Soil Biology and Biochemistry 104, 197–207.
Yanai, Y., Toyota, K., Okazaki, M., 2007. Effects of charcoal addition on N_2O emissions from soil resulting from rewetting air-dried soil in short-term laboratory experiments. Soil Science and Plant Nutrition 53, 181–188.
Zimmerman, A.R., Gao, B., Ahn, M.-Y., 2011. Positive and negative carbon mineralization priming effects among a variety of biochar-amended soils. Soil Biology and Biochemistry 43, 1169–1179.

Paper VI

Using the correlation between N_2O $\delta^{18}O$ and α position $\delta^{15}N$ as a tool to spot N_2O reduction process during denitrification in soils.

Wu, D., Cárdenas, L., Lewicka-Szczebak, D., Brüggemann, N., Well, R., Köster, J.R., Bol, R., 2017.

Draft manuscript

Using the correlation between N_2O $\delta^{18}O$ and α position $\delta^{15}N$ as a tool to spot N_2O reduction process during denitrification in soils

Di Wu[1]*, Laura M. Cárdenas[2], Dominika Lewicka-Szczebak[3], Nicolas Brüggemann[1], Reinhard Well[3], Jan Reent Köster[3], Hongjuan Zhang[1], Roland Bol[1]

[1] Institute of Bio- and Geosciences, Agrosphere (IBG-3), Forschungszentrum Jülich GmbH, 52425 Jülich, Germany

[2] Rothamsted Research, North Wyke, Okehampton EX20 2SB, UK

[3] Thünen Institute of Climate-Smart Agriculture, Federal Research Institute for Rural Areas, Forestry and Fisheries, Bundesallee 50, 38116 Braunschweig, Germany

*Corresponding author: w.di@fz-juelich.de

Abstract

The last step of denitrification, i.e. the reduction of N_2O to N_2, has been well studied in laboratory to understand denitrification process, predict nitrogen fertilizer losses and to establish mitigation strategy for N_2O. However, direct measurements of N_2 production via denitrification in situ field study are challenging due to the high atmospheric N_2 background. Recent studies indicate stable isotopologue analyses of emitted N_2O may help to spot N_2O reduction to N_2 process. In this study we investigated N_2O $\delta^{18}O$ and $\delta^{15}N\alpha$ obtained from six soil incubation studies conducted in soil incubation systems designed for measuring N_2O and N_2 emissions from soil directly by gas chromatography after replacing atmospheric air by a He-O_2 incubation atmosphere. The results indicate that the significant correlation and higher slope of $\delta^{18}O$ versus $\delta^{15}N^{\alpha}$ might be used as a promising approach for spotting N_2O reduction to N_2 process during denitrification in soils.

1. Introduction

Nitrous oxide (N_2O) is not only a potent greenhouse gas emitted by anthropogenic activities and also contributes largely to the destruction of the tropospheric ozone layer (Ravishankara et al., 2009). Soils are considered to be the largest source of N_2O emissions (Stocker et al., 2013), in which denitrification has been suggested as the dominant process responsible for the increase in atmospheric N_2O (Baggs, 2011). During the denitrification process, NO_3^- is reduced to NO_2^-, further to N_2O and N_2. The ratio of N_2O to N_2, often described as $N_2O/(N_2O+N_2)$ ratio, is highly variable with different NO_3^-concentration, available C content and O_2 availability in soil (Blackmer and Bremner, 1978; Senbayram et al., 2012). However, direct measurements of N_2 production in soils are challenging due to the high atmospheric N_2 background, especially in situ field study, while most indirect methods targeting N_2 production, e.g. the commonly used acetylene inhibition technique, are afflicted with artifacts (Groffman et al., 2006; Terry and Duxbury, 1985).

The N_2O site preference (SP) is defined as the difference between ^{15}N at the central (α position) and the terminal N atom (β position) in the asymmetric N_2O molecule, and has been proposed as a new tool for distinguish the different source of N_2O production pathways (Decock and Six, 2013; Toyoda and Yoshida, 1999). For bacterial denitrification, lower SP (-11‰ to 0‰) has been found than for nitrification (+31‰ to +37‰) (Sutka et al., 2006; Toyoda et al., 2015). However, the isotopic fractionation during N_2O reduction to N_2 could enrich ^{15}N at α position of the N_2O molecule and thereby increasing SP values (Well and Flessa, 2009). On one hand, this fractionation effect might lead to an erroneous source-partitioning of N_2O if not correctly compensated (Wu et al., 2016). On the other hand, this effect could lead to a significant correlation between N_2O ^{18}O and ^{15}N and thus could be possibly used as an indicator for N_2O reduction to N_2 process (Lewicka-Szczebak et al., 2017; Park et al., 2011; Well and Flessa, 2009).

In this study we investigated the relationship between N_2O $\delta^{18}O$ and $\delta^{15}N\alpha$ obtained from six soil incubation studies conducted in soil incubation systems designed for measuring N_2O as well as N_2 emissions from soil directly by gas chromatography after replacing atmospheric air by a He-O_2 incubation atmosphere. These systems facilitate regular gas sampling for N_2O isotopomer analysis by isotope ratio mass spectrometry (IRMS). The aim of this study was to investigate the possible approach to spot N_2O reduction process by using isotopic signature of N_2O.

2. Material and methods

N_2O isotopomer data were obtained from six soil incubation studies: Bol et al. (2003), Meijide et al. (2010), Bergstermann et al. (2011), Köster et al. (2015), and Lewicka-Szczebak et al. (2015), which were conducted at Rothamsted Research in North Wyke, Devon, UK, and Köster et al. (2013), which was conducted at Hanninghof Research Station in Dülmen, Germany. In total, we obtained 429 data points from soil incubation experiments conducted under conditions explicitly favoring denitrification. In all these studies the N_2O isotopomer ratios were analyzed by IRMS as described previously by Toyoda and Yoshida, (1999).

3. Results

The isotopic data were reorganized by $N_2O/(N_2O+N_2)$ ratio with different colors and plotted in Fig.1 as the relationship of $\delta^{18}O$ with $\delta^{15}N^{\alpha}$. As shown in Fig. 1, the points that have lower N_2O reduction effect (i.e. higher $N_2O/(N_2O+N_2)$ ratio) were found to have a smaller slope. In general, there was a significant positive correlation between $\delta^{18}O$ versus $\delta^{15}N^{\alpha}$ (Table. 1). We then calculated correlation of $\delta^{18}O$ with $\delta^{15}N^{\alpha}$ at three different N_2O reduction ranges, which are, high reduction ($N_2O/(N_2O+N_2)$ ratio<0.1), moderate ($0.1<N_2O/(N_2O+N_2)$ ratio<0.6), low ($0.6<N_2O/(N_2O+N_2)$ ratio <1). When the N_2O reduction effect is significant ($N_2O/(N_2O+N_2)$

ratio<0.1), which means most of N_2O has been reduced to N_2 by denitrification, the correlation between $\delta^{18}O$ versus $\delta^{15}N^{\alpha}$ (R^2=0.65, p<0.0001) showed the highest slope and R^2 values compared to others.

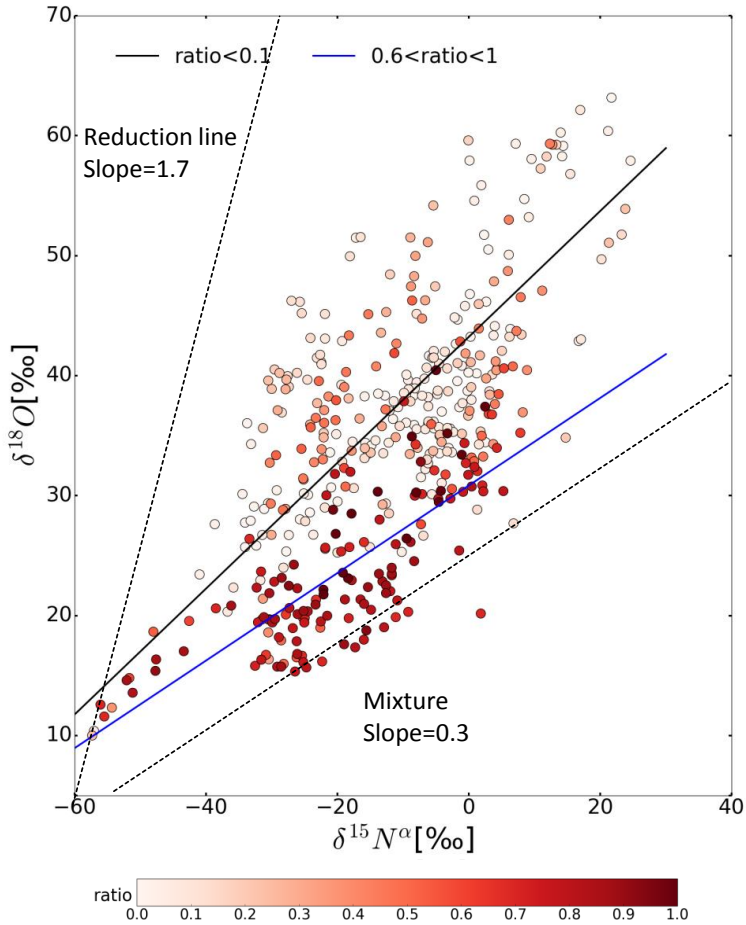

Figure 1. $\delta^{18}O$ versus $\delta^{15}N^{\alpha}$ at different N_2O/N_2O+N_2 ratio.

Table 1. Correlation between $\delta^{18}O$ versus $\delta^{15}N^{\alpha}$ at different ranges of N_2O/N_2O+N_2 ratio.

Range	ratio<0.1	0.1<ratio<0.6	0.6<ratio<1
n	128	172	129
Correlation	y=0.52x +43	y=0.37x +42	y=0.36x+31
R^2	0.65	0.35	0.60

4. Discussion

As N_2O reduction to N_2 process mainly involves the break of the bond between the central N (α position) and O, the remaining N_2O should therefore be enriched simultaneously in $\delta^{18}O$ and $\delta^{15}N\alpha$. If N_2O reduction is significant, the isotope effect should result in a positive correlation between $\delta^{18}O$ and $\delta^{15}N^{\alpha}$ and little to no correlation between $\delta^{18}O$ and $\delta^{15}N^{\beta}$ (Park et al., 2011). In line with Park et al. (2011), we found in general no significant correlation between $\delta^{18}O$ and $\delta^{15}N^{\beta}$ (data not shown), whilst the correlation between $\delta^{18}O$ and $\delta^{15}N^{\alpha}$ was more significant in high N_2O reduction conditions than the correlation in low reduction conditions (Table 1). However, a significant correlation between $\delta^{18}O$ and $\delta^{15}N^{\alpha}$ was also observed under low N_2O reduction conditions (R^2=0.60, $p<0.0001$). This indicates a significant correlation between $\delta^{18}O$ and $\delta^{15}N^{\alpha}$ might not be used alone as a reliable indicator for N_2O reduction. It has been suggested that a slope approaching 1 or greater was likely to be an indicator for N_2O reduction (Köster et al., 2011). In the study of Well and Flessa (2009) a relatively constant ratio between $\delta^{18}O$ versus $\delta^{15}N^{\alpha}$ was observed, ranging from 1.4 to 1.7. Similarly, Ostrom et al. (2007) reported the

correlation a slope of 1.7 for $\delta^{18}O$ versus $\delta^{15}N^{\alpha}$ when N_2O reduction occurs in the absence of production, and a slope of 0.3 with insignificant N_2O reduction in soil mesocosm and pure culture studies. Based on this, two slope dotted lines were drawn in Fig. 1 to compare with our data. In our study, most of the slopes of $\delta^{18}O$ / $\delta^{15}N^{\alpha}$ were close to 0.3 except for at high N_2O reduction conditions ($N_2O/(N_2O+N_2)$ ratio<0.1). The slope of $\delta^{18}O$ / $\delta^{15}N^{\alpha}$ at high N_2O reduction conditions was 0.65, which was lower than the slopes suggested by Ostrom and Well and Flessa, but close to the slopes found by Köster et al. 2011 in denitrification favored condition.

We could therefore conclude that the high correlation and large slope between $\delta^{18}O$ and $\delta^{15}N^{\alpha}$ could be used as a qualitative indicator for N_2O reduction to N_2 process. This would especially facilitate those in situ field experiments which have problems with direct N_2 measurement. It should be noted that the applicability of this method may require large isotopomer data set, which may be an issue for those current studies using laboratory-based isotope-ratio mass-spectrometry (IRMS). However, recently developed spectroscopic techniques like quantum cascade laser absorption spectroscopy (QCLAS) has enabled real-time analysis of N_2O isotope signatures and produced large data sets, indicating that the limited amount of data should not be a problem in the future (Mohn et al., 2012).

As oxygen of N_2O precursors could be exchanged with oxygen of soil water during denitrification and nitrification, the $\delta^{18}O$ value of N_2O has been shown to reflect not only the associated isotope effect, but also the isotope signature of the soil water (Casciotti et al., 2007; Kool et al., 2009). Lewicka-Szczebak et al. (2016) found that N_2O formation in a static anoxic incubation experiment was associated with oxygen isotope close to 100%, while flow-through experiments gave 56% oxygen isotope exchange. This may explain the variations of $\delta^{18}O/\delta^{15}N^{\alpha}$ and relatively stable $\delta^{18}O$ value in low N_2O reduction condition (Fig. 1).

Reference

Baggs, E.M., 2011. Soil microbial sources of nitrous oxide: recent advances in knowledge, emerging challenges and future direction. Current Opinion in Environmental Sustainability 3, 321–327.

Bergstermann, A., Cárdenas, L., Bol, R., Gilliam, L., Goulding, K., Meijide, A., Scholefield, D., Vallejo, A., Well, R., 2011. Effect of antecedent soil moisture conditions on emissions and isotopologue distribution of N_2O during denitrification. Soil Biology and Biochemistry 43, 240–250.

Blackmer, A.M., Bremner, J.M., 1978. Inhibitory effect of nitrate on reduction of N_2O to N_2 by soil microorganisms. Soil Biology and Biochemistry 10, 187–191.

Bol, R., Toyoda, S., Yamulki, S., Hawkins, J.M.B., Cardenas, L.M., Yoshida, N., 2003. Dual isotope and isotopomer ratios of N_2O emitted from a temperate grassland soil after fertiliser application. Rapid Communications in Mass Spectrometry 17, 2550–2556.

Casciotti, K.L., Boehlke, J.K., McIlvin, M.R., Mroczkowski, S.J., Hannon, J.E., 2007. Oxygen isotopes in nitrite: Analysis, calibration, and equilibration. Analytical Chemistry 79, 2427–2436.

Decock, C., Six, J., 2013. How reliable is the intramolecular distribution of ^{15}N in N_2O to source partition N_2O emitted from soil? Soil Biology and Biochemistry 65, 114–127.

Groffman, P.M., Altabet, M.A., Böhlke, J.K., Butterbach-Bahl, K., David, M.B., Firestone, M.K., Giblin, A.E., Kana, T.M., Nielsen, L.P., Voytek, M.A., 2006. Methods for measuring denitrification: diverse approaches to a difficult problem. Ecological Applications 16, 2091–2122.

Kool, D.M., Müller, C., Wrage, N., Oenema, O., Van Groenigen, J.W., 2009. Oxygen exchange between nitrogen oxides and H_2O can occur during nitrifier pathways. Soil Biology and Biochemistry 41, 1632–1641.

Köster, J.R., Well, R., Dittert, K., Giesemann, A., Lewicka-Szczebak, D., Mühling, K.-H., Herrmann, A., Lammel, J., Senbayram, M., 2013. Soil denitrification potential and its influence on N_2O reduction and N_2O isotopomer ratios. Rapid Communications in Mass Spectrometry 27, 2363–2373.

Köster, J.R., Cárdenas, L., Senbayram, M., Bol, R., Well, R., Butler, M., Mühling, K.H., Dittert, K., 2011. Rapid shift from denitrification to nitrification in soil after biogas residue application as indicated by nitrous oxide isotopomers. Soil Biology and Biochemistry 43, 1671–1677.

Köster, J.R., Cardenas, L.M., Bol, R., Lewicka-Szczebak, D., Senbayram, M., Well, R., Giesemann, A., Dittert, K., 2015. Anaerobic digestates lower N_2O emissions compared to cattle slurry by affecting rate and product stoichiometry of denitrification - An N_2O isotopomer case study. Soil Biology & Biochemistry 84, 65–74.

Lewicka-Szczebak, D., Well, R., Bol, R., Gregory, A.S., Matthews, G.P., Misselbrook, T., Whalley, W.R., Cardenas, L.M., 2015. Isotope fractionation factors controlling isotopocule signatures of soil-emitted N_2O produced by denitrification processes of various rates. Rapid Communications in Mass Spectrometry 29, 269–282.

Lewicka-Szczebak, D., Augustin, J., Giesemann, A., Well, R., 2017. Quantifying N_2O reduction to N_2 based on N_2O isotopocules – validation with independent methods (helium incubation and ^{15}N gas flux method). Biogeosciences 14, 711–732.

Lewicka-Szczebak, D., Dyckmans, J., Kaiser, J., Marca, A., Augustin, J., Well, R., 2016. Oxygen isotope fractionation during N_2O production by soil denitrification. Biogeosciences 13, 1129–1144.

Meijide, A., Cardenas, L.M., Bol, R., Bergstermann, A., Goulding, K., Well, R., Vallejo, A., Scholefield, D., 2010. Dual isotope and isotopomer measurements for the understanding of N_2O production and consumption during denitrification in an arable soil. European Journal of Soil Science 61, 364–374.

Mohn, J., Tuzson, B., Manninen, A., Yoshida, N., Toyoda, S., Brand, W.A., Emmenegger, L., 2012. Site selective real-time measurements of atmospheric N_2O isotopomers by laser spectroscopy. Atmospheric Measurement Techniques 5, 1601–1609.

Ostrom, N.E., Pitt, A., Sutka, R., Ostrom, P.H., Grandy, A.S., Huizinga, K.M., Robertson, G.P., 2007. Isotopologue effects during N_2O reduction in soils and in pure cultures of denitrifiers. Journal of Geophysical Research: Biogeosciences 112, G02005.

Park, S., Pérez, T., Boering, K.A., Trumbore, S.E., Gil, J., Marquina, S., Tyler, S.C., 2011. Can N_2O stable isotopes and isotopomers be useful tools to characterize sources and microbial pathways of N_2O production and consumption in tropical soils? Global Biogeochemical Cycles 25.

Ravishankara, A.R., Daniel, J.S., Portmann, R.W., 2009. Nitrous oxide (N_2O): the dominant ozone-depleting substance emitted in the 21st century. Science 326, 123–125.

Senbayram, M., Chen, R., Budai, A., Bakken, L., Dittert, K., 2012. N_2O emission and the $N_2O/(N_2O+N_2)$ product ratio of denitrification as controlled by available carbon substrates and nitrate concentrations. Agriculture, Ecosystems & Environment 147, 4–12.

Stocker, T., Qin, D., Plattner, G., Tignor, M., Allen, S., Boschung, J., Nauels, A., Xia, Y., Bex, B., Midgley, B., 2013. IPCC, 2013: climate change 2013: the physical science basis. Contribution of working group I to the fifth assessment report of the intergovernmental panel on climate change.

Sutka, R.L., Ostrom, N.E., Ostrom, P.H., Breznak, J.A., Gandhi, H., Pitt, A.J., Li, F., 2006. Distinguishing nitrous oxide production from nitrification and denitrification on the basis of isotopomer abundances. Applied and Environmental Microbiology 72, 638–644.

Terry, R.E., Duxbury, J.M., 1985. Acetylene decomposition in soils. Soil Science Society of America Journal 49, 90–94.

Toyoda, S., Yoshida, N., 1999. Determination of nitrogen isotopomers of nitrous oxide on a modified isotope ratio mass spectrometer. Analytical Chemistry 71, 4711–4718.

Toyoda, S., Yoshida, N., Koba, K., 2015. Isotopocule analysis of biologically produced nitrous oxide in various environments. Mass Spectrometry Reviews 2017

Well, R., Flessa, H., 2009. Isotopologue enrichment factors of N_2O reduction in soils. Rapid Communications in Mass Spectrometry 23, 2996–3002.

Wu, D., Köster, J.R., Cárdenas, L.M., Brüggemann, N., Lewicka-Szczebak, D., Bol, R., 2016. N_2O source partitioning in soils using ^{15}N site preference values corrected for the N_2O reduction effect. Rapid Communications in Mass Spectrometry 30, 620–626.

Paper VII

Effects of cattle slurry and nitrification inhibitor application on spatial soil O_2 dynamics and N_2O production pathways.

Nguyen, Q., **Wu, D**., Kong, X., Bol, R., Petersen, S., Jensen, L., Liu, S., Brüggemann, N., Glud, N., Larsen, M., Bruun, S., 2017

Soil Biology and Biochemistry 114: 200-209.

Soil Biology & Biochemistry 114 (2017) 200–209

Contents lists available at ScienceDirect

Soil Biology & Biochemistry

journal homepage: www.elsevier.com/locate/soilbio

Effects of cattle slurry and nitrification inhibitor application on spatial soil O_2 dynamics and N_2O production pathways

Quan Van Nguyen [a, *], Di Wu [b], Xianwang Kong [c], Roland Bol [b], Søren O. Petersen [c], Lars Stoumann Jensen [a], Shurong Liu [b], Nicolas Brüggemann [b], Ronnie N. Glud [d], Morten Larsen [d], Sander Bruun [a, **]

[a] Department of Plant and Environmental Sciences, University of Copenhagen, Thorvaldsensvej 40, Frederiksberg 1871, Copenhagen, Denmark
[b] Institute of Bio- and Geosciences, Agrosphere (IBG-3), Forschungszentrum Jülich GmbH, Jülich 52425, Germany
[c] Department of Agroecology, Aarhus University, Blichers Allé 20, Tjele 8830, Denmark
[d] Institute of Biology, Nordic Center for Earth Evolution (NordCEE), University of Southern Denmark, Odense M 5230, Denmark

ARTICLE INFO

Article history:
Received 20 January 2017
Received in revised form
11 July 2017
Accepted 14 July 2017

Keywords:
Soil oxygen
Optode
N_2O isotopomer
DMPP
GHGs mitigation
Grassland

ABSTRACT

Application of cattle slurry to grassland soil has environmental impacts such as ammonia volatilization and greenhouse gas emissions. The extent, however, depends on application method and soil conditions through their effects on infiltration and oxygen (O_2) availability during subsequent decomposition. Here, we applied O_2 planar optode and N_2O isotopomer techniques to investigate the linkage between soil O_2 dynamics and N_2O production pathways in soils treated with cattle slurry (treatment CS) and tested the effect of the nitrification inhibitor 3,4-dimethyl pyrazole phosphate, DMPP (treatment CSD). Two-dimensional planar optode images of soil O_2 over time revealed that O_2 depletion ultimately extended to 1.5 cm depth in CS, as opposed to 1.0 cm in CSD. The ^{15}N site preference (SP) and $\delta^{18}O$ of emitted N_2O varied between 11-25‰ and 35–47‰, respectively, indicating a mixture of production sources during the incubation. An early peak of N_2O emission occurred in both manure treated soils by day 1, with the highest SP values and $\delta^{18}O$-N_2O indicating that fungal denitrification of nitrate in the soil was the main contributor to the early peak. During the first five days, N_2O fluxes in CS and CSD treatments were similar, and hence nitrification did not influence N_2O emissions for several days under the experimental conditions of this study. The second peak of N_2O emission occurring only in CS peaking around day 14, could be due to both nitrification and bacterial denitrification of nitrate produced during incubation. Over 18 days, the application of DMPP substantially mitigated N_2O emissions by 60% compared to untreated CS in the investigated system which in terms of aeration status corresponded to wet or compacted grassland soil. Using this novel combination of O_2 planar optode imaging and N_2O isotopomer analysis, our results provide a better understanding of the coupled O_2 and N_2O dynamics in manure-amended soils, and they illustrate the roles of bacterial and fungal denitrification in N_2O production in grassland soil under high soil water content.

1. Introduction

Due to the high availability of degradable organic matter and ammonium, the application of animal slurry on agricultural soils will induce oxygen consumption through enhanced respiration and nitrification in a zone around the applied slurry (Petersen et al., 1996; Meyer et al., 2002). The added slurry-derived carbon (C) can also act as a C source, stimulating denitrification activity in these low-oxygen zones (Thompson, 1989). Since water from the applied slurry impedes O_2 supply, transient O_2 depletion zones may develop around the application area (Petersen et al., 2003; Zhu et al., 2015) and stimulate emissions of nitrous oxide (N_2O). In the soil environment, N_2O is formed mainly by ammonia-oxidizing bacteria as a by-product of nitrification or *via* nitrifier denitrification under aerobic conditions, and by heterotrophic denitrifiers under low-oxygen or anoxic conditions (Braker and Conrad, 2011; Butterbach-Bahl et al., 2013). Thus, O_2 distribution in slurry-

* Corresponding author.
** Corresponding author.
E-mail addresses: nguyen@plen.ku.dk (Q.V. Nguyen), sab@plen.ku.dk (S. Bruun).

http://dx.doi.org/10.1016/j.soilbio.2017.07.012
0038-0717/

amended soil plays an important role as a "controller" of N transformations, and may have a significant impact on N_2O emissions in terms of both magnitude and production pathways and/or dynamics (Zhu et al., 2015). Mapping the spatial and temporal distribution of soil O_2 is, therefore, essential for understanding the mechanisms governing N transformations, including the production of N_2O in soil. A mechanistic understanding of N_2O emissions requires that non-destructive methods are available to monitor soil conditions without disturbance. Recently, O_2 planar optode imaging was introduced for monitoring the dynamics of O_2 in soil amended with pig slurry (Zhu et al., 2014, 2015). Knowledge about the distribution and temporal dynamics of O_2 significantly improves the possibilities for making useful interpretations.

A potentially effective strategy to mitigate N_2O emissions from cattle slurry-treated soils is to inhibit nitrification. This is because, as stated above, nitrification may be a direct source of N_2O production. Also, when nitrification is inhibited, NO_2^- and NO_3^- formation, and thus electron acceptor availability for nitrifier-denitrification and denitrification processes, are limited (Zerulla et al., 2001). Synthetic nitrification inhibitors, such as 3,4-dimethyl pyrazole phosphate (DMPP), have been widely shown to restrict ammonia oxidation, which is the first step of nitrification (Dittert et al., 2001; Menéndez et al., 2006; Fangueiro et al., 2009; Chen et al., 2010; Bell et al., 2016).

In order to develop manure application strategies resulting in lower emissions of N_2O, it is important to understand which process is the dominating source under specific soil conditions. For this purpose, the N_2O isotopomer technique has been used to determine the intramolecular distribution of ^{15}N between the central (N^{α}) position ($^{14}N^{15}N^{16}O$) and the terminal (N^{β}) position ($^{15}N^{14}N^{16}O$) of N_2O molecules. From this information, site preference (SP) values can be calculated and compared with SP values measured in pure cultures of microorganisms with different N_2O production pathways, *i.e.* nitrification or bacterial and fungal denitrification (Toyoda and Yoshida, 1999). Subsequently, the SP values can be used to estimate the sources of N_2O production using a two-end-member mixing model (Bol et al., 2003b; Sutka et al., 2006; Jinuntuya-Nortman et al., 2008; Well et al., 2012; Mander et al., 2014; Köster et al., 2015; Wu et al., 2016). However, since the SP values of nitrification and fungal denitrification are in the same range *i.e.* between 33 and 37‰ in pure cultures (Sutka et al., 2006, 2008; Rohe et al., 2014), it can be challenging to distinguish the contribution from each of these processes. Recently, Lewicka-Szczebak et al. (2016) suggested using both the oxygen isotopic signature of the emitted N_2O ($\delta^{18}O$-N_2O) and SP values to separate the sources of N_2O, where the $\delta^{18}O$-N_2O can be used to distinguish nitrification from bacterial and fungal denitrification, and the SP values can be used to distinguish bacterial denitrification from fungal denitrification and nitrification.

The aim of this study was: 1) to examine how the distribution and dynamics of O_2 in the soil after surface application of cattle slurry affect the processes responsible for N_2O formation, and 2) to understand how these processes are affected by the amendment of DMPP to the slurry. It was hypothesized that: i) surface application of cattle slurry leads to the rapid development of a downward-migrating O_2 depletion zone, ii) application of DMPP in the slurry will decrease the temporal and spatial extent of O_2 depletion, and iii) DMPP application will reduce the production of N_2O from both nitrification and denitrification.

2. Material and methods

2.1. Soil, cattle slurry and DMPP

Soil was collected from 0 to 15 cm depth at a grassland site located in the Northern Eifel region in Rollesbroich, Germany (50°37′18″N, 6°18′15″E). The soil was characterized as a loamy silt soil with a bulk density of 0.94 ± 0.12 g cm^{-3} at 5 cm and 1.28 ± 0.15 at 20 cm depth (Qu et al., 2016). The collected soil sample was freshly sieved (<4 mm), homogenized and pre-incubated for three days at room temperature (18 °C) before use. The cattle slurry was obtained from a dairy cattle house at the Foulum campus of Aarhus University's experimental farm in Tjele, Denmark and kept at ~4 °C. A DMPP stock solution (1.49 kg L^{-1}, *i.e.* 36.35% DMPP by weight in phosphoric acid) was provided by EuroChem Agro (Mannheim, Germany). The moisture content of the soil and cattle slurry were determined by weight loss after drying the fresh samples at 105 °C for 24 h, and their organic matter contents or loss on ignition (LOI) were determined by weight loss after heating the dried samples in a muffle oven at 550 °C for 3 h. The total organic carbon and nitrogen of the soil were analyzed on the dried-ground soil samples using an elemental analyzer (vario PYRO cube, Elementar, Germany). The total nitrogen of the cattle slurry was measured by the Kjeldahl procedure (Foss, Kjeltec™ 2300). The properties and characteristics of the soil and cattle slurry are summarized in Table 1.

2.2. Planar optode imaging system and measurement of soil O_2

The O_2 planar optode system used to measure the O_2 distribution in the soil is described in detail by Zhu et al. (2014). Briefly, the system consisted of four components: i) twelve transparent optode chambers coated with optode foil containing an O_2 sensitive luminophore, ii) two DSLR cameras (Canon 1200D and Canon 1100 D) with lenses covered by a long-pass glass color filter, iii) an excitation source of the O_2 sensitive luminophores, and iv) a computer to control LEDs and obtain images. Details of the optode system are described in the on-line supplementary information.

The system was calibrated before use following the calibration procedure described in Larsen et al. (2011). Using the calibration curve, the O_2 concentration was calculated for each pixel in the images using ImageJ 1.48v software (Wayne, 2015). To increase the signal-to-noise ratio, three images were recorded within two seconds, and the average of these images was calculated. To further support data interpretation, the imaging area was divided into three O_2 concentration ranges, *i.e.* anoxic, hypoxic and oxic fractions corresponding to <1%, 1–30% and >30% O_2 air saturation respectively, and the size of each range was determined (Zhu et al., 2015).

2.3. Treatments and experimental setup

The experimental design included three treatments with four replicates, *i.e.* cattle slurry (CS), cattle slurry-amended with DMPP (CSD), and a control (CTR) treatment receiving water only. For each replicate, 122.7 g fresh soil (96 g dry wt.) was packed into each

Table 1
Physicochemical properties of soil and cattle slurry.

Measurement[a]	Soil	Cattle slurry
Water content (g kg^{-1})	278 ± 14	885 ± 12
Organic matter (% DM, LOI[b])	7.7 ± 0.2	83.1 ± 0.4
Total organic carbon (g kg^{-1} dry matter)	25.2	
Total nitrogen (g kg^{-1} DM)	2.9	45.0 ± 0.6
NH_4-N (mg kg^{-1} DM)	0.3 ± 0.1	18.7 ± 0.1
NO_3-N (mg kg^{-1} DM)	12.3 ± 3.4	nd[c]
pH	5.7 ± 0.0	7.0 ± 0.0

[a] Mean ± standard deviation, $n = 3$.
[b] LOI: loss on ignition (550 °C, 6 hs).
[c] nd: not determined.

optode chamber (H × L × W: 10 × 6 × 4 cm^3) following the packing procedure described by Zhu et al. (2015). The soil was packed to a depth of 4 cm soil, corresponding to a soil bulk density of 1.0 g cm^{-3}. This soil bulk density corresponded to the soil bulk density in the field (Rollesbroich, Germany), which was 0.94 ± 0.12 g cm^{-3} for the top 5 cm soil depth (Qu et al., 2016), although of course soil aggregation could not be exactly reproduced. Briefly, four portions of 30.65 g fresh soil were added sequentially. After each addition, the chamber was shaken vertically and the soil was gently compressed from the soil surface to achieve a soil layer of exactly 1 cm. In order to ensure contact between the soil and the optode sensors, we conducted pilot experiments which indicated that a water-filled pore space (WFPS) of 83% was sufficient to avoid border effects at the bulk density used here. Thus, prior to slurry application, all chambers received 26.9 ml water, to achieve 85% WFPS, and were left for 22 h to equilibrate and allow soil O_2 to stabilize (pre-incubation period).

Cattle slurry (2.75 g fresh weight) was applied to the central 50% of the soil surface area, which was delimited using a 12-cm^2 aluminum rectangular frame (30 mm × 40 mm). The application rate, which was calculated based on the volume of soil in each optode chamber, corresponded to 120 NH_4^+-N kg ha^{-1}. In the CSD treatment, cattle slurry was mixed with 0.5 ml DMPP stock solution before application, corresponding to 1.2 kg DMPP ha^{-1} or 1% by weight of applied NH_4-N; this rate has been reported to inhibit ammonia oxidation effectively (Zerulla et al., 2001). Part of the water in the cattle slurry would be retained at the soil surface by particulate organic matter (Petersen et al., 2003); the amount of water from slurry penetrating into the soil was estimated using equation (3) in Petersen et al. (2003) to be 0.22 ml. The untreated CTR soil, therefore, received 0.22 ml distilled water to ensure the same soil moisture content for all treatments.

Incubation took place in darkness at room temperature (18 °C). During the incubation, the lids of the optode chambers were closed to minimize evaporation, but one rubber stopper was removed from the rear side of the chambers to ensure aeration of the headspace. Optode images were taken automatically every 60 min during the incubation. Five days after slurry application, a precipitation event with an intensity of 1.25 mm was simulated by adding distilled water evenly to the soil surface, raising the soil water content to 90% WFPS. Incubation was then continued for an additional 13 days.

2.4. Gas and soil sampling

Gas sampling for flux measurements took place on days 0, 1, 2, 3, 5, 7, 11, 14 and 18, while additional samples for N_2O isotopomer analysis were taken on days 1, 3, 5, 7, 11 and 14. On each regular sampling day, one 25-ml gas sample was taken from each headspace (t_0) and then the chambers were closed for 40 min (t_{40}) when another sample was collected. The gas samples were injected into 22-ml pre-evacuated glass vials, and N_2O, CO_2 and CH_4 concentrations later analyzed by gas chromatography (Clarus 580, PerkinElmer, Rodgau, Germany). Due to the limited headspace in the optode chambers, samples for N_2O isotopomer analysis were collected by repeated (five times) sampling of 25-ml headspace gas as described above at five-minute intervals and combining them in 120 ml pre-evacuated crimped bottles. The gas fluxes were calculated from the increments in headspace concentration during chamber closure, assuming a linear increase over time (Zhu et al., 2014). Cumulative gas emissions were calculated using the trapezoidal integration method. By day 18, the 4-cm soil core contained in each optode chamber was sliced into four horizontal layers, each 1 cm thick. The pH of soil samples of each layer were measured in water (1:5 w/v). NH_4^+-N and NO_3^--N content were determined by extraction of 10 g soil (wet weight) in 40 ml 1 M KCl followed by measurement on a Foss FIAstar 5000, Flow Injection Analyzer (FOSS, Denmark).

2.5. N_2O isotopomer and isotope signatures

N_2O isotope signatures were determined by measuring *m/z* 44, 45, and 46 of intact N_2O^+ molecular ions and *m/z* 30 and 31 of NO^+ fragment ions (Toyoda and Yoshida, 1999) using an isotope ratio mass spectrometer (IsoPrime 100, Elementar Analysensysteme, Hanau, Germany). The analysis provides the average $\delta^{15}N$ of the N_2O molecule (bulk $^{15}N/^{14}N$ ratios or $\delta^{15}N^{bulk}$), as well as $\delta^{15}N^{\alpha}$ and $\delta^{18}O$ isotope signatures. The $\delta^{15}N^{\beta}$ was calculated using the equation $\delta^{15}N^{\beta} = 2 \times \delta^{15}N^{bulk} - \delta^{15}N^{\alpha}$ (Toyoda and Yoshida, 1999). The ^{15}N-N_2O site preference (SP) is defined as $SP = \delta^{15}N^{\alpha} - \delta^{15}N^{\beta}$. The measured $\delta^{18}O$ and $\delta^{15}N$ isotope signatures were expressed with reference to Vienna Standard Mean Ocean Water (VSMOW) and atmospheric air-N_2, respectively. The correction and calibration of the measurements are described in detail by Heil et al. (2015). The soil emitted N_2O isotope signatures on day *t* (R_t), including $\delta^{18}O$, $\delta^{15}N$ and SP values, were corrected using the N_2O isotope signatures of ambient air in the laboratory using the following equation:

$$R_t = \left(R_{sample(t)} \times N_2O_{sample(t)} - R_{air} \times N_2O_{air}\right) / \left(N_2O_{sample(t)} - N_2O_{air}\right) \quad (1)$$

where N_2O_{air} is the average N_2O concentration in the optode chambers before closure at t_0 (*i.e.* 269 ± 5 ppb); R_{air} is the corresponding average isotope signatures values of ambient air samples (*i.e.* $\delta^{18}O$, $\delta^{15}N$ and SP were 41.6‰, 4.6‰ and 17.5‰, respectively; Supplementary Table S5); $N_2O_{sample\ (t)}$ and $R_{sample\ (t)}$ are the soil derived N_2O concentration and their corresponding isotope signatures (*i.e.* $\delta^{18}O$, $\delta^{15}N$ or SP) of samples collected from optode chambers 40 min after closure (t_{40}) on day *t*.

The $\delta^{18}O$ values of soil emitted N_2O can be influenced greatly by O exchange between soil water and denitrification intermediates, hence resulting in a less precise estimation of N_2O source partitioning based on a two-end-member mixing model. For this reason, the SP value is much more robust for estimating the N_2O source partitioning (Well and Flessa, 2009b; Rohe et al., 2014). Therefore, the source partitioning of soil emitted N_2O production was calculated from the corrected SP values (Eq. (1)) based on a two-end-member isotopic mass balance equation (Toyoda and Yoshida, 1999) as follows:

$$fD = (R_t - SP_N \times fN)/SP_D \quad (2)$$

where fD defines the proportion (%) of N_2O derived from bacterial denitrification (BD), and fN the proportion derived from nitrification (NI) and/or fungal denitrification (FD) in N_2O released at time *t*. It was assumed that N_2O originated exclusively from NI/FD and BD (fN + fD = 100%). R_t represents the corrected SP values of soil-emitted N_2O obtained from Eq. (1), while SP_D and SP_N are the SP values of N_2O produced by BD and NI/FD.

The ranges of these end-member isotopic signatures were defined according to well-known literature data in pure culture studies as: for SP_D between −11‰ and 0‰ (average of −5‰) (Toyoda et al., 2005; Sutka et al., 2006), and for SP_N between 33‰ and 37‰ (average 35‰) (Sutka et al., 2006). The SP values of FD generally range between 34‰ and 37‰ (Sutka et al., 2006; Rohe et al., 2014) which makes it impossible to distinguish from N_2O produced by NI. In addition, N_2O isotopic signatures often vary

depending on the environment and experimental setup, *e.g.* between pure culture studies and soil, which may affect the estimation of N_2O source partitioning using the two-end-member mixing model (Eq. (2)), and therefore $\delta^{18}O$-N_2O data were used in combination with SP values to understand the shifting trends in sources of N_2O production during incubation. The end-members of $\delta^{18}O$-N_2O were defined according to literature data for N_2O emission from incubation studies, which for FD has been reported to range between 30‰ and 45‰ (Sutka et al., 2008; Rohe et al., 2014), for BD between 30‰ and 50‰ (Toyoda et al., 2005; Opdyke et al., 2009; Ostrom et al., 2010; Snider et al., 2013; Lewicka-Szczebak et al., 2014), and for NI between 13‰ and 35‰ (Snider et al., 2012, 2013).

2.6. Statistics

Statistical analyses were performed using one-way analysis of variance (ANOVA), and Tukey multiple comparisons tests to determine significant differences in mean gas fluxes, cumulative gas emission during 18 days, SP values, and N_2O source partitioning, respectively, between treatments. All differences were tested for significance at $P < 0.05$ using *Rstudio* (Rstudio Development Core Team, 2016).

3. Results

3.1. Dynamics of soil O_2 after slurry application

During the pre-incubation period, soil O_2 content stabilized at 85–90% air saturation in all treatments throughout the 4 cm × 4 cm soil cross-section (Fig. 1). Within the first day after slurry application, a zone of reduced O_2 content developed beneath the application area, which extended to a depth of approximately 1.5 cm in the cattle slurry (CS) treatment, and to 1 cm in the cattle slurry with DMPP (CSD) treatment. In the control soil (CTR), no zone with reduced O_2 developed. After approximately two days, soil O_2 depletion gradually diminished in both slurry treatments (Fig. 1 which shows profiles on day 5). Hypoxic zones (1–30% O_2 saturation) in treatments CS and CSD peaked at 7% and 4%, respectively, of the total cross-sectional area between 18 and 36 h, while the anoxic zones (<1% O_2 saturation) were largest after 30–48 h incubation in treatment CS, and after 24–42 h incubation in treatment CSD (Supp. Fig. S3). Below 1.5 cm soil depth, the O_2 content decreased by around 3% in all treatments, and there was no significant difference between the slurry treatments and CTR during the first five days.

Supplementary data related to this article can be found online at http://dx.doi.org/10.1016/j.soilbio.2017.07.012.

The simulated rain event of 1.25 mm by day 5 resulted in rapid expansion of the O_2 depletion zones in the upper 1.5 cm and 1.0 cm of the soil in treatments CS and CSD respectively. A more severe O_2 depletion in the CS treatment was reflected in anoxic and hypoxic areas developing more rapidly and being maintained for two days after water addition, whereas only the hypoxic area increased slightly in the CSD treatment and did not last as long (Supp. Fig. S3). In both amended treatments, soil O_2 status gradually reverted to the pre-incubation level for the remainder of the incubation. However, by the end of the incubation (425 h, day 18), a zone of anoxia remained in treatment CS in the upper 1 cm of soil, particularly in the central part of the soil profile where the slurry had been applied. In contrast, only a hypoxic zone was observed in treatment CSD that was limited to the upper 0.5 cm of the soil (Fig. 1).

3.2. Distribution of mineral N by the end of incubation

By day 18, vertical profiles of mineral N and pH of the soil (Fig. 2A–C) showed that NH_4^+-N and NO_3^--N concentrations, and pH, of the control soil were constant throughout the profile, but changed significantly with depth in the CS and CSD treatments. For

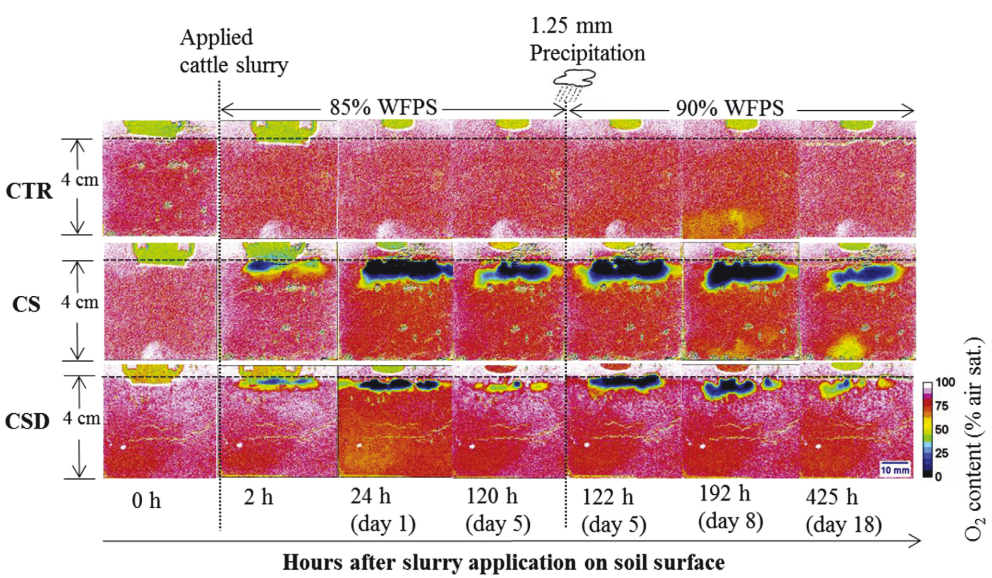

Fig. 1. Selected two-dimensional images of soil O_2 distribution (% air saturation) at different times after slurry application for a representative chamber (1 replicate) of the control (CTR), cattle slurry (CS), and cattle slurry-amended with DMPP treatment (CSD). Soil water content was 85% water-filled pore space (WFPS) at 2, 24 and 120 h, after which a 1.25 mm precipitation event was simulated, raising the soil water content to 90% WFPS at 122, 128 and 425 h of the incubation. For other replicates and more dynamics of soil O_2 during the incubation, see the supplementary information (Fig. S2 and Videos V1-3).

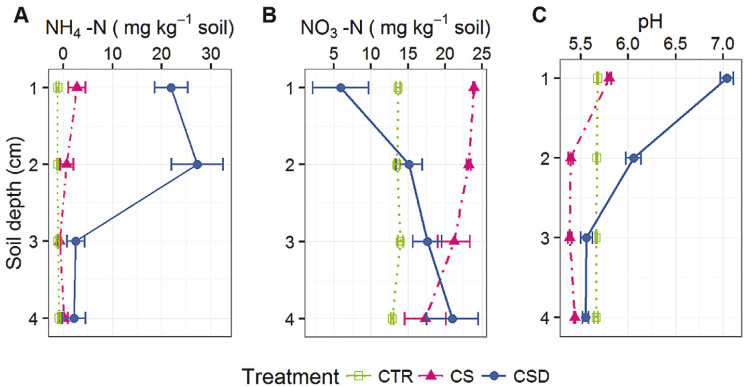

Fig. 2. (A) Vertical profiles of ammonium nitrogen content, (B) nitrate content and (C) pH by 1-cm layers from the soil surface at the end of the experiment. Bars indicate standard deviation of the mean ($n = 4$).

CSD, the highest soil NH_4^+-N concentrations were found at 1–2 cm soil depth, with 27.2 ± 5.3 mg N kg^{-1} dry wt. soil, which was significantly ($P < 0.001$) higher than that of CS in this layer, with 0.7 ± 1.4 mg N kg^{-1}. In contrast, NO_3^--N concentrations of CSD at 0–1 and 1–2 cm soil depth were significantly lower than those of CS in these layers, which were, in turn, lower than in the CTR treatment at a depth of 0–1 cm. NO_3^--N concentration of CSD increased with soil depth, while it decreased slightly from the soil surface towards the bottom layer in treatment CS. Below 2 cm soil depth, the NH_4^+-N and NO_3^--N concentrations of all three treatments were not significantly different. The soil pH of treatment CS was significantly lower than that of CTR and CSD treatments at all depths except for the upper 0–1 cm, where it was similar to CTR. In contrast, the soil pH of the CSD treatment in the upper 0–1 cm and 1–2 cm layers were significantly higher than in CTR, while the soil pH of CSD below 2 cm depth was much lower than that of CTR (Fig. 2C).

3.3. Trace gas emissions

During the incubation, CH_4, CO_2 and N_2O emissions from the CTR soil were negligible, whereas the gas fluxes were substantial in both CS and CSD (Fig. 3). Methane emissions from the cattle slurry amendments peaked immediately after slurry application, gradually leveled off from day 5 to day 7, and subsequently were not significantly different from CTR until the end of the incubation (Fig. 3A). Similarly, CO_2 evolution rates from the CS and CSD treatments peaked early, but remained significantly higher than CTR on most sampling days. The CO_2 emission rate of cattle slurry-amended soil peaked one day after application, then dropped off significantly in the following days. Nitrous oxide emissions were not significantly different between the two manure-amended soils during the first five days, and the highest N_2O fluxes coincided with the CO_2 peaks by day 1, at 47.8 ± 8.9 and 44.6 ± 2.2 μg N kg^{-1} soil per day for treatments CS and CSD, respectively (Fig. 3 C). After this early peak, the N_2O emissions of both slurry treatments declined dramatically. After the simulated rain event, a stimulation of N_2O emissions of similar magnitude was seen between days 5 and 7 but remained higher in CS than in CSD. From day 7, while N_2O emissions of treatment CSD declined and approached the background level of CTR, emissions of treatment CS increased steadily and reached a second peak of 41.1 ± 7.7 μg N kg^{-1} soil day^{-1} by day 14, before declining in the following days. By the end of the experiment, the N_2O emission of CS declined significantly to about 21.1 ± 6.8 μg N kg^{-1} soil per day, but this emission was still significantly higher than that of the CSD and CTR treatments.

Over the 18 days, cumulative CH_4 and CO_2 evolution did not differ between the CS and CSD treatments. In contrast, the total amount of emitted N_2O from the CS treatment was significantly higher than for CSD by approximately 60% (Supp. Table S2).

3.4. N_2O isotopomer and source partitioning

The SP values were between 10.9 ± 2.4‰ and 23.9 ± 1.2‰ during incubation (Fig. 4A). The highest SP values were observed in CS and CSD one day after slurry application, at 23.9 ± 1.2‰ and 23.5 ± 1.6‰, respectively. Given the two-end-member isotope signatures selected for the calculation of source partitioning (Eq. (2)), this is equivalent to roughly 30% of N_2O originating from bacterial denitrification (BD) in both the CS and CSD treatments (Table 2). This coincided with the largest area of hypoxia (1–30% air sat.) in the cattle slurry treatments, which occurred 18–30 h after application (Supp. Fig. S3). The SP values decreased significantly during the next two days, to 15.6 ± 1.3‰ for CS and 13.5 ± 1.3‰ for CSD by day 3, corresponding to approximately 50% of the N_2O originating from BD in the two treatments. After water addition, the soil O_2 contents of CS and CSD immediately declined to 45% and 60% air saturation, respectively, and remained at these levels for approximately 12 h before increasing gradually until the end of the experiment (Fig. 4B). Concomitantly, the SP values of these treatments dropped to their lowest levels at around 11.4‰ by day 7 for both CS and CSD, corresponding to around 60% of BD-derived N_2O production. For CS, the low SP value persisted until day 11 (11.2 ± 0.9‰) before slightly increasing to 14.7 ± 0.6‰ by day 14, while the SP for CSD increased more quickly and had already reached 20.1 ± 1.5‰ by day 14.

The end-member SP values used for N_2O source partitioning most often rely on results from pure culture studies, although SP may vary depending on the soil environment under field conditions (Well et al., 2006; Ostrom et al., 2010). Source partitioning calculations based on the two-end-member model (Eq. (2)) therefore provide only rough estimates of the contribution to soil-emitted N_2O. However, the relationship between SP values and $\delta^{18}O$ of soil-emitted N_2O (Fig. 5A) also indicated that N_2O emissions were not derived solely from NI/FD or BD, but from a combination of these sources. In general, the SP values and $\delta^{18}O$-N_2O of the CTR

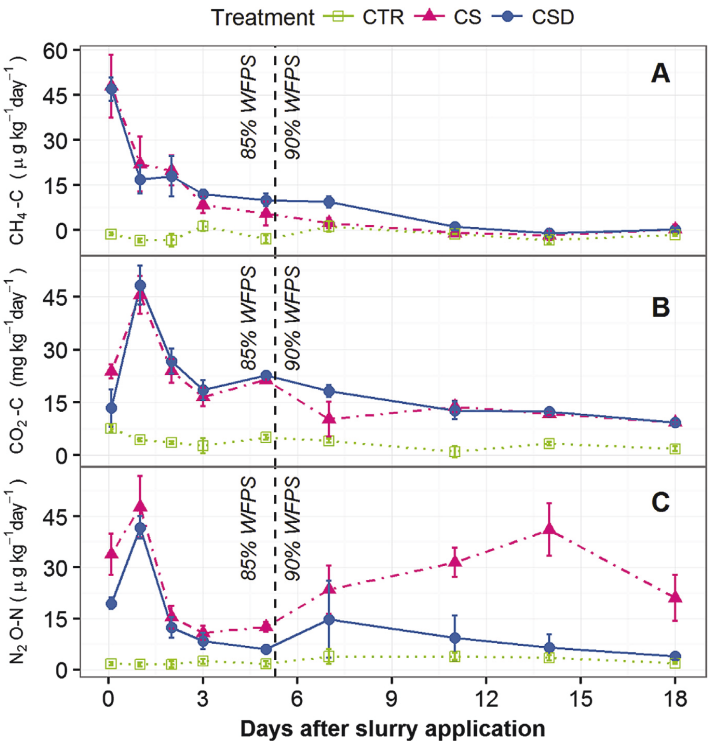

Fig. 3. Gas emission rates of CH_4, CO_2 and N_2O during 18 days of incubation ($n = 4$, mean ± standard deviation). The vertical dashed line indicates the time of water addition. Bars indicate the standard deviation of the mean ($n = 4$).

treatment and cattle slurry treatments fluctuated during incubation, probably reflecting a shift in the dominant source of N_2O between NI, FD and BD. The SP values were not clearly different between treatments on any sampling day except day 14. In contrast, the $\delta^{18}O$-N_2O differed between CSD (42‰–46‰), CS (35‰–42‰) and CTR (35‰–40‰). The increase in soil water content after simulated rainfall led to the depletion of $\delta^{18}O$-N_2O in all treatments from day 5 to day 7 (Fig. 5A), indicating a shift in N_2O production from NI/FD towards BD. The most pronounced shifts were found in CTR and CS and corresponded to the depletion of $\delta^{18}O$-N_2O by approximately 5‰ (from 41‰ to 36‰, and from 40‰ to 35‰, respectively), while the shift was slightly smaller for CSD (from 45‰ to 42‰).

The total N_2O emission (Fig. 5B) from treatment CS was significantly higher than those from treatments CSD and CTR, corresponding to approximately 60% higher N_2O in CS compared to CSD. However, the temporal dynamics of N_2O emission were complex. In the first five days, the cumulative N_2O emission was similar in the CS and CSD treatments (Supp. Table S3), while in the last 13 days the cumulative N_2O from treatment CSD was similar to CTR about 10% of that of CS ($P < 0.001$). Over the whole 18 days of incubation, the proportion of N_2O derived from BD tended to be higher (but not significantly) than that of NI/FD in all treatments; there was no difference between proportions of BD in any treatments (Fig. 5B).

4. Discussion

The spatial distribution of soil O_2 showed that NH_4^+ and labile C from surface-applied cattle slurry infiltrated and contributed to O_2 consumption in the upper 1.5 cm and 1.0 cm soil layer in CS and CSD treatments, respectively. This is likely to have been caused by the consumption of O_2 by heterotrophic respiration of dissolved organic matter (Bol et al., 2003a) and nitrification (Delin and Strömberg, 2011) of ammonical N which infiltrated and diffused into the upper cm of the soil. The observation that reactive C and N in cattle slurry can stimulate O_2 consumption through aerobic respiration and nitrification, causing depletion of O_2 in manure hotspots, has also been reported by, *e.g.*, Petersen et al. (1996) and Meyer et al. (2002). The difference in O_2 distribution between treatments CS and CSD indicated that nitrification could be responsible for a significant part of the O_2 depletion during the first few days after manure application, even though nitrification activity is usually considered to be limited as the organisms have to synthesize enzymes and multiply (Meyer et al., 2002). On the other hand, Petersen et al. (1992) observed a stimulation of potential ammonia oxidation rates around cattle manure hotspots after 24 h, indicating that nitrifier activity was already intense. Intensively managed grassland soil may have potential nitrification rates of 150–200 nmol NH_3 g^{-1} d^{-1} (Meyer et al., 2013), corresponding to 225–300 nmol O_2 g^{-1} d^{-1}. This can be compared with the observed CO_2 evolution rates (Fig. 3B) of 15–45 mg CO_2-C kg^{-1} d^{-1}, or 1250–3750 nmol CO_2-C g^{-1} d^{-1}. Assuming a CO_2:O_2 ratio close to 1 (Angert et al., 2015), it is evident that O_2 demand for nitrification could be quantitatively important, especially since nitrification activity was probably concentrated near soil-manure interfaces, unlike heterotrophic activity. Although cattle slurry in treatment

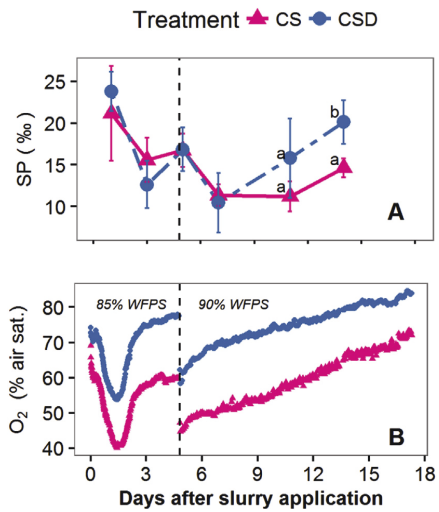

Fig. 4. (A) The corrected site preference values (SP) of soil emitted N_2O during incubation of slurry-amended soil, and (B) average oxygen content (% air saturation) in amended soils; the vertical dashed line indicates the time of the simulated rain event of 1.25 mm precipitation following gas sampling on day 5. Error bars present standard deviation of the SP mean ($n = 4$) and different letters indicate significant differences between the mean SP values of the CS and CSD treatments on each sampling day with $P < 0.05$.

Table 2
The proportion of N_2O emission derived from bacterial denitrification (fD[a] in %) during the incubation.

Day	CTR	CS	CSD
1	38.4 ± 1.7	34.5 ± 7.1	28.0 ± 3.0
3	57.8 ± 16.8	48.6 ± 3.3	56.0 ± 3.6
5	26.1 ± 12.5	45.6 ± 2.5	45.4 ± 3.3
7	62.2 ± 8.4	59.2 ± 1.7	61.4 ± 4.4
11	58.6 ± 5.5	59.6 ± 2.2	61.2 ± 14.1
14	42.8 ± 3.4	50.9 ± 1.4	47.4 ± 10.6

[a] fD calculated from site preference of emitted N_2O using a two-end-member mixing model (Eq. (2)), ($n = 4$, mean ± standard deviation).

CSD was amended with a nitrification inhibitor, nitrification in this treatment cannot be ruled out completely if NH_4^+ migrated further away from the zone of the original distribution than DMPP (Azam et al., 2001).

The recovery of O_2 concentrations in the CS and CSD treatments after just a few days reflected a decrease in oxidation activities. After the simulated rain event, the decreasing trend in soil O_2 content that followed in the CS and CSD treatments must have been caused by restrictions in the diffusional supply of O_2 from the headspace caused by the increased water content, combined with sustained O_2 consumption for oxidation of NH_4^+ and labile C (Bol et al., 2003a; Baral et al., 2016).

The similar total cumulative N_2O emissions obtained for CS and CSD during the early phase of incubation implies that the dominant N_2O production pathway during this period was unlikely to depend on nitrification (NI), and thus presumably denitrification using the NO_3^- already present in the soil was the main source. This also explains why the application of DMPP did not significantly mitigate N_2O emissions during the first five days. The early peak of N_2O emissions observed in the present study has also been reported and attributed to denitrification of soil NO_3^- in other studies (Petersen et al., 1992; Paul et al., 1993; Meyer et al., 2002; Thomsen et al., 2010; Markfoged et al., 2011). However, the SP values (around 25‰) of both CS and CSD for the N_2O peak were much higher than the values expected for bacterial denitrification of 1.3–13.8‰ in temperate grassland (Bol et al., 2003b), and of 2.6–14.6‰ in agricultural soils (Opdyke et al., 2009). Instead, these SP values were consistent with NI and/or FD being the dominant sources of N_2O production to the peak. A possible explanation for the high SP values of emitted N_2O in both the CS and CSD treatments during the early peak is that the contribution from FD was high. This would also be in accordance with the relatively high $\delta^{18}O$ values observed during this period. Fungal denitrification appears to be especially important in enhanced organic C soil environments (Robertson and Tiedje, 1987; Laughlin and Stevens, 2002; Marusenko et al., 2013; Jirout, 2015) and thus could play an important role in N_2O formation in grassland soil under sub-oxic conditions (Jirout et al., 2013; Chen et al., 2015). Moreover, the contribution of soil fungi to the total N_2O emissions has been reported to be as high as 65% in current and former intensive grazing pastures (Jirout, 2015). It can also be seen from Fig. 5A that $\delta^{18}O$-N_2O values by day 1 in cattle slurry amendments were in the transition zone between BD and FD, and more likely to be associated with FD based on the combination of both $\delta^{18}O$ and SP values of emitted N_2O.

It should be acknowledged that higher than expected SP values could be due to isotopic fractionation during N_2O reduction to N_2 (Ostrom et al., 2007; Jinuntuya-Nortman et al., 2008; Well and Flessa, 2009a; Köster et al., 2013), especially under conditions with low NO_3^- and high C availability (Senbayram et al., 2012). Thus, the proportion of NI/FD as a source of N_2O, as calculated from SP values with the two-end-member source partitioning model, could be overestimated (Wu et al., 2016). On the other hand, the significant positive correlation between $\delta^{18}O$-N_2O and SP values with a slope of 1.2 ($r = 0.08$, $P = 0.02$) had the characteristics of denitrification (Ostrom et al., 2007; Jinuntuya-Nortman et al., 2008; Köster et al., 2013; Mander et al., 2014).

The decline in N_2O emissions from both CS and CSD after the first peak occurred while the anoxic and hypoxic zones were largest, implying either that the NO_3^- supply limited denitrification or that denitrification products shifted towards the more complete reduction of N_2O to N_2. However, extensive reduction of N_2O to N_2 should increase SP values as a result of isotopic fractionation, as discussed above. The fact that the lowest SP values, implying BD as the dominant source of N_2O production in both the CS and CSD treatments, were measured on day 3 indicates that limitation of NO_3^- in the soil was most likely responsible for the decline in N_2O emissions during this period (Table 2 and Fig. 5A). Soil O_2 increased in both the CS and CSD treatments between days 3 and 5 and may have diminished the contribution of BD to N_2O emissions due to the inhibitory effect of O_2 to bacterial denitrification of NO_3^- (McKenney et al., 1994). However, the anoxic and hypoxic zones in CS remained larger than in CSD, which could have maintained bacterial denitrification at a relatively higher level in CS compared to CSD. This would be in accordance with the minor changes in SP and $\delta^{18}O$-N_2O values for CS between days 3 and 5 (Fig. 5A).

During the second peak of N_2O emissions, after soil moisture was increased through a simulated rain event, the N_2O emission of CTR slightly increased, presumably because O_2 depletion enhanced denitrification of soil NO_3^- in anaerobic microsites that were not visible in the optode images. It can be seen from Fig. 5A that both SP values and $\delta^{18}O$-N_2O declined, showing the greater contribution of BD to N_2O production during this period. For treatment CSD, the stimulation of N_2O emissions after the rain event was as high as in the CS treatment between days 5 and 7, and the concomitant decline in SP values observed during this period for both CS and CSD also suggest an increasing importance of BD for N_2O formation.

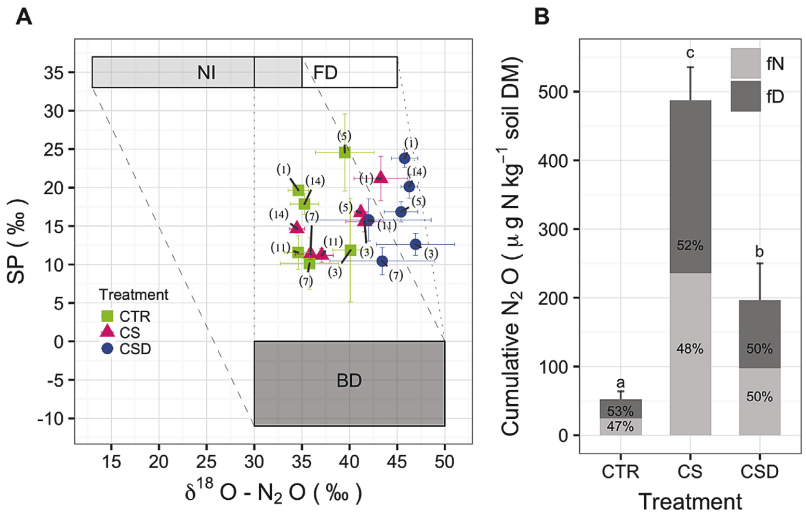

Fig. 5. (A) The end-member map with site preference values (SP) as a function of soil derived $\delta^{18}O$-N_2O (expressed with respect to Vienna Standard Mean Ocean Water - VSMOW) illustrates the trend shifting in source of N_2O production for the different treatments (control ■ CTR, cattle slurry ▲ CS and cattle slurry with DMPP treatment ● CSD), numbers in brackets indicate sampling days. The rectangles represent the areas corresponding to the ranges of literature data of N_2O isotopic signatures for the pure culture and soil incubation studies. SP for bacterial nitrification (NI), fungal denitrification (FD) and bacterial denitrification (BD) was based on literature data (see the method and methodology section). (B) Total cumulative N_2O over 18 days of incubation with the estimates of N_2O proportion (%) derived from NI/FD (fN) and BD (fD) based on the two-end-member mixing model. Bars indicate the standard deviation of the means ($n = 4$).

The O_2 content increased from day 7 in both CS and CSD, which could have diminished the contribution of BD-derived N_2O in the two treatments, and thus the predominant source of N_2O production may have shifted towards either NI or FD.

The sources of N_2O emissions in CS apparently remained constant between days 7 and 11, most likely dominated by BD, and then slightly changed towards NI and/or FD by day 14 (Fig. 5A). In contrast, BD was confirmed to be the main contributor to N_2O emissions in the CSD treatment until day 7, a contribution which then slightly declined until day 14 (Table 2). It has been reported that sub-oxic conditions favor fungal denitrification over bacterial denitrification as fungi require O_2 for cell growth (Zhou et al., 2001), while O_2 inhibits bacterial denitrification (McKenney et al., 1994). The distribution of NH_4^+ and NO_3^- at 3–4 cm depth at the end of the incubation indicated that nitrification had taken place at this depth in the CSD treatment (Fig. 2A and B). It is likely that little NH_4^+ and DMPP initially reached these layers, and that most nitrifiers here were unaffected by DMPP. Nitrification activity would have created a gradient leading to diffusion of NH_4^+ from upper soil layers. With soil moisture at 90% WFPS in the last part of the incubation, this nitrification activity could have contributed to the observed N_2O emissions between day 11 and 18 (Fig. 3C). Denitrification would be expected to continue to the extent that labile C and NO_3^- were available in anaerobic microsites. Therefore, it is proposed that N_2O emissions in the later phase likely derived from a mixture of either NI and BD, or of FD and BD. The contributions of NI and BD to N_2O emissions were higher for CS than CSD due to both the higher NO_3^- supply and larger anoxic and hypoxic zones. Consequently, the second peak of N_2O emission in CS was associated with the highest potential for nitrification of manure-derived NH_4^+ and was followed by the denitrification of already formed NO_3^- during the last 13 days of the incubation (Petersen et al., 1996; Meyer et al., 2002).

Evidence for the dominance of denitrification as a source of N_2O in the CSD and CS treatments also comes from the fact that the soil NO_3^- concentration by the end of the incubation in the 0–1 cm layer was lower in CSD than in CTR and CS, while soil pH was much higher for CSD than for CS and CTR (Fig. 2B and C). This is in accordance with the consumption of soil NO_3^- in the CSD treatment, and NO_3^- consumption together with nitrification activity in the CS treatment. The NO_3^- content remained higher in both CSD and CS compared to CTR by the end of the experiment. This is partly explained by Meyer et al. (2002), who used a nitrate-nitrite microsensor to profile NO_3^- and NO_2^- concentrations and reported that the maximum nitrification and denitrification rates at 0–10 mm distance from the soil-manure interface occurred around 10 days after application.

Further down the profile (3–4 cm), oxic conditions were maintained throughout the incubation (Fig. 1 and Supp. Fig. S2), promoting aerobic metabolism and preventing the reduction of NO_3^- (Wrage et al., 2001), and thus maintaining NO_3^- concentrations in both CS and CSD. Soil NO_3^- accumulated in the lower parts of the soil cores in the CSD treatment compared with CTR (Fig. 2B), which was not expected if DMPP blocked nitrification of $NH4^+$ added with cattle slurry. One explanation for this is that NH_4^+ diffused to the deeper layers to a greater extent than DMPP, as discussed previously. Removal of NH_4^+ *via* nitrification would have created a concentration gradient for NH_4^+, but not DMPP. Also, after the rain event, NO_3^- produced closer to the surface could have been transported to deeper soil layers.

The second peak of N_2O emissions in the CS treatment by day 14, which was absent in CSD, suggested that blocking of nitrification by DMPP largely suppressed N_2O emissions after the first week through NO_3^- limitation. Throughout the incubation period, the observation that addition of DMPP to cattle slurry did not affect total CH_4 and CO_2 accumulation is in line with several other studies (Dittert et al., 2001; Pereira et al., 2010; Menéndez et al., 2012; Kong et al., 2016). The significant reduction of total N_2O emission by approximately 60% after application of DMPP to cattle slurry was

comparable to that reported in previous laboratory studies (Chen et al., 2010; Zhu et al., 2016) and under field conditions (Di and Cameron, 2012). The N_2O mitigation of the CSD treatment in the present study was greater than in several field studies on grassland soil (Menéndez et al., 2006), but lower than in some cropland field experiments (Merino et al., 2006; Scheer et al., 2014; Abalos et al., 2016). The difference between the present study and these field studies with respect to N_2O mitigation is probably related to differences in experimental conditions, such as the initial soil nitrate content, availability of labile C, rainfall or water content (Abalos et al., 2016; Di and Cameron, 2016), soil temperature, manure application method (De Antoni Migliorati et al., 2014; Pereira et al., 2015) and dose of applied DMPP (Kong et al., 2016), which all influence the effectiveness of nitrification inhibitors. The present experiment was conducted at soil WFPS of 85–90%, and thus soil aeration was relatively poor. However, these conditions are commonly found during spring in wet temperate climates; for example, Harty et al. (2016) presented detailed information on WFPS across a two-year period in a multi-site study, and on several occasions fertilization coincided with soil WFPS >80%.

5. Conclusions

This study demonstrated, using planar optodes for non-destructive monitoring of O_2 availability, that surface application of cattle slurry creates a shallow zone of O_2 depletion in the soil beneath the slurry. The application of DMPP, equivalent to 1.2 kg ha^{-1}, reduced the extent of the O_2 depletion zone, presumably by inhibiting O_2 consumption by nitrification. The inhibition of the nitrification process also affected N_2O production in the grassland soil with a relatively high water content (85–90% WFPS). In the CS treatment, two peaks of N_2O production were observed, whereas the second peak was absent in the CSD treatment. Based on isotope analyses, the first peak was concluded to be mainly derived from fungal denitrification and bacterial denitrification based on the initial soil nitrate pool in both CS and CSD treatments. The second peak, observed in CS only, was associated with fungal and bacterial denitrification using nitrate formed by nitrification of manure ammonium. Given the fact that denitrification seemed to be the dominating process behind N_2O emissions, the results indicate that fungal denitrification could be playing an important role in this moderately acidic grassland soil at relatively high water content. The application of DMPP did not significantly reduce N_2O emissions during the initial phase, but clearly reduced the second peak, which quantitatively was the most important.

Acknowledgements

The current work was supported by the Danish Council for Strategic Research, under the "StrategicResearch in Sustainable Energy and Environment" research program, through the project "Optimization of value chains for biogas production in Denmark (BioChain)" (Grant number: 12-132631). We appreciate comments and suggestions from the reviewers to improve the manuscript.

Appendix A. Supplementary data

Supplementary data related to this article can be found at http://dx.doi.org/10.1016/j.soilbio.2017.07.012.

References

Abalos, D., Sanz-Cobena, A., Andreu, G., Vallejo, A., 2016. Rainfall amount and distribution regulate DMPP effects on nitrous oxide emissions under semiarid Mediterranean conditions. Agriculture, Ecosystems & Environment 238, 36–45.

Angert, A., Yakir, D., Rodeghiero, M., Preisler, Y., Davidson, E.A., Weiner, T., 2015. Using O_2 to study the relationships between soil CO_2 efflux and soil respiration. Biogeosciences (Online) 12, 2089–2099.

Azam, F., Benckiser, G., Müller, C., Ottow, J., 2001. Release, movement and recovery of 3,4-dimethylpyrazole phosphate (DMPP), ammonium, and nitrate from stabilized nitrogen fertilizer granules in a silty clay soil under laboratory conditions. Biology and Fertility of Soils 34, 118–125.

Baral, K.R., Arthur, E., Olesen, J.E., Petersen, S.O., 2016. Predicting nitrous oxide emissions from manure properties and soil moisture: an incubation experiment. Soil Biology and Biochemistry 97, 112–120.

Bell, M.J., Cloy, J.M., Topp, C.F.E., Ball, B.C., Bagnall, A., Rees, R.M., Chadwick, D.R., 2016. Quantifying N_2O emissions from intensive grassland production: the role of synthetic fertilizer type, application rate, timing and nitrification inhibitors. The Journal of Agricultural Science 154, 812–827.

Bol, R., Kandeler, E., Amelung, W., Glaser, B., Marx, M.C., Preedy, N., Lorenz, K., 2003a. Short-term effects of dairy slurry amendment on carbon sequestration and enzyme activities in a temperate grassland. Soil Biology and Biochemistry 35, 1411–1421.

Bol, R., Toyoda, S., Yamulki, S., Hawkins, J., Cardenas, L., Yoshida, N., 2003b. Dual isotope and isotopomer ratios of N2O emitted from a temperate grassland soil after fertiliser application. Rapid Communications in Mass Spectrometry 17, 2550–2556.

Braker, G., Conrad, R., 2011. Diversity, structure, and size of N_2O-producing microbial communities in soils–what matters for their functioning? Advances in Applied Microbiology 75, 33–70.

Butterbach-Bahl, K., Baggs, E.M., Dannenmann, M., Kiese, R., Zechmeister-Boltenstern, S., 2013. Nitrous oxide emissions from soils: how well do we understand the processes and their controls? Philosophical Transactions of The Royal Society 368, 20130122.

Chen, D., Suter, H.C., Islam, A., Edis, R., 2010. Influence of nitrification inhibitors on nitrification and nitrous oxide (N_2O) emission from a clay loam soil fertilized with urea. Soil Biology and Biochemistry 42, 660–664.

Chen, H., Mothapo, N.V., Shi, W., 2015. Soil moisture and pH control relative contributions of fungi and bacteria to N_2O Production. Microbial Ecology 69, 180–191.

De Antoni Migliorati, M., Scheer, C., Grace, P.R., Rowlings, D.W., Bell, M., McGree, J., 2014. Influence of different nitrogen rates and DMPP nitrification inhibitor on annual N_2O emissions from a subtropical wheat–maize cropping system. Agriculture, Ecosystems & Environment 186, 33–43.

Delin, S., Strömberg, N., 2011. Imaging-optode measurements of ammonium distribution in soil after different manure amendments. European Journal of Soil Science 62, 295–304.

Di, H.J., Cameron, K.C., 2012. How does the application of different nitrification inhibitors affect nitrous oxide emissions and nitrate leaching from cow urine in grazed pastures? Soil Use and Management 28, 54–61.

Di, H.J., Cameron, K.C., 2016. Inhibition of nitrification to mitigate nitrate leaching and nitrous oxide emissions in grazed grassland: a review. Journal of Soils and Sediments 16, 1401–1420.

Dittert, K., Bol, R., King, R., Chadwick, D., Hatch, D., 2001. Use of a novel nitrification inhibitor to reduce nitrous oxide emission from (15)N-labelled dairy slurry injected into soil. Rapid Commun Mass Spectrom 15, 1291–1296.

Fangueiro, D., Fernandes, A., Coutinho, J., Moreira, N., Trindade, H., 2009. Influence of two nitrification inhibitors (DCD and DMPP) on annual ryegrass yield and soil mineral N dynamics after incorporation with cattle slurry. Communications in Soil Science and Plant Analysis 40, 3387–3398.

Harty, M.A., Forrestal, P.J., Watson, C.J., McGeough, K.L., Carolan, R., Elliot, C., Krol, D., Laughlin, R.J., Richards, K.G., Lanigan, G.J., 2016. Reducing nitrous oxide emissions by changing N fertiliser use from calcium ammonium nitrate (CAN) to urea based formulations. Science of the Total Environment 563, 576–586.

Heil, J., Liu, S., Vereecken, H., Brüggemann, N., 2015. Abiotic nitrous oxide production from hydroxylamine in soils and their dependence on soil properties. Soil Biology and Biochemistry 84, 107–115.

Jinuntuya-Nortman, M., Sutka, R.L., Ostrom, P.H., Gandhi, H., Ostrom, N.E., 2008. Isotopologue fractionation during microbial reduction of N_2O within soil mesocosms as a function of water-filled pore space. Soil Biology and Biochemistry 40, 2273–2280.

Jirout, J., 2015. Nitrous oxide productivity of soil fungi along a gradient of cattle impact. Fungal Ecology 17, 155–163.

Jirout, J., Šimek, M., Elhottová, D., 2013. Fungal contribution to nitrous oxide emissions from cattle impacted soils. Chemosphere 90, 565–572.

Kong, X., Duan, Y., Schramm, A., Eriksen, J., Petersen, S.O., 2016. 3,4-Dimethylpyrazole phosphate (DMPP) reduces activity of ammonia oxidizers without adverse effects on non-target soil microorganisms and functions. Applied Soil Ecology 105, 67–75.

Köster, J.R., Cárdenas, L.M., Bol, R., Lewicka-Szczebak, D., Senbayram, M., Well, R., Giesemann, A., Dittert, K., 2015. Anaerobic digestates lower N_2O emissions compared to cattle slurry by affecting rate and product stoichiometry of denitrification–An N_2O isotopomer case study. Soil Biology and Biochemistry 84, 65–74.

Köster, J.R., Well, R., Dittert, K., Giesemann, A., Lewicka-Szczebak, D., Mühling, K.-H., Herrmann, A., Lammel, J., Senbayram, M., 2013. Soil denitrification potential and its influence on N_2O reduction and N_2O isotopomer ratios. Rapid Communications in Mass Spectrometry 27, 2363–2373.

Larsen, M., Borisov, S.M., Grunwald, B., Klimant, I., Glud, R.N., 2011. A simple and inexpensive high resolution color ratiometric planar optode imaging approach:

application to oxygen and pH sensing. Limnology and Oceanography: Methods 9, 361–379.
Laughlin, R.J., Stevens, R.J., 2002. Evidence for fungal dominance of denitrification and codenitrification in a grassland soil. Soil Science Society of America Journal 66, 1540.
Lewicka-Szczebak, D., Dyckmans, J., Kaiser, J., Marca, A., Augustin, J., Well, R., 2016. Oxygen isotope fractionation during N_2O production by soil denitrification. Biogeosciences (Online) 13, 1129–1144.
Lewicka-Szczebak, D., Well, R., Köster, J.R., Fuß, R., Senbayram, M., Dittert, K., Flessa, H., 2014. Experimental determinations of isotopic fractionation factors associated with N_2O production and reduction during denitrification in soils. Geochimica et Cosmochimica Acta 134, 55–73.
Mander, U., Well, R., Weymann, D., Soosaar, K., Maddison, M., Kanal, A., Lõhmus, K., Truu, J., Augustin, J., Tournebize, J., 2014. Isotopologue ratios of N_2O and N_2 measurements underpin the importance of denitrification in differently N-loaded riparian alder forests. Environmental Science & Technology 48, 11910–11918.
Markfoged, R., Nielsen, L.P., Nyord, T., Ottosen, L.D.M., Revsbech, N.P., 2011. Transient N_2O accumulation and emission caused by O_2 depletion in soil after liquid manure injection. European Journal of Soil Science 62, 541–550.
Marusenko, Y., Huber, D.P., Hall, S.J., 2013. Fungi mediate nitrous oxide production but not ammonia oxidation in aridland soils of the southwestern US. Soil Biology and Biochemistry 63, 24–36.
McKenney, D., Drury, C., Findlay, W., Mutus, B., McDonnell, T., Gajda, C., 1994. Kinetics of denitrification by Pseudomonas fluorescens: oxygen effects. Soil Biology and Biochemistry 26, 901–908.
Menéndez, S., Barrena, I., Setien, I., González-Murua, C., Estavillo, J.M., 2012. Efficiency of nitrification inhibitor DMPP to reduce nitrous oxide emissions under different temperature and moisture conditions. Soil Biology and Biochemistry 53, 82–89.
Menéndez, S., Merino, P., Pinto, M., González-Murua, C., Estavillo, J.M., 2006. 3,4-Dimethylpyrazol phosphate effect on nitrous oxide, nitric oxide, ammonia, and carbon dioxide emissions from grasslands. Journal of Environmental Quality 35, 973–981.
Merino, P., Menéndez, S., Pinto, M., González-Murua, C., Estavillo, J.M., 2006. 3, 4-Dimethylpyrazole phosphate reduces nitrous oxide emissions from grassland after slurry application. Soil Use and Management 21, 53–57.
Meyer, R.L., Kjær, T., Revsbech, N.P., 2002. Nitrification and denitrification near a soil–manure interface studied with a nitrate-nitrite biosensor. Soil Science Society of America Journal 66, 498–506.
Meyer, A., Focks, A., Radl, V., Keil, D., Welzl, G., Schöning, I., Boch, S., Marhan, S., Kandeler, E., Schloter, M., 2013. Different land use intensities in grassland ecosystems drive ecology of microbial communities involved in nitrogen turnover in soil. PloS One 8, e73536.
Opdyke, M.R., Ostrom, N.E., Ostrom, P.H., 2009. Evidence for the predominance of denitrification as a source of N_2O in temperate agricultural soils based on isotopologue measurements. Global Biogeochemical Cycles 23.
Ostrom, N.E., Pitt, A., Sutka, R., Ostrom, P.H., Grandy, A.S., Huizinga, K.M., Robertson, G.P., 2007. Isotopologue effects during N_2O reduction in soils and in pure cultures of denitrifiers. Journal of Geophysical Research 112.
Ostrom, N.E., Sutka, R., Ostrom, P.H., Grandy, A.S., Huizinga, K.M., Gandhi, H., von Fischer, J.C., Robertson, G.P., 2010. Isotopologue data reveal bacterial denitrification as the primary source of N2O during a high flux event following cultivation of a native temperate grassland. Soil Biology and Biochemistry 42, 499–506.
Paul, J.W., Beauchamp, E.G., Zhang, X., 1993. Nitrous and nitric oxide emissions during nitrification and denitrification from manure-amended soil in the laboratory. Canadian Journal of Soil Science 73, 539–553.
Pereira, J., Coutinho, J., Fangueiro, D., Trindade, H., 2015. Nitric oxide and nitrous oxide emissions from cattle-slurry and mineral fertiliser treated with nitrification inhibitor to an agricultural soil: a laboratory approach. Spanish Journal of Agricultural Research 13, 0305.
Pereira, J., Fangueiro, D., Chadwick, D.R., Misselbrook, T.H., Coutinho, J., Trindade, H., 2010. Effect of cattle slurry pre-treatment by separation and addition of nitrification inhibitors on gaseous emissions and N dynamics: a laboratory study. Chemosphere 79, 620–627.
Petersen, S.O., Nielsen, A.L., Haarder, K., Henriksen, K., 1992. Factors controlling nitrification and denitrification: a laboratory study with gel-stabilized liquid cattle manure. Microbial Ecology 23, 239–255.
Petersen, S.O., Nielsen, T.H., Frostegård, Å., Olesen, T., 1996. O_2 uptake, C metabolism and denitrification associated with manure hot-spots. Soil Biology and Biochemistry 28, 341–349.
Petersen, S.O., Nissen, H.H., Lund, I., Ambus, P., 2003. Redistribution of slurry components as influenced by injection method, soil, and slurry properties. Journal of Environmental Quality 32, 2399–2409.
Qu, W., Bogena, H.R., Huisman, J.A., Schmidt, M., Kunkel, R., Weuthen, A., Schiedung, H., Schilling, B., Sorg, J., Vereecken, H., 2016. The integrated water balance and soil data set of the Rollesbroich hydrological observatory. Earth Syst. Sci. Data 8, 517–529.
Robertson, G.P., Tiedje, J.M., 1987. Nitrous oxide sources in aerobic soils: nitrification, denitrification and other biological processes. Soil Biology and Biochemistry 19, 187–193.
Rohe, L., Anderson, T.-H., Braker, G., Flessa, H., Giesemann, A., Lewicka-Szczebak, D., Wrage-Mönnig, N., Well, R., 2014. Dual isotope and isotopomer signatures of nitrous oxide from fungal denitrification–a pure culture study. Rapid Communications in Mass Spectrometry 28, 1893–1903.
Rstudio Development Core Team, 2016. A Language and Environment for Statistical Computing, 0.99.902 ed. R Foundation for Statistical Computing, Vienna, Austria.
Scheer, C., Rowlings, D.W., Firrel, M., Deuter, P., Morris, S., Grace, P.R., 2014. Impact of nitrification inhibitor (DMPP) on soil nitrous oxide emissions from an intensive broccoli production system in sub-tropical Australia. Soil Biology and Biochemistry 77, 243–251.
Senbayram, M., Chen, R., Budai, A., Bakken, L., Dittert, K., 2012. N_2O emission and the $N_2O/(N_2O + N_2)$ product ratio of denitrification as controlled by available carbon substrates and nitrate concentrations. Agriculture, Ecosystems & Environment 147, 4–12.
Snider, D.M., Venkiteswaran, J.J., Schiff, S.L., Spoelstra, J., 2012. Deciphering the oxygen isotope composition of nitrous oxide produced by nitrification. Global Changen Biology 18, 356–370.
Snider, D.M., Venkiteswaran, J.J., Schiff, S.L., Spoelstra, J., 2013. A new mechanistic model of $\delta^{18}O$ N_2O formation by denitrification. Geochimica et Cosmochimica Acta 112, 102–115.
Sutka, R.L., Adams, G.C., Ostrom, N.E., Ostrom, P.H., 2008. Isotopologue fractionation during N_2O production by fungal denitrification. Rapid Communications in Mass Spectrometry 22, 3989–3996.
Sutka, R.L., Ostrom, N.E., Ostrom, P.H., Breznak, J.A., Gandhi, H., Pitt, A.J., Li, F., 2006. Distinguishing nitrous oxide production from nitrification and denitrification on the basis of isotopomer abundances. Applied and Environmental Microbiology 72, 638–644.
Thompson, R.B., 1989. Denitrification in slurry-treated soil: occurrence at low temperatures, relationship with soil nitrate and reduction by nitrification inhibitors. Soil Biology and Biochemistry 21, 875–882.
Thomsen, I.K., Pedersen, A.R., Nyord, T., Petersen, S.O., 2010. Effects of slurry pre-treatment and application technique on short-term N_2O emissions as determined by a new non-linear approach. Agriculture, Ecosystems & Environment 136, 227–235.
Toyoda, S., Mutobe, H., Yamagishi, H., Yoshida, N., Tanji, Y., 2005. Fractionation of N_2O isotopomers during production by denitrifier. Soil Biology and Biochemistry 37, 1535–1545.
Toyoda, S., Yoshida, N., 1999. Determination of nitrogen isotopomers of nitrous oxide on a modified isotope ratio mass spectrometer. Analytical Chemistry 71, 4711–4718.
Wayne, R., 2015. Image J 1.47v. National Institutes of Health, USA.
Well, R., Kurganova, I., Lopesdegerenyu, V., Flessa, H., 2006. Isotopomer signatures of soil-emitted N_2O under different moisture conditions—a microcosm study with arable loess soil. Soil Biology and Biochemistry 38, 2923–2933.
Well, R., Eschenbach, W., Flessa, H., von der Heide, C., Weymann, D., 2012. Are dual isotope and isotopomer ratios of N_2O useful indicators for N_2O turnover during denitrification in nitrate-contaminated aquifers? Geochimica et Cosmochimica Acta 90, 265–282.
Well, R., Flessa, H., 2009a. Isotopologue enrichment factors of N_2O reduction in soils. Rapid Communications in Mass Spectrometry 23, 2996–3002.
Well, R., Flessa, H., 2009b. Isotopologue signatures of N_2O produced by denitrification in soils. Journal of Geophysical Research: Biogeosciences 114.
Wrage, N., Velthof, G.L., Beusichem, M.L.v., Oenema, O., 2001. Role of nitrifier denitrification in the production of nitrous oxide. Soil Biology and Biochemistry 33, 1723–1732.
Wu, D., Köster, J.R., Cárdenas, L.M., Brüggemann, N., Lewicka-Szczebak, D., Bol, R., 2016. N_2O source partitioning in soils using ^{15}N site preference values corrected for the N_2O reduction effect. Rapid Communications in Mass Spectrometry 30, 620–626.
Zerulla, W., Barth, T., Dressel, J., Erhardt, K., Horchler von Locquenghien, K., Pasda, G., Rädle, M., Wissemeier, A., 2001. 3,4-Dimethylpyrazole phosphate (DMPP) - a new nitrification inhibitor for agriculture and horticulture. Biology and Fertility of Soils 34, 79–84.
Zhou, Z., Takaya, N., Sakairi, M.A.C., Shoun, H., 2001. Oxygen requirement for denitrification by the fungus Fusarium oxysporum. Archives of Microbiology 175, 19–25.
Zhu, K., Bruun, S., Jensen, L.S., 2016. Nitrogen transformations in and N_2O emissions from soil amended with manure solids and nitrification inhibitor. European Journal of Soil Science 67, 792–803.
Zhu, K., Bruun, S., Larsen, M., Glud, R.N., Jensen, L.S., 2014. Spatial oxygen distribution and nitrous oxide emissions from soil after manure application: a novel approach using planar optodes. Journal of Environmental Quality 43, 1809–1812.
Zhu, K., Bruun, S., Larsen, M., Glud, R.N., Jensen, L.S., 2015. Heterogeneity of O_2 dynamics in soil amended with animal manure and implications for greenhouse gas emissions. Soil Biology and Biochemistry 84, 96–106.

Paper VIII

Nitrification inhibitor's effect on mitigating N_2O emissions was weakened by urease inhibitor in calcareous soils.

Zhao, Z., **Wu, D.,** Bol, R., Shi, Y., Guo, Y., Meng, F., & Wu, W. 2017.

Atmospheric Environment 166,142-150

Atmospheric Environment 166 (2017) 142–150

Contents lists available at ScienceDirect

Atmospheric Environment

journal homepage: www.elsevier.com/locate/atmosenv

Nitrification inhibitor's effect on mitigating N_2O emissions was weakened by urease inhibitor in calcareous soils

Zichao Zhao [a], Di Wu [b], Roland Bol [b], Yuefeng Shi [a], Yanbin Guo [a], Fanqiao Meng [a, *], Wenliang Wu [a]

[a] Beijing Key Laboratory of Farmland Soil Pollution Prevention and Remediation, College of Resources and Environmental Sciences, China Agricultural University, Beijing 100193, China
[b] Institute of Bio- and Geosciences, Agrosphere (IBG–3), Research Centre Jülich, Jülich 52425, Germany

HIGHLIGHTS

- Inter-annual variation in N_2O emission was mainly due to differences of water input.
- Effect of DMPP on N_2O reduction was weakened by NBPT in calcareous soils.
- DMPP plus NBPT achieved higher crop yield and highest N efficiencies.

GRAPHICAL ABSTRACT

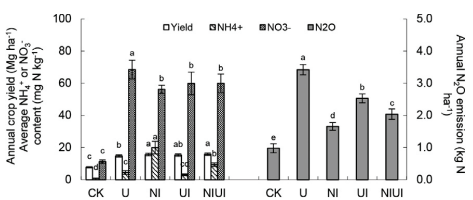

ARTICLE INFO

Article history:
Received 24 January 2017
Received in revised form
14 July 2017
Accepted 17 July 2017
Available online 18 July 2017

Keywords:
Nitrification inhibitor
Urease inhibitor
N_2O
Nitrogen use efficiency
Wheat–maize cropping system

ABSTRACT

The application of nitrification or urease inhibitors together with nitrogen (N) fertilizer has been proposed to reduce N losses, including nitrous oxide (N_2O) emissions, from agricultural soils. We measured N_2O fluxes, crop yield and plant N content over 3 years (2012–2015) to evaluate the long-term effects of nitrification and/or urease inhibitors on N_2O emissions, crop production and N use efficiency (NUE) in an intensively farmed wheat–maize system in northern China. The experiment consisted of the following five treatments: 1) CK, no N fertilizer; 2) U, urea; 3) NI, urea with 3,4-dimethylpyrazole phosphate (DMPP); 4) UI, urea with *N*-(*n*-butyl) thiophosphoric triamide (NBPT); and 5) NIUI, urea with combined DMPP and NBPT. Compared with the U treatment, the NI, NIUI and UI treatments mitigated cumulative N_2O emissions by 55%, 40% and 21% in the maize season, respectively, and 47%, 40% and 33% in the wheat season, respectively. The annual direct emission factors of N_2O for the U, NI, UI and NIUI treatments were 0.4%, 0.1%, 0.3% and 0.2%, respectively. The NIUI, NI and UI treatments increased the annual crop yield (7%, 6% and 4%) and the NUE (15%, 10% and 7%) relative to the U treatment. The NI treatment showed the best effect on mitigating N_2O emissions, but its efficacy was reduced when applied together with UI. This indicates that more studies are required focusing on the performances and mechanisms of these two inhibitors in alkaline and low organic carbon soils.

1. Introduction

Nitrous oxide (N_2O) is a potent and long-lived greenhouse gas with 298 times the global warming potential of carbon dioxide (CO_2) over a period of 100 years (IPCC, 2013). Agricultural soils are the major source of N_2O, accounting for 61% of the global N_2O emissions (IPCC, 2013). The North China Plain (NCP) is one of the most important agricultural regions in China, contributing 43.4% of the total national wheat–maize production (Shi et al., 2013). In

* Corresponding author.
E-mail address: mengfq@cau.edu.cn (F. Meng).

http://dx.doi.org/10.1016/j.atmosenv.2017.07.034
1352-2310/

this region, agricultural activities have relied on an increasing rate of nitrogen (N) fertilizer to sustain the increasing productivity over the past 30 years (Gu et al., 2015). Nitrogen is a highly active element that, if not managed well, can be lost in large amounts via pathways such as N_2O emissions, NO_3^- leaching and NH_3 volatilization, leading to a low N use efficiency (NUE) and subsequent environmental pollution in the NCP (Ju et al., 2009; Zaman et al., 2009; Cui et al., 2011). Hence, farmers in the region face the dual challenges of reducing N losses and increasing NUE under the prerequisite of maintaining high crop yield (Liu et al., 2013).

Application of nitrification and urease inhibitors has been suggested as promising farming practice to mitigate N losses including N_2O emissions (Zaman et al., 2013; Cahalan et al., 2015; Qiao et al., 2015). Nitrification inhibitors (NI) such as dicyandiamide (DCD) and 3,4-dimethylpyrazole phosphate (DMPP) are compounds that can prevent the conversion of NH_4^+ into mobile nitrate ions (NO_2^- and NO_3^-) by inhibiting the activity of ammonia-oxidizing bacteria in the soil, e.g. of the genus *Nitrosomonas* (Zerulla et al., 2001). The use of NI has been shown to reduce both N_2O emissions and NO_3^- leaching (Cui et al., 2011; Hill et al., 2014). Recent meta-analyses have found that NI could reduce N_2O losses by 39%–48% and increase crop yields by 6%–13% (Qiao et al., 2015; Gilsanz et al., 2016). Urease inhibitors (UI), such as *N*-(*n*-butyl) thiophosphoric triamide (NBPT), can be quickly converted into more effective oxon analogs following application to soil, after which a tridentate ligand is formed with the urease enzyme, which slows urea hydrolysis (Singh et al., 2013) and reduces N losses in the form of NH_3. In addition, NBPT can also reduce N_2O emissions and increase crop yields (Ding et al., 2010; Dawar et al., 2011). The application of DMPP or NBPT with urea was found to significantly reduce N_2O emissions by 37%–59% in the maize and wheat season (Ding et al., 2010; Hu et al., 2013; Liu et al., 2013; Ding et al., 2015). However, previous studies were mostly conducted in acidic or neutral soils using the NI of DCD (Qiao et al., 2015). As a result, these studies often exhibited different effects of NI, UI, or NI combined with UI on N losses, N uptake and crop production. For instance, NBPT or DMPP did not significantly increase crop yields (Ding et al., 2010; Sanz-Cobena et al., 2012; Hu et al., 2013; Liu et al., 2013; De Antoni Migliorati et al., 2014; Scheer et al., 2014; Ding et al., 2015), while NBPT alone was more effective at reducing total gaseous N emissions than NBPT combined with DMPP during cattle urine fertilization (Pereira et al., 2013).

Because the effectiveness of inhibitors is dependent on edaphic and climate conditions and farming measures (Abalos et al., 2014), field studies which lasted only 1 or 2 seasons cannot sufficiently address temporal variations across different farming years. Correspondingly, research conducted to date has not provided robust conclusions. Hence, in this study, we initiated a field experiment in an intensively farmed wheat–maize system on calcareous soils in the NCP to investigate the effects of NBPT, DMPP and NBPT + DMPP application on crop yields, N efficiencies and N_2O emissions. Specifically, we conducted year-round measurements of N_2O fluxes, crop yield and N uptake, soil mineral N content, and the main environmental factors over 3 years. The primary objectives of our study were (1) to evaluate the effects of DMPP, NBPT and DMPP plus NBPT on N efficiencies, N_2O emissions and crop production, (2) to examine the temporal variation in natural factors, soil moisture and mineral N contents and their relationship with N_2O mitigation, and (3) to identify good farming practices using inhibitors to maintain high crop yield and low N losses in northern China.

2. Materials and methods

2.1. Experimental setup and field management

A field experiment was established in June 2012 at the Agro-ecosystem Experimental Station of China Agricultural University, Huantai County, Shandong Province (36.57°N, 117.59°E). The region has a typical temperate monsoon climate, with a 30-year (1982–2012) annual mean air temperature and a mean precipitation of 12.5 °C and 542.8 mm, respectively. The soil in the region is aquic inceptisol (a calcareous, fluvo-aquic clay loam) with bulk density (BD) of 1.40 g cm^{-3}, pH of 7.8, soil organic matter of 17.3 g kg^{-1} and total N content of 1.1 g kg^{-1}. The soil consists of 38% clay, 32% silt and 30% sand (USDA). Prior to the experiment, fields were cropped with winter wheat and summer maize. The experiment consisted of five treatments: CK (no fertilizer N input), U (urea), NI (urea with DMPP), UI (urea with NBPT), and NIUI (urea with DMPP plus NBPT). Each treatment had four replicated plots (8×7.5 m^2). In the middle of June, wheat straw was mechanically chopped and ploughed into the field after harvest and maize was seeded in rows using a maize no-tillage planter. During the early October maize harvest, maize straw was also mechanically chopped and incorporated into the field. Wheat was sown using a wheat no-tillage planter. Inhibitor(s) and fertilizers during basal fertilization or topdressing were thoroughly mixed and then broadcasted onto the soil surface. Irrigation was conducted immediately after fertilization. Urea was applied at the local conventional fertilization level, i.e., 300 kg N ha^{-1} $season^{-1}$ (50% as basal fertilization and 50% as topdressing), for both the maize season and the wheat season. DMPP and NBPT were applied at a rate of 1% and 0.4% of applied fertilizer N, respectively. Phosphorus fertilizer (as triple superphosphate) was applied at a rate of 120 kg P_2O_5 ha^{-1} for wheat, while potassium fertilizer (as potassium sulfate) was applied at 100 kg K_2O ha^{-1} for maize. The application of herbicides and insecticides was similar to that of local conventional farming practice. The irrigation was implemented according to crop growth and soil moisture. Briefly, crops were irrigated four times (total 300 mm) during the three wheat seasons (2012–2013, 2013–2014 and 2014–2015), and twice (150 mm), once (75mm) and three times (225 mm) in the first (2012), second (2013) and third (2014) maize season, respectively.

2.2. N_2O emission measurements

We measured N_2O fluxes in each plot of all treatments from 16 June 2012 to 5 June 2015 using an opaque static chamber system as described by Shi et al. (2013). Briefly, one static chamber was installed in each replicated field plot and five gas samples from the chamber headspace were obtained with a 60-mL polypropylene syringe at 0, 8, 16, 24 and 32 min after chamber closure. Gas was sampled between 9:00 and 11:00 a.m. local time every day for a continuous duration of 7 days following fertilization and/or irrigation events, and twice a week during other periods of crop growth, and once per week during the winter season (Dec 15 to March 1 of the following year). The N_2O flux measurements were performed 80–100 times per year. All gas samples were analyzed on an Agilent 7820A gas chromatograph (Agilent Company, Shanghai, China) within 24 h of sampling. The N_2O fluxes and cumulative emissions were calculated using the linear model and linear interpolation method (Hu et al., 2013; Tan et al., 2017).

2.3. Auxiliary measurements

In addition to N_2O flux measurements, we also measured wheat

and maize yield, air temperature, precipitation, soil temperature (0–5 cm), soil moisture (0–10 cm), soil NO_3^--N and NH_4^+-N content (0–10 cm). Daily air temperature and precipitation were continuously measured by a meteorological station (AR5, Xinyuanshijie technology Co. Ltd, Beijing, China) located 100 m away from experimental plots. Soil temperature was determined with a digital thermometer (JM 624, Jinming Instrument Co. Ltd, Tianjin, China) at the time of gas sampling. At the time of gas sample collection, three fresh soil samples (0–10 cm) in each field plot were collected using a 2-cm diameter soil probe. Soil samples were then thoroughly mixed, homogenized and sieved (<2 mm), to measure soil moisture, soil NO_3^--N and soil NH_4^+-N content. Soil moisture was converted into water-filled pore space (WFPS; %) as follows:

$$\text{WFPS} = \text{water content (\%, w/w)} \times \text{BD/total soil porosity (\%)} \times 100\% \quad (1)$$

where water content was measured gravimetrically by drying the subsamples at 105 °C for 24 h, total soil porosity = 1 − (BD/2.65), with 2.65 g cm^{-3} as the mineral particle density of the soil, and BD is the soil bulk density (g cm^{-3}). The soil NO_3^--N and NH_4^+-N contents were measured using an Auto Analyzer 3 (BRAN + LUEBBE Co. Ltd., Hamburg, Germany) after extraction with 1 M KCl. The extracts for measuring soil NO_3^--N and NH_4^+-N contents were frozen and stored at −18 °C before analysis (Shi et al., 2013). At crop harvest, four sub-plots (7.5 m^2) from each treatment were harvested to measure the grain and straw yield of the crops. Total N content in aboveground biomass was analyzed using an elemental CN analyzer (Thermo Flash EA 1112 Flash, 2000; USA).

2.4. Calculation of the emission factor (EF) and NUE

The direct N_2O EF (%) of fertilizer N applied was calculated as follows (Cui et al., 2012):

$$EF = (E_F - E_0)/R_F \times 100\% \quad (2)$$

where E_F and E_0 are the annual or seasonal N_2O emissions (kg N_2O-N ha^{-1}) from the *N*-fertilized and CK plots, respectively; and R_F represents the annual or seasonal application rate of fertilizer N (kg N ha^{-1}).

The NUE (%) was calculated as follows (Hartmann et al., 2015):

$$NUE = (U_F - U_0)/R_F \times 100\% \quad (3)$$

where U_F and U_0 denote the annual or seasonal aboveground N uptake measured at harvest in the *N*-fertilized and CK plots (kg N ha^{-1}), respectively, and R_F is the annual or seasonal application rate of fertilizer N (kg N ha^{-1}).

2.5. Statistical analyses

The software SPSS 22.0 (IBM Corp., Armonk, NY, USA) was used for statistical analysis. Statistically significant differences in N_2O emissions, crop yield and NUE from all treatments were identified by one-way analysis of variance at a 0.05 level of probability followed by Duncan's test. The effects of the main driving factors on N_2O fluxes were investigated by analysis of pairwise correlations.

3. Results

3.1. Precipitation, temperature, soil moisture and inorganic N

The precipitation was quite high (563 mm) in the second maize season, but relatively low in the first (230 mm) and third (299 mm) maize seasons (Fig. 1a). The precipitation was 212, 125 and 147 mm during the first, second and third wheat seasons, respectively. Soil temperature varied from −1.6 to 29.7 °C over the 3 experimental

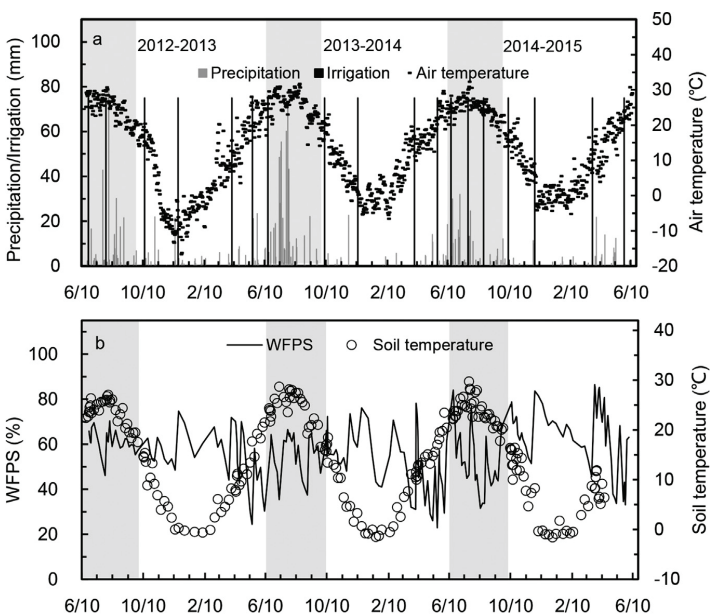

Fig. 1. Temporal variations of (a) precipitation, irrigation and air temperature and (b) soil temperature and water-filled pore space (WFPS) at the time of N2O sampling over the experimental period. Soil temperature and WFPS values are the means of four plot replicates. Grey background represents the maize season.

years (Fig. 1b). The average soil temperature was 10.1, 11.0 and 10.1 °C in the three wheat seasons and ranged from 24.6 to 24.9 °C during the maize seasons. Variations in air temperature were similar to those in soil temperature (Fig. 1a). The soil WFPS ranged from 23% to 86% (Fig. 1b), with the highest values appearing after irrigation or heavy rainfall events. For the 3 experimental years, the average WFPS during 7 and 30 days after N fertilization and during the entire maize season was 66%, 57% and 57%, respectively, while it was 70%, 63% and 58% for the wheat season, respectively (Table 1). No significant differences were observed in WFPS and temperature among the five treatments.

During the three examined durations (7 and 30 days after N fertilization and the entire crop season), inhibitors exerted similar effects on soil mineral N (Table 1): NO_3^--N and NH_4^+-N contents of *N*-fertilized soils increased significantly after N fertilization relative to the CK treatment (Fig. 2a and b; $P < 0.05$). During the maize season, the average soil NO_3^--N contents of all fertilization treatments were similar (Table 1); NI significantly increased soil NH_4^+-N compared with all other treatments ($P < 0.05$). For the wheat season, three inhibitor treatments (NI, UI and NIUI) significantly ($P < 0.05$) decreased soil NO_3^--N contents relative to U treatment at similar magnitudes (13%–29%). Soil NH_4^+-N contents were significantly ($P < 0.05$) decreased by UI (78% of U) and increased by NI (313% of U) and NIUI (133% of U), respectively. Soil NH_4^+-N and NO_3^--N contents were always higher in the wheat season than in the maize season (Table 1 and Fig. 2a and b). As the monitoring durations increased (i.e., from 7 days to 30 days after N fertilization and to the entire crop season), both the NH_4^+-N and NO_3^--N contents decreased (except the soil NH_4^+-N in the maize season, which was always within the range of 0.7–5.4 mg N kg^{-1}).

3.2. N_2O emissions and EF

Over the 3-year N_2O measurement period, the highest N_2O fluxes (150–1160 μg N m^{-2} h^{-1}) appeared after basal and topdressing N fertilization, while lower levels (<80 μg N m^{-2} h^{-1}) were observed on most other sampling dates (Fig. 2c). However, high N_2O fluxes were not observed after the N fertilizer topdressing (beginning of April) in the first and second wheat season. Most of the high soil NO_3^--N and NH_4^+-N contents in the wheat season did not cause high N_2O fluxes. The N_2O fluxes of CK, U, NI, UI and NIUI treatments ranged from −36 to 207 μg N m^{-2} h^{-1}, −3–1168 μg N m^{-2} h^{-1}, −3–392 μg N m^{-2} h^{-1}, −4–727 μg N m^{-2} h^{-1}, and −9 to 604 μg N m^{-2} h^{-1}, respectively, with means of 15, 81, 32, 58 and 43 μg N m^{-2} h^{-1}, respectively.

The cumulative N_2O emissions during 7 and 30 days after N fertilization accounted for 30%–56% and 71%–83% of the total maize seasonal N_2O emissions, respectively, and the corresponding values were 19%–32% and 45%–59% for the wheat season (Table 2). For CK, these proportions were < 20% and 45%–58% 7 days and 30 days after N fertilization, respectively. These findings indicate that about 80% and 50% of N_2O emissions occurred within only half of the maize season (i.e., (30 days after N basal fertilization + 30 days after N topdressing fertilization days)/123-day growth period) and within a quarter of the wheat season (i.e., (30 days after N basal fertilization + 30 days after N topdressing fertilization days)/243 days), respectively.

The cumulative seasonal N_2O emissions in the maize and wheat seasons decreased in the following sequence: U > UI > NIUI > NI > CK (Table 3). The N_2O emissions were similar among the three maize seasons, but higher in the second wheat season than in the first and third, particularly for the CK and NI treatments ($P < 0.05$). When compared with the U treatment, the *N*-fertilized treatments of NI, NIUI and UI mitigated the

Table 1
Average WFPS, soil mineral N contents and N_2O fluxes during 7 and 30 days after N fertilization and during the entire maize and wheat season. All data shown are the means of the 3-year period from 2012 to 2015.

Period	Treatment	Maize season				Wheat season			
		WFPS (%)	NO_3^--N (mg N kg^{-1})	NH_4^+-N (mg N kg^{-1})	N_2O (μg N m^{-2} h^{-1})	WFPS (%)	NO_3^--N (mg N kg^{-1})	NH_4^+-N (mg N kg^{-1})	N_2O (μg N m^{-2} h^{-1})
7 days after N fertilization	CK	66.9 ± 2.3a	28.2 ± 4.4b (45%)	1.1 ± 0.1b (71%)	28.4 ± 0.2e (9%)	69.5 ± 1.8a	9.2 ± 0.8d (8%)	3.1 ± 0.1c (14%)	29.7 ± 4.5d (21%)
	U	66.7 ± 2.6a	63.1 ± 3.6a (100%)	1.5 ± 0.1b (100%)	304 ± 13a (100%)	70.4 ± 2.4a	109 ± 4.6a (100%)	22.5 ± 1.7b (100%)	141 ± 11a (100%)
	NI	65.8 ± 2.3a	53.2 ± 2.6a (84%)	5.4 ± 1.1a (358%)	78.7 ± 4.5d (26%)	69.6 ± 2.3a	78.6 ± 2.7c (72%)	70.5 ± 8.1a (313%)	58.3 ± 3.9c (41%)
	UI	64.2 ± 2.8a	56.5 ± 2.6a (90%)	1.7 ± 0.1b (110%)	210 ± 6.0b (69%)	69.4 ± 1.6a	85.1 ± 8.0bc (78%)	17.5 ± 3.6b (78%)	70.3 ± 5.0b (50%)
	NIUI	66.2 ± 2.1a	58.3 ± 1.0a (92%)	2.6 ± 0.5b (173%)	148 ± 29c (49%)	70.2 ± 2.2a	95.0 ± 3.5ab (87%)	30 ± 2.5b (133%)	50.3 ± 1.6c (36%)
30 days after N fertilization	CK	55.8 ± 2.7a	20.5 ± 2.4b (39%)	0.8 ± 0.1c (67%)	25.1 ± 0.3e (14%)	62.7 ± 2.3a	8.0 ± 0.5c (8%)	1.8 ± 0.1d (13%)	20.1 ± 2.7d (21%)
	U	57.5 ± 2.2a	52.1 ± 2.2a (100%)	1.2 ± 0.1bc (100%)	186 ± 8.3a (100%)	63.2 ± 2.1a	97.5 ± 5.7a (100%)	13.7 ± 1.8c (100%)	95.8 ± 7.5a (100%)
	NI	56.5 ± 2.1a	47.1 ± 3.0a (90%)	3.1 ± 0.5a (252%)	58.4 ± 3.1d (31%)	63.1 ± 2.5a	77.5 ± 1.9b (79%)	47.1 ± 3.9a (345%)	41.1 ± 3.2c (43%)
	UI	55.1 ± 2.9a	48.8 ± 1.8a (94%)	1.4 ± 0.1bc (113%)	131 ± 3.0b (71%)	62.0 ± 2.4a	82.8 ± 5.5b (85%)	9.2 ± 1.1c (67%)	56.2 ± 4.3b (59%)
	NIUI	57.2 ± 2.1a	49.8 ± 0.9a (96%)	1.8 ± 0.2b (143%)	95.7 ± 1.3c (52%)	63.8 ± 2.8a	84.8 ± 3.8b (87%)	21.4±2b (157%)	36.6 ± 1.3c (38%)
Entire season	CK	57.1 ± 2.1a	16.8 ± 1.5b (38%)	0.7 ± 0.1c (61%)	25.5 ± 0.4e (17%)	58.3 ± 2.8a	8.0 ± 0.3c (10%)	1.1 ± 0.1d (15%)	13.3 ± 1.0d (22%)
	U	57.7 ± 2.2a	44.5 ± 1.9a (100%)	1.1 ± 0.1bc (100%)	153 ± 9.3a (100%)	58.0 ± 2.1a	84.2 ± 3.7a (100%)	7.6 ± 1.1c (100%)	60.6 ± 4.5a (100%)
	NI	57.2 ± 2.1a	40.8 ± 2.3a (92%)	2.4 ± 0.4a (224%)	52.1 ± 3.0d (34%)	58.6 ± 2.2a	66.7 ± 0.6b (79%)	34.9 ± 3.4a (458%)	27.8 ± 2.0c (46%)
	UI	56.4 ± 2.1a	41.9 ± 1.7a (94%)	1.2 ± 0.1bc (109%)	111 ± 3.8b (73%)	57.9 ± 2.2a	72.1 ± 5.0b (86%)	4.9 ± 0.5cd (64%)	38.3 ± 3.9b (63%)
	NIUI	57.3 ± 2.0a	42.7 ± 1.1a (96%)	1.5 ± 0.2b (136%)	81.2 ± 11.9c (53%)	58.7 ± 2.1a	71.4 ± 4.3b (85%)	17.3 ± 1.0b (227%)	27.1 ± 0.8c (45%)

Mean ± standard error ($n = 4$). Different letters indicate significant differences between treatments at $P < 0.05$. Data within parentheses are the proportion of NH_4^+-N, NO_3^--N contents and N_2O fluxes of all treatments relative to U.

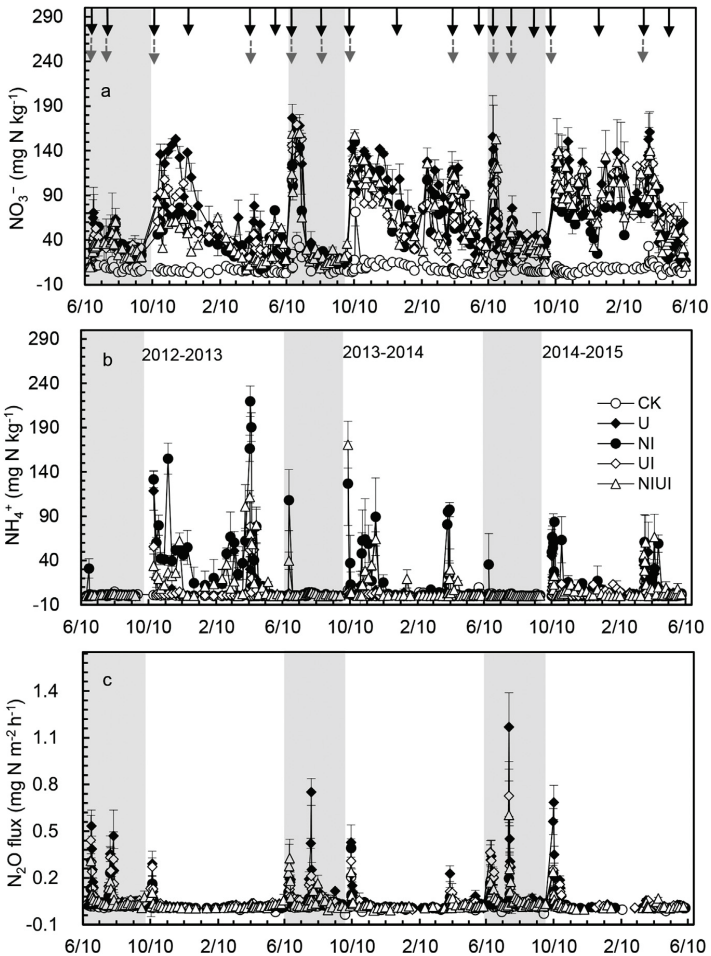

Fig. 2. (a) Soil NO3− content and (b) soil NH4+ content at the time of N2O sampling, and (c) soil N2O flux over the experimental period. Data are the means ± the standard error (n = 4). Solid and dashed line arrows indicate the timing of irrigation and fertilizer application, respectively. Grey background represents the maize season.

cumulative N_2O emissions by 55%, 40% and 21% in the maize season, respectively, and 47%, 40% and 33% in the wheat season, respectively. Therefore, NI always had the lowest EF (0.11%) in the maize season, significantly lower ($P < 0.05$) than that of NIUI (0.20%), UI (0.33%) and U (0.47%). In the wheat season, the EF of inhibitor treatments (NI, NIUI and UI) did not differ significantly (0.11%–0.23%; $P > 0.05$), but they were significantly lower than that of U (0.35%, $P < 0.05$) (Table 3).

Table 2
Average cumulative N_2O emissions (kg N ha^{-1}) during 7 and 30 days after N fertilization and during the entire crop season. All data shown are the means of the 3-year period from 2012 to 2015.

Treatment	Maize season			Wheat season		
	7 days after N fertilization	30 days after N fertilization	Entire season	7 days after N fertilization	30 days after N fertilization	Entire season
CK	0.09 ± 0.01e (15%)	0.35 ± 0.03e (58%)	0.60 ± 0.04e (100%)	0.07 ± 0.01d (18%)	0.17 ± 0.02d (45%)	0.38 ± 0.04d (100%)
U	1.12 ± 0.06a (56%)	1.66 ± 0.07a (83%)	2.01 ± 0.06a (100%)	0.45 ± 0.05a (32%)	0.82 ± 0.10a (58%)	1.41 ± 0.09a (100%)
NI	0.27 ± 0.01d (30%)	0.65 ± 0.04d (71%)	0.91 ± 0.04d (100%)	0.17 ± 0.01c (23%)	0.35 ± 0.02c (47%)	0.75 ± 0.04c (100%)
UI	0.75 ± 0.07b (47%)	1.25 ± 0.06b (79%)	1.59 ± 0.05b (100%)	0.25 ± 0.02b (27%)	0.55 ± 0.04b (59%)	0.94 ± 0.06b (100%)
NIUI	0.47 ± 0.06c (39%)	0.95 ± 0.07c (79%)	1.20 ± 0.07c (100%)	0.16 ± 0.01c (19%)	0.38 ± 0.03c (45%)	0.84 ± 0.04bc (100%)

Mean ± standard error ($n = 4$). Different letters indicate significant differences between treatments at $P < 0.05$. Data within parentheses are the proportion of N_2O emissions of all treatments relative to U.

Table 3
Seasonal and annual N_2O emissions (kg N ha^{-1}), emission factors (EF, %), crop yield (t ha^{-1}) and NUE (%) over the experimental period.

	Treatment	2012–2013			2013–2014			2014–2015		
		Maize	Wheat	Annual	Maize	Wheat	Annual	Maize	Wheat	Annual
N_2O	CK	0.55 ± 0.06dA	0.34 ± 0.02cB	0.89 ± 0.07eB	0.69 ± 0.07eA	0.54 ± 0.05cA	1.23 ± 0.10eA	0.54 ± 0.03dA	0.28 ± 0.02cB	0.82 ± 0.04eB
	U	2.15 ± 0.13aA	1.19 ± 0.09aA	3.34 ± 0.11aA	2.00 ± 0.08aA	1.53 ± 0.08aA	3.53 ± 0.10aA	1.86 ± 0.09aA	1.51 ± 0.23aA	3.37 ± 0.19aA
	NI	0.88 ± 0.10cA	0.67 ± 0.03bB	1.55 ± 0.09dB	0.98 ± 0.06dA	0.88 ± 0.09bA	1.86 ± 0.10dA	0.87 ± 0.04cA	0.68 ± 0.06bB	1.55 ± 0.05dB
	UI	1.60 ± 0.09bA	0.81 ± 0.09bA	2.41 ± 0.11bA	1.61 ± 0.06bA	1.06 ± 0.14bA	2.67 ± 0.08bA	1.57 ± 0.11aA	0.95 ± 0.04bA	2.52 ± 0.13bA
	NIUI	1.08 ± 0.12cA	0.80 ± 0.08bA	1.88 ± 0.12cA	1.27 ± 0.07cA	0.93 ± 0.09bA	2.20 ± 0.14cA	1.23 ± 0.16bA	0.81 ± 0.03bA	2.04 ± 0.14cA
EF	U	0.53 ± 0.04aA	0.28 ± 0.03aA	0.41 ± 0.02aA	0.44 ± 0.03aA	0.33 ± 0.03aA	0.38 ± 0.02aA	0.44 ± 0.03aA	0.41 ± 0.08aA	0.43 ± 0.03aA
	NI	0.11 ± 0.03cA	0.11 ± 0.01bA	0.11 ± 0.02cA	0.10 ± 0.02dA	0.12 ± 0.03bA	0.11 ± 0.02dA	0.11 ± 0.01cA	0.14 ± 0.02bA	0.12 ± 0.01dA
	UI	0.35 ± 0.03bA	0.16 ± 0.03bA	0.25 ± 0.02bA	0.31 ± 0.02bA	0.18 ± 0.05bA	0.24 ± 0.01bA	0.34 ± 0.04abA	0.23 ± 0.01bA	0.28 ± 0.02bA
	NIUI	0.17 ± 0.04cA	0.15 ± 0.03bA	0.16 ± 0.02cA	0.20 ± 0.02cA	0.13 ± 0.03bA	0.16 ± 0.02cA	0.23 ± 0.05bA	0.18 ± 0.01bA	0.20 ± 0.02cA
Crop yield	CK	6.1 ± 0.2cA	2.4 ± 0.1bA	8.5 ± 0.2cA	4.2 ± 0.2bB	2.3 ± 0.1cA	6.5 ± 0.2cB	6.0 ± 0.2cA	2.3 ± 0.2bA	8.3 ± 0.2cA
	U	9.3 ± 0.2bA	6.3 ± 0.2aAB	15.6 ± 0.2bA	8.5 ± 0.2aB	5.8 ± 0.1bB	14.3 ± 0.2bB	8.0 ± 0.1bB	6.5 ± 0.1aA	14.5 ± 0.2bB
	NI	9.7 ± 0.1abA	6.4 ± 0.1aA	16.1 ± 0.1abA	9.0 ± 0.4aA	6.7 ± 0.2aA	15.7 ± 0.4aA	8.8 ± 0.3aA	6.6 ± 0.1aA	15.4 ± 0.1aA
	UI	9.4 ± 0.2bA	6.2 ± 0.2aA	15.6 ± 0.4bA	8.9 ± 0.2aAB	6.7 ± 0.1aA	15.6 ± 0.3aA	8.5 ± 0.2abB	6.5 ± 0.3aA	15.0 ± 0.3abA
	NIUI	10 ± 0.2aA	6.4 ± 0.2aA	16.4 ± 0.4aA	9.3 ± 0.2aA	6.7 ± 0.1aA	16.0 ± 0.2aAB	9.0 ± 0.2aA	6.2 ± 0.1aA	15.2 ± 0.1aB
NUE	U	31.1 ± 1.3bA	33.2 ± 1.2aAB	32.2 ± 0.8bA	33.0 ± 1.5aA	32.1 ± 1.0bB	32.6 ± 0.6bA	26.4 ± 1.0bB	36.2 ± 0.7aA	31.3 ± 0.7bA
	NI	34.4 ± 0.8abA	34.3 ± 0.7aA	34.3 ± 0.3abB	37.1 ± 2.9aA	38.0 ± 1.7aA	37.5 ± 1.6aA	32.0 ± 1.8aA	36.4 ± 1.0aA	34.2 ± 0.4aB
	UI	32.0 ± 1.5bAB	32.9 ± 1.6aB	32.4 ± 1.5bB	36.3 ± 1.6aA	38.3 ± 0.9aA	37.3 ± 1.2aA	29.8 ± 1.3abB	37.3 ± 1.9aAB	33.5 ± 1.3abAB
	NIUI	37.5 ± 1.7aA	34.7 ± 1.3aB	35.9 ± 1.4aAB	39.4 ± 1.6aA	38.2 ± 0.8aA	38.8 ± 0.7aA	33.9 ± 1.6aA	36.7 ± 1.1aAB	35.3 ± 0.5aB

Mean ± standard error ($n = 4$). Different lowercase and uppercase letters indicate significant differences between treatments and years at $P < 0.05$, respectively.

3.3. Crop yield and NUE

Maize yields of NIUI, NI and UI were significantly higher (4.3%–12.5%, $P < 0.05$) than those of U and CK (except in the second maize season), and NIUI and NI always had the highest grain yields, followed by UI (Table 3). Wheat yields of NI, UI and NIUI were similar to those of U (except that they were higher than U in the second year; Table 3), and were significantly higher ($P < 0.05$) than that of CK. For NIUI and NI, the maize had a similar NUE to wheat, while for U and UI, maize had a significantly lower ($P < 0.05$) NUE than wheat (except the second experimental year).

The first and second experimental year had the highest maize and wheat yield, respectively, among the three experimental years. Mainly because of the differences in crop yields, the 3-year averaged NUE varied between treatments in the following sequence: NIUI (maize: 36.9%; wheat: 36.5%) ≈ NI (maize: 34.5%; wheat: 36.2%) > UI (maize: 32.8%; wheat: 36.2%) > U (maize: 30.2%; wheat: 33.8%). This indicates that, compared with U treatment, the NIUI, NI and UI treatments significantly ($P < 0.05$) increased the NUE by 22.2%, 14.3% and 8.3% for the maize season, respectively, and by 8.0%, 7.1% and 7.1% for the wheat season, respectively, but there was no significant difference among the three inhibitor treatments. For the three inhibitor treatments (NIUI, UI and NI), the second year had a significantly ($P < 0.05$) higher NUE than the first and third years.

3.4. Effects of soil temperature, moisture and soil mineral N content on N_2O emissions

During the entire maize and wheat season, N_2O flux was positively correlated ($P < 0.05$) with soil temperature and WFPS (for WFPS only in the maize season) for all treatments and positively correlated with soil NO_3^--N and NH_4^+-N contents only in the U treatment (Table 4). However, this positive correlation diminished as the duration (after fertilization) decreased: during the 30 days after N fertilization, only positive correlation of N_2O with soil NO_3^--N occurred in the U treatment (Table 4; Fig. S1). During the first 7 days after fertilization, there was no significant correlation between N_2O flux and temperature and WFPS, and the correlations between N_2O fluxes and soil mineral N contents (particularly NH_4^+) were not statistically significant and tended to become negative. The WFPS (controlled by precipitation and irrigation) tended to be positively correlated with the soil mineral N contents, and this relationship occurred during the entire crop season and 30 days after N fertilization (Table S1). Few significant correlations between soil NH_4^+-N and NO_3^--N were exhibited for fertilization treatments during the periods of 7 and 30 days after N fertilization and during the entire crop season.

4. Discussion

4.1. Effect of inhibitor(s) on N_2O emissions

Emissions of N_2O are derived from nitrification, nitrifier denitrification and denitrification in farmland soils (Weiske et al., 2001; Venterea et al., 2012; Zhu et al., 2013). Our experiment was conducted in an area with a sub-arid climate, low soil organic carbon (1.0%–1.5%) and an alkaline soil (pH 7.5–8.5), where nitrification and/or nitrifier denitrification are reported to be mainly responsible for N_2O production (Ju et al., 2011; Zhu et al., 2013; Huang et al., 2014). Even for the period of peak N_2O fluxes (7 days after N fertilization and irrigation) when soil water content was high, the average WFPS values were less than 70% (maize season: 64%–67%; wheat season: 69%–70%), under which conditions it is difficult for NO_3^- to be reduced, and rather NH_4^+ is oxidized to NO_2^- or NO_3^- (Rütting et al., 2011; Huang et al., 2014). These moisture levels were optimum in agricultural soils for nitrification and nitrifier denitrification processes (Pihlatie et al., 2004; Menéndez et al., 2012; Huang et al., 2014), which occur prior to denitrifier denitrification (from NO_3^- to NO_2^- and/or $NO/N_2O/N_2$) (Baggs, 2008; Venterea et al., 2012).

Inhibitors exhibited a significant mitigation effect on N_2O emissions: NI > NIUI > UI; this is consistent with the fact that conditions favored nitrification and nitrifier denitrifications as the likely pathways to N_2O production. The lower effect of UI than NI is acceptable because UI (NBPT) could only reduce the quantity of NH_4^+ (Singh et al., 2013; Hagenkamp-Korth et al., 2015), the initial substrate for N_2O generation, but it did not inhibit the oxidation of NH_4^+. The high clay content in the study soils (38%) may also reduce the mitigation effect of NBPT on N_2O emissions (Gioacchini et al., 2002). Moreover, NBPT would immediately decompose in the first few days after fertilization under high soil temperatures (>20 °C) in the maize season (Soares et al., 2012). The incorporation of crop straw and surface N fertilization in our study also enhanced

Table 4
Correlations between N_2O flux and soil temperature, WFPS, NO_3^--N and NH_4^+-N during 7 and 30 days after N fertilization and during the entire crop season.

Period	Treatment	T		WFPS		NO_3^--N		NH_4^+-N	
		Maize	Wheat	Maize	Wheat	Maize	Wheat	Maize	Wheat
7 days after N basal fertilization	CK	−0.579	0.093	0.636	0.048	−0.248	−0.537	−0.099	0.595
	U	−0.171	0.324	0.494	0.809	0.675	−0.183	0.183	0.346
	NI	−0.363	0.292	−0.016	−0.218	−0.543	−0.445	−0.451	−0.591
	UI	−0.396	0.149	0.297	0.420	−0.580	−0.529	−0.340	−0.272
	NIUI	−0.305	0.246	0.055	0.430	−0.285	−0.450	−0.397	−0.434
7 days after N topdressing fertilization	CK	0.376	−0.228	−0.257	−0.006	0.801	0.402	0.821	0.347
	U	0.783	−0.311	−0.160	0.157	0.418	−0.091	−0.419	0.735
	NI	0.811	−0.629	−0.260	0.425	−0.433	−0.245	−0.021	0.557
	UI	0.635	0.331	0.233	−0.376	0.311	−0.407	−0.325	−0.083
	NIUI	0.859*	0.368	−0.591	−0.609	−0.085	−0.241	−0.593	−0.531
30 days after N basal fertilization	CK	0.090	0.250	0.207	0.282	−0.233	−0.248	−0.185	0.668**
	U	−0.757**	0.564**	0.651**	0.803**	0.900**	−0.183	0.320	0.346
	NI	−0.505*	0.490*	0.396	0.297	0.273	0.088	−0.451	−0.076
	UI	−0.718**	0.435	0.489*	0.376	0.366	0.073	−0.389	−0.186
	NIUI	−0.680**	0.456*	0.523*	0.523*	−0.027	0.245	−0.017	−0.021
30 days after N topdressing fertilization	CK	−0.171	−0.027	−0.414	0.266	0.105	0.105	−0.192	0.321
	U	0.446*	−0.133	0.571**	0.376	0.737**	0.576**	0.350	0.457*
	NI	0.584**	−0.034	0.454**	0.069	0.294	−0.058	0.425	0.453
	UI	0.420	0.099	0.548**	−0.055	0.617**	0.132	0.300	0.105
	NIUI	0.552*	0.447	0.335	−0.090	0.290	−0.093	0.338	0.042
Entire season	CK	0.254**	0.271**	−0.174	−0.057	−0.057	0.014	0.195*	0.176*
	U	0.340**	0.251**	0.421**	0.303*	0.227*	0.277**	0.274*	0.225*
	NI	0.310**	0.385**	0.324**	0.101	0.237*	0.193*	−0.010	0.092
	UI	0.317**	0.396**	0.384**	0.137	0.216	0.155	0.163	−0.040
	NIUI	0.237*	0.465**	0.265**	0.128	0.248*	0.124	0.027	0.021

*$P < 0.05$, **$P < 0.01$.

urease activity and increased NH_3 volatilization, leading to a reduced NBPT effect (Soares et al., 2012). Unlike the findings of other studies (Zaman et al., 2009; Ding et al., 2010), the effect of NIUI was lower than NI in the present study (Table 1). We speculate that this was because: (1) DMPP was used as the NI in our study, rather than DCD used in other studies; (2) the low pH values of DMPP (2.5–3.0, Zerulla et al., 2001) tend to promote the decomposition of NBPT, which has a 1–2 h half-life at pH 5.1 (Engel et al., 2015); and (3) there may be some other reactions when DMPP is mixed with NBPT, as Sanz-Cobena et al. (2012) suggested for DCD + NBPT. Hence, the weakened effectiveness of DMPP by NBPT (Table 2) should be further investigated, with a particular focus on microorganisms (Shi et al., 2016) and changes of DMPP under the addition of NBPT.

4.2. Implications for crop production, N_2O mitigation and N efficiency improvement

There was a significant positive relationship between N_2O flux and WFPS in our study. The WFPS was mainly driven by precipitation and/or irrigation, as described in Fig. S1. Total irrigation and precipitation during the second year was 1137 mm, greater than in the first (886 mm) and third (827 mm) years, especially for the period of the maize season in which N_2O was mainly produced. Hence, the difference in water input (total irrigation and precipitation) across crop season/year could explain the inter-annual variation. The low fertilizer *N*-induced N_2O flux peaks and low cumulative N_2O emissions following topdressing during the wheat season was due to the low soil temperature (Figs. 1b and 2c; Ding et al., 2015). More correlations occurred as the duration after N fertilization increased, indicating that soil moisture and temperature are important factors for N_2O fluxes (Menéndez et al., 2012). As the duration after fertilization increased, there were more frequent changes of WFPS and soil temperature that coincided with or significantly influenced the production and diffusion of N_2O. The average N_2O fluxes during the summer maize season were about 1.4–3 times greater than those during the winter wheat season (Table 1), which also indicates that temperature strongly affects N_2O production in agricultural soils.

In the U treatment, urea was immediately hydrolyzed after fertilization and irrigation. Subsequently, as ammonium oxidation proceeded, soil NH_4^+-N contents decreased and NO_3^--N contents increased, which coincided with the generation of N_2O (Fig. S1), leading to a positive correlation between N_2O fluxes and soil mineral N contents. Contrary to the U treatment, in the nitrification treatments (NI and NIUI), soil NO_3^--N contents were decreased by 4%–28% but were still >40 mg N kg^{-1} for the maize season and >70 mg N kg^{-1} for the wheat season. This indicates that the conversion of NH_4^+ to NO_3^- still occurred relatively rapidly. However, in the NI and NIUI treatments, soil NH_4^+ accumulated (instead of decreased in the U treatment) and the increases of soil NO_3^--N contents were slower than under the U treatment (Table 1; Fig. S1). Therefore, the correlation of N_2O fluxes vs. soil mineral N contents became weaker. Under the UI treatment, the hydrolysis of urea was blocked and soil NH_4^+-N contents were considerably lower than the U treatment or even below the detectable level (Table 1, Fig. S1), indicating that the rapid increase of soil NO_3^- and production of N_2O was also inhibited. As a result, we did not find a significant correlation between N_2O and soil mineral N in the UI treatment.

The total N_2O emitted only accounted for <1% of fertilizer N applied (Table 3), indicating that an adequate N substrate was not the limiting factor for N_2O production in the N fertilization treatments. In our study region, high NH_3 volatilization (6.9%–21.8% of N applied; Ju et al., 2009; Wang et al., 2016; Bellarby et al., 2017) and NO_3^- leaching (3.3%–22.5% of N applied; Li et al., 2007; Ju et al., 2009; Huang et al., 2015) are the dominant pathways of N losses. This highlights that the substantial losses via NH_3 volatilization and NO_3^- leaching should be assessed together in future research. Besides the N_2O emissions, NH_3 volatilization and NO_3^- leaching, a large proportion of fertilizer N was immobilized within the soil, especially in the wheat season (Chen et al., 2016). On the one hand, the immobilized fertilized N in soils (22%–40% of fertilizer N; Ju et al., 2009; Wang et al., 2016) could be used in following seasons, which is important for maintaining a high soil fertility (Wang

et al., 2016). On the other hand, our findings imply that indirect N_2O emissions (0.7–3.1, 0.2–2.0 and 0.3–2.2 kg N ha^{-1} for NI, UI and NIUI, respectively) should not be neglected (IPCC, 2006).

In our study, cumulative N_2O peak emissions after topdressing in the wheat season were very low (0.01–0.07 kg N ha^{-1}) in all *N*-fertilized treatments, only accounting for 0.2%–2.3% of the annual N_2O emissions. Considering that the wheat yield did not increase significantly, we propose that application of inhibitors with topdressing during the wheat season was not necessary. The EFs of N_2O in our study were in the range of 0.38%–0.43%. This was lower than those of most studies on upland crops in China, which ranged from 0.40% to 1.54% (Cai et al., 2013; Cui et al., 2012; Liu et al., 2014; Shepherd et al., 2015). The dual effects of DMPP on N_2O mitigation and EFs and on crop production were better than DMPP + NBPT, and NBTP alone had the smallest effect. However, throughout the three-year experimental period, NIUI had similar lowest level of EF with NI, the highest crop yields and NUE (Table 3). This emphasizes that the effect of NI on mitigating N_2O emissions was weakened by UI, and the comprehensive performances of NIUI should be further assessed in future research.

5. Conclusions

Differences in water input (irrigation and precipitation) between years is one of the main reasons for inter-annual variations in N_2O emissions from farmland soils. To the best of our knowledge, this is the first 3-year study examining the efficacy and stability of nitrification and urease inhibitors on N_2O mitigation and crop production in northern China. The cumulative N_2O peak emissions after topdressing during the wheat season were negligible (0.2%–2.3% of the annual) due to the low soil temperature. Therefore, the application of inhibitors during this period was deemed to be unnecessary. The combination of DMPP and NBPT achieved a high crop yield and the highest NUE. Moreover, DMPP exhibited a remarkable effect on the mitigation of N_2O emissions (55% and 47% for maize and wheat season, respectively) and led to a high crop yield, but its efficacy was reduced if applied together with urease inhibitor (NBPT).

Acknowledgments

We thank Zhengjiang Hu, Shuxian Chen, Rongchao Liu and Fengmei Geng for their efforts in managing the plots. This study was financially supported by the National Key Research and Development Program of China (Grant no: 2016YFD0800104).

Appendix A. Supplementary data

Supplementary data related to this article can be found at http://dx.doi.org/10.1016/j.atmosenv.2017.07.034.

References

Abalos, D., Jeffery, S., Sanz-Cobena, A., Guardia, G., Vallejo, A., 2014. Meta-analysis of the effect of urease and nitrification inhibitors on crop productivity and nitrogen use efficiency. Agric. Ecosyst. Environ. 189, 136–144.

Baggs, E.M., 2008. A review of stable isotope techniques for N_2O source partitioning in soils: recent progress, remaining challenges and future considerations. Rapid Commun. Mass Spectrom. 22, 1664–1672.

Bellarby, J., Siciliano, G., Smith, L.E.D., Xin, L., Zhou, J., Liu, K., Jie, L., Meng, F., Inman, A., Rahn, C., Surridge, B., Haygarth, P.M., 2017. Strategies for sustainable nutrient management: insights from a mixed natural and social science analysis of Chinese crop production systems. Environ. Dev. 21, 52–65.

Cahalan, E., Ernfors, M., Müller, C., Devaney, D., Laughlin, R.J., Watson, C.J., Hennessy, D., Grant, J., Khalil, M.I., McGeough, K.L., Richards, K.G., 2015. The effect of the nitrification inhibitor dicyandiamide (DCD) on nitrous oxide and methane emissions after cattle slurry application to Irish grassland. Agric. Ecosyst. Environ. 199, 339–349.

Cai, Y., Ding, W., Luo, J., 2013. Nitrous oxide emissions from Chinese maize–wheat rotation systems: a 3-year field measurement. Atmos. Environ. 65, 112–122.

Chen, Z., Wang, H., Liu, X., Liu, Y., Gao, S., Zhou, J., 2016. The Effect of N Fertilizer placement on the fate of Urea-^{15}N and yield of winter wheat in Southeast China. PloS One 11, e0153701.

Cui, F., Yan, G., Zhou, Z., Zheng, X., Deng, J., 2012. Annual emissions of nitrous oxide and nitric oxide from a wheat–maize cropping system on a silt loam calcareous soil in the North China Plain. Soil Biol. Biochem. 48, 10–19.

Cui, M., Sun, X., Hu, C., Di, H.J., Tan, Q., Zhao, C., 2011. Effective mitigation of nitrate leaching and nitrous oxide emissions in intensive vegetable production systems using a nitrification inhibitor, dicyandiamide. J. Soils Sediments 11, 722–730.

Dawar, K., Zaman, M., Rowarth, J.S., Blennerhassett, J., Turnbull, M.H., 2011. Urease inhibitor reduces N losses and improves plant-bioavailability of urea applied in fine particle and granular forms under field conditions. Agric. Ecosyst. Environ. 144, 41–50.

De Antoni Migliorati, M., Scheer, C., Grace, P.R., Rowlings, D.W., Bell, M., McGree, J., 2014. Influence of different nitrogen rates and DMPP nitrification inhibitor on annual N_2O emissions from a subtropical wheat–maize cropping system. Agric. Ecosyst. Environ. 186, 33–43.

Ding, W.X., Chen, Z.M., Yu, H.Y., Luo, J.F., Yoo, G.Y., Xiang, J., Zhang, H.J., Yuan, J.J., 2015. Nitrous oxide emission and nitrogen use efficiency in response to nitrophosphate, N-(n-butyl) thiophosphoric triamide and dicyandiamide of a wheat cultivated soil under sub-humid monsoon conditions. Biogeosciences 12, 803–815.

Ding, W.X., Yu, H.Y., Cai, Z.C., 2010. Impact of urease and nitrification inhibitors on nitrous oxide emissions from fluvo-aquic soil in the North China Plain. Biol. Fert. Soils 47, 91–99.

Engel, R.E., Towey, B.D., Gravens, E., 2015. Degradation of the urease inhibitor NBPT as affected by soil pH. Soil Sci. Soc. Am. J. 79, 1674.

Gilsanz, C., Báez, D., Misselbrook, T.H., Dhanoa, M.S., Cárdenas, L.M., 2016. Development of emission factors and efficiency of two nitrification inhibitors, DCD and DMPP. Agric. Ecosyst. Environ. 216, 1–8.

Gioacchini, P., Nastri, A., Marzadori, C., Giovannini, C., Vittori Antisari, L., Gessa, C., 2002. Influence of urease and nitrification inhibitors on N losses from soils fertilized with urea. Biol. Fert. Soils 36, 129–135.

Gu, B., Ju, X., Chang, J.C., Ge, Y., Vitousek, P.M., 2015. Integrated reactive nitrogen budgets and future trends in China. Proc. Natl. Acad. Sci. U. S. A. 112, 8792–8797.

Hagenkamp-Korth, F., Haeussermann, A., Hartung, E., 2015. Effect of urease inhibitor application on urease activity in three different cubicle housing systems under practical conditions. Agric. Ecosyst. Environ. 202, 168–177.

Hartmann, T.E., Yue, S., Schulz, R., He, X., Chen, X., Zhang, F., Müller, T., 2015. Yield and N use efficiency of a maize–wheat cropping system as affected by different fertilizer management strategies in a farmer's field of the North China Plain. Field Crops Res. 174, 30–39.

Hill, A.M., Di, H.J., Cameron, K., Podolyan, A., 2014. The effect of animal trampling and DCD on ammonia oxidisers, nitrification, and nitrate leaching under simulated winter forage grazing conditions. J. Soils Sediments 15, 972–981.

Hu, X.K., Su, F., Ju, X.T., Gao, B., Oenema, O., Christie, P., Huang, B.X., Jiang, R.F., Zhang, F.S., 2013. Greenhouse gas emissions from a wheat-maize double cropping system with different nitrogen fertilization regimes. Environ. Pollut. 176, 198–207.

Huang, M., Liang, T., Wang, L., Zhou, C., 2015. No-tillage and fertilization management on crop yields and nitrate leaching in North China Plain. Ecol. Evol. 5, 1143–1155.

Huang, T., Gao, B., Hu, X.K., Lu, X., Well, R., Christie, P., Bakken, L.R., Ju, X.T., 2014. Ammonia-oxidation as an engine to generate nitrous oxide in an intensively managed calcareous fluvo-aquic soil. Sci. Rep. 4, 3950.

IPCC, 2006. IPCC Guidelines for National Greenhouse Gas Inventories. Institute for Global Environmental Strategies, Kanagawa.

IPCC, 2013. Climate change 2013: the physical science basis in contribution of working group I to the fifth assessment report of the intergovernmental panel on climate change. Camb. N. Y. 710–716.

Ju, X., Lu, X., Gao, Z., Chen, X., Su, F., Kogge, M., Romheld, V., Christie, P., Zhang, F., 2011. Processes and factors controlling N_2O production in an intensively managed low carbon calcareous soil under sub-humid monsoon conditions. Environ. Pollut. 159, 1007–1016.

Ju, X., Xing, G., Chen, X., Zhang, S., Zhang, L., Liu, X., Cui, Z., Yin, B., Christie, P., Zhu, Z., Zhang, F., 2009. Reducing environmental risk by improving N management in intensive Chinese agricultural systems. Proc. Natl. Acad. Sci. U. S. A. 106, 3041–3046.

Li, X., Hu, C., Delgado, J.A., Zhang, Y., Ouyang, Z., 2007. Increased nitrogen use efficiencies as a key mitigation alternative to reduce nitrate leaching in north china plain. Agric. Water Manag. 89, 137–147.

Liu, C., Wang, K., Zheng, X., 2013. Effects of nitrification inhibitors (DCD and DMPP) on nitrous oxide emission, crop yield and nitrogen uptake in a wheat–maize cropping system. Biogeosciences 10, 2427–2437.

Liu, C., Yao, Z., Wang, K., Zheng, X., 2014. Three-year measurements of nitrous oxide emissions from cotton and wheat–maize rotational cropping systems. Atmos. Environ. 96, 201–208.

Menéndez, S., Barrena, I., Setien, I., González-Murua, C., Estavillo, J.M., 2012. Efficiency of nitrification inhibitor DMPP to reduce nitrous oxide emissions under different temperature and moisture conditions. Soil Biol. Biochem. 53, 82–89.

Pereira, J., Barneze, A.S., Misselbrook, T.H., Coutinho, J., Moreira, N., Trindade, H., 2013. Effects of a urease inhibitor and aluminium chloride alone or combined with a nitrification inhibitor on gaseous N emissions following soil application

of cattle urine. Biosyst. Eng. 115, 396–407.
Pihlatie, M., Syväsalo, E., Simojoki, A., Esala, M., Regina, K., 2004. Contribution of nitrification and denitrification to N_2O production in peat, clay and loamy sand soils under different soil moisture conditions. Nutr. Cycl. Agroecosyst 70, 135–141.
Qiao, C., Liu, L., Hu, S., Compton, J.E., Greaver, T.L., Li, Q., 2015. How inhibiting nitrification affects nitrogen cycle and reduces environmental impacts of anthropogenic nitrogen input. Glob. Chang. Biol. 21, 1249–1257.
Rütting, T., Boeckx, P., Müller, C., Klemedtsson, L., 2011. Assessment of the importance of dissimilatory nitrate reduction to ammonium for the terrestrial nitrogen cycle. Biogeosciences 8, 1779–1791.
Sanz-Cobena, A., Sánchez-Martín, L., García-Torres, L., Vallejo, A., 2012. Gaseous emissions of N_2O and NO and NO_3^- leaching from urea applied with urease and nitrification inhibitors to a maize (Zea mays) crop. Agric. Ecosyst. Environ. 149, 64–73.
Scheer, C., Rowlings, D.W., Firrel, M., Deuter, P., Morris, S., Grace, P.R., 2014. Impact of nitrification inhibitor (DMPP) on soil nitrous oxide emissions from an intensive broccoli production system in sub-tropical Australia. Soil Biol. Biochem. 77, 243–251.
Shepherd, A., Yan, X., Nayak, D., Newbold, J., Moran, D., Dhanoa, M.S., Goulding, K., Smith, P., Cardenas, L.M., 2015. Disaggregated N_2O emission factors in China based on cropping parameters create a robust approach to the IPCC Tier 2 methodology. Atmos. Environ. 122, 272–281.
Shi, X., Hu, H., He, J., Chen, D., Suter, H.C., 2016. Effects of 3,4-dimethylpyrazole phosphate (DMPP) on nitrification and the abundance and community composition of soil ammonia oxidizers in three land uses. Biol. Fert. Soils 52, 927–939.
Shi, Y., Wu, W., Meng, F., Zhang, Z., Zheng, L., Wang, D., 2013. Integrated management practices significantly affect N_2O emissions and wheat–maize production at field scale in the North China Plain. Nutr. Cycl. Agroecosyst 95, 203–218.
Singh, J., Kunhikrishnan, A., Bolan, N.S., Saggar, S., 2013. Impact of urease inhibitor on ammonia and nitrous oxide emissions from temperate pasture soil cores receiving urea fertilizer and cattle urine. Sci. Total Environ. 465, 56–63.
Soares, J.R., Cantarella, H., Menegale, M.L.D.C., 2012. Ammonia volatilization losses from surface-applied urea with urease and nitrification inhibitors. Soil Biol. Biochem. 52, 82–89.
Tan, Y., Xu, C., Liu, D., Wu, W., Lal, R., Meng, F., 2017. Effects of optimized N fertilization on greenhouse gas emission and crop production in the North China Plain. Field Crops Res. 205, 135–146.
Venterea, R.T., Halvorson, A.D., Kitchen, N., Liebig, M.A., Cavigelli, M.A., Grosso, S.J.D., Motavalli, P.P., Nelson, K.A., Spokas, K.A., Singh, B.P., Stewart, C.E., Ranaivoson, A., Strock, J., Collins, H., 2012. Challenges and opportunities for mitigating nitrous oxide emissions from fertilized cropping systems. Front. Ecol. Environ. 10, 562–570.
Wang, X., Zhou, W., Liang, G., Pei, X., Li, K., 2016. The fate of ^{15}N-labelled urea in an alkaline calcareous soil under different N application rates and N splits. Nutr. Cycl. Agroecosyst 106, 311–324.
Weiske, A., Benckiser, G., Herbert, T., Ottow, J., 2001. Influence of the nitrification inhibitor 3,4-dimethylpyrazole phosphate (DMPP) in comparison to dicyandiamide (DCD) on nitrous oxide emissions, carbon dioxide fluxes and methane oxidation during 3 years of repeated application in field experiments. Biol. Fert. Soils 34, 109–117.
Zaman, M., Saggar, S., Blennerhassett, J.D., Singh, J., 2009. Effect of urease and nitrification inhibitors on N transformation, gaseous emissions of ammonia and nitrous oxide, pasture yield and N uptake in grazed pasture system. Soil Biol. Biochem. 41, 1270–1280.
Zaman, M., Zaman, S., Adhinarayanan, C., Nguyen, M.L., Nawaz, S., Dawar, K.M., 2013. Effects of urease and nitrification inhibitors on the efficient use of urea for pastoral systems. Soil Sci. Plant Nutr. 59, 649–659.
Zerulla, W., Barth, T., Dressel, J., Erhardt, K., Horchler von Locquenghien, K., Pasda, G., Rädle, M., Wissemeier, A., 2001. 3,4-Dimethylpyrazole phosphate (DMPP) - a new nitrification inhibitor for agriculture and horticulture. Biol. Fert. Soils 34, 79–84.
Zhu, X., Martin, B., Doane, T.A., Horwath, W.R., 2013. Ammonia oxidation pathways and nitrifier denitrification are significant sources of N_2O and NO under low oxygen availability. Proc. Natl. Acad. Sci. U. S. A. 110, 6328–6333.

Paper IX

Interactive effects of MnO_2, organic matter and pH on abiotic formation of N_2O from hydroxylamine in artificial soil mixtures.

Liu S., Berns AE., Vereecken H., **Wu, D**., Brüggemann., N., 2017

Scientific Reports, 7, 39590.

SCIENTIFIC REPORTS

OPEN

Interactive effects of MnO_2, organic matter and pH on abiotic formation of N_2O from hydroxylamine in artificial soil mixtures

Received: 22 February 2016
Accepted: 24 November 2016
Published: 01 February 2017

Shurong Liu, Anne E. Berns, Harry Vereecken, Di Wu & Nicolas Brüggemann

Abiotic conversion of the reactive nitrification intermediate hydroxylamine (NH_2OH) to nitrous oxide (N_2O) is a possible mechanism of N_2O formation during nitrification. Previous research has demonstrated that manganese dioxide (MnO_2) and organic matter (OM) content of soil as well as soil pH are important control variables of N_2O formation in the soil. But until now, their combined effect on abiotic N_2O formation from NH_2OH has not been quantified. Here, we present results from a full-factorial experiment with artificial soil mixtures at five different levels of pH, MnO_2 and OM, respectively, and quantified the interactive effects of the three variables on the NH_2OH-to-N_2O conversion ratio ($R_{NH2OH\text{-}to\text{-}N2O}$). Furthermore, the effect of OM quality on $R_{NH2OH\text{-}to\text{-}N2O}$ was determined by the addition of four different organic materials with different C/N ratios to the artificial soil mixtures. The experiments revealed a strong interactive effect of soil pH, MnO_2 and OM on $R_{NH2OH\text{-}to\text{-}N2O}$. In general, increasing MnO_2 and decreasing pH increased $R_{NH2OH\text{-}to\text{-}N2O}$, while increasing OM content was associated with a decrease in $R_{NH2OH\text{-}to\text{-}N2O}$. Organic matter quality also affected $R_{NH2OH\text{-}to\text{-}N2O}$. However, this effect was not a function of C/N ratio, but was rather related to differences in the dominating functional groups between the different organic materials.

Nitrous oxide (N_2O) is a potent greenhouse gas that can be formed by several soil processes, such as microbial nitrification and denitrification. The N_2O production from nitrification, especially from its reactive intermediate hydroxylamine (NH_2OH), has received increasing attention in the recent past, fostered by the development of analytical techniques for the determination of the ^{15}N site preference in the N_2O molecule that allows for constraining the contribution of different source processes to total N_2O formation[1–4]. Also, increasing knowledge from molecular biological and genetic studies has contributed to elucidating the different N_2O formation mechanisms during nitrification[3]. Still, the role of NH_2OH in N_2O formation in the soil is insufficiently understood. While there is evidence, e.g., from measurements in wastewater treatment systems that NH_2OH can contribute about 65% of total N_2O formation[2], the formation of N_2O from NH_2OH in soil and its controlling factors have rarely been studied[5,6].

Hydroxylamine was first identified by Lees (1952)[7] as an intermediate of the first step of nitrification by ammonia oxidizing bacteria (AOB), in which ammonia is oxidized to nitrite. Understanding the nitrification process in ammonia-oxidizing archaea (AOA), however, is much more fragmentary, but NH_2OH has been identified as an intermediate of ammonia oxidation also in AOA[8]. In most circumstances, NH_2OH is quickly oxidized to nitrite in the periplasm of the AOB, and N_2O may be produced as a side product during this process[3]. However, also a leakage of NH_2OH from the periplasm across the outer membrane of the AOB into the soil matrix, followed by a chemical reaction with soil constituents yielding N_2O, could be a potential mechanism of N_2O formation during nitrification. This assumption is supported by the fact that AOB can take up NH_2OH from the surrounding medium[9] as well as by the observation that the medium of AOB cultures contains measurable amounts of NH_2OH. The latter was found for *Nitrosomonas europaea* under oxic conditions, both for wild-type *N. europaea* and even more so for NirK and NorB-deficient mutants[10]. In accordance with this assumption, a positive relationship between NH_2OH content of the soil and soil N_2O emissions under oxic conditions has been detected in

Institute of Bio- and Geosciences – Agrosphere (IBG-3), Forschungszentrum Jülich GmbH, 52425, Jülich, Germany. Correspondence and requests for materials should be addressed to N.B. (email: n.brueggemann@fz-juelich.de)

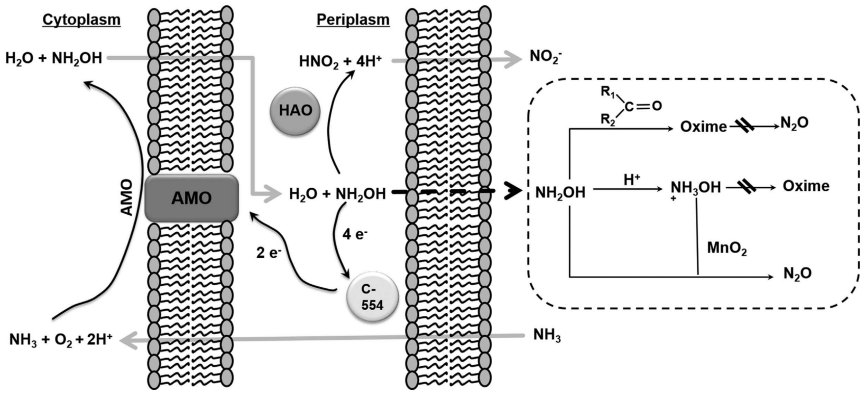

Figure 1. Hypothetical model of NH_2OH release by ammonia-oxidizing bacteria to the soil environment and potential abiotic reactions of NH_2OH with MnO_2 and organic matter in the soil at different pH conditions ($R_1R_2C{=}O$ represents carbonyl groups of SOM). AMO is ammonia monooxygenase; HAO is hydroxylamine oxidoreductase.

natural forest soil samples[11]. In addition, abiotic formation of N_2O from NH_2OH has been observed in sterilized soil samples from different ecosystems[6].

In soil, N_2O can be formed chemically, among a range of possible reactions, according to the following equations[12]:

$$NH_2OH + NO_2^- \rightarrow N_2O + H_2O + OH^- \quad (1)$$

$$2MnO_2 + 2NH_2OH \rightarrow 2MnO + N_2O + 3H_2O. \quad (2)$$

Owing to its high oxidization potential, manganese dioxide (MnO_2) acts as a strong oxidant in soil that plays an important role not only in the turnover of organic substances[13,14], but also in the N cycle[15], even under anoxic conditions[16,17]. Soil organic matter (SOM) plays a crucial role in the storage and release of N as well as in the emission of N_2O from soils. Quick disappearance of nitrite and nitrate within a few hours after addition has been observed in forest soils[18–20], whereas NH_2OH disappeared completely in soil several minutes after addition[5,11]. Abiotic reactions of SOM and inorganic N may contribute to the quick disappearance, as nitrite and nitrate can react with SOM or dissolved organic carbon (DOC), leading to the formation of organic N, such as nitroso and nitro compounds[21,22], while NH_2OH can also react with carbonyl groups to form oximes[23,24]:

$$R_1(R_2)C = O + NH_2OH \rightarrow R_1(R_2)C = NOH + H_2O \quad (3)$$

The quality of SOM, or more specifically the C/N ratio and the type and abundance of functional groups, influence the bonding of inorganic N to SOM[22]. Phenolic lignin derivatives, an important constituent of SOM, can covalently bind reactive N compounds and thereby stabilize N in soil[25,26]. The N binding form can be affected by the plant species from which the SOM is derived due to the different characteristics of phenolic compounds, e.g. condensed or hydrozable tannin[27].

Soil pH is another key factor influencing most nitrogen transformations in soil. High pH can lead to an increase of chemical N_2O production involving nitrite by favoring nitrite accumulation, either directly through increasing nitrite stability, or indirectly by inhibiting biological nitrite oxidation due to a higher concentration of free NH_3 (an inhibitor of nitrite oxidizers) in the soil[28]. In contrast, high soil N_2O emissions have also been observed in acid forest soils[29,30]. In this case, the effect of pH on enzyme activities during denitrification and nitrification was suggested as the main reason[31]. However, also chemical reactions that produce N_2O in the soil, such as the reaction of nitrite with SOM and the reaction of NH_2OH with MnO_2, are subject to a strong pH dependence and can contribute substantially to N_2O emissions under acidic conditions[32–34].

The aim of this study was to quantify the interactive effects of the major control factors of abiotic N_2O formation from NH_2OH in soil, i.e. MnO_2 content, pH and OM quantity and quality, by means of experiments with artificial soil mixtures. We hypothesized that the control factors interact with each other in the following way: At higher pH, unprotonated NH_2OH would react more readily with carbonyl groups of OM, leading to oxime formation and making NH_2OH less available for oxidation to N_2O by MnO_2. Lower soil pH would lead to increased protonation of NH_2OH, making NH_2OH more stable against the reaction with carbonyl groups of OM and more prone to the reaction with MnO_2, leading to higher N_2O formation from the same amount of NH_2OH (Fig. 1). To test these hypotheses, we performed two laboratory experiments with artificial soil mixtures, which were produced from pure quartz sand, quartz powder, kaolin clay, MnO_2 powder and different plant-derived organic materials, resembling SOM of different quality, at different mixing ratios. In these experiments, N_2O formation was determined after NH_2OH addition to the different mixtures at different pH levels and related to the different control factors.

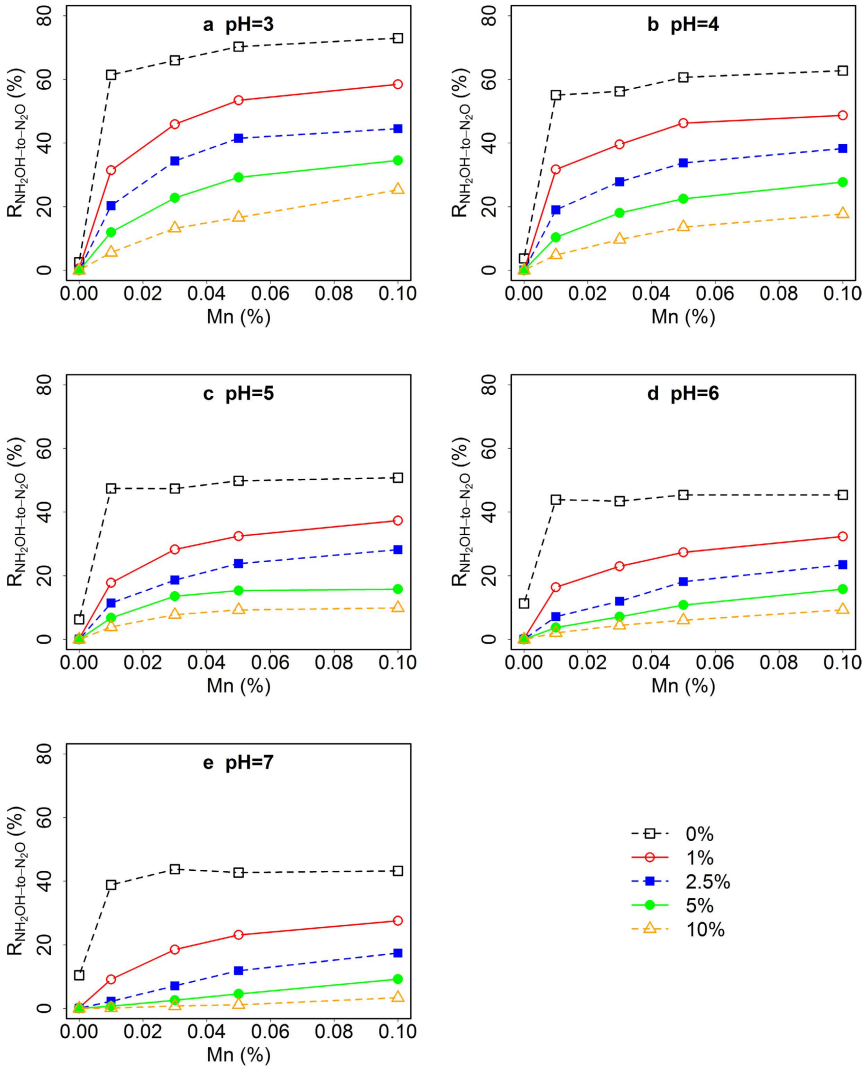

Figure 2. Mean NH_2OH-to-N_2O conversion ratios ($R_{NH2OH-to-N2O}$) in artificial soil mixtures at different pH as well as MnO_2 and organic matter (OM, peat moss) contents. The total amount of NH_2OH added was 5 nmol (equivalent to 70 μg N per kg dry material). Different symbols represent $R_{NH2OH-to-N2O}$ at different OM content (n = 3, SD < 5%, not shown).

Results and Discussion

$R_{NH2OH-to-N2O}$ at different pH, MnO_2 and OM contents (%). In the present study all three factors, i.e. pH, MnO_2 and OM content, affected $R_{NH2OH-to-N2O}$ from peat moss significantly (Fig. 2, S1 and S2). The $R_{NH2OH-to-N2O}$ increased greatly with an increase in MnO_2 content from 0% to 0.1% (Fig. 2). This finding is consistent with Bremner *et al.*[5], who studied 19 soils with a wide range of properties and found that the formation of N_2O by decomposition of NH_2OH was highly correlated with oxidized Mn content of the soils. The fact that NH_2OH was used in the past for the selective extraction of Mn oxides from soil samples[35] indicates that NH_2OH can efficiently reduce Mn(IV) to Mn(II) or Mn(III) (and in turn is oxidized to N_2O) in natural soil samples. With increasing OM content, $R_{NH2OH-to-N2O}$ decreased remarkably, especially at high pH (Fig. 2c,d,e). For example, an increase in OM by only 1% at 0.01% MnO_2 led to about 50% and 80% decrease in N_2O emissions at pH 3 and pH 7, respectively (Fig. 2e, S2). This could be caused by the oxime-forming reaction between NH_2OH and carbonyl groups of OM, such as in quinones. The oximes may undergo a tautomeric equilibrium with their corresponding nitrosophenol

forms[23]. In fact, NH_2OH has been used in a number of previous studies to determine the carbonyl content of humic substances[36], indicating a high affinity of NH_2OH to OM that contains carbonyl groups. In the absence of OM and MnO_2, increasing pH led to a slight increase in $R_{NH2OH\text{-}to\text{-}N2O}$ due to the self-decomposition of NH_2OH at higher pH, whereas in the presence of OM and absence of MnO_2 nearly no NH_2OH was converted to N_2O (Fig. S2a). In contrast, the effect of increasing pH on $R_{NH2OH\text{-}to\text{-}N2O}$ became negative already in the presence of 0.01% MnO_2 (Fig. S2b). This finding suggests that acidic conditions are favorable for the redox reaction between NH_2OH and MnO_2.

Also strong interactive effects of pH and MnO_2, pH and OM, and OM and MnO_2 were observed for the conversion of NH_2OH to N_2O. The largest $R_{NH2OH\text{-}to\text{-}N2O}$ found in the present experiment was 81.5% in the absence of SOM at pH 3, and with a MnO_2 content of 0.1% (Fig. 2a), while the lowest $R_{NH2OH\text{-}to\text{-}N2O}$ was about 9%, when SOM content was 10% in the presence of 0.1% MnO_2 at pH 7 (Fig. 2e). This suggests that even at the highest MnO_2 level and in all other respects optimal conditions a small fraction of NH_2OH had not been converted to N_2O, but to some other unidentified product.

In the treatments without OM, MnO_2 had only a small effect on $R_{NH2OH\text{-}to\text{-}N2O}$ at all pH conditions, while it had a larger effect especially at higher OM content (Fig. 2, S1), suggesting a strong competition between OM and MnO_2 for NH_2OH. The competition was biased by pH, with lower pH favouring the reaction of NH_2OH and MnO_2, while higher pH favoured the reaction of NH_2OH with OM. These findings confirmed our hypothesis that at low pH NH_2OH is more protected against reaction with OM and more available for the oxidation by MnO_2 due to the higher degree of NH_2OH protonation at lower pH.

$R_{NH2OH\text{-}to\text{-}N2O}$ as a function of pH, MnO_2 content and OM quality. Organic matter quality had a clear influence on $R_{NH2OH\text{-}to\text{-}N2O}$ in this study (Fig. 3, S3, and S4). Most of the OM types were associated with a significantly lower $R_{NH2OH\text{-}to\text{-}N2O}$ compared to the mixtures without OM within the pH range of the experiment. In general, the inhibitory effect of the organic materials on the conversion of NH_2OH to N_2O showed a clear pH dependency, but was not a function of C/N ratio (Fig. 3, S3). At acidic conditions (pH 3–4), peat moss and watermilfoil with their relatively large C/N ratio inhibited $R_{NH2OH\text{-}to\text{-}N2O}$ the least, while the cyanobacterium material and clover had a stronger inhibitory effect on $R_{NH2OH\text{-}to\text{-}N2O}$ despite their smaller C/N ratio (Fig. 3a,b). The differences between peat moss, cyanobacterium and watermilfoil material as OM became smaller at higher pH, and were no longer significant at pH 7 in the presence of 0.01% MnO_2 (Fig. 3e), while clover showed always the smallest $R_{NH2OH\text{-}to\text{-}N2O}$ at all pH levels. In the absence of MnO_2, all OM forms showed a $R_{NH2OH\text{-}to\text{-}N2O}$ close to zero, except for the watermilfoil material that was associated with a $R_{NH2OH\text{-}to\text{-}N2O}$ significantly above zero within the pH range 3–6 (Fig. S4a). A possible explanation could be the fact that, in contrast to the other OM sources, the watermilfoil material contained about 0.03% Mn (Table 1), which could have caused the N_2O emission after NH_2OH addition even without external MnO_2 addition.

We assumed that $R_{NH2OH\text{-}to\text{-}N2O}$ would be a function of the C/N ratio of the different SOM types, as larger C/N ratios would be indicative of a lower degree of N-containing functional groups, i.e. leaving a higher chance for NH_2OH to react with SOM and not to be converted to N_2O. However, as stated above we did not observe any clear relationship between C/N ratio and $R_{NH2OH\text{-}to\text{-}N2O}$, e.g. peat moss had the largest C/N ratio, but did not lead to the lowest $R_{NH2OH\text{-}to\text{-}N2O}$. Instead, clover with a much lower C/N ratio had the largest inhibitory effect on $R_{NH2OH\text{-}to\text{-}N2O}$. The addition of 2.5% dry clover powder (C/N ratio = 11.3) to the artificial soil mixture decreased $R_{NH2OH\text{-}to\text{-}N2O}$ by 48% at pH 3 (Fig. 3a), which was similar to the effect of 10% peat moss (C/N ratio = 67.2) at the same pH (Fig. 2a). The reason for this observation could lie in the differences in functional groups between the different organic materials used in this study.

A better insight into the effects of C and N functional groups of the different organic materials was obtained from NMR analysis. The peat moss OM had the lowest proportion of ester or amide carbonyl at around 170 ppm of all materials (Fig. 4, Table 2). This is in accordance with the observation that – despite having the largest C/N ratio – peat moss OM had a lower inhibitory effect on $R_{NH2OH\text{-}to\text{-}N2O}$ compared to clover and watermilfoil OM (if the background MnO_2 effect was subtracted), i.e. the lack of almost any carbonyl groups in peat moss was clearly visible in its chemical behaviour toward NH_2OH. In addition, peat moss OM exhibited the largest proportion of O-substituted aliphatic compounds, which might have also contributed to the relatively low inhibitory effect on $R_{NH2OH\text{-}to\text{-}N2O}$ in comparison to clover and watermilfoil OM. In contrast, cyanobacterium OM had the highest proportion of acid/amide carbonyl of all four organic materials, suggesting the highest inhibitory effect on $R_{NH2OH\text{-}to\text{-}N2O}$ due to the competitive reaction of carbonyl groups with NH_2OH. The clover material, however, contained lower amounts of O-substituted aliphatics and di-O-substituted C in comparison to peat moss and watermilfoil OM, which may have increased its affinity for NH_2OH. For the proportion of unsaturated C no clear trend emerged across the different materials, suggesting that the effect of unsaturated C on $R_{NH2OH\text{-}to\text{-}N2O}$ is of minor importance.

Development of a stepwise multiple regression model from the artificial soil mixtures and application to natural soils. The multiple regression model obtained from the first experiments was $R_{NH2OH\text{-}to\text{-}N2O} = 45.9 - 3.1\ SOM + 241.1\ MnO_2 - 4.5\ pH$, $R^2 = 0.62$ ($P < 0.01$), which could explain about 62% variation of $R_{NH2OH\text{-}to\text{-}N2O}$, and the contributions of pH, Mn and SOM content to the model's performance were all significant ($P < 0.01$). It could well explain the observations (Fig. 3) for peat moss, watermilfoil and clover OM (R^2 close to 0.8, $P < 0.01$, Fig. 5). This demonstrated the general applicability of the model for the OM derived from the different plant and cyanobacterium materials, with different N content, aliphatic C content and C/N ratios. In contrast, the model proved to be not appropriate for the artificial soil mixture without any MnO_2, indicated by the decreased goodness of the simulation.

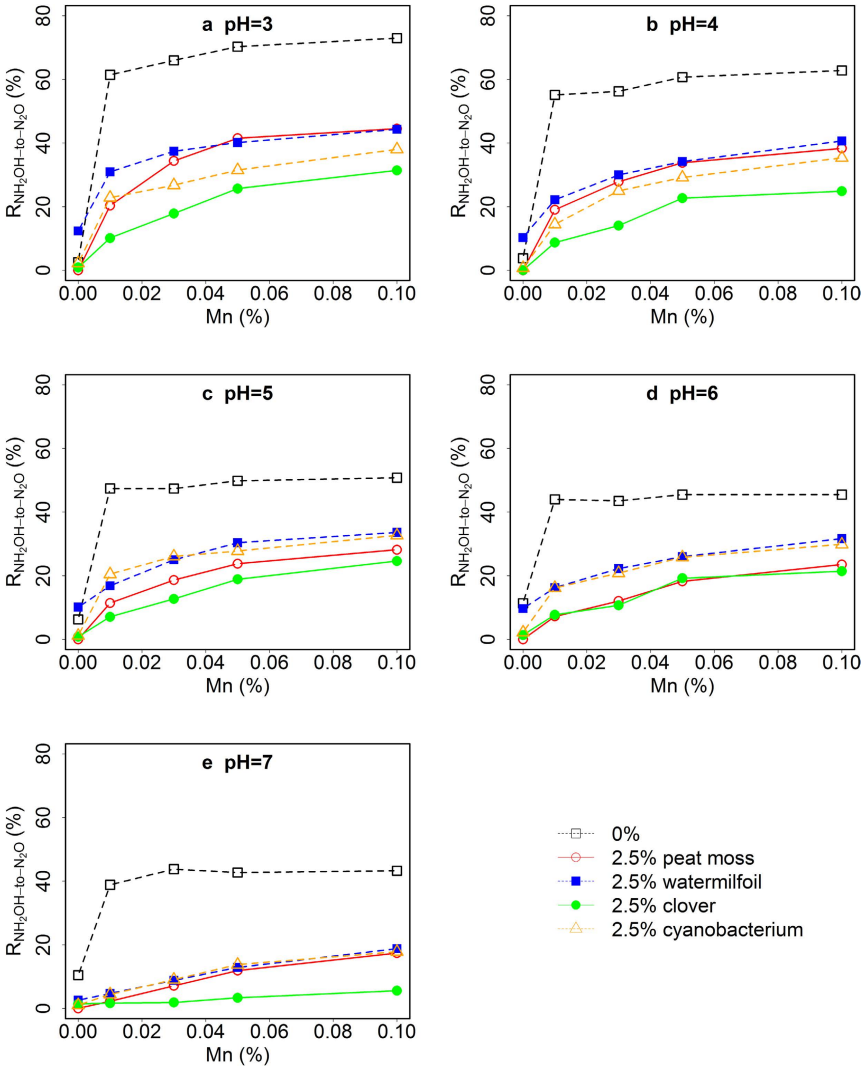

Figure 3. Mean NH_2OH-to-N_2O conversion ratios ($R_{NH2OH-to-N2O}$) in artificial soils at different pH and MnO_2 content, and for organic matter of different origins at a fixed content of 2.5% (w/w). The total amount of NH_2OH added was 5 nmol. Different symbols represent $R_{NH2OH-to-N2O}$ for the artificial soil mixtures with the different organic materials (n = 3, SD < 5%, not shown).

	C	N	C/N	Al	Ca	Fe	K	Mg	Mn	Na	P	Si
Peat moss	41.3[1]	0.6	67.2	0.03	0.13	0.06	0.06	0.07	<0.01	0.01	0.03	0.08
Watermilfoil	35.4	2.1	17.0	0.12	2.26	0.11	1.21	0.25	0.031	0.67	0.12	0.21
Clover	41.4	3.7	11.3	<0.01	1.10	0.01	2.68	0.20	<0.01	<0.01	0.34	0.03
Cyanobacterium	44.9	9.9	4.5	0.02	0.31	0.09	1.22	0.31	<0.01	1.36	0.92	0.07

Table 1. Element contents (%) and C/N ratios of the organic materials used in this study. All elements are reported as % of dry weight (mean of three replicates). The standard deviation is 3% for the values larger than 1%, 20% for the values smaller than 0.1%, and 10% for the values in the range of 0.1% to 1%.

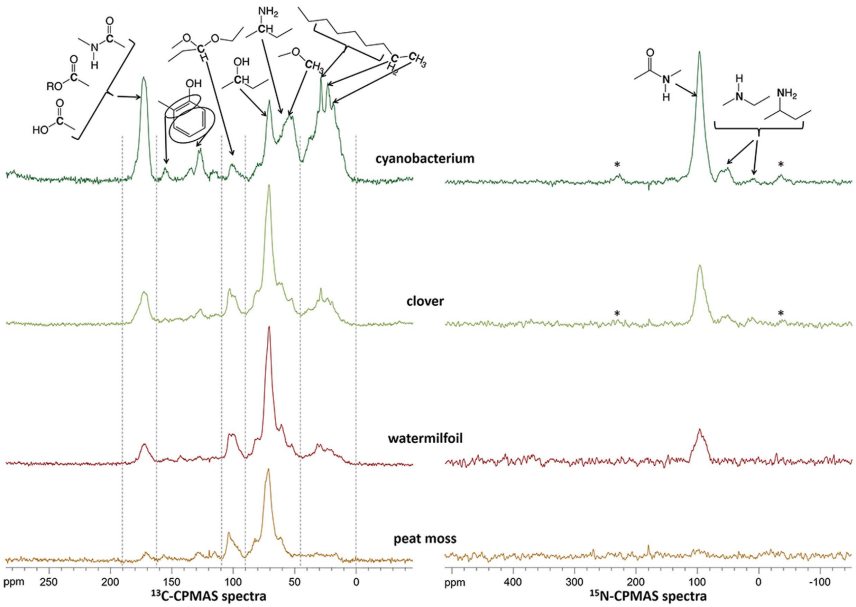

Figure 4. ^{13}C- and ^{15}N-CPMAS-NMR spectra of the different organic materials (cyanobacterium, clover, watermilfoil, peat moss) used in the experiment.

Spectral range (ppm)	Chemical features	Found in	Cyanobacterium (%)	Clover (%)	Watermilfoil (%)	Peat moss (%)
45–0	Aliphatic compounds	waxes, suberin, cutin, cyanophycin, chlorophyll (a,b,d)	41	17	15	11
64.5–45	N- and O-substituted aliphats	amino acids, amino sugars, lignin, cyanophycin	19	14	14	12
90–64.5	O-substituted aliphats	polysaccharides, cellulose, hemi-cellulose, starch, pectin, lignin	14	38	42	49
109–90	di-O-substituted C	polysaccharides, cellulose, hemi-cellulose, starch, pectin	3	11	12	14
162–109	unsaturated C, aromatic C	suberin, lignin, chlorophyll	7	11	10	11
190–162	acid, ester, amide	cutin, proteins, cyanophycin, chlorophyll	17	10	7	4

Table 2. Relative proportions of chemical features of the different plant materials derived from ^{13}C CPMAS NMR spectra. Sums within columns greater than 100 are due to rounding errors.

Finally, $R_{NH2OH\text{-}to\text{-}N2O}$ was simulated with the same regression model for the natural soils described in Heil *et al.*[6]. The results showed that the application of the model to natural soils was promising, no matter if it was applied to fumigated or fresh soils (Fig. 6). The simulated $R_{NH2OH\text{-}to\text{-}N2O}$ explained more than 90% of the observed rates, especially for cropland, grassland and deciduous forest soils. However, the model failed at correctly predicting $R_{NH2OH\text{-}to\text{-}N2O}$ for the spruce forest soil of Heil *et al.*[6], which could be related to the high SOM and relatively low MnO_2 content of the spruce soil as compared to the other soils. This finding suggests that there is a threshold value for the SOM content of 10% above which – and a MnO_2 content of 0.01% below which – the model fails to predict the correct $R_{NH2OH\text{-}to\text{-}N2O}$ values.

Soil pH, MnO_2 and SOM content were identified as crucial control variables of $R_{NH2OH\text{-}to\text{-}N2O}$, i.e. the conversion ratio of NH_2OH to N_2O in the artificial soil experiments of this study. Organic matter derived from different plant species and a cyanobacterium also affected $R_{NH2OH\text{-}to\text{-}N2O}$ due to the differences in composition, type and abundance of functional groups, as more carbonyl C leads to higher reactivity of NH_2OH with organic matter, thereby lowering its availability for the oxidation to N_2O by MnO_2. The multiple regression model of pH, MnO_2 and OM developed here could explain about 60% of the variance of $R_{NH2OH\text{-}to\text{-}N2O}$ in the artificial soil mixtures, and proved also to be promising for the prediction of $R_{NH2OH\text{-}to\text{-}N2O}$ of chemical N_2O production from NH_2OH in natural soils, when SOM content was below 10% and Mn content was larger than 0.01%. If these findings can

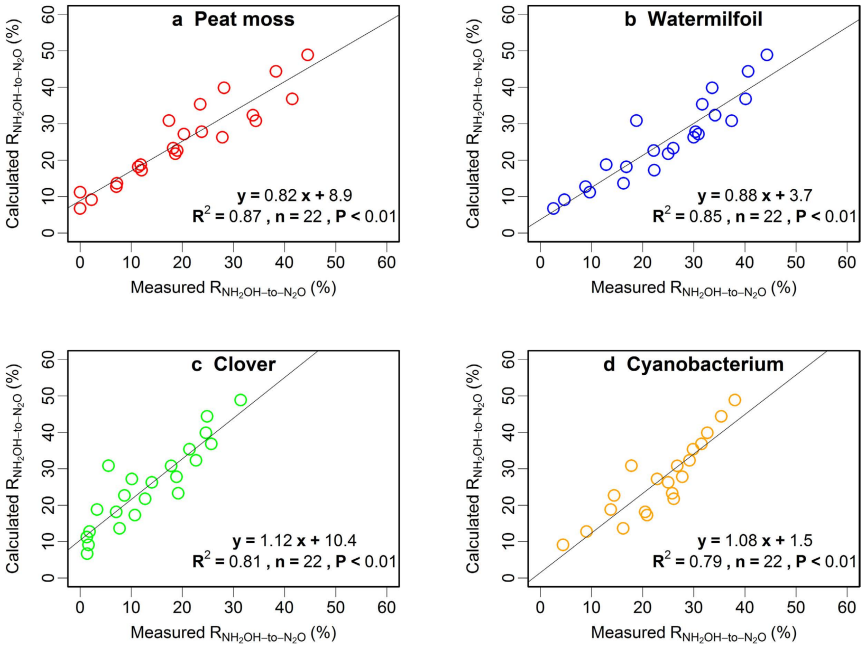

Figure 5. Results of the application of the artificial soil regression model for the calculation of NH_2OH-to-N_2O conversion ratios ($R_{NH2OH\text{-}to\text{-}N2O}$) to artificial soil mixtures amended with the different organic materials (n = 22). The three points for which $R_{NH2OH\text{-}to\text{-}N2O}$ was determined at pH 3, 4, and 5 without MnO_2 addition were excluded from the simulation.

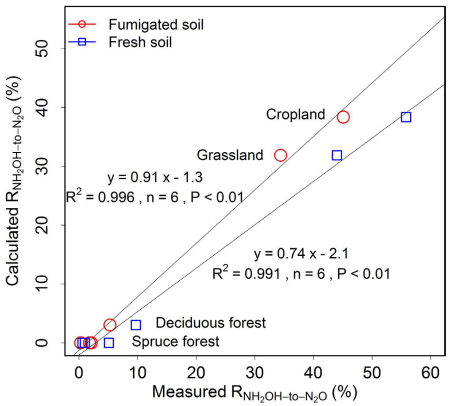

Figure 6. Results of the application of the artificial soil regression model for the calculation of NH_2OH-to-N_2O conversion ratios ($R_{NH2OH\text{-}to\text{-}N2O}$) to six natural fresh and chloroform-fumigated soils as reported in Heil *et al.*[6].

be confirmed for other soils from different ecosystems, this improved understanding of the controls of N_2O formation from the reactive nitrification intermediate NH_2OH in soils can have large implications for developing appropriate management options, such as adding organic amendments with suitable chemical characteristics, for mitigating N_2O emissions from agricultural land, the largest anthropogenic source of N_2O to the atmosphere.

Methods

Experimental setup. Two full-factorial artificial soil experiments were conducted. The first experiment comprised three factors (pH, MnO_2 and OM content) and five levels of each factor. The scond experiment comprised also three factors (pH, MnO_2 and OM quality) with five levels of pH and MnO_2, and four different organic materials at the same concentration level (2.5% w/w on a dry weight basis), but of different quality. Each experiment was conducted in triplicate.

Preparation of the artificial soil mixtures. The artificial soil mixtures consisted of 15% (expressed as percentage of dry weight) fine quartz sand (50% of the particles 0.05–0.2 mm), representing the sand fraction, 65% quartz powder (0.002–0.063 mm), representing the silt fraction, and 20% kaolin clay (≤0.002 mm), representing the clay fraction, mimicking the soil texture of the agricultural Terrestrial Environmental Observatories (TERENO) field site Selhausen[37]. Freeze-dried, finely ground and sieved (<0.75 mm) peat moss (*Sphagnum magellanicum*, collected from Dürres Maar, Eifel, Germany) was amended as SOM to the artificial soil mixtures at levels of 0%, 1%, 2.5%, 5%, 10% dry weight, while the relative amount of sand, clay and silt was reduced according to the amount of peat moss added. The water holding capacity (WHC) was determined for each of the artificial soil mixtures. The WHC increased with increasing organic matter (OM) content, and amounted to 29%, 44%, 55%, 76%, and 132% for the five OM contents, respectively. Each of those artificial soil mixtures was amended with MnO_2 (Merck, Darmstadt, Germany) at five different levels (0%, 0.01%, 0.025%, 0.05%, 0.1% Mn), then the ingredients were thoroughly homogenized.

Preparation of artificial soil mixtures with different OM qualities. Organic materials with different C/N ratios (Table 1) were derived from two different plant species, i.e. watermilfoil (*Myriophyllum* spec.) and clover (*Trifolium repens*), and from a cyanobacterium (*Spirulina platensis*). Watermilfoil and clover had been collected previously on the campus of Forschungszentrum Jülich (2004 and 2014, respectively), while the cyanobacterium material had been purchased in 2006 (Concept Vitalprodukte, Schwerte, Nordrhein-Westfalen, Germany). The finely ground, freeze-dried and sieved (<0.75 mm) organic material was amended to the inorganic quartz-kaolin mixture as described above at a rate of 2.5% dry weight, while the relative amount of sand, clay and silt was reduced accordingly. Also for this experiment, each of the artificial soil mixtures was amended with MnO_2 at five different levels (0%, 0.01%, 0.025%, 0.05%, 0.1% Mn), and again mixed thoroughly to obtain a homogeneous composition.

Addition of NH_2OH to the artificial soil mixtures and analysis of the N_2O formed. One gram of each artificial soil mixture was weighed into individual 22-mL gas chromatograph (GC) vials. Subsequently, NH_2OH in different buffer solutions was added to each vial to obtain a soil water content of 50% WHC, which required addition of varying volumes of buffer solution to the different soil mixtures depending on the OM content, and adaptation of the NH_2OH concentration of each of the buffer solutions accordingly. The total amount of NH_2OH added to each of the soil mixtures was always 5 nmol (equivalent to 70 μg N per kg dry material). The pH buffer solutions at pH 3, 4, 5 and 6 were prepared with citric acid (0.1 M) and sodium citrate (0.1 M) according to Gomori[38], whereas the buffer at pH 7 was prepared with tris(hydroxymethyl)aminomethane and maleate (Tris-maleate buffer). The vials were closed immediately after NH_2OH addition. After 10 hours of incubation, the N_2O concentration in the headspace of the vials was measured with a GC equipped with an electron capture detector (Clarus 580, PerkinElmer, Rodgau, Germany). Details of the GC setup and analytical conditions have been described previously[11].

Calculation of the NH_2OH-to-N_2O conversion ratio. The NH_2OH-to-N_2O conversion ratio ($R_{NH2OH\text{-}to\text{-}N2O}$, moles N_2O-N per mole NH_2OH-N, %) was determined according to the following equation:

$$R_{NH_2OH-to-N_2O} = (c_1 - c_0) \cdot V/V_m \cdot 2/n \cdot 100 \quad (4)$$

where c_0 is the background N_2O mixing ratio in the headspace of the control with the same amount of water instead of NH_2OH solution (nL L^{-1}); c_1 is the N_2O mixing ratio in the headspace of the sample with NH_2OH addition (nL L^{-1}); the factor 2 represents the molar N ratio of N_2O and NH_2OH; V is the volume of the vial headspace (0.022 L); V_m is the molar volume of N_2O at standard pressure and room temperature (24.465 L mol^{-1}); n is the amount of NH_2OH added to the sample vials (5 nmol).

Determination of the basic properties of the organic materials. Three replicates of each organic material were analyzed to determine its basic properties. The C and N content of the different organic materials was analyzed by weighing 200–300 μg dry material into tin capsules, followed by combustion at 1080 °C in an elemental analyzer (EuroEA, EuroVector, Milan, Italy) interfaced to an isotope-ratio mass spectrometer (Isoprime, Isoprime Ltd, Stockport, United Kingdom). The C and N content was determined through peak integration of m/z 44 (CO_2) and 28 (N_2), respectively, and calibrated against elemental standards.

The elemental composition of the organic materials was analyzed by using inductively coupled plasma optical emission spectrometry (ICP-OES) in the central analytical laboratory (ZEA-3) of Forschungszentrum Jülich. Briefly, 100 mg of sample material were mixed with 3 mL HNO_3 and 2 mL H_2O_2, heated in the microwave at 800 W for 30 min. The mixtures were subsequently filled up to 14 mL and diluted 10-fold with deionized water followed by the ICP-OES measurement.

For the determination of characteristic molecule structures and functional groups of the different organic materials used in the experiments, ^{13}C and ^{15}N cross-polarisation magic-angle spinning (CPMAS) nuclear magnetic resonance (NMR) spectra were obtained. ^{13}C CPMAS spectra were obtained on a 7.05 T Varian INOVA™ Unity (Varian Inc., Palo Alto, CA, USA) at a ^{13}C resonance frequency of 75.4 MHz. ^{15}N CPMAS spectra were

obtained on a 14.09 T Varian NMR system (Varian Inc., Palo Alto, CA, USA) at a ^{15}N resonance frequency of 60.8 MHz. Samples were packed into 6 mm diameter cylindrical zirconia rotors with Vespel® drive tips and spun at 8000 ± 3 Hz in an HX Apex probe. The spectra were collected with a sweep width of 25 kHz and an acquisition time of 20 ms. In preliminary experiments, the optimal contact time and recycle delay for the cross-polarization experiment were determined. A contact time of 1 ms and a 5 s recycle delay time were used for ^{13}C, whereas a contact time of 1 ms and a 1 s recycle delay time were used for ^{15}N. During cross-polarization the ^{1}H radio frequency (RF) field strength was set to 47 kHz for ^{13}C and to 33.7 kHz for ^{15}N, respectively. The ^{13}C and ^{15}N RF field strength was set to 41 and 41.7 kHz, respectively. An ascending ramp of 15 and 12.2 kHz on the ^{1}H-RF field was used for ^{13}C and ^{15}N during contact time to account for inhomogeneities of the Hartmann-Hahn condition, respectively[39]. Proton decoupling was done using a spinal sequence with a ^{1}H field strength of 50 and 35.6 kHz, a phase of 4.5° and 5.5°, and a pulse length of 12 and 9.5 μs, respectively.

The free induction decays (FID) were recorded with VnmrJ (Version 1.1 RevisionD, Varian Inc., Palo Alto, CA, USA) and processed with Mestre-C (Version 4.9.9.9, Mestrelab Research, Santiago de Compostela, Spain). All FIDs were fourier-transformed with an exponential filter function with a line broadening (LB) of 20 to 50 Hz. Baseline correction was done using the manual baseline correction function of Mestre-C.

The ^{13}C chemical shifts are reported relative to tetramethylsilane (=0 ppm) using adamantane as an external reference. The relative intensities of the regions were determined using the integration routine of the MestRe-C software. The ^{15}N chemical shifts are reported relative to ammonium nitrate ($NH_4^+ = 0$ ppm).

Data analysis. The homogeneity of variance was tested with the Bartlett test. One-way analysis of variance (one-way ANOVA) of the main controlling factors in the two experiments was performed, followed by a Tukey Honest Significant Difference (HSD) test. A stepwise multiple regression model for the NH_2OH-to-N_2O conversion ratio was developed on the basis of the co-variables pH, MnO_2 and SOM content by using the data from the first experiment. In this case, significance was tested with the F test. Linear regression was performed for simulated and measured $R_{NH2OH\text{-}to\text{-}N2O}$ in artificial and natural soils described in Heil *et al.*[6] and tested for significance. All analyses were performed with the R software package (version 3.1.0, R Development Core Team, 2013)[40].

References

1. Sutka, R. L. *et al.* Distinguishing nitrous oxide production from nitrification and denitrification on the basis of isotopomer abundances. *Appl. Environ. Microb.* **72,** 638–644 (2006).
2. Rathnayake, R. M. L. D. *et al.* Source identification of nitrous oxide on autotrophic partial nitrification in a granular sludge reactor. *Water Res.* **47,** 7078–7086 (2013).
3. Stein, L. Y. 6 Surveying N_2O-Producing Pathways in Bacteria In *Methods in enzymology* (ed Klotz, M. G.) 131–152 (Elsevier, 2011).
4. Wunderlin, P. *et al.* Isotope Signatures of N_2O in a Mixed Microbial Population System: Constraints on N_2O Producing Pathways in Wastewater Treatment. *Environ. Sci. Technol.* **47,** 1339–1348 (2012).
5. Bremner, J. M., Blackmer, A. M. & Waring, S. A. Formation of nitrous oxide and dinitrogen by chemical decomposition of hydroxylamine in soils. *Soil Biol. Biochem.* **12,** 263–269 (1980).
6. Heil, J., Liu, S., Vereecken, H. & Brüggemann, N. Abiotic nitrous oxide production from hydroxylamine in soils and their dependence on soil properties. *Soil Biol. Biochem.* **84,** 107–115 (2015).
7. Lees, H. Hydroxylamine as an Intermediate in Nitrification. *Nature* **169,** 156–157 (1952).
8. Vajrala, N. *et al.* Hydroxylamine as an intermediate in ammonia oxidation by globally abundant marine archaea. *Proc. Natl. Acad. Sci. USA* **110,** 1006–1011 (2013).
9. Schmidt, I., Look, C., Bock, E. & Jetten, M. S. M. Ammonium and hydroxylamine uptake and accumulation in Nitrosomonas. *Microbiology* **150,** 1405–1412 (2004).
10. Schmidt, I., van Spanning, R. J. M. & Jetten, M. S. M. Denitrification and ammonia oxidation by Nitrosomonas europaea wild-type, and NirK- and NorB-deficient mutants. *Microbiology* **150,** 4107–4114 (2004).
11. Liu, S., Vereecken, H. & Brüggemann, N. A highly sensitive method for the determination of hydroxylamine in soils. *Geoderma* **232–234,** 117–122 (2014).
12. Bremner, J. Sources of nitrous oxide in soils. *Nutr. Cycl. Agroecosys.* **49,** 7–16 (1997).
13. Lehmann, R. G., Cheng, H. H. & Harsh, J. B. Oxidation of Phenolic Acids by Soil Iron and Manganese Oxides. *Soil Sci. Soc. Am. J.* **51,** 352–356 (1987).
14. Li, C., Zhang, B., Ertunc, T., Schaeffer, A. & Ji, R. Birnessite-Induced Binding of Phenolic Monomers to Soil Humic Substances and Nature of the Bound Residues. *Environ. Sci. Technol.* **46,** 8843–8850 (2012).
15. Luther, G. III & Popp, J. Kinetics of the Abiotic Reduction of Polymeric Manganese Dioxide by Nitrite: An Anaerobic Nitrification Reaction. *Aquat. Geochem.* **8,** 15–36 (2002).
16. Hulth, S. *et al.* Nitrogen removal in marine environments: Recent findings and future research challenges. *Mar. Chem.* **94,** 125–145 (2005).
17. Hulth, S., Aller, R. C. & Gilbert, F. Coupled anoxic nitrification/manganese reduction in marine sediments. *Geochim. Cosmochim. Acta* **63,** 49–66 (1999).
18. Dail, D., Davidson, E. & Chorover, J. Rapid abiotic transformation of nitrate in an acid forest soil. *Biogeochemistry* **54,** 131–146 (2001).
19. Davidson, E. A., Chorover, J. & Dail, D. B. A mechanism of abiotic immobilization of nitrate in forest ecosystems: the ferrous wheel hypothesis. *Global Change Biol.* **9,** 228–236 (2003).
20. Schmidt, B. M. & Matzner, E. Abiotic reaction of nitrite with dissolved organic carbon? Testing the Ferrous Wheel Hypothesis. *Biogeochemistry* **93,** 291–296 (2009).
21. El Azhar, S., Verhe, R., Proot, M., Sandra, P. & Verstraete, W. Binding of nitrite-N on polyphenols during nitrification. *Plant Soil* **94,** 369–382 (1986).
22. Thorn, K. A. & Mikita, M. A. Nitrite Fixation by Humic Substances Nitrogen-15 Nuclear Magnetic Resonance Evidence for Potential Intermediates in Chemodenitrification. *Soil Sci. Soc. Am. J.* **64,** 568–582 (2000).
23. Thorn, K. A., Arterburn, J. B. & Mikita, M. A. Nitrogen-15 and carbon-13 NMR investigation of hydroxylamine-derivatized humic substances. *Environ. Sci. Technol.* **26,** 107–116 (1992).
24. Nelson, D. Transformations of hydroxylamine in soils. *Proc. Indiana Acad. Sci.* **87,** 409–413 (1977).
25. Halvorson, J. J. & Gonzalez, J. M. Tannic acid reduces recovery of water-soluble carbon and nitrogen from soil and affects the composition of Bradford-reactive soil protein. *Soil Biol. Biochem.* **40,** 186–197 (2008).
26. Olk, D. C. *et al.* Chemical stabilization of soil organic nitrogen by phenolic lignin residues in anaerobic agroecosystems. *Soil Biol. Biochem.* **38,** 3303–3312 (2006).

27. Kraus, T. E. C., Zasoski, R. J., Dahlgren, R. A., Horwath, W. R. & Preston, C. M. Carbon and nitrogen dynamics in a forest soil amended with purified tannins from different plant species. *Soil Biol. Biochem.* **36,** 309–321 (2004).
28. Venterea, R. T., Clough, T. J., Coulter, J. A. & Breuillin-Sessoms, F. Ammonium sorption and ammonia inhibition of nitrite-oxidizing bacteria explain contrasting soil N_2O production. *Sci. Rep.* **5** (2015).
29. Šimek, M. & Cooper, J. E. The influence of soil pH on denitrification: progress towards the understanding of this interaction over the last 50 years. *Eur. J. Soil Sci.* **53,** 345–354 (2002).
30. Martikainen, P. J., Lehtonen, M., Lång, K., De Boer, W. & Ferm, A. Nitrification and nitrous oxide production potentials in aerobic soil samples from the soil profile of a Finnish coniferous site receiving high ammonium deposition. *FEMS Microbiology Ecology* **13,** 113–121 (1993).
31. Liu, B., Mørkved, P. T., Frostegård, Å. & Bakken, L. R. Denitrification gene pools, transcription and kinetics of NO, N_2O and N_2 production as affected by soil pH. *FEMS Microbiology Ecology* **72,** 407–417 (2010).
32. Samarkin, V. A. *et al.* Abiotic nitrous oxide emission from the hypersaline Don Juan Pond in Antarctica. *Nature Geosci.* **3,** 341–344 (2010).
33. van Cleemput, O. Subsoils: chemo-and biological denitrification, N_2O and N_2 emissions. *Nutr. Cycl. Agroecosys.* **52,** 187–194 (1998).
34. Venterea, R. T. Nitrite-driven nitrous oxide production under aerobic soil conditions: kinetics and biochemical controls. *Global Change Biol.* **13,** 1798–1809 (2007).
35. Chao, T. T. Selective Dissolution of Manganese Oxides from Soils and Sediments with Acidified Hydroxylamine Hydrochloride1. *Soil Sci. Soc. Am. J.* **36,** 764–768 (1972).
36. Gierer, J. & Söderberg, S. Über die Carbonylgruppen des Lignins. *Acta Chem. Scand.* **13,** 1 (1959).
37. Bornemann, L., Herbst, M., Welp, G., Vereecken, H. & Amelung, W. Rock Fragments Control Size and Saturation of Organic Carbon Pools in Agricultural Topsoil. *Soil Sci. Soc. Am. J.* **75,** 1898–1907 (2011).
38. Gomori, G. Preparation of buffers for use in enzyme studies In *Handbook of Biochemistry and Molecular Biology 4th edn* (eds Lundblad, R. L. & F. M. MacDonald) 138–146 (CRC Press, 2010).
39. Berns, A. E. & Conte, P. Effect of ramp size and sample spinning speed on CPMAS ^{13}C NMR spectra of soil organic matter. *Org. Geochem.* **42,** 926–935 (2011).
40. R Development Core Team. R: A language and environment for statistical computing. R Foundation for Statistical Computing. Vienna, Austria. ISBN 3-900051-07-0, URL http://www.R-project.org/ (2013).

Acknowledgements

The authors wish to thank Holger Wissel for his analytical and technical assistance, Jannis Heil for providing the data for the simulations with the multiple regression model, Volker Nischwitz for the analysis of plant elemental composition, and Daniel Weymann and Franz Leistner for their assistance in the gas chromatography. This study was supported by the Chinese Scholarship Council (scholarship no. 201206760007).

Author Contributions

N.B. and S.L. conceived the experiments. S.L. conducted the experiments, analysed the data and drafted the manuscript. A.E.B. performed the NMR measurements. D.W. conducted the work related to the exclusion of biological nitrification activity in the artificial soil samples. All authors interpreted the data and contributed to writing the manuscript.

Additional Information

Supplementary information accompanies this paper at http://www.nature.com/srep

Competing financial interests: The authors declare no competing financial interests.

How to cite this article: Liu, S. *et al.* Interactive effects of MnO_2, organic matter and pH on abiotic formation of N_2O from hydroxylamine in artificial soil mixtures. *Sci. Rep.* **6**, 39590; doi: 10.1038/srep39590 (2016).

Publisher's note: Springer Nature remains neutral with regard to jurisdictional claims in published maps and institutional affiliations.

Paper X

Biogas digester hydraulic retention time affects oxygen consumption patterns and greenhouse gas emissions after application of digestate to soil.

Nguyen, Q., Jensen L, N., Bol, R., **Wu, D**., Triolo, J., Jensen,. Vazifehkhoran, A., Bruun, S., 2017.

Journal of Environmental Quality. Accepted

Published online August 31, 2017

Journal of Environmental Quality

TECHNICAL REPORTS

WASTE MANAGEMENT

Biogas Digester Hydraulic Retention Time Affects Oxygen Consumption Patterns and Greenhouse Gas Emissions after Application of Digestate to Soil

Quan Van Nguyen,* Lars Stoumann Jensen, Roland Bol, Di Wu, Jin Mi Triolo, Ali Heidarzadeh Vazifehkhoran, and Sander Bruun

Abstract

Knowledge about environmental impacts associated with the application of anaerobic digestion residue to agricultural land is of interest owing to the rapid proliferation of biogas plants worldwide. However, virtually no information exists concerning how soil-emitted N_2O is affected by the feedstock hydraulic retention time (HRT) in the biogas digester. Here, the O_2 planar optode technique was used to visualize soil O_2 dynamics following the surface application of digestates of the codigestion of pig slurry and agro-industrial waste. We also used N_2O isotopomer analysis of soil-emitted N_2O to determine the N_2O production pathways, i.e., nitrification or denitrification. Two-dimensional images of soil O_2 indicated that anoxic and hypoxic conditions developed at 2.0- and 1.5-cm soil depth for soil amended with the digestate produced with 15-d (PO15) and 30-d (PO30) retention time, respectively. Total N_2O emissions were significantly lower for PO15 than PO30 due to the greater expansion of the anoxic zone, which enhanced N_2O reduction via complete denitrification. However, cumulative CO_2 emissions were not significantly different between PO15 and PO30 for the entire incubation period. During incubation, N_2O emissions came from both nitrification and denitrification in amended soils. Increasing the HRT of the biogas digester appears to induce significant N_2O emissions, but it is unlikely to affect the N_2O production pathways after application to soil.

Core Ideas

- O_2 planar optode images system and N_2O isotopomer analysis were deployed.
- O_2 consumption was greater for digestate with a hydraulic retention time of 15 d than 30 d.
- N_2O production was smaller for digestate with a 15-d hydraulic retention time.
- Lower N_2O emission for 15-d retention time digestate was due to higher complete denitrification.

J. Environ. Qual.
doi:10.2134/jeq2017.03.0117
Supplemental material is available online for this article.
Received 27 Mar. 2017.
Accepted 1 Aug. 2017.
*Corresponding author (nguyen@plen.ku.dk; nvquan189@gmail.com).

Reportedly, one of the main advantages of anaerobic digestion is the reduction in greenhouse gas emissions from the manure handling system, including storage and land application. Anaerobic digestion residues—digestates—have been reported to reduce nitrous oxide (N_2O) emissions after application to soils compared with undigested materials (Petersen et al., 1996; Köster et al., 2015). The main reason for this has been ascribed to the fact that easily degradable organic matter is degraded and transformed into methane (CH_4) during anaerobic digestion. However, there is also reason to believe that digestates could increase the production of N_2O after land application, depending on the properties of the digestates applied (Abubaker et al., 2013). The high water content of digestates may induce N_2O production immediately on application to soils because it limits atmospheric oxygen (O_2) diffusion into the soil, thus favoring denitrification (Firestone et al., 1989). At the same time, the residual content of easily degradable organic matter in digestates applied to soil increases O_2 consumption by soil respiration, which is driven by the supply of available carbon (C). This means that the application of digestate enhances the O_2 depletion zones where denitrifiers are able to produce N_2O (Bollmann and Conrad, 1998; Zhu et al., 2015).

The added organic C can also be used as an electron donor in the denitrification process (Tiedje, 1988). Thus, a reduction in organic matter in the digester will subsequently reduce the depletion area and propensity for denitrification, resulting in less N_2O formation from soil after digestate application. However, anaerobic digestion generally results in the digestates having a higher ammonia content, which can be oxidized by nitrification and produce N_2O as a by-product. This process requires O_2 for oxidation and thereby enhances O_2 depletion in the soil following application (Zhu et al., 2014). Hence, the effect of anaerobic digestion on N_2O emissions in the field is complex and depends

Q.V. Nguyen, L.S. Jensen, and S. Bruun, Dep. of Plant and Environmental Sciences, Univ. of Copenhagen, Thorvaldsensvej 40, Frederiksberg 1871, Copenhagen, Denmark; Q.V. Nguyen, Dep. of Environmental Research for Livestock, National Institute of Animal Science, Hanoi 10000, Vietnam; R. Bol and D. Wu, Institute of Bio- and Geosciences, Agrosphere (IBG-3), Forschungszentrum Jülich GmbH, Jülich 52425, Germany; J.M. Triolo and A.H. Vazifehkhoran, Institute of Chemical Engineering, Biotechnology and Environmental Technology, Univ. of Southern Denmark, Campus Vej 55, Odense M 5230, Denmark. Assigned to Associate Editor Mindy Spiehs.

Abbreviations: DM, dry matter; HRT, hydraulic retention time; PO15, hydraulic retention time of 15 d; PO30, hydraulic retention time of 30 d; SP, site preference; VSMOW, Vienna Standard Mean Ocean Water; WFPS, water-filled pore space.

on the properties of the digestate resulting from the different feedstocks used, the residence time in the digester, and interactions with climate and soil types.

These complex and interacting effects have so far been examined only to a limited extent. One of the few studies was undertaken by Clemens et al. (2006), who examined the direct linkage between hydraulic retention time (HRT) of the digester and N_2O emissions after land application of the digestate. They reported that increasing HRT from 0 to 29 and 59 d decreased emissions of N_2O. However, they did not study the underlying mechanisms in any detail; therefore, a more thorough understanding of these mechanisms is needed.

It is well documented that the supply of organic C and soil O_2 are some of the most important factors driving nitrogen (N) transformation processes (Tiedje, 1988; Bollmann and Conrad, 1998; Morley and Baggs, 2010). However, the way in which the distribution of O_2 in soil is influenced by the distribution and degradability of the organic matter applied, and in turn how this affects N_2O production, has not yet been fully investigated. A visualization of soil spatiotemporal O_2 dynamics by planar O_2 optodes has proved useful for enhancing understanding of the processes leading to N_2O emissions after application of organic materials (Zhu et al., 2014, 2015; Nguyen et al., 2017). Furthermore, N_2O isotopomer techniques have been used widely to investigate the source of N_2O production pathways (Toyoda and Yoshida, 1999; Bol et al., 2003b; Sutka et al., 2006; Jinuntuya-Nortman et al., 2008; Ostrom et al., 2010; Köster et al., 2013; Wu et al., 2017). More recently, a combination of these techniques was used to quantify the effects of cattle slurry application on soil O_2 distribution and N_2O emission pathways (Nguyen et al., 2017).

The objectives of this study were (i) to quantify the effect of HRT during biogas production on N_2O emissions after land application of digestates and (ii) to understand the role of O_2 dynamics for the determination of the N_2O production through different N_2O production pathways (i.e., bacterial denitrification and nitrification). It has been reported that the shorter HRT of biogas production led to a higher biodegradable fraction in digestates compared with digestates produced with a longer HRT (Vazifehkhoran and Triolo, 2015). Thus, the HRT of the biogas digesters could influence the O_2 consumption in soil after application of digestates to the soils. The resulting spatial and temporal distribution of soil O_2 consequently would affect N_2O formation and emission. Therefore, we hypothesized that digestates produced with a shorter HRT would induce larger anoxic zones and N_2O reduction compared with the digestates produced with a longer HRT when using the same feedstock.

Materials and Methods

Digestates and Soil

Digestates from the codigestion of pig slurry and agro-industrial waste were produced in 20-L continuously stirred anaerobic reactors operated with a HRT of 15 d (PO15) or 30 d (PO30). The feedstocks consisted of 75% pig slurry (wet weight) and 25% agro-industrial waste (a mixture of supermarket, brewery, and slaughterhouse waste). The temperature in the reactors was mesophilic with 37°C, and the digestates were collected daily and stored at −20°C for later use. The procedure used to produce the digestates was previously described in detail by Vazifehkhoran and Triolo (2015). Before application, the digestates were thawed and analyzed for physicochemical properties. Soil was collected from an experimental field in Foulum, Denmark, and was characterized as a sandy loam soil (79.1% total sand, 9.6% silt, 8.9% clay, 2.4% humus w/w). It was freshly sieved, field moist (<2 mm) just before the start of the experiment.

The dry matter contents of the digestates and the soil were determined by weight loss at 105°C for 24 h, and their total organic matter contents (loss on ignition) were determined after ignition at 550°C for 3 h. To determine the total organic N contents and total organic C of the digestates and the soil, the fresh samples of the digestates were dried at 70°C for 48 h, and samples of the soil were dried at 105°C for 24 h. These were then ground and analyzed using an elemental analyzer (vario PYRO cube; Elementar). The mineral N content of the digestates and the soil samples were measured after extraction with 1 M KCL (1:25 w/v). The extraction was then analyzed for NH_4^+ and NO_3^- concentrations by flow injection analysis (FIA-Series 8000; QuickChem). The total inorganic C content of the digestates was determined by measuring the carbon dioxide (CO_2) content released after acidification of 10 g fresh digestate samples with equivalent amounts of 1 M H_2SO_4 acid to reach pH 2.0 for each of the digestates using gas chromatography (450-GC; Bruker). The samples were kept in 0.75-L closed glass jars for 2 h. The physicochemical properties of the digestates and soil samples are presented in Table 1.

Incubation Experiment

An incubation experiment was conducted under laboratory conditions for 5 d to evaluate the dynamics of soil O_2 distribution and CO_2 and N_2O emissions after application of the digestates. The experiment consisted of three treatments: PO15, PO30, an untreated control soil (COTR). All treatments were performed with three replicates. The soil was packed in Plexiglas boxes (10 by 6 by 4 cm) fitted with planar O_2 optode foil on the front and rubber septa at the rear for gas sampling (Supplemental Fig. S1). The soil was compressed to a bulk density of 1.3 g cm^{-3}. Before digestate application, 17 mL of water was added to all optode chambers to achieve ~73% water-filled pore space (WFPS) and

Table 1. Properties of the soil and digestates used in the incubation experiment.

Measurements	Unit	Soil	PO15†	PO30†
Dry matter	g 100 g^{-1}	86.9	4.0	3.6
Organic matter (LOI‡)	% DM		64.8	66.2
Ammonium nitrogen (NH_4^+–N)	g kg^{-1} DM	2.2×10^{-3}	20.9	32.2
Nitrate (NO_3–N)	mg kg^{-1} DM	13.9	nil§	nil
Total organic N	% DM	0.25	2.63	2.58
Total organic C	% DM	2.0	36.0	35.2
Total inorganic C	g kg^{-1} DM		16.5	19.52
C/N ratio		8.2	13.7	13.7
pH		6.7	8.6	8.1

† Digestate of 75% pig slurry codigested with 25% agro-industrial waste (wet weight basis) at hydraulic retention times of 15 d (PO15) and 30 d (PO30).

‡ LOI: loss on ignition, 550°C oven for 3 h.

§ nil: negligible ~ 0 (mg kg^{-1} dry matter).

left for 48 h to equilibrate and for soil O_2 to stabilize. After this period, the digestates were applied to 50% of the soil surface at the rate corresponding to 100 kg NH_4^+ ha^{-1} (equivalent to 33.3 mg N kg^{-1} soil dry matter [DM]) for both PO15 and PO30 treatments, producing a final WFPS of 85% for all treatments, which was maintained throughout the incubation. The soil was left to incubate for 5 d at a temperature of 19 to 20°C. The detailed calculation of application rate is presented in the Supplemental Material (Supplemental Table S1).

Oxygen Optode and Soil Oxygen Imaging

During the incubation, images of the O_2 distribution were recorded every 30 min using the optode system (Supplemental Fig. S1). The system was previously described in detail by Zhu et al. (2015) and is based on the measurement principles described in Larsen et al. (2011). The optode system was calibrated using two calibration points of 0% and 100% of O_2 concentration in air-saturated water solution (Larsen et al., 2011). Soil O_2 content was calculated as the average O_2 content obtained for the entire optode window cross-sectional area (5 by 4 cm) and expressed as a percentage of air saturation using a free software ImageJ v. 1.50i (National Institutes of Health, 2016). Soil O_2 conditions were defined as anoxic, hypoxic, and oxic condition corresponding to <1%, 1 to 30%, and >30% air saturation, respectively (Zhu et al., 2014).

Trace Gas Emissions

Headspace gas sampling was performed 6, 24, 48, 72, and 96 h after digestate application to determine gas emissions and to perform N_2O isotopomer analysis. On each sampling occasion, the chamber was closed, and 5 mL headspace gas samples were taken every 20 min for 1 h, after which the chamber was opened again. Gas samples were injected into 3-mL pre-evacuated glass vials (Labco), and the concentrations of N_2O, CO_2 and CH_4 were determined by gas chromatography (GC-450; Bruker). Gas emission rates were calculated as the slope of a straight line fitted to the concentration of the gases in the headspace during the closed period. Cumulative gas emissions were calculated from the emission rates using the trapezoidal integration rule.

Nitrous Oxide Isotopomer and Source Partitioning

For N_2O isotopomer analysis, 25-mL gas samples were taken after a 1-h closed time on four occasions: 6, 24, 48, and 96 h after digestate application. By repeating this process, five 25-mL gas samples were collected and bulked into a 120-mL pre-evacuated crimped bottle to measure the N_2O isotopomer samples. The N_2O isotope signatures of soil-emitted N_2O gas samples, $\delta^{15}N^{\alpha}$, $\delta^{18}O$, the average $\delta^{15}N$ of the N_2O molecule ($\delta^{15}N^{bulk}$), were determined by measuring mass-to-charge ratio (*m/z*) 44, 45, 46 of intact N_2O^+ molecular ions, and *m/z* 30, 31 of NO^+ fragment ions using an isotope ratio mass spectrometer (IRMS-IsoPrime 100; Elementar Analysensysteme). The site preference (SP) value of soil-emitted N_2O is defined as SP = $\delta^{15}N^{\alpha} - \delta^{15}N^{\beta}$, where $\delta^{15}N^{\beta}$ is the isotopic signature of $\delta^{15}N$ at the terminal position, which was calculated as $\delta^{15}N^{\beta} = 2\times\delta^{15}N^{bulk} - \delta^{15}N^{\alpha}$ (Toyoda and Yoshida, 1999). The soil emitted N_2O isotope signatures on day t (R_t) including $\delta^{18}O$, $\delta^{15}N$, and SP values were corrected with the reference N_2O isotope signatures of the ambient air in the laboratory using Eq. [1]. The measured $\delta^{18}O$ and $\delta^{15}N$ isotope signatures were expressed with respect to Vienna Standard Mean Ocean Water (VSMOW) and air standards, respectively. The correction and calibration of the measurements are detailed by Heil et al. (2015).

$$R_t = \frac{(R_{\text{sample}(t)} \times N_2O_{\text{sample}(t)} - R_{\text{air}} \times N_2O_{\text{air}})}{(N_2O_{\text{sample}(t)} - N_2O_{\text{air}})} \quad [1]$$

where N_2O_{air} and R_{air} are the average N_2O concentration and the corresponding $\delta^{18}O$, $\delta^{15}N$, and SP values of the laboratory air samples in the optode chambers before closure at t_0 (269 ± 5 ppb), and $N_2O_{sample(t)}$ and $R_{sample(t)}$ are the soil-derived N_2O concentration and their corresponding isotope signatures (i.e., either $\delta^{18}O$, $\delta^{15}N$, or SP) of the samples collected from optode chambers 40 min after closure (t_{40}) at day t.

The source partitioning of N_2O production was used to separate N_2O derived from either nitrification/fungal denitrification or bacterial denitrification. This was done by a two-end-member isotopic mass balance equation:

$$SP_t = SP_D \times f_D + SP_N \times f_N \quad [2]$$

where SP_t is the corrected site preference of soil-emitted N_2O obtained from Eq. [1], SP_D and SP_N are the SP values of N_2O produced by bacterial denitrification and bacterial nitrification or fungal denitrification in pure cultures, which ranges between −10 and 0‰ (average −5‰) and 33 to 37‰ (average 35‰), respectively (Toyoda et al., 2005; Sutka et al., 2006), and f_D and f_N are the portions of N_2O derived from bacterial denitrification and nitrification and/or fungal denitrification to total N_2O release ($f_D + f_N = 100\%$). Rearranging Eq. [2], the following equation was obtained:

$$f_D = [SP_t - SP_N \ (1 - f_N)]/SP_D \quad [3]$$

which can be used to calculate the contribution of bacterial denitrification to total N_2O production, f_D.

Statistical Analyses

All statistical analyses were performed using one-way analysis of variance (ANOVA) and Tukey multiple comparisons in RStudio (version 0.99.878) to determine the significant differences in the means of gas fluxes, cumulative gas emissions, N_2O isotopic signatures, SP values, and O_2 concentration between treatments. The significant differences were accepted at the level of probability of $P < 0.05$. Linear regression analyses were performed to examine the relationships between isotopic signatures of the soil-emitted N_2O between each treatment and for all treatments. Pearson correlation coefficients were obtained for the correlation between ^{18}O–N_2O and $^{15}N^{\alpha}$–N_2O.

Results and Discussion

Temporal and Spatial Distribution of Soil Oxygen

During the 48-h pre-incubation period, the soil O_2 content stabilized at approximately 75% air saturation throughout the soil cores of all treatments. However, the O_2 content was substantially depleted in the digestate-treated soils approximately 12 h

after digestate application (Fig. 1). In contrast, the O_2 content remained stable in the control soil after the addition of water. This is in line with Zhu et al. (2014), who observed rapid development of the anoxic and hypoxic zones within the first 5 h of pig manure application to soil, either in layers or mixed into the soil. Similarly, Nguyen et al. (2017) applied cattle slurry to the soil surface and observed a depletion zone developing beneath the application area after just 2 h, with the most extensive depletion between 18 and 24 h.

The recorded depletion zone clearly covered a larger area for PO15 than for PO30 (Fig. 1 and Supplemental Videos S2–S3). Within the first 24 h, anoxic zones developed rapidly for PO15 and peaked on approximately 30% of the total 4- by 6-cm image area, as opposed to only 10% for PO30 (Supplemental Fig. S2). The anoxic area that developed in the current study was much less extensive than in the study by Zhu et al. (2014) due to lower biodegradable organic matter in the digestate compared with undigested material. Hypoxic zones were similar in size for PO15 and PO30 within the first 24 h after digestates application, but it was much larger and remained the predominant soil condition in PO15 from 24 to 48 h compared with PO30, where the hypoxic zone was quickly reduced during this period.

The fact that the O_2 depletion zones were much larger for PO15 than PO30 suggests that more easily biodegradable organic C in the PO15 digestate still remained as a result of the shorter 15-d HRT. This resulted in a higher demand for O_2 after application compared with that of the PO30 digestate produced with 30-d HRT. The obvious explanation for this is that during anaerobic digestion, easily degradable organic C in the substrates is gradually transformed into CH_4, and this process works more efficiently when the substrates have a longer retention time in biogas digesters (Vazifehkhoran and Triolo, 2015; Fitamo et al., 2016). The presence of more biodegradable organic matter applied in the PO15 treatment—a total organic C of 478.7 mg kg^{-1} soil dry weight for PO15 compared with 388.2 mg kg^{-1} for PO30 (Supplemental Table S2)—therefore stimulated greater microbial activity, which is the main reason for the more severe depletion of O_2 in the PO15 treatment. Another possible explanation for the stronger depletion of the O_2 content in the PO15 treatment compared with the PO30 treatment could be higher consumption by nitrification. However, since the application of the digestates was based on the same total amount of NH_4^+ for PO15 and PO30, it was assumed that O_2 consumption for nitrification would be similar for both PO15 and PO30.

The O_2 images showed that the O_2 depletion zones developed immediately beneath the area where the digestates were applied and expanded both downward and horizontally in both directions (Fig. 1). The stronger O_2 depletion in the upper soil layers (0–2 cm) was caused by their proximity to the applied manure, with most of the O_2 consumption occurring in the upper layer of soil through which dissolved organic matter percolates. This is supported by Bol et al. (2003a), who reported that easily biodegradable, cattle manure-derived C is likely to be the main source of C for soil microbial respiration within the first 48 h in the top 2-cm soil layer after application. Recently, Nguyen et al. (2017) also observed a depletion zone in the upper 1.5 cm after application of cattle slurry on the soil surface. However, in that study, there was a tendency for a less intensive depletion of soil O_2 below the soil surface, presumably because of a higher influx of O_2 from the surface. It is not clear why this influx is more restricted in the current study, but it could be related to the physical properties of the soil (e.g., soil bulk density, pore size, and soil WPFS) and their interaction with soil biological processes (Balaine et al., 2013, 2016; Owens et al., 2017). Soil porosity and macroporosity declines with increasing soil bulk density (Balaine et al., 2013). Therefore, the higher soil bulk density of 1.3 g cm^{-3} for the present study could lead to a lower O_2 diffusion from the

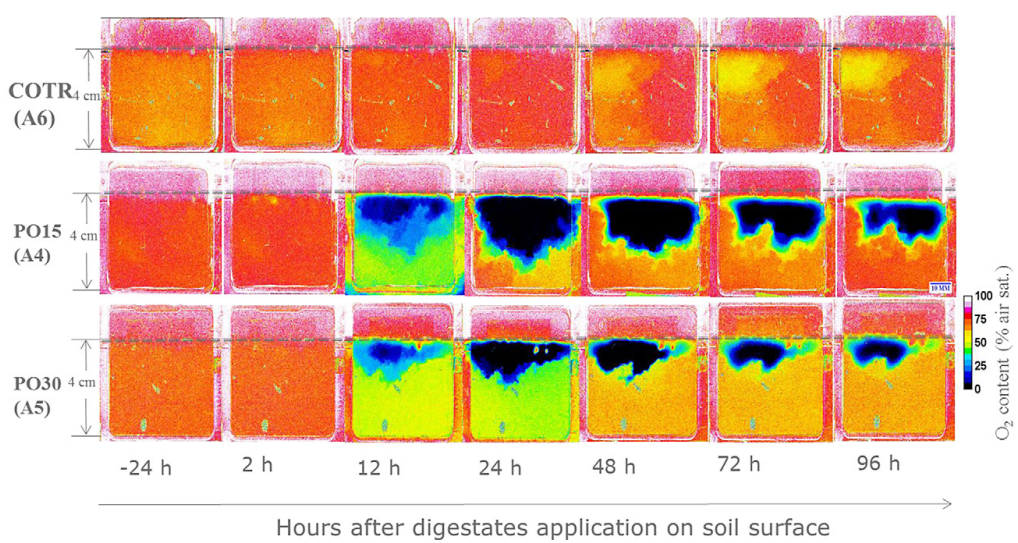

Fig. 1. Selected two-dimensional images of soil O_2 distribution (% air saturation) at different times after digestate application for a representative chamber (1 replicate) of the control (COTR, Supplemental Video S1), digestate with a 15-d retention time (PO15, Supplemental Video S2) and a 30-d retention time (PO30, Supplemental Video S3). For others replicates during the incubation, see Supplemental Videos S4–S9).

soil surface into the deeper soil layers compared with 1.0 g cm^{-3} in Nguyen et al. (2017). Also, the relatively high dry matter content of the cattle slurry (11.5% w/w) in their study compared with that of the digestates (3.6–4.0% w/w) in the present study is likely to limit the infiltration of easily biodegradable, soluble or fine particulates into the soil, thereby causing fewer O_2 depletion zones beneath the application areas.

It is apparent from the optode images that O_2 from the headspace of the chambers diffused into the soil through the surface areas on which the digestates were not applied (Fig. 1). This clearly diminished the O_2 depletion zones for both the PO15 and the PO30 treatments in the upper soil layer and led to the increase in soil O_2 content outside the application area (Supplemental Videos S2–S3). This implies that O_2 consumption was lower in the areas without digestate application than in the application areas. After 48 h, soil O_2 increased throughout the soil cores for both PO15 and PO30 (Fig. 1, Supplemental Fig. S2). This demonstrates that the demand for O_2 for microbial respiration and nitrification decreased, presumably because the applied active labile C and N had been consumed by this time and the influx of O_2 from ambient air was greater than O_2 consumption. Although the soil water content was as high as 85% WFPS in the control soil, oxic conditions dominated in the soil cores throughout the incubation period. This was due to the low O_2 demand for both microbial respiration and ammonium oxidation since soil organic C (2% DM) and soil NH_4^+ (2.2 mg kg^{-1} DM) were relatively limited (Table 1).

Greenhouse Gas Emissions

During the incubation, CH_4 emissions from all treatments remained at a very low level (<0.1 μg kg^{-1} soil h^{-1}); however, the CO_2 and N_2O emissions from digestate-treated soils were substantially higher than from the control soil (Fig. 2A–B). The CH_4 emissions (data not shown) were comparable to previous incubation studies for digestate soil amendments (Odlare et al., 2012; Abubaker et al., 2013). In both digestate soil amendments, CO_2 emissions already occurred at a considerable rate (~1.2 mg C kg^{-1} soil h^{-1}) at 6 h after digestate application but then declined toward the end of the incubation, whereas CO_2 emissions from the control soil were negligible (~0.05 mg C kg^{-1} soil h^{-1}) and relatively constant. This is in line with previous studies (Köster et al., 2011, 2015; Alburquerque et al., 2012), which reported a pronounced initial peak of CO_2 evolution during the initial 24 h after application of a digestate from the codigestion of pig slurry and/or cattle manure with agro-industrial wastes with HRT about 56 d. It is assumed that the main difference between the digestates with retention times of 15 and 30 d is the content of labile biodegradable C, with less difference in the recalcitrant organic C content. Thus, since most of the labile C was respired by aerobic microbes at the start of the incubation, the recalcitrant organic C was left behind in the soil and decomposed at slower rates in both PO15 and PO30, resulting in the decline in CO_2 evolution and lower demand for O_2 consumption for soil respiration. Although the total organic C applied in PO15 was much higher than in PO30 (Supplemental Table S2), the total C mineralization (% CO_2–C released of C added) over the 5-d incubation for PO15 was not significantly higher than that of PO30 (Supplemental Table S3). This could be due to the higher anoxic conditions developing in PO15, which limited the magnitude of soil aerobic respiration and reduced the magnitude of difference in CO_2 evolution compared with PO30.

For N_2O emissions, both digestate treatments induced a significant N_2O flux compared with the control, but the magnitude of this stimulation varied between the digested materials. The N_2O emissions from the control were negligible (~0.01 μg N kg^{-1} soil h^{-1}) throughout the incubation, as expected, due to the low NH_4^+ content in the soil and hence limited nitrification. Also, the high O_2 content throughout the soil matrix (75% air saturation) limited denitrification (Smith and Tiedje, 1979). However, for the digestate-amended soils, both processes could have occurred where the presence of added NH_4^+ and organic C caused considerably higher N_2O emissions (Fig. 2A, C).

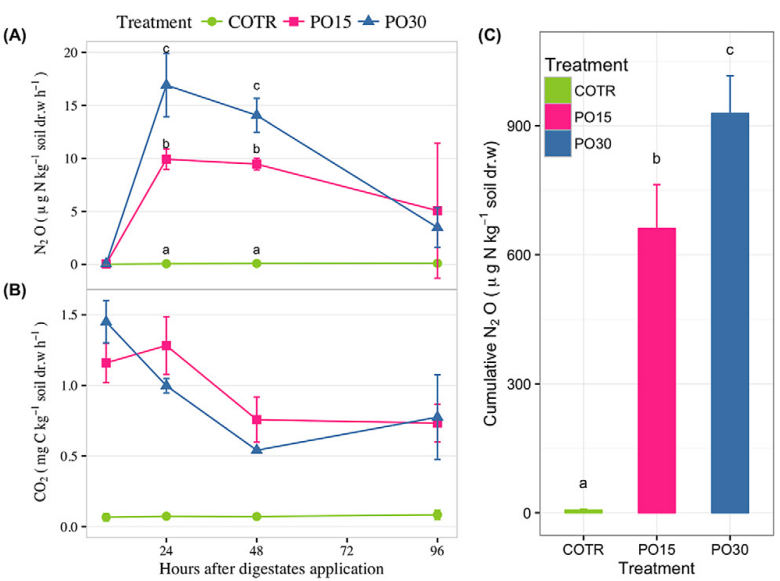

Fig. 2. Gas fluxes (A) N_2O, (B) CO_2 and (C) total cumulative N_2O emissions over the entire 5-d incubation period for the control (COTR), soil treated with digestate with a 15-d retention time (PO15), and soil treated with digestate with a 30-d retention time (PO30). Letters indicate significant differences with $P < 0.05$; error bars indicate standard deviation of the mean values.

Higher N_2O emissions after the application of digestates to soils compared with the unfertilized control soils were previously reported (Köster et al., 2011; Rodhe et al., 2012; Abubaker et al., 2013). Our study showed that N_2O emissions were still very low (<0.1 μg N kg^{-1} soil h^{-1}) in both PO15 and PO30 6 h after application, when oxic conditions remained the dominant condition in all treatments (Supplemental Fig. S2). However, after this, N_2O increased dramatically and peaked after 24 h for both digestate treatments, simultaneously with the strongest O_2 depletion in the soils. This initial peak of N_2O was previously reported after slurry application (Petersen et al., 1996, 2016; Nguyen et al., 2017) and digestate application (Köster et al., 2011, 2015; Abubaker et al., 2013).

The N_2O flux was nearly twice as high in PO30 as in PO15 at its peak and remained greater over the next few days, resulting in significantly higher cumulative N_2O emissions over the entire 5-d incubation period for PO30 than for PO15. This could suggest that the higher O_2 consumption in PO15 during the initial 48 h, which was due to the higher respiration activities as previously discussed, significantly decreased soil-emitted N_2O. The most plausible explanation for this is that the widespread anoxia developing in the PO15 treatment within the first 24 h after application did more to stimulate complete denitrification, where N_2O is reduced to N_2. In contrast, this step did not occur to the same extent in the PO30 treatment because of the relatively lower anoxia areas compared with PO15. This explanation is partly supported by Miller et al. (2009), who reported the negative correlation between respiration rate and N_2O molar ratio, that is, $N_2O/(N_2O + N_2)$, in liquid manure-amended soils. These authors therefore proposed that a higher C substrate availability in soil enhances the reduction of N_2O to N_2.

The complete denitrification step was previously observed with the high water content in digestate-amended soil where no immediate N_2O peak was reported after the application of anaerobically digested cattle manure (Köster et al., 2015), although in their study, the relatively high initial soil nitrate (31 mg kg^{-1} soil DM) at 90% WFPS soil moisture level contents usually resulted in N_2O peaking shortly after the application of digestate. In the present study, the application of higher labile C clearly increased demand for terminal electron acceptors (NO_3^-) in PO15 relative to PO30. Consequently, readily available soil NO_3^- (13.9 mg kg^{-1} soil DM) was used preferentially, and immediately, within the initial 24 h to produce N_2O (Cho et al., 1997) in the digestate-amended soils. However, the anoxia was approximately 10 and 15% of the total area for the PO30 and PO15, respectively, at the peak of N_2O emissions by 24 h, whereas the hypoxia fraction was close to 60% of the total area for both PO15 and PO30 (Supplemental Fig. S2). This condition was not optimum for the dominance of complete denitrification in digestate-amended soils.

The N_2O emission rate gradually reduced over the following days and approached the background level after 96 h for both PO30 and PO15, with oxic conditions returning in >80% of the total soil area (Fig. 1, Supplemental Fig. S2). Thus, at this point, it was concluded that either a lack of electron donor (digestate-derived organic C) and electron acceptor (soil NO_3^-) supply for denitrification or the dominance of oxic conditions in soils inhibited N_2O production from the denitrification process.

Nitrous Oxide Isotopomer Signatures and Source Partitioning

Nitrous oxide isotopomer signatures showed that the SP values, $\delta^{18}O$ (VSMOW), and $\delta^{15}N^{\alpha}$ of soil-emitted N_2O for digestate-treated soils fluctuated, whereas the values were almost constant for the untreated control soil during the incubation period (Fig. 3). For the control soil, N_2O emissions were very low; hence, the SP values of emitted N_2O for the control were similar to those of the ambient air, approximately 17‰ (Yoshida and Toyoda, 2000). In contrast, the SP values of digestate-treated soils clearly increased from 17 to 24‰ in both digestate treatments during the initial 24 h, thereafter gradually declining over the next few days (Fig. 3B).

The SP values of soil-emitted N_2O from PO15 and PO30 at most of the sampling times, except at 24 h, were within the range

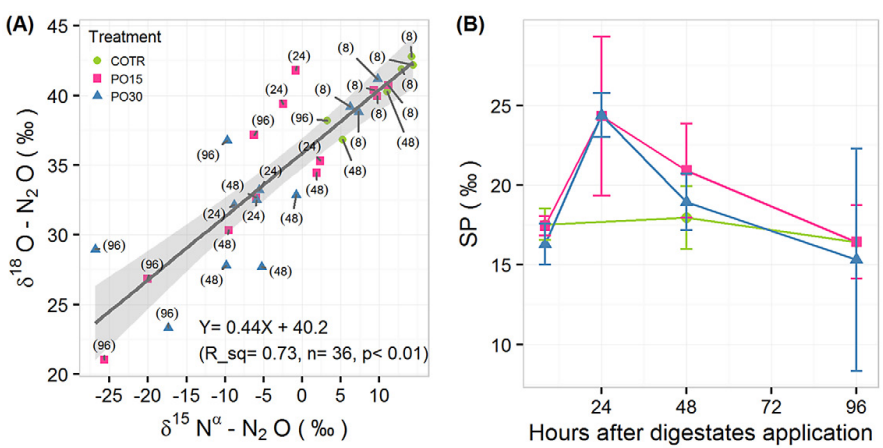

Fig. 3. (A) Correlation between $\delta^{18}O$-N_2O (Vienna Standard Mean Ocean Water) and $\delta^{15}N^{\alpha}$-N_2O for treatment control (COTR), digestates with a 15-d retention time (PO15), and digestates with a 30-d retention time (PO30). Data represent each single measurement for replicates. Numbers in parentheses indicate sampling time (hours after application). The individual correlation between the isotopic signatures within each treatment is shown in Supplemental Table S4. (B) Site preference (SP) values of soil-emitted N_2O during the entire 5-d incubation period.

of predominant bacterial denitrification-produced N_2O in soil environments (Bol et al., 2003b; Well et al., 2006; Opdyke et al., 2009; Köster et al., 2011, 2015). Within the initial hours and/or days after slurry-related material application to soils, the initial peak of N_2O has often been observed and attributed to denitrification of the soil nitrate following the addition of active C and N. This stimulates activities of nitrifiers and denitrifiers at the manure "hot-spot," thus creating O_2 depletion zones and inducing N_2O production (Paul et al., 1993; Petersen et al., 1996; Meyer et al., 2002; Köster et al., 2011; Markfoged et al., 2011; Abubaker et al., 2013). However, by 24 h, the highest SP values for both PO15 and PO30 were around 25‰, at the peak of N_2O emissions, corresponding to approximately only 26% of the estimated N_2O originating from bacterial denitrification according to the two-end-member equation (Supplemental Table S5). A likely explanation for these relatively high SP values is the isotope fractionation effects of the N_2O reduction via complete denitrification (Ostrom et al., 2007; Jinuntuya-Nortman et al., 2008; Well and Flessa, 2009; Köster et al., 2013). Thus, the estimation of N_2O derived from bacterial denitrification based on a two-end-member calculation using Eq. [3] can be underestimated (Wu et al., 2016).

Against this backdrop, it could be expected that complete denitrification occurred in both PO15 and PO30. However, the extent of this could not be quantified since N_2 emissions were not measured in the present study. It has been reported that the SP fractionation factor of N_2O reduction values ranges from −16.4 to −1.9‰ (Well and Flessa, 2009). Taking this variation into account, the increasing SP values in the present study are a good indication that N_2O reduction via complete denitrification occurred within the initial 24 h after digestate application. This is also supported by Köster et al. (2015), who reported that the $N_2O/(N_2O + N_2)$ product ratio was close to zero during the initial period (<24 h) after either cattle slurry or its digestate were applied to soils, and this ratio then increased in the later stages.

Alternatively, Nguyen et al. (2017) proposed that an early peak of N_2O occurring within the initial 24 h after cattle slurry applied on the soil surface could be associated with fungal denitrification in an acidic grassland soil (pH 5.7). Although fungal denitrification was also reported as a major source of N_2O production at the relative neutral soil pH 6.3 (Laughlin and Stevens, 2002), the soil moisture content in their study was relatively low at 65% WFPS, which significantly influenced the contribution from fungal denitrification. Chen et al. (2015) demonstrated that the fungal-to-bacterial contribution ratio at high WFPS such as 85 and 90% were significantly lower than that of 65 and 75% WFPS. Therefore, in the present study, the higher soil pH 6.7 and soil moisture content (85% WFPS) were not likely optimal conditions for fungal denitrification. In addition, the potential for fungal denitrification to produce N_2O remains in soils with enhanced organic C (Laughlin and Stevens, 2002; Köster et al., 2015) and under subanoxic conditions (Jirout et al., 2013; Chen et al., 2015; Lewicka-Szczebak et al., 2016). In the present study, the O_2 optode images showed that anoxic and subanoxic conditions (hypoxia) dominated within the first 24 h; thus, fungal denitrification could play a role in N_2O production during this period. The contribution from fungal denitrification could be also considerable after the initial 24 h in the PO15 treatment since the hypoxia remained widespread in PO15 until 48 h (Supplemental Fig. S2). However, the SP values had declined substantially between 24 h and 48 h (Fig. 3B), indicating that fungal denitrification was unlikely the dominating source of N_2O production after the first 24 h in the present study. Therefore, the N_2O fluxes from fungal denitrification was possibly important during the first 24 h but unlikely to be the dominant source for the entire course of the incubation under the present experimental setup.

After 24 h, since the N and O isotopic signatures of soil-emitted N_2O were gradually depleted toward the end of the incubation from 0 to −25‰ and from 40 to 30‰, respectively, the dominant source of N_2O production appeared to be shifting toward bacterial denitrification (Mandernack et al., 2000). This was evidenced by the significant positive correlation between $\delta^{18}O\text{-}N_2O$ and $\delta^{15}N^{\alpha}\text{-}N_2O$ with a slope of 0.44 (Fig. 3A, Supplemental Table S4), which is typical for systems in which N_2O is produced and consumed simultaneously (Mandernack et al., 2000; Ostrom et al., 2007). These observations were in accordance with the decline of SP values after 24 h toward the end of the incubation.

The estimated contribution of bacterial denitrification to N_2O increased from 26 to 35 and 46% for PO15 and from 26 to 45 and 55% for PO30 between 24, 48, and 96 h after application, respectively (Supplemental Table S5). This seemingly contrasts with the fact that significantly lower CO_2 fluxes observed compared with the fluxes within the initial 24 h is indicating the depletion of the electron donor (organic C) in the later phases (48 h, 96 h). This could diminish the extent of denitrification in both digestate treatments. It has been reported that aerobic respiration is positively correlated with denitrifier community abundance in slurry-amended soils (Miller et al., 2009; Köster et al., 2015). Furthermore, either the development of oxic conditions toward the end of the experiment after 48 h, which could inhibit NO_3^- reduction, or limited supply of soil NO_3^- presumably resulted in a reduction in denitrification in the later phase of the incubation. In addition, higher labile C applied to the soil for PO15 provided more available energy for denitrifier organisms compared with PO30, leading to an expectation of higher denitrification in PO15 than in PO30. However, the estimated bacterial denitrification for these two treatments on each sampling day were similar, indicating that denitrification was unlikely to be limited by the C supply in the digestate-amended soils. Consequently, the effect of HRT on the source partitioning of soil-emitted N_2O was not significant in the present study.

During the 5-d incubation period, the contribution of either nitrification and/or fungal denitrification or bacterial denitrification to N_2O production from digestate-treated soils was not influenced by HRT. The estimation of sources of N_2O production based on the two-end-member of the SP values indicated that nitrification appeared to be the dominant N_2O production contributor in the digestate treatments (Supplemental Table S5), even though denitrification was expected to be the main production pathway at a high soil moisture content in this experimental setup. This is partly because of the relatively low emission rates measured during the incubation for both digestate treatments compared with the peak after 24 h, which resulted in a small contribution of bacterial denitrification to the total cumulative N_2O for the entire incubation period.

Conclusions

Soil O_2 content was substantially depleted in the 0- to 2-cm soil depth after surface application of the digestates. Higher O_2 consumption in the PO15 compared with PO30 treatment resulted in larger anoxic and hypoxic zones for at least 48 h after application. The larger area of anoxia led to an apparently more complete reduction of NO_3^- to N_2 in the PO15 treatment, thus reducing N_2O emissions. The longer hydraulic retention time of digestate induced significantly higher N_2O emissions after soil application, probably due to lower microbial O_2 consumption and hence the lesser extent of anoxia. The N_2O source partitioning was not significantly affected by the biogas digester retention time ($P > 0.05$). During the incubation, the N_2O isotopomer signatures indicated that both denitrification and nitrification apparently contributed to produce N_2O emission for both digestates. The isotopic fractionation during the reduction of N_2O to N_2 in the initial 24 h may have led to some underestimation of N_2O produced by bacterial denitrification.

Acknowledgments

We acknowledge the research funding from the Danish Council for Strategic Research (DSF), through the project "Optimization of value chains for biogas production in Denmark (BioChain)" (Grant number: 12-132631). We are grateful to Søren O. Petersen and Khagendra Raj Baral of Aarhus University, Denmark, for their comments on the experimental design and for providing the soil samples. Thanks to Ronnie N. Glud and Morten Larsen of the University of Southern Denmark for their advice and technical support with oxygen optode imaging systems. We appreciate constructive feedbacks from two anonymous reviewers.

References

Abubaker, J., M. Odlare, and M. Pell. 2013. Nitrous oxide production from soils amended with biogas residues and cattle slurry. J. Environ. Qual. 42:1046–1058. doi:10.2134/jeq2012.0247

Alburquerque, J.A., C. de la Fuente, and M.L. Bernal. 2012. Chemical properties of anaerobic digestates affecting C and N dynamics in amended soils. Agric. Ecosyst. Environ. 160:15–22. doi:10.1016/j.agee.2011.03.007

Balaine, N., T.J. Clough, M.H. Beare, S.M. Thomas, and E.D. Meenken. 2016. Soil gas diffusivity controls N_2O and N_2 emissions and their ratio. Soil Sci. Soc. Am. J. 80(3):529–540. doi:10.2136/sssaj2015.09.0350

Balaine, N., T.J. Clough, M.H. Beare, S.M. Thomas, E.D. Meenken, and J.G. Ross. 2013. Changes in relative gas diffusivity explain soil nitrous oxide flux dynamics. Soil Sci. Soc. Am. J. 77(5):1496–1505. doi:10.2136/sssaj2013.04.0141

Bol, R., E. Kandeler, W. Amelung, B. Glaser, M.C. Marx, N. Preedy, and K. Lorenz. 2003a. Short-term effects of dairy slurry amendment on carbon sequestration and enzyme activities in a temperate grassland. Soil Biol. Biochem. 35:1411–1421. doi:10.1016/S0038-0717(03)00235-9

Bol, R., S. Toyoda, S. Yamulki, J.M.B. Hawkins, L.M. Cardenas, and N. Yoshida. 2003b. Dual isotope and isotopomer ratios of N_2O emitted from a temperate grassland soil after fertiliser application. Rapid Commun. Mass Spectrom. 17:2550–2556. doi:10.1002/rcm.1223

Bollmann, A., and R. Conrad. 1998. Influence of O_2 availability on NO and N_2O release by nitrification and denitrification in soils. Glob. Change Biol. 4:387–396. doi:10.1046/j.1365-2486.1998.00161.x

Chen, H., N.V. Mothapo, and W. Shi. 2015. Soil moisture and pH control relative contributions of fungi and bacteria to N2O production. Microb. Ecol. 69(1):180–191. doi:10.1007/s00248-014-0488-0

Cho, C.M., D.L. Burton, and C. Chang. 1997. Kinetic formulation of oxygen consumption and denitrification processes in soil. Can. J. Soil Sci. 77:253–260. doi:10.4141/S96-056

Clemens, J., M. Trimborn, P. Weiland, and B. Amon. 2006. Mitigation of greenhouse gas emissions by anaerobic digestion of cattle slurry. Agric. Ecosyst. Environ. 112:171–177. doi:10.1016/j.agee.2005.08.016

Firestone, M., E. Davidson, M. Andreae, and D. Schimel. 1989. Microbiological basis of NO and N2O production and consumption in soil. In: M.O. Andreae and D.S. Schimel, editors, Exchange of trace gases between terrestrial ecosystems and the atmosphere. John Wiley & Sons, New York. p. 7–21.

Fitamo, T., A. Boldrin, K. Boe, I. Angelidaki, and C. Scheutz. 2016. Co-digestion of food and garden waste with mixed sludge from wastewater treatment in continuously stirred tank reactors. Bioresour. Technol. 206:245–254. doi:10.1016/j.biortech.2016.01.085

Heil, J., S. Liu, H. Vereecken, and N. Brüggemann. 2015. Abiotic nitrous oxide production from hydroxylamine in soils and their dependence on soil properties. Soil Biol. Biochem. 84:107–115. doi:10.1016/j.soilbio.2015.02.022

Jinuntuya-Nortman, M., R.L. Sutka, P.H. Ostrom, H. Gandhi, and N.E. Ostrom. 2008. Isotopologue fractionation during microbial reduction of N_2O within soil mesocosms as a function of water-filled pore space. Soil Biol. Biochem. 40:2273–2280. doi:10.1016/j.soilbio.2008.05.016

Jirout, J., M. Šimek, and D. Elhottová. 2013. Fungal contribution to nitrous oxide emissions from cattle impacted soils. Chemosphere 90(2):565–572. doi:10.1016/j.chemosphere.2012.08.031

Köster, J.R., L. Cárdenas, M. Senbayram, R. Bol, R. Well, M. Butler, K.H. Mühling, and K. Dittert. 2011. Rapid shift from denitrification to nitrification in soil after biogas residue application as indicated by nitrous oxide isotopomers. Soil Biol. Biochem. 43:1671–1677. doi:10.1016/j.soilbio.2011.04.004

Köster, J.R., L.M. Cárdenas, R. Bol, D. Lewicka-Szczebak, M. Senbayram, R. Well, A. Giesemann, and K. Dittert. 2015. Anaerobic digestates lower N_2O emissions compared to cattle slurry by affecting rate and product stoichiometry of denitrification: An N_2O isotopomer case study. Soil Biol. Biochem. 84:65–74. doi:10.1016/j.soilbio.2015.01.021

Köster, J.R., R. Well, K. Dittert, A. Giesemann, D. Lewicka-Szczebak, K.-H.H. Mühling, A. Herrmann, J. Lammel, and M. Senbayram. 2013. Soil denitrification potential and its influence on N_2O reduction and N_2O isotopomer ratios. Rapid Commun. Mass Spectrom. 27:2363–2373. doi:10.1002/rcm.6699

Larsen, M., S.M. Borisov, B. Grunwald, I. Klimant, and R.N. Glud. 2011. A simple and inexpensive high resolution color ratiometric planar optode imaging approach: Application to oxygen and pH sensing. Limnol. Oceanogr. Methods 9:348–360. doi:10.4319/lom.2011.9.348

Laughlin, R.J., and R.J. Stevens. 2002. Evidence for fungal dominance of denitrification and codenitrification in a grassland soil. Soil Sci. Soc. Am. J. 66(5):1540–1548. doi:10.2136/sssaj2002.1540

Lewicka-Szczebak, D., J. Dyckmans, J. Kaiser, A. Marca, J. Augustin, and R. Well. 2016. Oxygen isotope fractionation during N_2O production by soil denitrification. Biogeosciences 13:1129–1144. doi:10.5194/bg-13-1129-2016

Mandernack, K.W., T. Rahn, C. Kinney, and M. Wahlen. 2000. The biogeochemical controls of the $\delta^{15}N$ and $\delta^{18}O$ of N_2O produced in landfill cover soils. J. Geophys. Res. Atmos. 105:17709–17720. doi:10.1029/2000JD900055

Markfoged, R., L.P. Nielsen, T. Nyord, L.D.M. Ottosen, and N.P. Revsbech. 2011. Transient N_2O accumulation and emission caused by O_2 depletion in soil after liquid manure injection. Eur. J. Soil Sci. 62:541–550. doi:10.1111/j.1365-2389.2010.01345.x

Meyer, R.L., T. Kjaer, and N.P. Revsbech. 2002. Nitrification and denitrification near a soil–manure interface studied with a nitrate-nitrite biosensor. Soil Sci. Soc. Am. J. 66:498–506. doi:10.2136/sssaj2002.4980

Miller, M.N., B.J. Zebarth, C.E. Dandie, D.L. Burton, C. Goyer, and J.T. Trevors. 2009. Influence of liquid manure on soil denitrifier abundance, denitrification, and nitrous oxide emissions. Soil Sci. Soc. Am. J. 73:760–768. doi:10.2136/sssaj2008.0059

Morley, N., and E.M. Baggs. 2010. Carbon and oxygen controls on N_2O and N_2 production during nitrate reduction. Soil Biol. Biochem. 42:1864–1871. doi:10.1016/j.soilbio.2010.07.008

National Institutes of Health. 2016. ImageJ. v. 1.50i. National Institutes of Health, Bethesda, MD. http://imagej.nih.gov/ij.

Nguyen, Q.V., D. Wu, X. Kong, R. Bol, S.O. Petersen, L.S. Jensen, S. Liu, N. Brüggemann, R.N. Gludd, M. Larsen, and S. Bruun. 2017. Effects of cattle slurry and nitrification inhibitor application on spatial soil O_2 dynamics and N_2O production pathways. Soil Biol. Biochem. 114:200–209

Odlare, M., J. Abubaker, J. Lindmark, M. Pell, E. Thorin, and E. Nehrenheim. 2012. Emissions of N_2O and CH_4 from agricultural soils amended with two types of biogas residues. Biomass Bioenergy 44:112–116. doi:10.1016/j.biombioe.2012.05.006

Opdyke, M.R., N.E. Ostrom, and P.H. Ostrom. 2009. Evidence for the predominance of denitrification as a source of N_2O in temperate agricultural soils based on isotopologue measurements. Global Biogeochem. Cycles 23:GB4018. doi:10.1029/2009GB003523

Ostrom, N.E., A. Pitt, R. Sutka, P.H. Ostrom, A.S. Grandy, K.M. Huizinga, G.P. Robertson, A. Piit, R. Sutka, P.H. Ostrom, A.S. Grandy, K.M. Huizinga, and G.P. Robertson. 2007. Isotopologue effects during N_2O reduction in soils and in pure cultures of denitrifiers. J. Geophys. Res. Biogeosci. 112:G02005. doi:10.1029/2006JG000287

Ostrom, N.E., R. Sutka, P.H. Ostrom, A.S. Grandy, K.M. Huizinga, H. Gandhi, J.C. von Fischer, and G.P. Robertson. 2010. Isotopologue data reveal bacterial denitrification as the primary source of N_2O during a high flux event following cultivation of a native temperate grassland. Soil Biol. Biochem. 42:499–506. doi:10.1016/j.soilbio.2009.12.003

Owens, J., T.J. Clough, J. Laubach, J.E. Hunt, and R.T. Venterea. 2017. Nitrous oxide fluxes and soil oxygen dynamics of soil treated with cow urine. Soil Sci. Soc. Am. J. 81:289–298. doi:10.2136/sssaj2016.09.0277

Paul, J.W., E.G. Beauchamp, and X. Zhang. 1993. Nitrous and nitric oxide emissions during nitrification and denitrification from manure-amended soil in the laboratory. Can. J. Soil Sci. 73:539–553. doi:10.4141/cjss93-054

Petersen, S.O., K.R. Baral, and E. Arthur. 2016. Manure distribution as a predictor of N_2O emissions from soil. Anim. Prod. Sci. 56:549–556. doi:10.1071/AN15534

Petersen, S.O., T.H. Nielsen, Å. Frostegård, and T. Olesen. 1996. O_2 uptake, C metabolism, and denitrification associated with manure hot-spots. Soil Biol. Biochem. 28:341–349. doi:10.1016/0038-0717(95)00150-6

Rodhe, L.K.K., J. Abubaker, J. Ascue, M. Pell, and Å. Nordberg. 2012. Greenhouse gas emissions from pig slurry during storage and after field application in northern European conditions. Biosystems Eng. 113:379–394. doi:10.1016/j.biosystemseng.2012.09.010

Smith, M.S.S., and J.M. Tiedje. 1979. Phases of denitrification following oxygen depletion in soil. Soil Biol. Biochem. 11:261–267. doi:10.1016/0038-0717(79)90071-3

Sutka, R.L., N.E. Ostrom, P.H. Ostrom, J.A. Breznak, H. Gandhi, A.J. Pitt, and F. Li. 2006. Distinguishing nitrous oxide production from nitrification and denitrification on the basis of isotopomer abundances. Appl. Environ. Microbiol. 72:638–644. doi:10.1128/AEM.72.1.638-644.2006

Tiedje, J. 1988. Ecology of denitrification and dissimilatory nitrate reduction to ammonium. In: A.J.B. Zehnder, editor, Biology of anaerobic microorganisms. John Wiley & Sons, New York. p. 179–244.

Toyoda, S., H. Mutobe, H. Yamagishi, N. Yoshida, and Y. Tanji. 2005. Fractionation of N_2O isotopomers during production by denitrifier. Soil Biol. Biochem. 37:1535–1545. doi:10.1016/j.soilbio.2005.01.009

Toyoda, S., and N. Yoshida. 1999. Determination of nitrogen isotopomers of nitrous oxide on a modified isotope ratio mass spectrometer. Anal. Chem. 71:4711–4718. doi:10.1021/ac9904563

Vazifehkhoran, A.H., and J.M. Triolo. 2015. Anaerobic co-digestion of pig manure and organic waste materials as affected by different hydraulic retention time. In: RAMIRAN Abstracts, 16th International Conference on Rural-Urban Symbiosis, Hamburg, Germany. p. 527–530.

Well, R., and H. Flessa. 2009. Isotopologue signatures of N_2O produced by denitrification in soils. J. Geophys. Res. 114:GO2020. doi:10.1029/2008JG000804

Well, R., I. Kurganova, V. Lopesdegerenyu, and H. Flessa. 2006. Isotopomer signatures of soil-emitted N_2O under different moisture conditions: A microcosm study with arable loess soil. Soil Biol. Biochem. 38:2923–2933. doi:10.1016/j.soilbio.2006.05.003

Wu, D., J.R. Köster, L.M. Cárdenas, N. Brüggemann, D. Lewicka-Szczebak, and R. Bol. 2016. N_2O source partitioning in soils using ^{15}N site preference values corrected for the N_2O reduction effect. Rapid Commun. Mass Spectrom. 30:620–626. doi:10.1002/rcm.7493

Wu, D., M. Senbayram, R. Well, N. Brüggemann, B. Pfeiffer, N. Loick, B. Stempfhuber, K. Dittert, and R. Bol. 2017. Nitrification inhibitors mitigate N_2O emissions more effectively under straw-induced conditions favoring denitrification. Soil Biol. Biochem. 104:197–207. doi:10.1016/j.soilbio.2016.10.022

Yoshida, N., and S. Toyoda. 2000. Constraining the atmospheric N_2O budget from intramolecular site preference in N_2O isotopomers. Nature 405:330–334. doi:10.1038/35012558

Zhu, K., S. Bruun, M. Larsen, R.N. Glud, and L.S. Jensen. 2014. Spatial oxygen distribution and nitrous oxide emissions from soil after manure application: A novel approach using planar optodes. J. Environ. Qual. 43:1809–1812. doi:10.2134/jeq2014.03.0125

Zhu, K., S. Bruun, M. Larsen, R.N. Glud, and L.S. Jensen. 2015. Heterogeneity of O_2 dynamics in soil amended with animal manure and implications for greenhouse gas emissions. Soil Biol. Biochem. 84:96–106. doi:10.1016/j.soilbio.2015.02.012

Paper XI

Potential inhibitor effect of hippuric acid on nitrous oxide emissions from grassland on a heavy clay soil.

Ciganda V, S., Aizpun. M,. Repullo. M., **Wu, D**., J, Terra, Elustondo, D., Clough, T., Cardenas. L,. 2017

Under review in *Journal of Plant Nutrition and Soil Science.*

SOIL NITROUS OXIDE EMISSIONS FROM GRASSLAND: POTENTIAL INHIBITOR EFFECT OF HIPPURIC ACID.

Verónica S. Ciganda[a], María López-Aizpún[b], Miguel A. Repullo[c], Di Wu[d], José A. Terra[e], David Elustondo[b], Tim Clough[f], Laura M. Cardenas [g].

AFFILIATIONS

[a] National Institute for Agricultural Research, INIA- La Estanzuela, Ruta 50 km 11, Colonia, Uruguay

[b] LICA, Department of Chemistry, University of Navarre, Irunlarrea, 1-31008 Pamplona, Spain

[c] Institute of Agricultural Research and Training (IFAPA), Cordoba, Spain

[d] Institute of Bio- and Geosciences, Agrosphere (IBG-3), Forschungszentrum Jülich GmbH, 52425 Jülich, Germany

[e] National Institute for Agricultural Research, INIA-Treinta y Tres, Ruta 8 km 282, Treinta y Tres, Uruguay

[f] Faculty of Agriculture and Life Sciences, Lincoln University, Lincoln, Canterbury, New Zealand

[g] Rothamsted Research, North Wyke, Okehampton, Devon, EX20 2SB, UK

Keywords: bovine urine, N_2O emissions, natural nitrification inhibition, heavy clay soil

Abstract

In grassland systems, cattle and sheep urine patches are recognized as nitrous oxide (N_2O) emission hot spots due to the high urinary nitrogen (N) concentrations. Hippuric acid (HA) is one of the constituents of ruminant urine that has been reported as a natural inhibitor of soil N_2O emissions. The aim of this study was to examine the potential for elevated ruminant urine HA concentrations to reduce N_2O emissions, in situ, on an acidic heavy clay soil under poorly drained conditions (WFPS > 85%). A randomized complete block design experiment with three replications and four treatments was conducted using the closed-static-flux chamber methodology. The four treatments were applied inside the chambers: control with no artificial urine application (C), control artificial urine (U), and enriched artificial urine containing two rates of HA (55.8 and 90 mM, U+HA1, U+HA2). Soil inorganic-N, soil dissolved organic carbon (DOC), soil pH as well as N_2O and methane (CH_4) fluxes were monitored over a 79-day period. Although N_2O emissions were not affected by the HA enriched urine treatments, U+HA2 positively affected the retention of N as NH_4^+ until day 3, when the soil pH dropped to values <5. Subsequently, as a consequence of rainfall events and soil acidification, it is likely that leaching or sorption onto clay reduced the efficacy of HA, masking any treatment differential effect on N_2O emissions. Moreover, CH_4 fluxes as well as DOC results reflected the soil anaerobic conditions which did not favour nitrification processes. Further research is needed to determine the fate of HA into the soil which might clarify the lack of an *in situ* effect of this compound.

1 Introduction

Up to 9% of the United Kingdom's greenhouse gas (GHG) emissions result from agriculture, with 55% of these GHG emissions in the form of nitrous oxide (N_2O) (*DEFR*A, 2011). In grassland systems, cattle and sheep urine patches are recognized N_2O emission hot spots due to the high urinary nitrogen (N) concentrations that may range from 3 to 20.5 g N L^{-1} urine (*Spek* et al., 2012; *Bristow* et al., 1992). In England and Wales, over 42% of the agricultural land area, or 26% of the total area, is under permanent grassland (SEISMIC1 v.2.0.6. software 2000 dataset). Within this agricultural grassland, approximately 50% occurs on poorly drained soils with a shallow impermeable substrate and they are frequently found in western Britain, where high levels of rainfall can lead to seasonal water logging when drainage systems have not been installed (*Granger* et al., 2010). This greatly reduces the soil aerobic status and favours the occurrence of anaerobic processes. Except for winter time, when cattle are usually removed from the land, such agricultural grasslands are permanently loaded during spring, summer and autumn with urine-N from ruminant depositions. Soil inorganic-N, derived from ruminant urine, is prone to being lost as N_2O or N_2 via nitrifier-denitrification, denitrification, or codenitrification processes since increasing water-filled pore space (WFPS) enhances anaerobic conditions (*Linn* and *Doran*, 1984; *Balaine* et al. 2013; *Selbie* et al. 2015).

Studies performed in soils under grasslands of varying texture, affected by ruminant urine, and under varying WFPS conditions, report N_2O emissions ranging from 0.02 to 2.33 % of ruminant urine-N applied (*Zaman* et al., 2012; *Luo* et al., 2008; *de Klein* et al., 2011; *Baral* et al., 2014; *Misselbrook* et al., 2014; *Krol* et al., 2015; *Kelly* et al., 2008; *Wachendorf* et al., 2008; *Boon* et al., 2014). This oscillation in N_2O emissions may be a consequence of variation in ruminant urine composition, which is controlled by the animal's diet (*Martin*, 1970 a, b; *Kreula* et al., 1978; *Van Vuuren* and *Simits*., 1997). In this sense, some of the constituents in the ruminant urine have been reported to affect subsequent soil N_2O emissions (*Van Groenigen* et al., 2005a, b; *Van Groenigen* et al., 2006; *Kool* et al., 2006). That is the case of Hippuric acid (HA), a constituent naturally present in ruminant

urine at concentrations between 0.37 and 0.70 g N L^{-1} (*Dijkstra* et al., 2013) depending on animal diet (*Kreula* et al., 1978). *In vitro*, HA has been shown to mitigate N_2O emissions from soil (*Van Groenigen* et al., 2006; *Kool* et al., 2006; *Bertram* et al. 2009) presumably due to the presence of benzoic acid (BA), a break-down product (*Bristow* et al., 1992) which, along with its demonstrable antimicrobial activity in acidic mediums (*Marwan* and *Nagel*, 1986), is known as a denitrification inhibitor (*Her* and *Huang*, 1995). Benzoic acid may be adsorbed onto soil particles via van der Waal or hydrogen bonding and subsequently released as a consequence of decreasing soil solution strength or as a result of competing ions (*Dalton*, 1999). Using ^{14}C labelled benzoic acid, *Inderjit* and *Bhowmik* (2004) found that increasing soil clay content and soil organic matter content influenced the sorption of benzoic acid onto soil particles with the sorption of the benzoic acid onto soil particles increasing with concentration. Also, adsorption of benzoic acid by soil components is greatly affected by soil pH: at soil pH values below its pKa (approximately 4.5), molecules are nonionized and may be adsorbed to organic matter and clay through weak physical adsorption forces (*Dalton, 1999*).

HA has been reported to reduce soil N_2O emissions due to its inhibitory effect on both nitrification and denitrification processes (*Bertram* et al., 2009). In addition, the concentration of HA in urine has been reported to have a controlling effect on both the hydrolysis of urine-N and on NH_3 volatilization, and thus it may further influences N_2O emission factors by altering substrate supply for microbial mechanisms of N_2O production (*Van Groenigen*, et al., 2005).

Field studies carried out *in situ* on silt loam soils with WFPS ranging from 18% to 51% reported no effect on N_2O emissions with increasing urine HA concentration (*Clough* et al., 2009). Similarly, *Krol* et al., (2015) found no effect *in situ*, on a loam soil where WFPS ranged from 60% to 80%. By contrast, the inhibitory effect of HA under anaerobic conditions (WFPS 92%) has been proved under laboratory conditions (*Kool* et al., 2006). However, there are no reports on the *in situ* effects of urinary HA concentration on N_2O emissions for heavy clay soils, with high values of WFPS (>85%), as commonly found in grazed perennial pastures from the southwest of England.

The aim of this study was to examine the potential for elevated ruminant urine HA concentrations to reduce *in situ* N_2O emissions on an acidic heavy clay soil under poorly drained soil conditions (WFPS > 85%). Based on previous *in situ* studies (*Kool* et al., 2006; *Clough* et al., 2009; *Krol* et al., 2015) we hypothesized that an increase in ruminant urine HA content could inhibit N_2O emissions when urine was applied to acidic soils with a high clay content, due to the potential retention of HA by the clay in the soil and due to the favourable pH conditions (<5.2) making viable the antimicrobial activity of benzoic acid (*Chipley*, 1983).

2 Materials and methods

2.1 Site location

The field trial was carried out in 2015 on a permanent grassland, dominated by ryegrass (*Lolium perenne* L.) and white clover (*Trifolium repens* L.), from September 29th to December 16th at Rothamsted Research, North Wyke, Devon, UK (50:46:10N, 3:54:05W). The climate is a temperate maritime climate (*Koppen*, 1931), typical of South-West England. The soil used for the experiment is defined by the British soil classification (*Avery*, 1980) as a clayey typical non-calcareous pelosol of the Halstow series: the soil type is described as either a stagnivertic cambisol, or as an aeric haplaquept by the FAO and USDA taxonomic classification systems, respectively. The soil has a brownish clay loam A horizon while the B horizon is clayey with marked gleying confined below 40 cm (*Harrod* and *Hogan*, 2008). It is characterized, with an unusually low cation exchange capacity (C.E.C.) relative to clay content, which is partly an expression of the micaceous nature of its clay minerals and partly of the relatively coarse size and therefore small surface area of the clay (*Harrod* and *Hogan*, 2008).

This soil is water-logged for considerable periods of the year. The impermeable nature is confirmed by the low fraction of drainable pores and it has very slow hydraulic conductivity (*Harrod* and *Hogan*, 2008).

Initial analysis of the upper 10 cm of the soil profile indicated: 2 mg NO_3^--N kg^{-1} dry $soil^{-1}$, 6 mg NH_4^+-N kg^{-1} dry $soil^{-1}$, pH of 5.1 and bulk density (BD) of 1.11 Mg m^{-3}. Meteorological data, consisting of air temperature and precipitation, was collected from a station located 500 m away from the field site.

2.2 Experimental and chamber design

A randomized complete block design experiment was set up with three replicate plots per each of four treatments. Blocks were 3 m apart and replicate plots were 5.6 m^2 (2 m x 2.8 m) with a 1 m separation as buffer. Five chambers were installed within each replicate plot (i.e., 60 chambers in total) and an area of 1 m^2 (1 m x 1 m) was delineated next to each replicate plot for soil sampling.

The closed static chamber technique was used (*Rochette* and *Erisksen-Hamel*, 2008) for determining soil gas fluxes. Chambers comprised white polyvinyl chloride (PVC) open ended boxes with a volume of 0.032 m^3 (length 0.4 m, width 0.4 m, height 0.25 m; *Cardenas* et al., 2010). The lid was fitted with a sampling port with a three-way valve. In order to ensure a good seal between the chamber and soil, the chambers were inserted into the soil to a depth of 0.1 m more than 24 h before the flux measurements began (*Parkin* and *Venterea*, 2010). The effective height of each chamber was recorded internally at the centre of each wall and in the centre of the chamber to use in the calculation of the fluxes. The resultant chamber effective height was the weighted mean of the 5 points taken (including two times the centre height), and ranged between 0.09 and 0.18 m.

2.3 Treatments

On September 30th, four treatments were applied inside the chambers: control with no artificial urine application (C), control artificial urine containing HA 37 mM (U), enriched artificial urine containing HA 55.8 mM (U+HA1), and enriched artificial urine containing HA 90 mM (U+HA2).The

respective N application rates for the C, U, U+HA1, and U+HA2 were 0, 516, 528, and 552 kg N ha-1 HA concentrations applied were defined based on previous studies (Table 1). Treatments were prepared the day before the application using the recipe described by *Doak* (1952), and stored at 4°C overnight. Urine was applied using a watering can at a rate of 5 L m^{-2} and when applied its average temperature was 16.4°C.

2.5 Greenhouse gas measurements

Greenhouse gases, including N_2O and methane (CH_4), were monitored one day before treatment application and on 22 occasions after treatment application over a 79-day period. Gas samples were taken between 11:00 a.m and 2:00 p.m on each sampling day, four times a week for the first two weeks, twice weekly for the next five weeks, and weekly thereafter (*Misselbrook* et al., 2014). Sampling was conducted according to *Chadwick* et al. (2014). Atmospheric samples were collected at the start and the end (three at each time) of the sampling run to provide background values. Chamber lids were placed on the chambers sequentially across the paddocks and after 40 min a gas sample was collected from each closed chamber (T40) via a sampling port fixed in the lid using a plastic 50 mL syringe fitted with a 3-way luer-lok tap. The sample was then transferred to a pre-evacuated (-1 atm.) *22* mL vial, using a hypodermic needle, that had a chloro-butyl rubber septum (Chromacol). Samples were analysed within two days by gas chromatography on a Perkin Elmer Clarus 500 GC and TurboMatrix 110 auto headspace sampler equipped with an electron capture detector (ECD) and a flame ionization detector (FID). The separation column employed was a Perkin Elmer EliteQ PLOT megabore capillary (30 m long, 0.53 mm i.d.), operated at 35°C. The ECD detector was set at 300°C and the carrier gas was N_2. Gas fluxes were calculated based on the linear increase in the gas concentration inside the chamber from T0 (ambient) to T40 (Smith and Dobbie, 2001). Confirmation of the linearity of the gas flux was confirmed by taking four gas samples from one of

the chambers that received urine at T0, T20, T40 and T60 on every sampling occasion. Soil surface temperature was measured at the beginning and at the end on each sampling day.

2.6 Soil analysis

Soil samples, taken on every gas sampling occasion, were dried for 48 h at 105 °C to determine gravimetric water content (θ_g). Soil BD was calculated after treatment application in each plot. Then WFPS was calculated using the BD, an assumed soil particle density (2.65 g cm^{-3}) and θ_g. Average WFPS between the four treatments for every sampling date was calculated. Soil mineral N was determined weekly by extracting soil in 2 M KCl (20 g of fresh soil: 40 mL 2 M KCl, shaken for 1 h). The extracts were analysed with colorimetric analysis, using an Aquakem 600 discrete analyser, for NH_4^+-N and for NO_3^--N.

Soil samples were collected for pH determination on seven occasions within the experimental period in a 1:2.5 (vol/vol) fresh soil-water suspension shaken for 15 minutes (*Ministry of Agriculture Fisheries and Food*, 1986) using a pH meter fitted with a general-purpose combination electrode.

The same soil samples were analyzed for dissolved organic carbon (DOC) by shaking 50 g of soil (dry weight) in 200 mL of ultrapure water at 120 revolutions per minute, for 60 minutes at room temperature. Extracts were then centrifuged for 15 minutes at 4600 g and filtered through 0.45-µm cellulose acetate filter papers (*Guigue* et al., 2014) before analyzing them on a total organic carbon analyser (Shimadzu TOC-L).

2.7 Data analysis

The N_2O flux data had a skewed distribution so it was log transformed as ln (N_2O flux + 1). A one-way analysis of variance (ANOVA) was performed on the transformed data to determine the effect of the

treatments on the N_2O emissions, with treatment means for each sampling date compared using least significant difference (LSD) test at 5% level of probability using the R software (*Fox*, 2005).

3 Results

3.1 Meteorological data

Total precipitation over the experimental period was 170.8 mm with the highest event (13.6 mm) in November 29th (Fig. 1). Initially, WFPS was 85% and steadily increased until the soil was saturated, with an average of 97.9% for the experiment, with values > 100% when water was lying on the soil surface (Fig.1). Soil surface temperature averaged 14^{o}C with a steady decrease from a maximum of 18 ^{o}C to a minimum of 10 ^{o}C on day 79 (Fig. 1).

Insert Figure 1

3.2 Nitrous oxide emissions

During the first 20 days of the experiment, daily N_2O fluxes showed no significant differences between the control and the urine treatments with fluxes < 20 g of N_2O-N ha^{-1} day^{-1} with a small peak, five days after application (Figure 2). The highest fluxes from the urine treatments appeared on day 22, with other peaks on days 38, 45 and 56 in all urine treatments. Emissions from the control ranged from -1.87 to 1.79 g N_2O-N ha $^{-1}$ day^{-1} while N_2O emissions from U, U+HA1 and U+HA2 ranged from -1.64 to 28.13, from -1.63 to 41.71 and from -0.74 to 24.57 g N_2O-N ha $^{-1}$ day^{-1}, respectively. The variability measured in the fluxes from the control was smaller than that observed in the urine treatments on all sampling dates. On days 22, 28, 35, 45 and 50 the emissions from the urine treatments were higher than from the control ($P < 0.05$). However, there were no significant

differences between the U and the U+HA treatments on these sampling days with the three treatments having similar N_2O-N fluxes trends.

Insert Figure 2

Cumulative emissions from the U, U+HA1 and U+HA2 treatments were 660 (±187), 757 (±377), and 564 (±289) g N_2O-N ha^{-1}, respectively, and did not differ significantly. These values were higher ($p<0.05$) than the cumulative emissions from the control which averaged 5.89 g N_2O-N ha^{-1} day^{-1} (Figure 3). As a percentage of the urine-N applied, the cumulative N_2O-N fluxes for the urine treatments averaged 0.13% (± 0.03).

Insert Figure 3

3.3 CH_4 emissions

Soil CH_4 emissions for all treatments, including the control, were < 5 g ha^{-1} d^{-1} until day 28. After this time, CH_4 emissions steadily increased in all treatments, including the control, peaking at 40 g CH_4 ha^{-1} day^{-1} at the end of the experiment (Figure 4). Cumulative CH_4 emissions did not significantly differ among the four treatments and averaged 623.5 g CH4 ha^{-1}.

Insert Figure 4

3.4 Nitrogen content in soil

By day 3 the soil NH_4^+-N concentrations had increased in all urine treatments, up to 379.5 mg NH_4^+-N kg dry $soil^{-1}$ (Figure 5). On day 3, the U+HA2 treatment had a significantly higher NH_4^+-N soil concentration than either the U and U+HA1 ($p<0.05$) treatments, but after day 3 soil NH_4^+-N concentrations did not differ among treatments and declined over time to about 50 mg NH_4^+-N kg dry $soil^{-1}$. Concentrations of NH_4^+-N in the control treatment were close to zero and significantly lower than in the urine treatments ($p<0.01$) throughout the experiment.

Insert Figure 5

Soil NO_3^--N concentrations ranged from 0 to 10 mg NO_3^--N and there were no significant differences between urine treatments and the control, except for days 35 and 64 when the soil NO_3^--N concentration in the control was lower ($p<0.05$) than in the urine treatments.

Insert Figure 6

3.5 Soil pH and DOC

Initially the soil pH averaged 5.11 (± 0.15) prior to treatment application. On day 3, after the urine treatments were applied, pH values decreased to 4.84, 4.85, and 4.98 for the U, U+HA1 and U+HA2 treatments, respectively. The pH remained < 5.0 until the end of the experiment, with the lowest pH values measured on day 35 (Figure 7).

Insert Figure 7

Soil DOC ranged from 11 to 61 mg kg^{-1} during the study. The U and the U+HA2 treatment peaked (59 and 61 mg DOC kg^{-1}, respectively) three days after treatment application with a second peak, < 44 mg DOC kg^{-1}, on day 22 (Figure 8). Meanwhile, DOC concentrations in the U+HA1 treatment were ≤ 30 mg DOC kg^{-1} throughout the study. The control DOC concentrations ranged from 19 to 39 mg DOC kg^{-1}, following a similar trend as described for the U and U+HA2 treatments. After day 35, all treatments had average DOC concentrations < 25 mg DOC kg^{-1}.

Insert Figure 8

4 Discussion

4.1 Soil properties

The range of HA concentrations applied in this study were selected based on previous work (Table 1) and are comparable with what is found in ruminant urine (*Kehraus* et al., 2006). The effect of the synthetic urine treatments on soil properties (changes in inorganic-N, soil pH and DOC) can be explained by the hydrolysis of the urea, contained in the urine, applied. The higher soil NH_4^+ concentration (>379 NH_4^+-N kg dry $soil^{-1}$) and lower NO_3^--N (<1.7 mg) in the U+HA2 treatment on day 3 show an inhibitory effect on nitrification when HA was applied at its highest concentration. The fact that this pattern was not observed for the remainder of the experiment might be explained by the leaching of the HA due as a consequence of the rainfall events recorded on days 6, 7, and 8 (Figure 1) when 22.2 mm of rainfall occurred. Alternatively, biological degradation of benzoic acid (*Razika* et al., 2010), as well as sorption of this compound onto soil particles (*Indejirt* and *Prasanta*, 2004), may explain the lack of a continued HA effect. However, due to the acidic soil pH, biological degradation of the benzoic acid seems less likely since the microbial degradation of phenolic compounds has been reported to be favoured at neutral-alkaline pH values (*Razika* et al., 2010; *Prabhakaran* et al., 2012). The decrease in soil pH after day 3, however, might have favoured the adsorption of benzoic acid to clay through weak physical forces (*Indejirt* and *Prasanta*, 2004). Thus, it seems probable that HA leaching and benzoic acid sorption onto clay were responsible for the lack of a HA effect on soil NH_4^+-N after day 3. Also, it might have ocurred that the HA effect was not large enough to affect N_2O emissions due to the spatial variability between chambers.

The decline in soil NH_4^+-N after day 3 indicated that it was probably nitrified, and this promoted the decrease in soil pH due to the released of free H^+, as a consequence of the nitrification process, which is similar to the results reported by *Krol* et al. (2015) (Figure 7). Moreover, the formation of benzoic acid from HA might have also contributed to the soil pH decrease. While the occurrence of nitrification is evident from the increases in NO_3^- concentrations, these concentrations were much lower than values previously reported in similar studies (e.g. *Clough* et al., 2009). The lower NO_3^- concentrations measured in this study might be explained either by either pasture N uptake or by

the high WFPS recorded, that provided conditions suitable for promoting the development of anaerobic microsites suitable for denitrification. The rate of nitrification also appeared slow when compared to prior studies where the nitrification is often complete within a month under urine patches on pasture soil (e.g. REF). Thus, the lower NO_3^--N concentrations indicated that nitrification was slowly progressing under the anaerobic conditions and/or the produced NO_3^--N was quickly taken up by the pasture or denitrified as either N_2O or N_2 (*Kool* et al., 2006).

The DOC values increased as a result of urea hydrolysis increasing soil pH but they then decreased to < 25 mg DOC kg $soil^{-1}$ when WFPS was > 100%. Such changes in DOC with increasing WFPS are indicative of anaerobic heterotrophic processes such as denitrification consuming DOC. This indicates a low or negligible supply of oxygen, which would also have slowed or prevented nitrification processes, further explaining the relatively prolonged and slow decline in soil NH_4^+-N concentrations.

4.2 Effect of HA on the GHG emissions

The lack of a HA effect on N_2O fluxes after day 3 under our field conditions is the opposite to that found by Kool et al. (2006) in a laboratory experiment under similar anaerobic conditions. In this sense, our results ratify previous results under more aerobic conditions (*Clough* et al., 2009; *Krol* et al., 2015) in terms of potential *in situ* effects of HA.

The percentage of N applied subsequently emitted as N_2O reported in this study was similar to that reported by *Di* and *Cameron* (2006) and by *Taghizadeh-Toosi* et al. (2012) but lower than that reported by *Clough* et al. (2009) and *Krol* et al. (2015). This lower percentage of N emitted might be explained by the occurrence of the higher values of WFPS registered when compared to *Clough* et al. (2009) and *Krol* et al. (2015). High WFPS reduces relative soil gas diffusivity increasing soil anaerobic

conditions, which leads to higher losses of N as N_2 instead of N_2O (*Balaine* et al. 2016). Alternatively, the acidic soil pH (< 5.0) could have favoured chemodenitrification processes as a result of nitrite, formed as a consequence of nitrification or denitrification, producing nitrous acid and reacting with soil organic matter (*Heil* et al., 2016), and thus further reducing the substrate available for N_2O production. However, the percentage of N applied emitted as N_2O (0.13 %) was considerably lower than that reported in the laboratory study conducted by *Kool* et al. (2006) under similar anaerobic conditions (2.1 % for the high HA treatment; WFPS=97 %). Although such experiment was conducted on a different soil type, the difference in the the percentage of N applied emitted as N_2O may be a consequence of plant uptake of mineral N in our study, which might decrease N susceptible of being emitted as N_2O. However, values of soil NH_4^+-N were similar to those reported by *Kool* et al. (2006). Nevertheless, the effect of HA on N_2O emissions appears not to be related to the amount of mineral N present in the soil (*Koo*l et al., 2006).

It has previously been shown that CH_4 production in rice paddies and soil suspensions occurs under much stronger reducing conditions than observed for N_2O (*Yu* et al., 2001; 2003). The steady increase of CH_4 emissions for all treatments after day 35 coincided with WFPS values greater than 100% and a decline in DOC concentrations. Such anaerobic conditions would have favoured the decomposition process of soil organic material through which CH_4 was produced, via DOC fermentation catalyzed by methanogenic microorganisms (Rizzo et al, 2013). Thus, the CH_4 emissions further demonstrate the favourable soil conditions for denitrification. The higher U+HA treatment inhibited nitrification as soil NH_4 remained as NH_4 until day 3. However, as N_2O emission was not inhibited it means that N_2O was not the result of the nitrification from the added NH_4, but from denitrification possibly from the soil NO_3. On day 3, WFPS was ~80% so the soil was not saturated and nitrification did occur. Indeed, soil NO_3 concentration was higher in the U and U+HA treatments compared to the control indicating NO_3 formation.

Furthermore, *Van Groenigen* et al. (2006) reported that the HA inhibition effect occurred at a concentration of 3.9 mmol HA kg^{-1} soil, which is the same concentration as in the U+HA2 treatment in the current study (allowing for the soil bulk density and assuming that urine was absorbed to a depth of 10 cm). However, the permanent soil water logging conditions after day 3 (WFPS > 85%) may have resulted in leaching of the HA and the formed BA after treatments application, which may have resulted in a decrease in the soil HA-BA concentration, contributing to the lack of effect of HA as an inhibitor of N_2O emissions after day 3. At the same time, soil pH (4.6 after HA application) was optimal for antimicrobial activity of BA. Therefore, a treatment effect on N_2O emission could be expected since the antimicrobial activity is proportional to the BA concentration. However, as mentioned above, this soil pH might have favoured the sorption of BA onto clay preventing not only its antimicrobial action but also its inhibition effect on denitrification with the soil acidification that occurred in all treatments. The potential sorption of HA onto clay and/or organic matter confounds the interpretation of the results with respect to the efficacy of HA in limiting N_2O producing processes. *Inderjit* and *Bhowmik* (2004) reported sorption of benzoic acid by soil from ca. 2 to 1000 $\mu g\ g^{-1}$ soil as solution concentrations varied from ca. 2 to 1000 $\mu g\ ml^{-1}$, respectively. Thus, in theory the efficacy of the HA at the highest rate in the current experiment (3.9 mmol HA kg^{-1}), equating to ca 700 $\mu g\ g^{-1}$ soil, could have been negated due to sorption onto soil.

In view of the above, an inhibitor effect was observed for the highest U+HA treatment just until day 3, as soil NH_4^+ remained as NH_4^+ more than the other treatments. However, such inhibitor effect was not reflected both on soil NO_3^- concentration and on N_2O emissions. After day 3, it seems likely that a combination of soil HA and BA leaching under the permanent soil water logging conditions and a sorption of BA into clay under optimal soil pH may explain the lack of an observed HA effect.

5 Conclusions

While the soil NH_4^+-N concentration was elevated until day 3 under the highest rate of HA applied, the N_2O emissions from artificial urine applied to grassland on an acidic heavy clay soil and under high water content conditions (WFPS >85%) were not affected by the addition of different concentrations of HA. Whereas the mitigation effect of HA under similar soil water conditions has been proven in vitro we have ratified the lack of such an effect in situ under strongly reducing conditions. Soil HA and BA leaching under the permanent soil water logging conditions and the likely sorption of BA onto clay under optimal soil pH may explain the lack of observed HA effect. Our study showed that the potential manipulation of ruminant urine, via diet selection, to optimise HA concentration will not mitigate N_2O emissions. Further studies using ^{13}C labelled benzoic acid or HA should be performed to determine the residence time and fate of HA in soil.

Acknowledgements

The authors are grateful to the BBSRC for supporting this study, particularly the projects: Delivering sustainable systems (BB-J004286-1) and Soils to Nutrition (BB/P01268X/1). Also, we are grateful to NERC under project Uplands N_2O (NE/MO13847/1). We are also grateful for The Stapledon Memorial Trust and to the "Agencia Nacional de Investigación e Innovación" of Uruguay for providing funding in the form of research fellowships for Dr. Ciganda. Also thanks to INIA – Uruguay for partially funding this work. During this study M. López-Aizpún was recipient of a research grant from the "la Caixa Banking Foundation" which is kindly acknowledged, and Dr. M. Repullo was under a postdoctoral contract from the IFAPA (Andalucía, Spain). We thank Liz Dixon, Neil Donovan and Enrique Cancer-Berroya for technical support.

References

Avery, B. W. (1980): Soil Classification for England and Wales (Higher Categories). Soil Survey of England and Wales. Soil Survey Technical Monograph No. 14, Harpenden, UK.

Balaine, N., Clough, T. J., Beare, M. H., Thomas, S. M., Meenken, E. D., Ross, J. G. (2013): Changes in Relative Gas Diffusivity Explain Soil Nitrous Oxide Flux Dynamics. *Soil Sci. Soc. Am. J.* 77, 5, 1496-1505.

Balaine, N., Clough, T. J., Beare, M. H., Thomas, S. M., Meenken, E. D.(2016): Soil Gas Diffusivity Controls N_2O and N_2 Emissions and their Ratio. *Soil Sci. Soc. Am. J.* 80, 529-540.

Baral, K. R., Thomsen, A. G., Olesen, J. E., Peterson, S. O. (2014): Controls of nitrous oxide emission after simulated cattle urine deposition. *Agric. Ecosyst. Environ*. 188, 103-110.

Bertram, J. E., Clough, T. J., Sherlock, R. R., Condron, L. M., O' Callaghan, M., Wells, N. S., Ray, J. L. (2009): Hippuric acid and benzoic acid inhibition of urine derived N_2O emissions from soil. *Glob. Change Bio.* 15, 2067-2077.

Boon, A., Robinson, J. S., Chadwick, D. R., Cardenas, L. M. (2014): Effect of cattle urine addition on the surface emissions and subsurface concentrations of greenhouse gases in a UK peat grassland. *Agric. Ecosyst. Environ.* 186, 23-32.

Bristow, A. W., Whitehead, D. C., Cockburn, J.E. (1992): Nitrogenous constituents in the urine of cattle, sheep and goats. *J. Sci. Food Agr.* 59, 387–394.

Cardenas, L. M., Thorman, R., Ashlee, N., Butler, M., Chadwick, D., Chambers, B., Cuttle, S., Donovan, N., Kingston, H., Lane, S., Dhanoa, M. S., Scholefield, D. (2010): Quantifying annual N_2O emission fluxes from grazed grassland under a range of inorganic fertiliser nitrogen inputs. *Agric. Ecosyst. Environ.* 136, 218–26.

Clough, T. J., Ray, J. L., Buckthought, L. E., Calder, J., Baird, D., O'Callaghan, M., Sherlock, R. R., Condron, L. M. (2009): The mitigation potential of hippuric acid on N_2O emissions from urine patches: An in situ determination of its effect. *Soil Biol. Biochem.* 41, 2222-2229.

Chadwick, D. R., Cardenas, L., Misselbrook, T. H., Smith, K. A., Rees, R. M., Watson, C. J., McGeough, K. L., Williams, J. R., Cloy, J. M., Thorman, R. E., Dhanoa, M. S. (2014): Optimizing chamber methods for measuring nitrous oxide emissions from plot- based agricultural experiments. *Eur. J. Soil Sci.* 65, 295–307.

Chipley, J.R. (1983): Sodium benzoate and benzoic acid. In: Branen, A.L., Davidson, P.M. (Eds.), Antimicrobials in Foods. M. Decker, New York, pp. 11–35.

Dalton, B.R. (1999): The occurrence and behavior of plant phenolic acids in soil environment and their potential involvement in allelochemical interference interactions: methodological limitations in establishing conclusive proof of allelopathy. In: Inderjit, Dakshini KMM, Foy CL (eds) Principles and practices in plant ecology: allelochemical interactions. CRC, BocaRaton, Fla., pp. 57–74.

Defra. (2011): Greenhouse Gas Emission Projections for UK Agriculture to 2030. http://www.defra.gov.uk/corporate/evidence/economics/ (accessed 15.11.20).

de Klein, C. A. M., Barton, L., Sherlock, R. R., Li, Z., Littlejohn, R. P. (2003): Estimating a nitrous oxide emission factor for animal urine from some New Zealand pastoral soils. *Aust. J. Soil Res.* 41, 381-389.

de Klein, C. A. M., Cameron, K. C., Di, H. J., Rys, G., Monaghan, R. M., Sherlock, R. R. (2011): Repeated annual use of the nitrification inhibitor dicyandiamide (DCD) does not alter its effectiveness in reducing N_2O emissions from cow urine. *Animal Feed Sci. Technol.* 166, 480–491.

de Klein, C. A. M., Luo, J., Woodward, K. B., Styles, T., Wise, B., Lindsey, S., Cox, N. (2014): The effect of nitrogen concentration in synthetic cattle urine on nitrous oxide emissions. *Agric. Ecosyst. Environ.* 188, 85-92.

Di, H. J., Cameron, K. C. (2006): Nitrous oxide emissions from two dairy pasture soils as affected by different rates of a fine particle suspension nitrification inhibitor, dicyandiamide. *Biol. Fertil. Soils.* 42, 472-480.

*Dijkstra, J., Onema, O., van Groenigen, J. W., Spek, J. W., van Vuuren, A. M., Bannink, A. (*2013): Diet effects on urine composition of cattle and N_2O emissions. *Animal* 7, 292-302.

Doak, B. W. (1952): Some chemical changes in the nitrogenous constituents of urine when voided on pasture. *J. Agric. Sci.* 42, 162–171.

Fox, J. (2005): The R Commander: a basic-statistics graphical user interface to R. *J. Stat. Softw.* 14, 9.

Granger, S. J., Bol, R., Meier-Augenstein, W., Leng , M. J., Kemp H. F., Heaton, T. H. E., White, S. M. (2010): The hydrological response of heavy clay grassland soils to rainfall in south-west England using δ2H. *Rapid Commun. Mass Spectrom.* 24, 475–482.

Guigue, J., Mathieu, O., Lévêque, J., Mounier, S., Laffont, R., Maron, P. A., Navarro, N., Chateau, C., Amiotte-Suchet, P., Lucas, Y.(2014): A comparison of extraction procedures for water-extractable organic matter in soils. *Eur. J. Soil Sci.* 65, 520–530.

Harrod, T. R., Hogan, D. V.(2008): The Soils of North Wyke and Rowden. Unpublished Report to North Wyke Research, Revised Edition of Original Report by TR Harrod, *Soil Survey of England and Wales*.

Heil, J., Vereecken, H., Brüggemann, N. (2016): A review of chemical reactions of nitrification intermediates and their role in nitrogen cycling and nitrogen trace gas formation in soil. *Eur. J. Soil Sci.* 67, 23–39

Her J., Huang, J., (1995): Influences of carbon source and C/N ratio on nitrate/nitrite denitrification and carbon breakthrough. *Bioresource Technol.* 54, 45–51.

Inderjit, Bowhmik, P. C. (2004): Sorption of benzoic acid onto soil colloids and its implications for allelopathy studies. *Biol. Fertil. Soils* 40, 345–348.

Kelly, K. B., Phillips, F. A., Baigent, R. (2008): Impact of dicyandiamide application on nitrous oxide emissions from urine patches in northern Victoria, Australia. *Aust. J. Exp. Agric.* 48, 156-159.

Kehraus, S., Südekum, J. H., Pfeffer, E. (2006): Einflussfactoren auf die ausscheidung N-haltiger verbindungen im harn von wiederkäuern. *Übersichten Tierernährung* 34, 125–164.

Köppen, W. (1931): Grundriss der Klimakunde. Walter de Gruyter, Berlin.

Kool, D. M., Hoffland, E., Hummelink, E. W. J., Van Groenigen, J. W. (2006): Increased hippuric acid content of urine can reduce soil N_2O fluxes. *Soil Biol. Biochem.* 38, 1021–1027.

Kreula, M., Rauramaa, A., Ettala, T. (1978): The effect of feeding on the hippuric acid content of cow's urine. *J. Agr. Sci. Finland* 50, 372–377.

Krol, D. J., Forrestal, P. J., Lanigan, G. J., Richards, K. G. (2015): In situ N_2O emissions are not mitigated by hippuric and benzoic acids under denitrifying conditions. *Sci. Total Environ*. 511, 362-368.

Linn, D. M., Doran J. W.(1984): Effect of water-filled pore space on carbon dioxide and nitrous oxide production in tilled and non-tilled soils. *Soil Sci. Soc. Am. J.* 48, 1267-1272.

Luo, J., Lindsey, S. B., Ledgard, S. F. (2008): Nitrous oxide emissions from animal urine application on a New Zealand pasture. *Biol. Fertil. Soils* 44, 463–470.

Martin, A.K. (1970a): The urinary aromatic acids excreted by sheep given S24 perennial ryegrass cut at six stage of maturity. *Br. J. Nutr.* 24, 943–959.

Martin, A.K. (1970b): Effect of stage of maturity of perennial ryegrass on its content of some organic acids and phenolic compounds. *J. Sci. Food Agr*. 21, 496–501.

Marwan, A. G., Nagel, C. W. (1986): Quantitative determination of infinite inhibition concentrations of antimicrobial agents. *Appl. Environ. Microb.* 51, 559–561.

Ministry of Agriculture, Fisheries and Food. (1986): The Analysis of Agricultural Materials, 3rd edn Reference book 427. HMSO, London.

Misselbrook, T. H., Cardenas, L. M., Camp, V., Thorman, R. E., Williams, J. R., Rollett, A. J., Chambers, B. J. (2014): An assessment of nitrification inhibitors to reduce nitrous oxide emissions from UK agriculture. *Environ. Res. Lett.* 9, 115006.

Parkin, T. B., Venterea, R. T. (2010): USDA-ARS GRACEnet Proyect Protocols. In: Follet, R.F (Eds), Chapter 3. Chamber-Based Traze Gas Flux Measurements. Sampling Protocols, Beltsville, MD, 1–39.

Prabhakaran, S. P., Santhosh Kumar, R., Jaganath, J., Naveena, B., Gomathi Priya, P., 2012. Biodegradation Studies on Phenolic Compounds. *Adv. Mater. Res*. 584, 455-459.

Razika, B., Abbes, B., Messaoud, C., Soufi, K. (2010): Phenol and benzoic acid degradation by Pseudomonas Aeruginosa. *J. Water Resource Prot.* 2, 788-791.

Rizzo, A., Boano, F., Revelli, R., Ridolfi, L., 2013. Role of water flow in modelling methane emissions from flooded paddy soils. *Adv. Water Resour.* 52, 261–274.

Rochette, P., Erisksen-Hamel, N. S. (2008): Chamber measurements of soil nitrous oxide flux: are absolute values reliable? *Soil Sci. Soc. Am. J.* 72,331–342.

Sánchez-Martín, L., Vallejo, A., Dick, J., Skiba, U. M. (2008): The influence of soluble carbon and fertilizer nitrogen on nitric oxide and nitrous oxide emissions from two contrasting agricultural soils. *Soil Biol. Biochem.* 40, 142–151.

Selbie, D. R., Lanigan, G. J., Laughlin, R. J., Di, H. J., Moir, J. L., Cameron, K. C., Clough, T. J., Watson, C. J., Grant, J., Somers, C., Richards, K. G. (2015): Confirmation of co-denitrification in grazed grassland. *Sci. Rep.* 5, 17361.

Smith, K. A., Dobbie, K. E.(2001): The impact of sampling frequency and sampling times on chamber-based measurements of N_2O emissions from fertilized soils. *Global Change Biol*. 7, 933–945.

Spek J. W., Bannink A., Gort G., Hendriks W. H., Dijkstra J. (2012): Effect of sodium chloride intake on urine volume, urinary urea excretion, and milk urea concentration in lactating dairy cattle. *J. Dairy Sci.* 95, 7288–7298.

Stange, C. F., Spott, O., Arriaga, H., Menendez, S., Estavillo, J. M., Merino, P. (2013): Use of the inverse abundance approach to identify the sources of NO and N_2O release from Spanish forest soils under oxic and hypoxic conditions. *Soil Biol. Biochem.* 57, 451-458.

Taghizadeh-Toosi, A., Clough, T. J., Sherlock, R. R., Condron, L. M. (2012). A wood based low-temperature biochar captures NH_3-N generated from ruminant urine-N, retaining its bioavailability. *Plant Soil* 353, 73-84.

Van Groenigen, J. W., Kuikman, P. J., De Groot, W. J. M., Velthof, G. L. (2005ª): Nitrous oxide emission from urine-treated soil as influenced by urine composition and soil physical conditions. *Soil Biol. Biochem.* 37, 463–473.

Van Groenigen, J. W., Velthof, G. L., Van der Bolt, F. J. E., Vos, A., Kuikman, P. J. (2005b): Seasonal variation in N_2O emissions from urine patches: effects of urine concentration, soil compaction and dung. *Plant Soil* 273, 15–27.

Van Groenigen, J. W., Palermo, V., Kool, D. M, Kuikman, P. J. (2006): Inhibition of denitrification and N_2O emission by urine-derived benzoic and hippuric acid. *Soil Biol. Biochem.* 38, 2499-2502.

Van Vuuren, A. M., Smits, M. C. J. (1997): Effect of nitrogen and sodium chloride intake on production and composition of urine in dairy cows. In Gaseous nitrogen emissions from grasslands (ed. SC Jarvis and BF Pain), 195–199. CAB International, Wallingford, UK.

Wachendorf, C., Lampe, C., Taube, F., Dittert, K. (2008): Nitrous oxide emissions and dynamics of soil nitrogen under ^{15}N-labeled cow urine and dung patches on a sandy grassland soil. *J. Plant Nutr. Soil Sci.* 171, 171-180.

Yu, K., Wang, Z., Vermoesen, A., Patrick Jr., W., Van Cleemput, O. (2001): Nitrous oxide and methane emissions from different soil suspensions: effect of soil redox status. *Biol. Fertil. Soils* 34, 25–30.

Yu, K., Patrick Jr., W. H. (2003): Redox range with minimum nitrous oxide and methane production in a rice soil under different pH. *Soil Sci. Soc. America J.* 67, 1952-1958.

Zaman, M., Nguyen, M. L. (2012): How application timings of urease and nitrification inhibitors affect N losses from urine patches in pastoral system. *Agric. Ecosyst. Environ.* 156, 37–48.

Zhang, J. B., Cai, Z. C., Zhu, T. B. (2011): N_2O production pathways in the subtropical acid forest soils in China. *Environ. Res.* 111, 643-649.

Table 1. Range of hippuric acid (HA) concentrations in cattle urine reported in different studies.

HA concentration (mM)	Reference
23 to 68	Kool et al., 2006
23 to 68	van Groenigen et al., 2006
46 to 96	Bertram et al. 2009
56 to 90	Clough et al.,2009
8 to 82	Krol et al., 2015

Figure 1. Precipitation (mm), WFPS (%) and soil surface temperature (°C) over the experimental period.

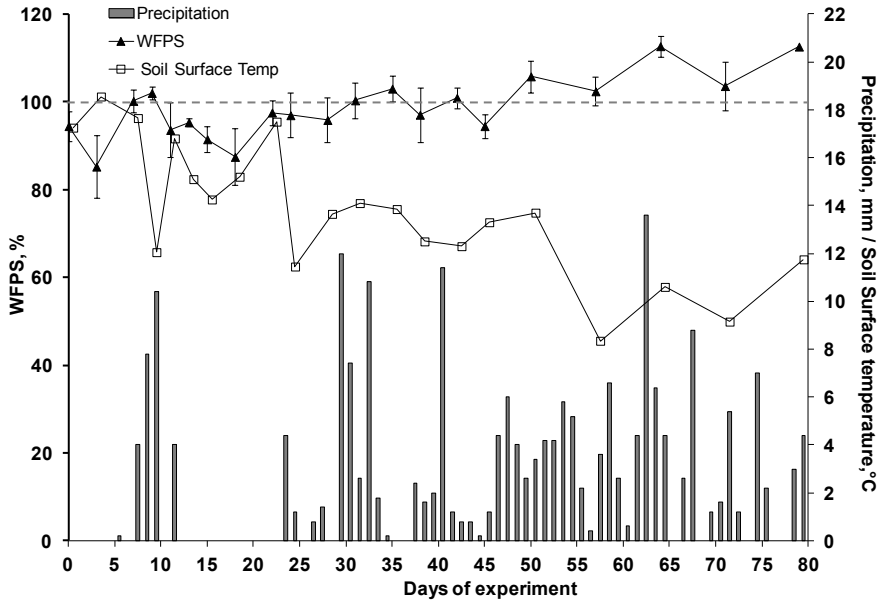

Figure 2. Daily mean N_2O flux (g N_2O-N ha^{-1} d^{-1}) over the experimental period. Vertical bars show standard error of the treatment means (n=3). Significant differences ($\alpha<0.05$) from the control are marked with an asterisk.

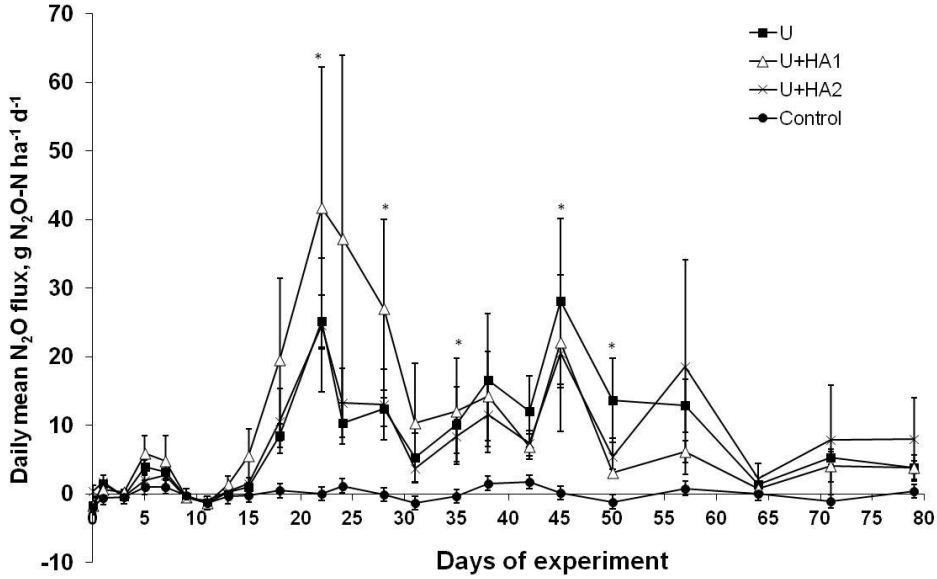

Figure 3. Cumulative N_2O emissions (g N_2O-N ha^{-1}) over the experimental period. Vertical bars show standard error of the treatment means (n=3). Means with different letters are significantly different at the 5% level.

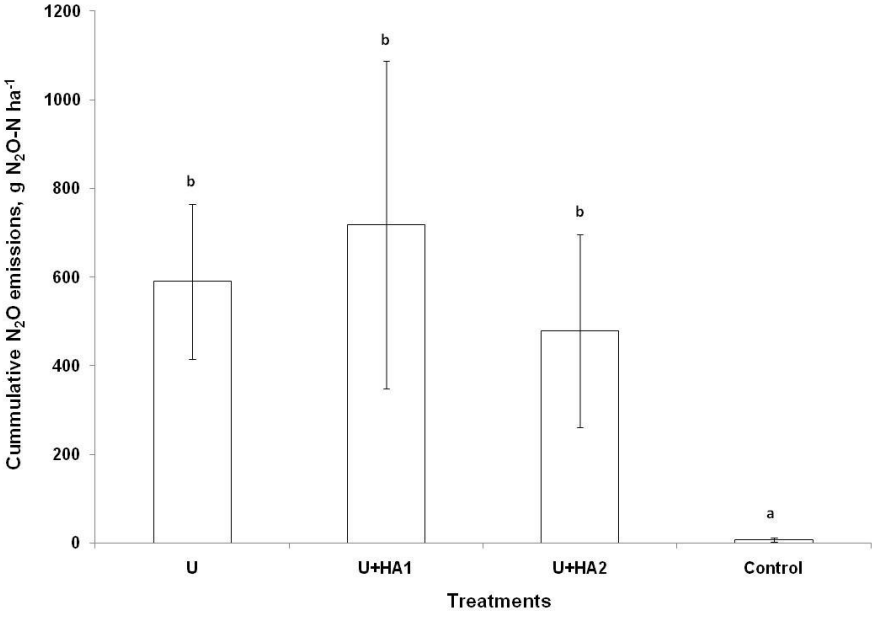

Figure 4. Daily mean CH_4 flux (g CH_4 ha^{-1} d^{-1}) for all treatments over the experimental period. Vertical bars show standard error of the treatment means (n=3).

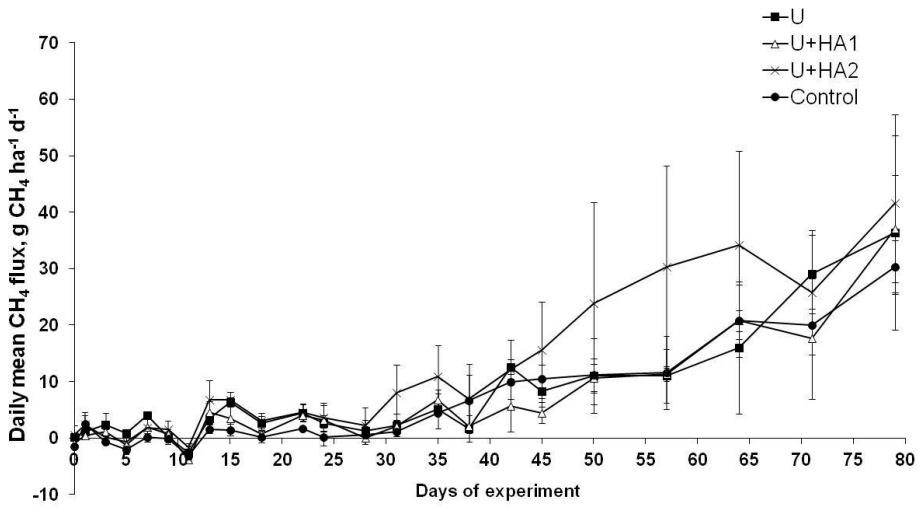

Figure 5. Soil NH_4^+ - N content (mg NH_4^+ - N kg^{-1}) per treatment over the experimental period. Vertical bars show standard error of the treatment means (n=3).

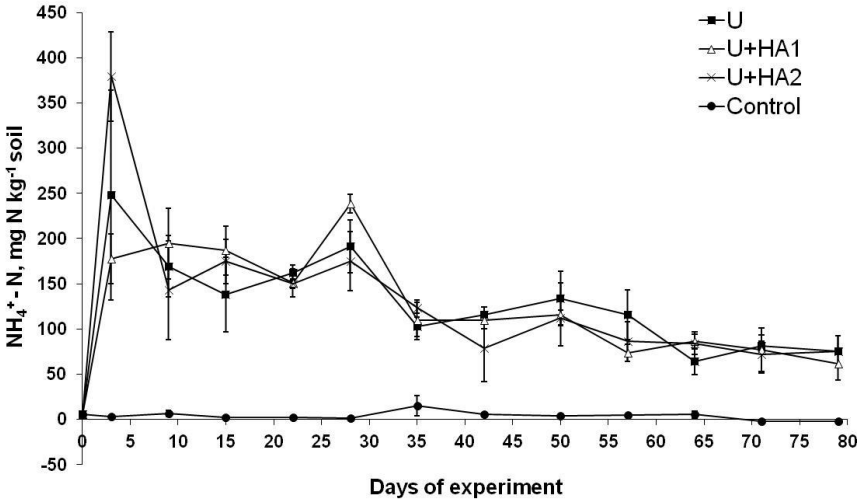

Figure 6. Soil NO_3^--N content (mg NO_3^--N kg^{-1}) per treatment over the experimental period. Vertical bars show standard error of the treatment means (n=3).

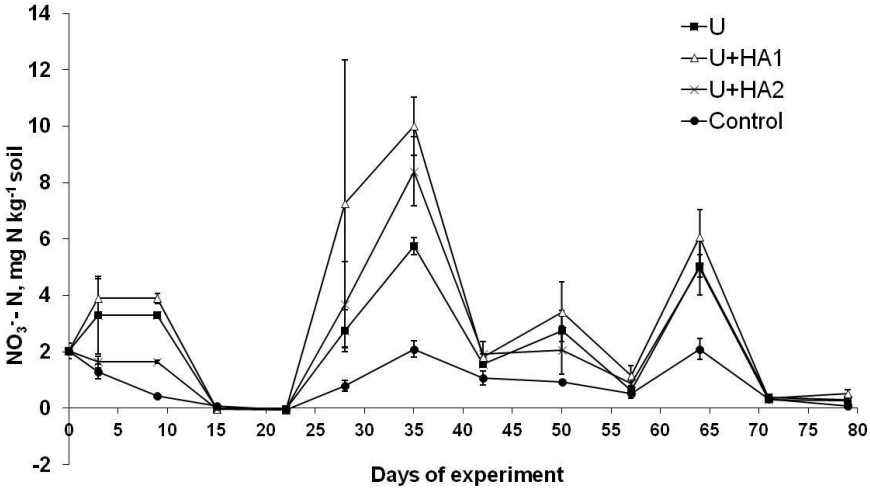

Figure 7. Soil pH measured per treatment over the experimental period. Vertical bars show standard error of the treatment means (n=3).

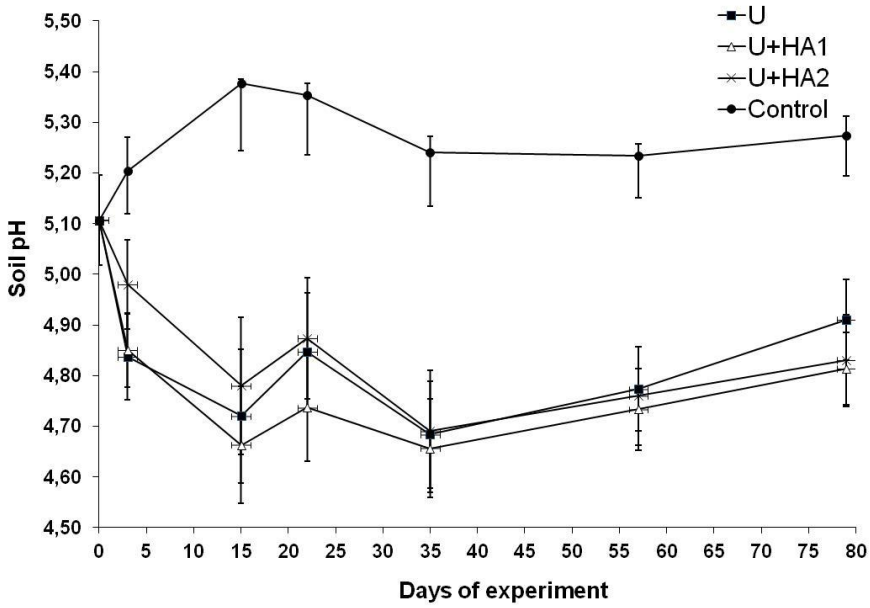

Figure 8. Dissolved organic carbon (DOC, mg C kg soil^{-1}) in soil per treatment over the experimental period. Vertical bars show standard error of the treatment means (n=3).

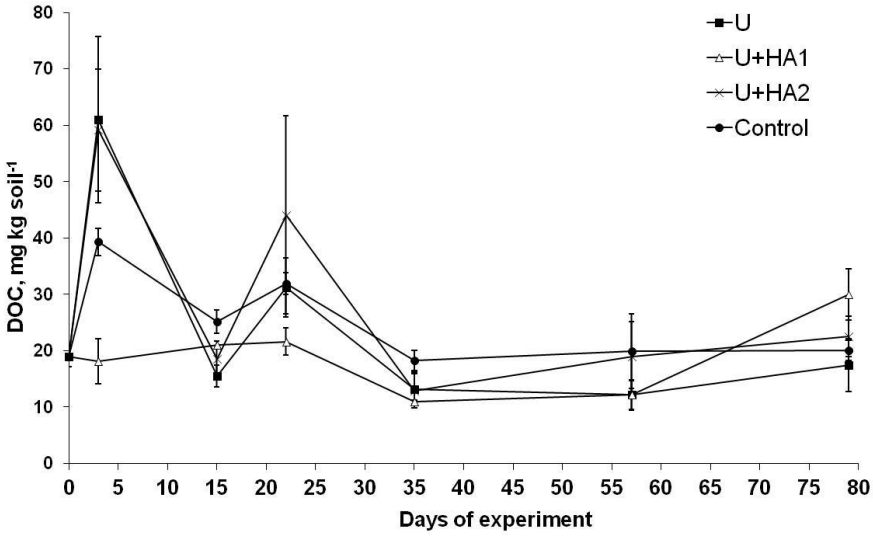

Band / Volume 376
Drying front formation in topmost soil layers as evaporative restraint
Non-invasive monitoring by magnetic resonance and numerical simulation
S. Merz (2017), xxii, 108 pp
ISBN: 978-3-95806-234-4

Band / Volume 377
Low Temperature Thin-Film Silicon Solar Cells on Flexible Plastic Substrates
K. Wilken (2017), 194 pp
ISBN: 978-3-95806-235-1

Band / Volume 378
Dissolution Behaviour of Innovative Inert Matrix Fuels for Recycling of Minor Actinides
E. L. Mühr-Ebert (2017), xii, 164 pp
ISBN: 978-3-95806-238-2

Band / Volume 379
Charakterisierung und Modifizierung von Kupferoxid- und Kupfersulfid-Nanopartikeln für Dünnschichtsolarzellen
J. Flohre (2017), 141, iii pp
ISBN: 978-3-95806-241-2

Band / Volume 380
Einzelfaserkomposite aus Pulvermetallurgischem Wolfram-faserverstärktem Wolfram
B. Jasper (2017), v, 92, XVIII pp
ISBN: 978-3-95806-248-1

Band / Volume 381
Untersuchungen zur Deckschichtbildung auf $LiNi_{0,5}Mn_{1,5}O_4$-Hochvoltkathoden
Die Kathoden/Elektrolyt-Grenzfläche in Hochvolt-Lithium-Ionen-Batterien
K. Wedlich (2017), xvi, 157, xvii-xxvi pp
ISBN: 978-3-95806-249-8

Band / Volume 382
Charakterisierung gradierter Eisen/Wolfram-Schichten für die erste Wand von Fusionsreaktoren
S. Heuer (2017), x, 234 pp
ISBN: 978-3-95806-252-8

Band / Volume 383
High resolution imaging and modeling of aquifer structure
N. Güting (2017), viii, 107 pp
ISBN: 978-3-95806-253-5

Band / Volume 384
IEK-3 Report 2017
Sektorkopplung –
Forschung für ein integriertes Energiesystem
(2017), 182 pp
ISBN: 978-3-95806-256-6

Band / Volume 385
Bestimmung der Wolframerosion mittels optischer Spektroskopie unter ITER-relevanten Plasmabedingungen
M. Laengner (2017), vi, 184, XI pp
ISBN: 978-3-95806-257-3

Band / Volume 386
IEK-3 Report 2017
Sector Coupling –
Research for an Integrated Energy System
(2017), 175 pp
ISBN: 978-3-95806-258-0

Band / Volume 387
Photochemistry of Highly Oxidized Multifunctional Organic Molecules: a Chamber Study
L. I. M. Pullinen (2017), II, 96, xviii pp
ISBN: 978-3-95806-260-3

Band / Volume 388
Poröse Transportschichten für die Polymerelektrolytmembran-Wasserelektrolyse
M. Höh (2017), VI, 186 pp
ISBN: 978-3-95806-262-7

Band / Volume 389
Modelling of High Temperature Polymer Electrolyte Fuel Cells
Q. Cao (2017), 173 pp
ISBN: 978-3-95806-263-4

Band / Volume 390
Potential use of nitrification inhibitors for mitigating N_2O emission from soils
D. Wu (2017), 206 pp
ISBN: 978-3-95806-264-1

Weitere ***Schriften des Verlags im Forschungszentrum Jülich*** unter
http://wwwzb1.fz-juelich.de/verlagextern1/index.asp

Energie & Umwelt /
Energy & Environment
Band / Volume 390
ISBN 978-3-95806-264-1